Composite Action in the Reinforced

Concrete Beam

Composite Action in the Reinforced Concrete Beam

by

ABDUL SHAKOOR UPPAL, B.Sc.Eng.

A Thesis

submitted to the Faculty of Graduate Studies

in Partial Fulfilment of the Requirements

for the Degree of

Master of Engineering

McMaster University

January, 1969

MASTER OF ENGINEERING (1969)   MCMASTER UNIVERSITY

(CIVIL ENGINEERING)   Hamilton, Ontario

TITLE: Composite Action in the Reinforced Concrete

            Beam

AUTHOR: A. Shakoor Uppal, B.Sc.Eng. (Panjab University)

SUPERVISOR: Dr. H. Robinson

NUMBER OF PAGES: xii, 195

SCOPE AND CONTENTS:

        This thesis involves the treatment of the reinforced

        concrete beam as a composite beam with incomplete

        interaction. Influence of the loss of interaction

        and other parameters on the flexural cracking, and

        the moment capacity of the remaining uncracked

        portion of the reinforced concrete beam is studied

        analytically.

ACKNOWLEDGEMENTS

TABLE OF CONTENTS

List of Figures

ix

x

CHAPTER I

INTRODUCTION

1.1 Introduction

The conventional theories for the reinforced con-
crete beam assume that concrete and the steel reinforcement
act together and that there is no slip between them. How-
ever, it has been well recognized from the experiments of
various research workers[1,20,25,29] that the concrete does
not perfectly act together with the steel reinforcement, and
that there is always some relative movement taking place
between them.

During the past few decades, a large number of
experiments have been carried out in order to classify the
modes and determine the causes of different types of
failures[4,6,7,10,12,22]. Similarly, on the other hand,
analytical studies are under way to find out the theoretical
interpretation[13,17,21,24,28] of these experimental findings.

It is thought that the conventional theories for the
reinforced concrete beam are insufficient to give a satis-
factory answer to the cracking and failure phenomenon. They
have not provided a comprehensive explanation of the cause
of the diagonal failure. As a result, new approaches are
being undertaken[11,20,27,29] in particular those which could
account for the effect of slip between the reinforcement
and the concrete.

1

It was suggested[11], that a reinforced concrete beam should be treated as a composite beam with incomplete interaction.

It will be demonstrated that a qualitative explanation of various experimental phenomenon such as cracking patterns[17,24], variations of the internal forces[7,29], strains[8] and the influence of various parameters on the moment carrying capacity[4,10] of a beam, etc., can be achieved by treating the reinforced concrete beam in this manner.

By considering the reinforced concrete beam as a composite beam with incomplete interaction, it is also hoped that a rational explanation of the occurrence of diagonal cracking in the shear span may ultimately be achieved.

1.2 Literature Survey

Since the early stages of development of reinforced concrete, research workers have been attempting to understand the phenomenon of the so-called "Shear Failure".

Before the year 1900, there were at least two schools of thought existing. One considered horizontal shear as the basic cause of shear failure, while the other considered diagonal tension as the basic cause of shear failure. However the origin of the later concept is unknown, a clear explanation of the diagonal tension was first presented by Ritter as early as 1899.

Morsch[6] in 1900, conducted laboratory tests and in the light of his experiments, strongly supported the concept of diagonal tension. Further he developed the following classical expression for the nominal shear.

$$v = \frac{V}{bjd} \qquad 1.1$$

This became accepted to the extent that today, codes of practice in many countries recommend this for computing the shear stresses.

Later in 1909 Talbot observed that Morsch's expression does not seem to be in general agreement with the test results and in particular it fails to account for such variables as shear arm ratio $\frac{u}{d}$, the percentage of steel p, and other factors influencing the stiffness of a beam.

In the early 1950's Clark[6] following Talbot's notion first introduced a mathematical expression for the shear in beams, involving, span to depth ratio, percentage of longitudinal reinforcement and the strength of the concrete. Subsequently researchers developed several empirical formulas relating the effects of various factors that they observed in their experiments. The ACI-ASCE Committee[6] 326 has reported most of these empirical relationships and suggested a new criterion for design. The committee stated that the problem of shear failure and diagonal tension has not been fundamentally and conclusively solved and that further research work be undertaken to establish a more rational

theory to describe the effects of shear and diagonal tension on the behaviour of reinforced concrete members.

Kani[10] in his paper "The riddle of shear failure and its solution" used the "concrete teeth" and "comblike structure" concept to describe the cracking process. He also suggested that redistribution of stresses takes place by the transformation of a beam with bond to a tied arch without bond. The final failure due to him results in diagonal compression instead of diagonal tension as conceived earlier by others.

In 1964 Broms[13,15] carried out an analytical investigation of the distribution of flexural, shear and normal stress across the depth of beams at various points along their spans. He also attempted to explain the cause of different failure phenomenon as a result of excessive stresses either due to a single or a combination of these stresses. He further reported that the diagonal tension failure could be due to the occurrence of higher shear stresses near the neutral axis of a cracked beam.

A year later Leonhardt and Walther[4] reported that principal tensile stresses govern the crack formation in concrete and that shear stress is neither decisive for the carrying capacity nor for the crack formation. Similarly Ferguson suggested that the theory of combined stresses could possibly be employed more constructively in connection

with rational studies of diagonal cracking. In his paper he described failure patterns also in terms of the conventional theory of combined stresses.

More recent analytic studies by Krahl, Kachaturian and Siess[17] and MacGregor and Walters[24], on the development and stability of tensile cracks have contributed, a great deal towards this problem.

Acharya[16] in 1965 suggested that after the beam has taken the form of a comblike structure, about sixty percent of the shear is carried by the beam through dowel action. Fenwick and Pauley[29] in 1968 concluded from their experiments that after the cracking has taken place, a considerable amount of shear must be carried by the aggregate interlock and dowel action in a beam.

A number of so far suggested mechanisms of shear failures have been well summarized in a recent review by Bresler and MacGregor[20].

Although a considerable amount of experimental research as well as analytical studies have been conducted to provide a rational explanation of the cause of shear failure, no definite answer has been found.

In a discussion of Plowman's[8] paper Robinson[11] stated that while conducting preliminary investigations on composite beams with cellular zone between the concrete slab and I-beam, he discovered that in spite of the fact

that there was no distinct interfacial plane between the concrete slab and the steel beam, the strain distribution at any section had been observed to be essentially linear in the elastic range. He also suggested that a reinforced concrete beam may be considered as a composite beam with incomplete interaction.

Wong[18] following Robinson's notion, stated that although a reinforced concrete beam did not have a distinct interfacial plane between the concrete and the steel reinforcement, through a slight modification of the approach by Newmark at el[3] (for conventional composite beams) the theory be applied to a reinforced concrete beam provided a psuedo-interface is assumed. He utilized this concept to estimate the extremeties of a potential zone of flexural cracking in a reinforced concrete beam. These computed crack profiles, in case of a beam with two point loading indicate that the height of the flexural cracks are greatest under the load points in spite of the fact that there is a constant moment applied between the two load points. This trend becomes more pronounced as the interaction between the steel and concrete is reduced.

Further the strain variations along the tensile reinforcement, estimated by him qualitatively characterized those by Plowman[8]. The increase in the top strain under the load point indicated by his computation was similar to

the experimental observations by Kar[26].

Ho[19] in an extension of Wong's[18] work stated
that the study of the strain trajectories, the principal
strain magnitudes and their directions in the remaining
uncracked zone did not appear to give much insight into the
nature of development of the diagonal crack. He also sug-
gested that micro cracks must occur between the major cracks.

Although his investigations did not explain the
cause of shear failure, they did impart sufficient hope that
the application of composite theory and concept of combined
stresses may lead to a rational explanation of this problem.

1.3 Objective and Extent of Investigation

The objective of this investigation is to treat the
reinforced concrete beam as a composite beam with incomplete
interaction, and to attempt to study its cracking behaviour
and carrying capacity analytically.

A simply supported beam carrying two symmetrically
situated point loads was taken as a typical case and in-
fluence of the factors, such as interaction coefficient,
percentage of steel, location and intensity of the point
loads on the flexural crack profiles were studied.

Crack profiles were computed also for the cases of
fixed end, as well as of continuous beams, for different
values of the interaction coefficient $\frac{1}{c}$. Moment carrying
capacity curves for the typical cracked beam were computed.

This study was extended further to record the influence of various parameters on the carrying capacity of a beam.

Distribution of the bond stress and the amount of slip occurring along the length of a cracked beam were also computed. The results of these investigations were compared with experimental observations by other research workers.

Finally a determination of the vertical shear distribution was carried out using methods similar to Ho[19] and Broms[13]. The shear stresses were combined with the strains due to flexure to compute the magnitude and direction of the maximum and minimum principal strains across the depth of a beam. However, although these investigations of the principal strains did not lead to a definite conclusion (owing to certain drawbacks in the approaches followed), they do offer prospects that further investigations may reveal more insight into the problem of diagonal cracking, particularly if small incremental loading is utilized.

CHAPTER II

REINFORCED CONCRETE BEAM

2.1   The conventional working stress theory for the
reinforced concrete beam assumes that the concrete and the
steel reinforcement act together and that there is no slip
permitted.   However it is well recognized by the experi-
ments of various research workers[1,20,25,29] that the
concrete does not perfectly act together with the reinforce-
ment and that there is always some relative movement or slip
taking place.   This phenomenon is quite pronounced
especially in the case of a cracked beam where slip is
partially due to the breakdown in bond and partially due to
deformation of the concrete teeth.

Moreover the reinforced concrete beam, unlike a
composite beam, does not possess a definite interface.   How-
ever if a psuedo-interface is assumed the composite beam
theory can be applied.   The following principal assumptions
were made for the analysis, corresponding to the composite
theory summarized in Appendix I.

It is assumed that

1)   The concrete and steel are perfect elastic
materials.

2)   There is a linear strain variation across the
depth of a section.

3)   The bond-slip characteristic for a given

9
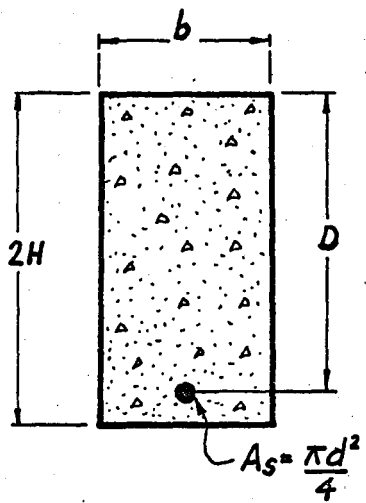
a) Uncracked
   Section
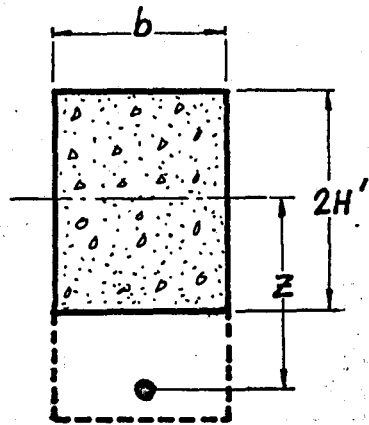
b) Cracked
   Section
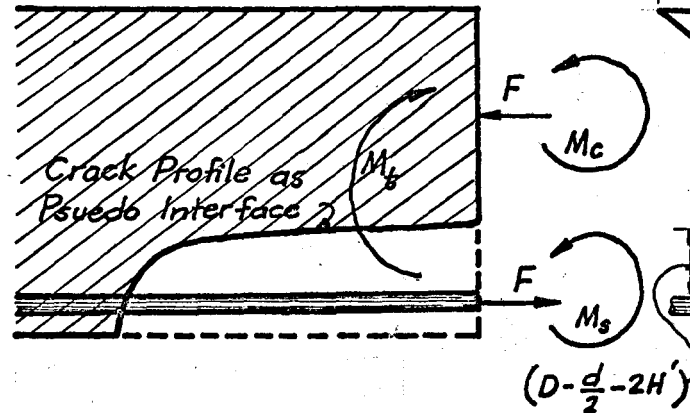
c) Forces
   $(M_t = M_c + M_s + F \cdot Z)$
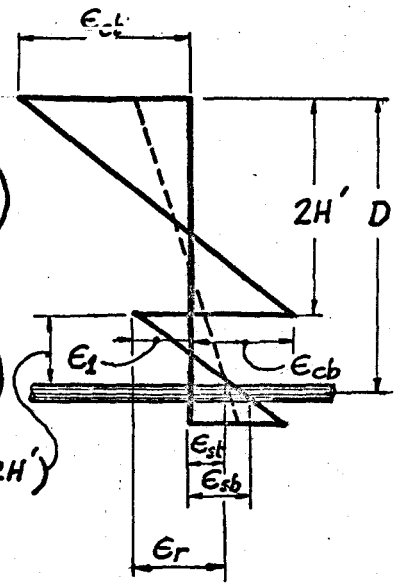
d) Strains

APPLICATION OF COMPOSITE THEORY TO THE REINFORCED CONCRETE BEAM

FIG . 2.1

interaction coefficient is assumed to remain constant be-
fore and after cracking and is uniform and continuous along
the length of the reinforced concrete beam.

4) The amount of relative movement between the
concrete and the steel is directly proportional to the
horizontal shear.

5) Concrete and steel reinforcement deflect equal
amounts at all points along the length of a beam.

The line joining the extremeties of the flexural
cracks will be referred to as the crack profile. This
profile will be treated as a psuedo-interface, Fig. 2.1,
and then the "slip-strain" at the pseudo-interface
(analogous to Eq. A1.3) can be written:

$$\frac{d\gamma}{dx} = \varepsilon_b - \varepsilon_s \qquad\qquad \text{A1.3}$$

$$= \varepsilon_1 - \varepsilon_{cb}$$

$$\text{now} \quad \varepsilon_1 = -(\varepsilon_r - \varepsilon_{st})$$

$$\therefore \quad \frac{d\gamma}{dx} = \varepsilon_{st} - \varepsilon_r - \varepsilon_{cb} \qquad\qquad 2.1$$

From the similarity of shaded triangles,

$$\varepsilon_r = (\varepsilon_{sb} - \varepsilon_{st}) \left(\frac{D - \frac{d}{2} - 2H'}{d} \right) \qquad\qquad 2.2$$

where ε_r is the strain due to distortion of the concrete
'teeth' in a cracked beam. Since the strain distribution
has been assumed to be linear across the section, analogous

to Eq. A1.5(a & b), following expressions can be written:

$$\varepsilon_{sb} = \frac{F}{E_s A_s} + \frac{M_s C_s}{E_s I_s}$$

$$\varepsilon_{st} = \frac{F}{E_s A_s} - \frac{M_s C_s}{E_s I_s}$$

$$\varepsilon_{cb} = - \frac{F}{E_s A_s} + \frac{M_c C_c}{E_c I_c}$$ 2.3

$$\varepsilon_{ct} = - \frac{F}{E_s A_s} - \frac{M_c C_c}{E_c I_c}$$

Therefore

$$\varepsilon_r = \left(\frac{\cancel{F}}{E_s A_s} + \frac{M_s C_s}{E_s I_s} - \frac{\cancel{F}}{E_s A_s} + \frac{M_s C_s}{E_s I_s} \right) \left(\frac{D - \frac{d}{2} - 2H'}{d} \right)$$

$$\varepsilon_r = - \frac{2 M_s C_s}{E_s I_s} \left(\frac{D - \frac{d}{2} - 2H'}{d} \right)$$

Now substituting this value of ε_r in Eq. 2.1, the rate of change of slip will be

$$\frac{d\gamma}{dx} = \varepsilon_{st} - \varepsilon_{cb} - \frac{2 M_s C_s}{E_s I_s d} \left(D - \frac{d}{2} - 2H' \right)$$ 2.4

The compatibility condition, Eq. A1.7 can be rewritten as

$$\frac{d\gamma}{dx} = \frac{1}{k} \frac{d^2 F}{dx^2}$$, setting s = 1 for the reinforced

concrete beam.

Therefore, Eq. 2.4 will then be

$$\frac{1}{k} \frac{d^2 F}{dx^2} = \varepsilon_{st} - \varepsilon_{cb} - \frac{2 M_s C_s}{E_s I_s d} \left(D - \frac{d}{2} - 2H' \right)$$ 2.4A

Substituting values of ε_{st} and ε_{cb} in Eq. 2.4A from Eq. 2.3

$$\frac{1}{k}\frac{d^2F}{dx^2} = \left(\frac{F}{E_sA_s} - \frac{M_sC_s}{E_sI_s}\right) - \left(-\frac{F}{E_cA_c} + \frac{M_cC_c}{E_cI_c}\right) - \frac{2M_sC_s}{E_sI_sd}\left(D-\frac{d}{2}-2H'\right)$$

Re-arranging

$$\frac{1}{k}\frac{d^2F}{dx^2} = F\left(\frac{1}{E_sA_s} + \frac{1}{E_cA_c}\right) - \left[\frac{M_sC_s}{E_sI_s} + \frac{M_cC_c}{E_cI_c} + \frac{2M_sC_s}{E_sI_sd}\left(D - \frac{d}{2} - 2H'\right)\right]$$

Since it is assumed that the concrete and steel reinforcement deflect equally at all points, i.e. they have equal curvatures, the moments M_s and M_c are related as follows:

$$\frac{M_s}{E_sI_s} = \frac{M_c}{E_cI_s}$$

Also from equilibrium of the composite section

$$M_t = M_c + M_s + F.Z \qquad\qquad 2.5$$

Therefore

$$\frac{M_c}{E_cI_c} = \frac{M_s}{E_sI_s} = \frac{M_t - F.Z}{\Sigma EI} \qquad\qquad 2.6$$

where by definition

$$\Sigma EI = E_sI_s + E_cI_c$$

$$C_c = H \text{ and } C_s = \frac{d}{2}$$

Substituting values of Eq. 2.6 in the expression above

$$\frac{1}{k}\frac{d^2F}{dx^2} = F\left(\frac{1}{E_sA_s} + \frac{1}{E_cA_c}\right) - \frac{M_t - F.Z}{\Sigma EI}\left[C_s + C_c + \frac{2C_s}{d}\left(D - \frac{d}{2} - 2H'\right)\right]$$

or

$$\frac{1}{k}\frac{d^2F}{dx^2} = F\left\{\frac{1}{E_sA_s} + \frac{1}{E_cA_c} + \frac{z^2}{\Sigma EI}\right\} - \frac{M_t.Z}{\Sigma EI}$$

where

$$Z = C_s + C_c + \frac{2C_s}{d} (D - \frac{d}{2} - 2H')$$

Re-arranging the terms, yields

$$\frac{d^2F}{dx^2} - F \cdot k \cdot \frac{\overline{EI}}{\overline{EA}\Sigma EI} = - k \frac{Z}{\Sigma EI} \cdot M_t(x) \qquad 2.7$$

For an uncracked section, where there are no concrete teeth, $D - \frac{d}{2} - 2H' = 0$ and so $\varepsilon_r = 0$, therefore Eq. 2.4 reduces to

$$\frac{d\gamma}{dx} = \varepsilon_{st} - \varepsilon_{cb}$$

which is identical to Newmark's Eq. A1.3. This means slip occurs only between the reinforcement and the concrete surrounding it, whereas in a cracked beam ($\varepsilon_r \neq 0$), there would be an additional slip due to deformation of the concrete teeth.

It, therefore, could be concluded that the differential equation 2.7 is applicable to both, a cracked as well as an uncracked section of a reinforced concrete beam.

2.2 Solution of Differential Equation 2.7

Complete solutions for Eq. 2.7 were obtained for a variety of beam cases. Only a beam, carrying two symmetrically placed point loads, with different cases of end conditions will be considered here.

2.2.1 Case I – Simply Supported Beam with Symmetrically Placed Two Point Loads
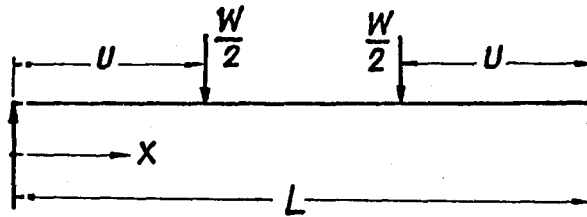
Fig. 2.2

The moment expressions are:

$$M_t(x) = \frac{W}{2} x \qquad \text{for } 0 \leqslant x \leqslant u$$

and

$$M_t(x) = \frac{W}{2} u \qquad \text{for } 0 \leqslant x \leqslant \frac{L}{2}$$

2.8

Two differential equations for these two ranges of moment can be solved for F_L and F_R using the following boundary conditions

$$\text{at } x = 0 \quad ; \quad F_L = 0$$

$$\text{at } x = u \quad ; \quad F_L = F_R \text{ and } \frac{dF_L}{dx} = \frac{dF_R}{dx}$$

and

$$\text{at } x = \frac{L}{2} \quad ; \quad \frac{dF_R}{dx} = 0$$

2.9

The solutions for the interaction force F are

$$F_L = \frac{\overline{EA}}{\overline{EI}}.z.\frac{WL}{2}\left\{ \frac{x}{L} - \frac{\sqrt{C}}{\pi} \frac{\text{Cosh} \frac{\pi}{\sqrt{C}}\left(\frac{1}{2} - \frac{u}{L}\right)}{\text{Cosh} \frac{\pi}{2\sqrt{C}}} \text{Sinh}\left(\frac{\pi}{\sqrt{C}}\frac{x}{L}\right)\right\}$$

2.10a

$$F_R = \frac{\overline{EA}}{\overline{EI}}.z.\frac{WL}{2}\left\{ \frac{u}{L} - \frac{\sqrt{C}}{\pi} \frac{\text{Sinh}\left(\frac{\pi}{\sqrt{C}}\frac{u}{L}\right)}{\text{Cosh} \frac{\pi}{2\sqrt{C}}} \text{Cosh} \frac{\pi}{\sqrt{C}}\left(\frac{1}{2} - \frac{x}{L}\right)\right\}$$

2.10b

$$F_L = \frac{\overline{EA}}{\overline{EI}} \cdot Z \cdot \frac{WL}{2} \left\{ \frac{X}{L} - \frac{\sqrt{C}}{\pi} \cdot \frac{Cosh \frac{\pi}{\sqrt{C}}\left(\frac{1}{2} - \frac{U}{L}\right)}{Cosh \frac{\pi}{2\sqrt{C}}} \cdot Sinh \frac{\pi}{\sqrt{C}}\left(\frac{X}{L}\right) \right\} \cdot \text{—} \quad Eq:2.10a$$

$$F_R = \frac{\overline{EA}}{\overline{EI}} \cdot Z \cdot \frac{WL}{2} \left\{ \frac{U}{L} - \frac{\sqrt{C}}{\pi} \cdot \frac{Sinh \frac{\pi}{\sqrt{C}}\left(\frac{U}{L}\right)}{Cosh \frac{\pi}{2\sqrt{C}}} \cdot Cosh \frac{\pi}{\sqrt{C}}\left(\frac{1}{2} - \frac{X}{L}\right) \right\} \cdot \text{—} \quad Eq:2.10b$$

where: $\frac{\overline{EA}}{\overline{EI}} \cdot Z \cdot \frac{WL}{2}$ is assumed unity for this plot.

U=.33L   U=.33L

END SLIP PERMITTED

$\frac{1}{C} = 100.0$ $\frac{1}{C} = \infty$ $\frac{1}{C} = 50.0$

$\frac{1}{C} = 5.0$

$\frac{1}{C} = 2.0$

$\frac{1}{C} = 1.0$

$\frac{1}{C} = 0.5$

F

X/L

VARIATION OF INTERACTION FORCE - SIMPLY SUPPORTED BEAM

FIG.2.3

16

$$q_L = \frac{\overline{EA}}{EI} \cdot Z \cdot \frac{W}{2} \left\{ 1 - \frac{Cosh \frac{\pi}{\sqrt{c}}\left(\frac{1}{2} - \frac{U}{L}\right)}{Cosh \frac{\pi}{\sqrt{c}}} \cdot Cosh \frac{\pi}{\sqrt{c}}\left(\frac{x}{L}\right) \right\} \quad \text{------- Eq: 2.14a}$$

$$q_R = \frac{\overline{EA}}{EI} \cdot Z \cdot \frac{W}{2} \left\{ \frac{Sinh \frac{\pi}{\sqrt{c}}\left(\frac{U}{L}\right)}{Cosh \frac{\pi}{\sqrt{c}}} \cdot Sinh \frac{\pi}{\sqrt{c}}\left(\frac{1}{2} - \frac{U}{L}\right) \right\} \quad \text{------- Eq: 2.14b}$$

where $\frac{\overline{EA}}{EI} \cdot Z \cdot \frac{W}{2}$ is assumed unity for this plot.

VARIATION IN VALUE OF UNIT HORIZONTAL SHEAR - SIMPLY SUPPORTED BEAM.

FIG. 2.4

where $\frac{1}{C}$, the interaction coefficient, is a dimensionless quantity, introduced mainly for convenience, and is given by

$$\frac{1}{C} = \frac{k}{s} \cdot \frac{L^2 \overline{EI}}{\pi^2 \overline{EA}\Sigma EI} \qquad 2.11$$

where s = unity. The interaction coefficent, $\frac{1}{C}$, depends on the geometry and the bond-slip characteristics of a beam. It has been found that for complete interaction, $\frac{1}{C}$ is ∞, and for no interaction, $\frac{1}{C} = 0$. Similarly a value of $\frac{1}{C} = 200$ indicates a high interaction and $\frac{1}{C} = 0.5$, a low interaction.

Therefore for complete interaction, i.e. $\frac{1}{C} = \infty$, we obtain

$$F_L' = \frac{\overline{EA}}{\overline{EI}} \cdot z \cdot \frac{Wx}{2} \qquad 2.12a$$

$$F_R' = \frac{\overline{EA}}{\overline{EI}} \cdot z \cdot \frac{Wu}{2} \qquad 2.12b$$

The degree of interaction, $\alpha = \frac{F}{F'}$, for each range of x is

$$\frac{F_L}{F_L'} = 1. - \frac{\sqrt{C}}{\pi} \cdot \frac{\text{Cosh} \frac{\pi}{\sqrt{C}} \left(\frac{1}{2} - \frac{u}{L}\right)}{\frac{x}{L} \cdot \text{Cosh} \frac{\pi}{2\sqrt{C}}} \text{Sinh} \left(\frac{\pi}{\sqrt{C}} \frac{x}{L}\right) \qquad 2.13a$$

$$\frac{F_R}{F_R'} = 1. - \frac{\sqrt{C}}{\pi} \cdot \frac{\text{Sinh} \frac{\pi}{\sqrt{C}} \frac{u}{L}}{\frac{u}{L} \text{Cosh} \frac{\pi}{2\sqrt{C}}} \cdot \text{Cosh} \frac{\pi}{\sqrt{C}} \left(\frac{1}{2} - \frac{x}{L}\right) \qquad 2.13b$$

$$\frac{F_L}{F_{L'}} = 1 - \frac{\sqrt{c}}{\pi} \cdot \frac{\text{Cosh}\ \frac{\pi}{\sqrt{c}}\left(\frac{1}{2} - \frac{U}{L}\right)}{\frac{x}{L}\ \text{Cosh}\ \frac{\pi}{2\sqrt{c}}} \cdot \text{Sinh}\ \frac{\pi}{\sqrt{c}}\left(\frac{x}{L}\right) \quad \text{———} \cdot \text{———} \cdot \text{———} \cdot \text{Eq}: 2.13a$$

$$\frac{F_R}{F_{R'}} = 1 - \frac{\sqrt{c}}{\pi} \cdot \frac{\text{Sinh}\ \frac{\pi}{\sqrt{c}}\left(\frac{U}{L}\right)}{\frac{U}{L}\ \text{Cosh}\ \frac{\pi}{2\sqrt{c}}} \cdot \text{Cosh}\ \frac{\pi}{\sqrt{c}}\left(\frac{1}{2} - \frac{x}{L}\right) \text{———} \cdot \text{———} \cdot \text{——} \cdot \text{Eq}: 2.13b$$
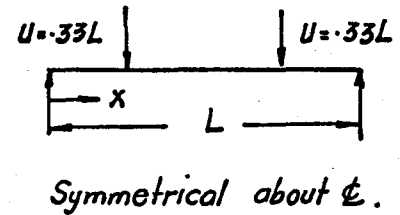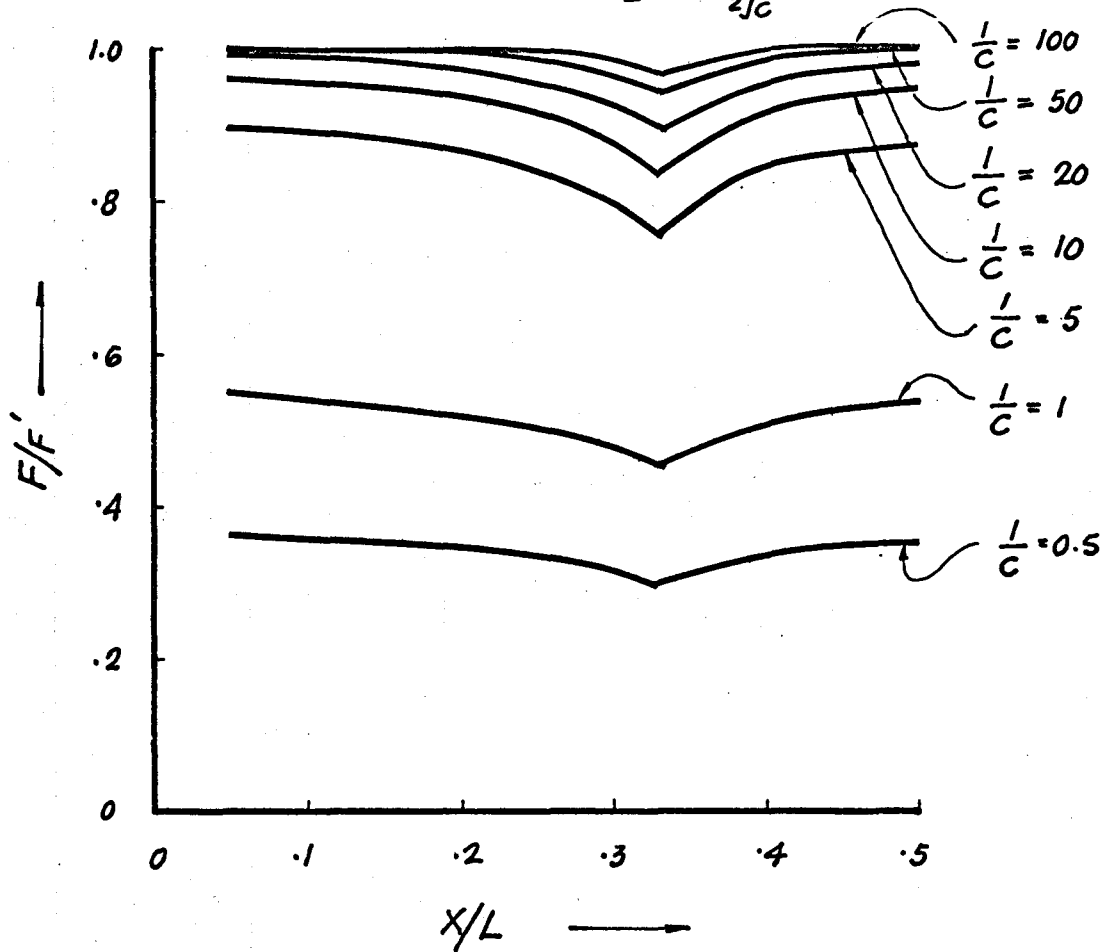
VARIATION IN DEGREE OF INTERACTION – SIMPLY SUPPORTED BEAM

FIG. 2.5

The expressions for load per unit length transmitted between the ccncrete and the reinforcement (i.e. horizontal shear force per unit length) can be found by Eq. A1.6 and are:

$$q_L = \frac{\overline{EA}}{\overline{EI}} \cdot z \cdot \frac{W}{2} \left\{ 1. - \frac{\text{Cosh } \frac{\pi}{\sqrt{C}}\left(\frac{1}{2} - \frac{u}{L}\right)}{\text{Cosh } \frac{\pi}{2\sqrt{C}}} \cdot \text{Cosh}\left(\frac{\pi}{\sqrt{C}} \frac{x}{L}\right) \right\} \quad 2.14a$$

$$q_R = \frac{\overline{EA}}{\overline{EI}} \cdot z \cdot \frac{W}{2} \left[\frac{\text{Sinh}\left(\frac{\pi}{\sqrt{C}} \frac{u}{L}\right)}{\text{Cosh } \frac{\pi}{2\sqrt{C}}} \cdot \text{Sinh } \frac{\pi}{\sqrt{C}}\left(\frac{1}{2} - \frac{x}{L}\right) \right] \quad 2.14b$$

Plots showing variations of F, q, and $\frac{F}{F\tau}$, along the length of a beam for this case, with varying values of the interaction coefficient $\frac{1}{C}$ are given in Figs. 2.3, 2.4 and 2.5.

2.2.2 Case II - Simply Supported Beam with Symmetrically
      Placed Two Point Loads - End Slip Restricted

This case is same as case I, except that slip at free ends of the beam, is kept zero by imposing the condition that at x = o and L, $\frac{dF}{dx}$ = 0 in the solution of the differential equation 2.7.

The solutions for the interaction force F are:

$$F_L = \frac{\overline{EA}}{\overline{EI}} \cdot z \cdot \frac{WL}{2} \left\{ \frac{\sqrt{c}}{\pi} \left(\frac{Cosh \frac{\pi}{2\sqrt{c}} - Cosh \frac{\pi}{\sqrt{c}}\left(\frac{1}{2} - \frac{u}{L}\right)}{Sinh \frac{\pi}{2\sqrt{c}}} \right) Cosh \frac{\pi}{\sqrt{c}}\left(\frac{x}{L}\right) - \frac{\sqrt{c}}{\pi} Sinh \frac{\pi}{\sqrt{c}}\left(\frac{x}{L}\right) + \frac{x}{L} \right\} \cdot \underline{\qquad} \cdot Eq: 2.15a$$

$$F_R = \frac{\overline{EA}}{\overline{EI}} \cdot z \cdot \frac{WL}{2} \left\{ \frac{\sqrt{c}}{\pi} \left(\frac{1 - Cosh \frac{\pi}{\sqrt{c}}\left(\frac{u}{L}\right)}{Sinh \frac{\pi}{2\sqrt{c}}} \right) Cosh \frac{\pi}{\sqrt{c}}\left(\frac{1}{2} - \frac{x}{L}\right) + \frac{u}{L} \right\} \cdot \underline{\qquad \cdot \qquad} \cdot Eq: 2.15b$$

where $\frac{\overline{EA}}{\overline{EI}} \cdot z \cdot \frac{WL}{2}$ assumed unity for this plot

0.25L   0.25L

L

End Slip Restricted
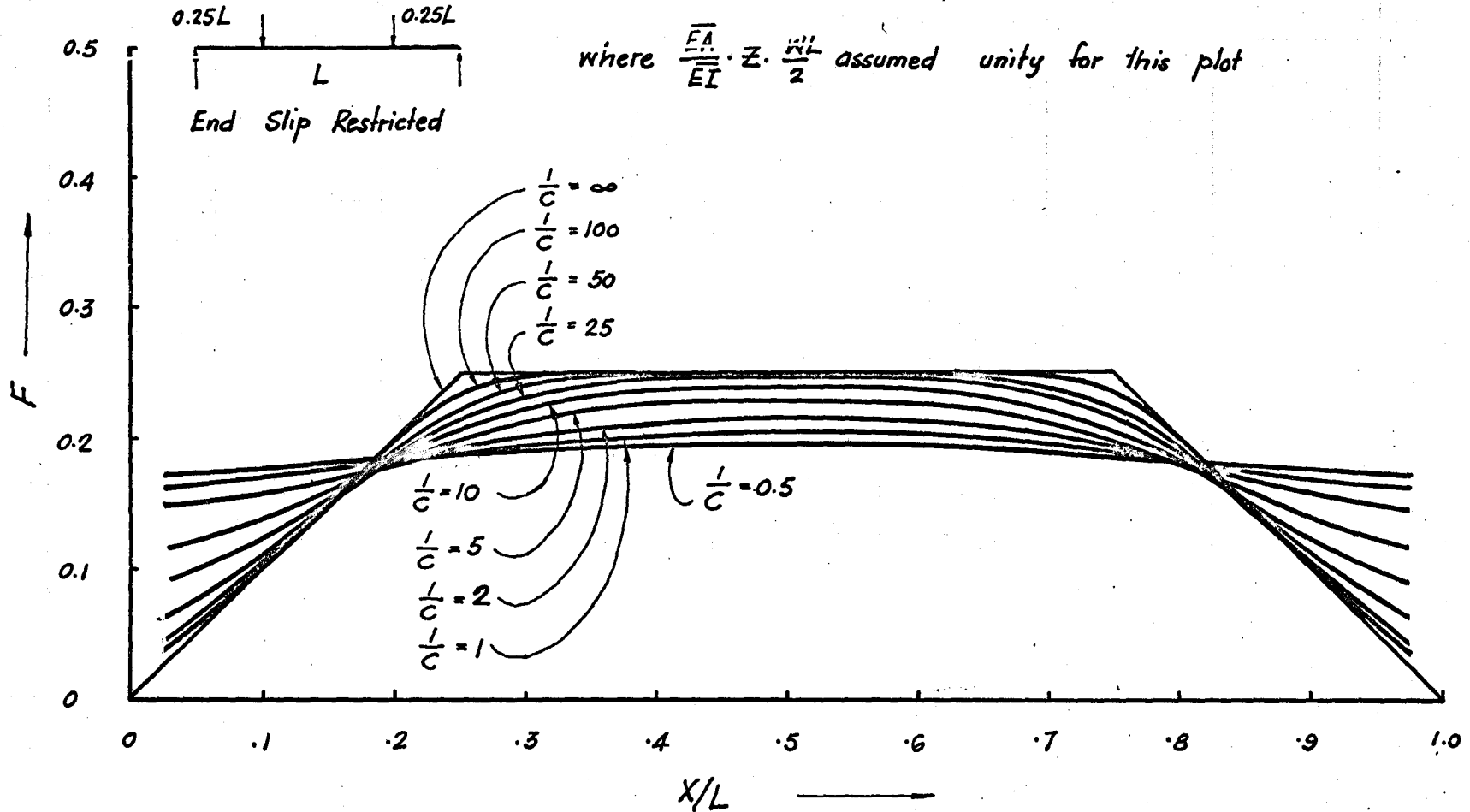
VARIATION OF INTERACTION FORCE - SIMPLY SUPPORTED BEAM.

FIG. 2.6

$$q_L = \frac{\overline{EA}}{\overline{EI}} \cdot Z \cdot \frac{W}{2} \left\{ \left(\frac{Cosh \frac{\pi}{2\sqrt{C}} - Cosh \frac{\pi}{\sqrt{C}} \left(\frac{1}{2} - \frac{u}{L} \right)}{Sinh \frac{\pi}{2\sqrt{C}}} \right) Sinh \frac{\pi}{\sqrt{C}} \left(\frac{x}{L} \right) - Cosh \frac{\pi}{\sqrt{C}} \left(\frac{x}{L} \right) + 1 \right\} \cdot \text{——— } Eq: 2.18_a$$

$$q_R = \frac{\overline{EA}}{\overline{EI}} \cdot Z \cdot \frac{W}{2} \left\{ \left(\frac{Cosh \frac{\pi}{\sqrt{C}} \left(\frac{u}{L} \right) - 1}{Sinh \frac{\pi}{2\sqrt{C}}} \right) Sinh \frac{\pi}{\sqrt{C}} \left(\frac{1}{2} - \frac{x}{L} \right) \right\} \text{—— · —— · —— } Eq: 2.18_b$$

VARIATION IN VALUE OF UNIT HORIZONTAL SHEAR -SIMPLY SUPPORTED BEAM

FIG . 2.7

END SLIPS RESTRICTED.

$$\frac{F_L}{F_L'} = 1 + \frac{\sqrt{c}}{\pi}\left(\frac{L}{x}\right)\left\{\left(\frac{Cosh\frac{\pi}{2\sqrt{c}} - Cosh\frac{\pi}{\sqrt{c}}\left(\frac{1}{2} - \frac{u}{L}\right)}{Sinh\frac{\pi}{2\sqrt{c}}}\right)Cosh\frac{\pi}{\sqrt{c}}\left(\frac{x}{L}\right) - Sinh\frac{\pi}{\sqrt{c}}\left(\frac{x}{L}\right)\right\} \quad Eq. \ 2.17_a$$

$$\frac{F_R}{F_R'} = 1 + \frac{\sqrt{c}}{\pi}\left(\frac{L}{u}\right)\left\{\left(\frac{1 - Cosh\frac{\pi}{\sqrt{c}}\left(\frac{u}{L}\right)}{Sinh\frac{\pi}{2\sqrt{c}}}\right)Cosh\frac{\pi}{\sqrt{c}}\left(\frac{1}{2} - \frac{x}{L}\right)\right\} \quad Eq. \ 2.17_b$$

$\frac{1}{c} = 0.5$

$\frac{1}{c} = 1.0$

$\frac{1}{c} = 2.0$

$\frac{1}{c} = 5.0$

$\frac{1}{c} = 10$

$\frac{1}{c} = 25$

$\frac{1}{c} = 50$

$\frac{1}{c} = 100$

VARIATION IN DEGREE OF INTERACTION - SIMPLY SUPPORTED BEAM

FIG. 2.8

23

$$F_L = \frac{\overline{EA}}{\overline{EI}} \cdot z \cdot \frac{WL}{2} \left\{ \frac{\sqrt{C}}{\pi} \left(\frac{\text{Cosh } \frac{\pi}{2\sqrt{C}} - \text{Cosh } \frac{\pi}{\sqrt{C}} \left(\frac{1}{2} - \frac{u}{L} \right)}{\text{Sinh } \frac{\pi}{2\sqrt{C}}} \right) \text{Cosh } \frac{\pi}{\sqrt{C}} \frac{x}{L} \right.$$

$$\left. - \frac{\sqrt{C}}{\pi} \text{Sinh } \frac{\pi}{\sqrt{C}} \frac{x}{L} + \frac{x}{L} \right\} \qquad \qquad 2.15a$$

$$F_R = \frac{\overline{EA}}{\overline{EI}} \cdot z \cdot \frac{WL}{2} \left\{ \frac{\sqrt{C}}{\pi} \left(1 - \text{Cosh } \frac{\pi}{\sqrt{C}} \frac{u}{L} \right) \frac{\text{Cosh } \frac{\pi}{\sqrt{C}} \left(\frac{1}{2} - \frac{x}{L} \right)}{\text{Sinh } \frac{\pi}{2\sqrt{C}}} + \frac{u}{L} \right\} \quad 2.15b$$

For complete interaction, when $\frac{1}{C} = \infty$, we have

$$F_L' = \frac{\overline{EA}}{\overline{EI}} \cdot z \cdot \frac{WL}{2} \left(\frac{x}{L} \right) \qquad \qquad 2.16a$$

$$F_R' = \frac{\overline{EA}}{\overline{EI}} \cdot z \cdot \frac{WL}{2} \left(\frac{u}{L} \right) \qquad \qquad 2.16b$$

The degree of interaction $\frac{F}{F'}$ for each range of x is

$$\frac{F_L}{F_L'} = 1 + \frac{\sqrt{C}}{\pi} \frac{L}{x} \left\{ \left(\frac{\text{Cosh } \frac{\pi}{2\sqrt{C}} - \text{Cosh } \frac{\pi}{\sqrt{C}} \left(\frac{1}{2} - \frac{u}{L} \right)}{\text{Sinh } \frac{\pi}{2\sqrt{C}}} \right) \text{Cosh } \frac{\pi}{\sqrt{C}} \frac{x}{L} \right.$$

$$\left. - \text{Sinh } \frac{\pi}{\sqrt{C}} \frac{x}{L} \right\} \qquad \qquad 2.17a$$

and

$$\frac{F_R}{F_R'} = 1 + \frac{\sqrt{C}}{\pi} \frac{L}{u} \left\{ \left(\frac{1 - \text{Cosh } \frac{\pi}{\sqrt{C}} \frac{u}{L}}{\text{Sinh } \frac{\pi}{2\sqrt{C}}} \right) \text{Cosh } \frac{\pi}{\sqrt{C}} \left(\frac{1}{2} - \frac{x}{L} \right) \right\} \qquad 2.17b$$

The expressions for the horizontal shear force per unit length, from Eq. A1.6 are:

$$q_L = \frac{\overline{EA}}{\overline{EI}} \cdot z \cdot \frac{W}{2} \left\{ \left(\frac{\text{Cosh } \frac{\pi}{2\sqrt{C}} - \text{Cosh } \frac{\pi}{\sqrt{C}} \left(\frac{1}{2} - \frac{u}{L} \right)}{\text{Sinh } \frac{\pi}{2\sqrt{C}}} \right) \text{Sinh } \frac{\pi}{\sqrt{C}} \frac{x}{L} \right.$$

$$\left. - \text{Cosh } \frac{\pi}{\sqrt{C}} \frac{x}{L} + 1 \right\} \qquad\qquad 2.18a$$

and

$$q_R = \frac{\overline{EA}}{\overline{EI}} \cdot z \cdot \frac{W}{2} \left[-\left(\frac{1 - \text{Cosh } \frac{\pi}{\sqrt{C}} \frac{u}{L}}{\text{Sinh } \frac{\pi}{2\sqrt{C}}} \right) \text{Sinh } \frac{\pi}{\sqrt{C}} \left(\frac{1}{2} - \frac{x}{L} \right) \right\} \qquad 2.18b$$

Plots showing variations of F, q, and $\frac{F}{F'}$ along the length of a beam with point loads at quarter span, and for varying values of the interaction coefficient $\frac{1}{C}$ are given as Figs. 2.6, 2.7 and 2.8.

2.2.3 Case III - Fixed End Beam with Symmetrically Placed Two Point Loads
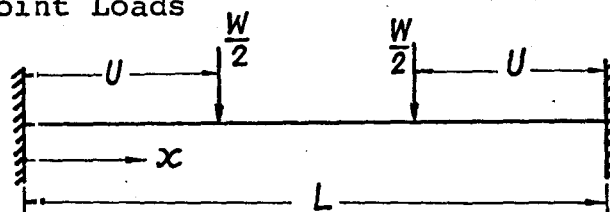
Fig. 2.9

The moment expressions are:

$$M_{(x)} = - \frac{Wu}{2L} (L-u) + \frac{W}{2} x \qquad \text{for } 0 \leqslant x \leqslant u$$

and

$$M_{(x)} = - \frac{Wu}{2L} (L-u) + \frac{W}{2} u \qquad \text{for } u \leqslant x \leqslant \frac{L}{2}$$

$$\left. \right\} \quad 2.19$$

Two differential equations for these two ranges of moment can be solved for F_L and F_R using the following boundary conditions:

$$\text{at } x = 0 \; ; \quad \frac{dF}{dx} = 0$$

$$\text{at } x = u \; ; \quad F_L = F_R \text{ and } \frac{dF_L}{dx} = \frac{dF_R}{dx}$$

and

$$\text{at } x = \frac{L}{2} \; ; \quad \frac{dF}{dx} = 0$$

$$\left. \right\} \quad 2.20$$

The solutions for the interaction force F are

$$F_L = \frac{EA}{EI} . z . \frac{WL}{2} \left[\frac{\sqrt{C}}{\pi} \left\{ \left(\frac{\text{Cosh } \frac{\pi}{2\sqrt{C}} - \text{Cosh } \frac{\pi}{2\sqrt{C}} \left(\frac{1}{2} - \frac{u}{L} \right)}{\text{Sinh } \frac{\pi}{2\sqrt{C}}} \right) \text{Cosh } \frac{\pi}{\sqrt{C}} \frac{x}{L} \right. \right.$$

$$\left. \left. - \text{Sinh } \frac{\pi}{\sqrt{C}} \frac{x}{L} \right\} - \frac{u}{L} \left(1 - \frac{u}{L} \right) + \frac{x}{L} \right] \qquad 2.21a$$

where: $\dfrac{\overline{EA}}{EI} \cdot Z \cdot \dfrac{WL}{2}$ assumed unity for this plot.

$$F_L = \dfrac{\overline{EA}}{EI} \cdot Z \cdot \dfrac{WL}{2}\left[\dfrac{\sqrt{c}}{\pi}\left\{\left(\dfrac{Cosh\,\dfrac{\pi}{2\sqrt{c}}-Cosh\,\dfrac{\pi}{\sqrt{c}}\left(\dfrac{1}{2}-\dfrac{U}{L}\right)}{Sinh\,\dfrac{\pi}{2\sqrt{c}}}\right)Cosh\,\dfrac{\pi}{\sqrt{c}}\left(\dfrac{x}{L}\right)-Sinh\,\dfrac{\pi}{\sqrt{c}}\left(\dfrac{x}{L}\right)\right\}\right] \text{---}Eq.\,2.21a$$

$$F_R = \dfrac{\overline{EA}}{EI} \cdot Z \cdot \dfrac{WL}{2}\left[\dfrac{\sqrt{c}}{\pi}\left\{\left(\dfrac{1-Cosh\,\dfrac{\pi}{\sqrt{c}}\left(\dfrac{U}{L}\right)}{Sinh\,\dfrac{\pi}{2\sqrt{c}}}\right)Cosh\,\dfrac{\pi}{\sqrt{c}}\left(\dfrac{1}{2}-\dfrac{x}{L}\right)-\dfrac{U}{L}\left(1-\dfrac{U}{L}\right)+\dfrac{U}{L}\right\}\right] \text{---}Eq.\,2.21b$$

$X/L \longrightarrow$
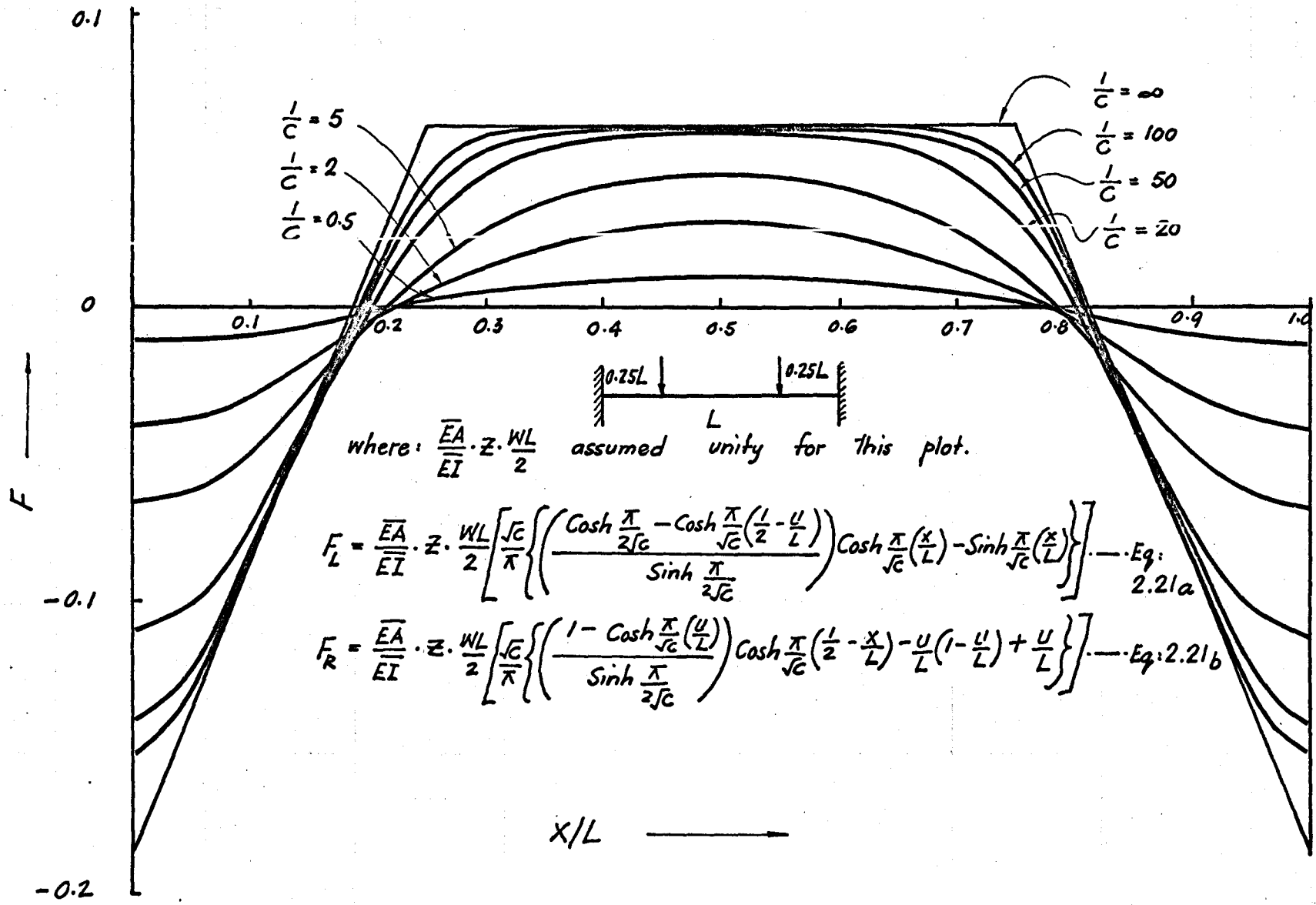
VARIATION OF INTERACTION FORCE — FIXED END BEAM

FIG. 2.10

$$q_L = \frac{\overline{EA}}{\overline{EI}} \cdot Z \cdot \frac{W}{2} \left\{ \left(\frac{\cosh \frac{\pi}{2\sqrt{c}} - \cosh \frac{\pi}{\sqrt{c}} \left(\frac{1}{2} - \frac{U}{L}\right)}{\sinh \frac{\pi}{2\sqrt{c}}} \right) \sinh \frac{\pi}{\sqrt{c}} \frac{x}{L} - \cosh \frac{\pi}{\sqrt{c}} \frac{x}{L} + 1 \right\} \quad \text{------} \quad Eq \ 2.24a$$

$$q_R = \frac{\overline{EA}}{\overline{EI}} \cdot Z \cdot \frac{W}{2} \left\{ - \left(\frac{1 - \cosh \frac{\pi}{\sqrt{c}} \frac{U}{L}}{\sinh \frac{\pi}{2\sqrt{c}}} \right) \sinh \frac{\pi}{\sqrt{c}} \left(\frac{1}{2} - \frac{x}{L}\right) \right\} \quad \text{------} \quad Eq \ 2.24b$$
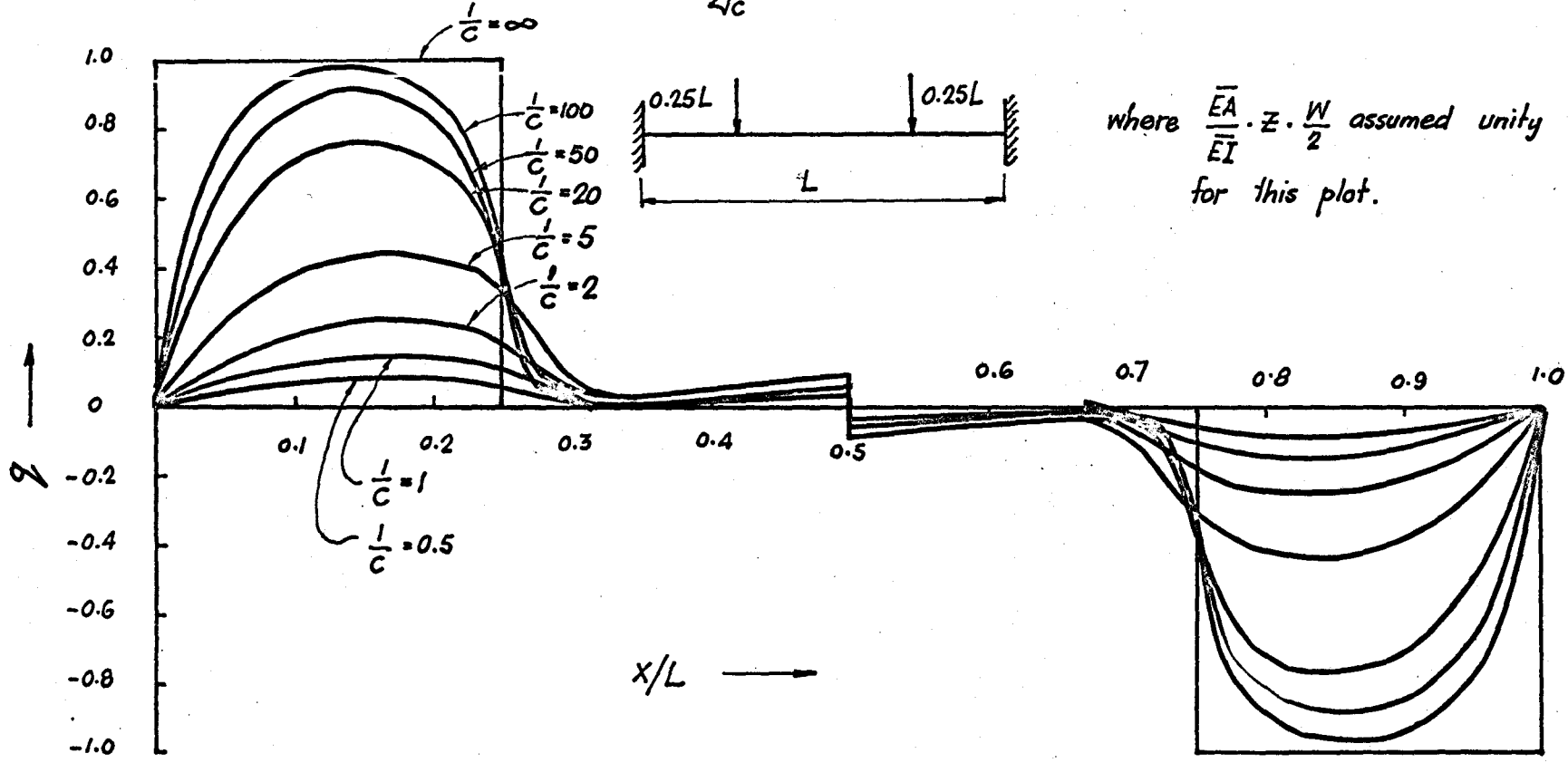
where $\dfrac{\overline{EA}}{\overline{EI}} \cdot Z \cdot \dfrac{W}{2}$ assumed unity for this plot.

VARIATION IN VALUE OF UNIT HORIZONTAL SHEAR — FIXED END BEAM

FIG. 2.11

$$F_R = \frac{\overline{EA}}{EI} \cdot z \cdot \frac{WL}{2} \left[\frac{\sqrt{C}}{\pi} \left\{ \left(\frac{1 - \text{Cosh} \frac{\pi}{\sqrt{C}} \frac{u}{L}}{\text{Sinh} \frac{\pi}{2\sqrt{C}}} \right) \text{Cosh} \frac{\pi}{\sqrt{C}} \left(\frac{1}{2} - \frac{x}{L} \right) \right\} \right.$$

$$\left. - \frac{u}{L} \left(1 - \frac{u}{L} \right) + \frac{u}{L} \right] \tag{2.21b}$$

For complete interaction, when $\frac{1}{C} = $ we have:

$$F_L' = \frac{\overline{EA}}{EI} \cdot z \cdot \frac{WL}{2} \left[- \frac{u}{L} \left(1 - \frac{u}{L} \right) + \frac{w}{L} \right] \tag{2.22a}$$

$$F_R' = \frac{\overline{EA}}{EI} \cdot z \cdot \frac{WL}{2} \left[- \frac{u}{L} \left(1 - \frac{u}{L} \right) + \frac{u}{L} \right] \tag{2.22b}$$

The degree of interaction, $\frac{F}{F'}$ for each range of x is:

$$\frac{F_L}{F_L'} = 1 + \frac{\sqrt{C}}{\pi} \cdot \frac{1}{\left[- \frac{u}{L} \left(1 - \frac{u}{L} \right) + \frac{x}{L} \right]} \left\{ \left(\frac{\text{Cosh} \frac{\pi}{2\sqrt{C}} - \text{Cosh} \frac{\pi}{\sqrt{C}} \left(\frac{1}{2} - \frac{u}{L} \right)}{\text{Sinh} \frac{\pi}{2\sqrt{C}}} \right) \text{Cosh} \frac{\pi}{\sqrt{C}} \frac{x}{L} \right.$$

$$\left. - \text{Sinh} \frac{\pi}{\sqrt{C}} \frac{x}{L} \right\} \tag{2.23a}$$

and

$$\frac{F_R}{F_R'} = 1 + \frac{\sqrt{C}}{\pi} \cdot \frac{1}{\left[- \frac{u}{L} \left(1 - \frac{u}{L} \right) + \frac{u}{L} \right]} \left\{ \left(\frac{1 - \text{Cosh} \frac{\pi}{\sqrt{C}} \frac{u}{L}}{\text{Sinh} \frac{\pi}{2\sqrt{C}}} \right) \cdot \text{Cosh} \frac{\pi}{\sqrt{C}} \left(\frac{1}{2} - \frac{x}{L} \right) \right\} \tag{2.23b}$$

The expressions for the horizontal shear force per unit length are derived from Eq. 2.6 as:

$$\frac{F_L}{F_L'} = 1 - \frac{\sqrt{c}}{\pi} \cdot \frac{\cosh \frac{\pi}{\sqrt{c}}\left(\frac{1}{2} - \frac{U}{L}\right)}{\frac{X}{L} \cdot \cosh \frac{\pi}{2\sqrt{c}}} \cdot \sinh\left(\frac{\pi}{\sqrt{c}} \frac{X}{L}\right) \text{ --- --- } Eq: 2.23a$$

$$\frac{F_R}{F_R'} = 1 - \frac{\sqrt{c}}{\pi} \cdot \frac{\sinh \frac{\pi}{\sqrt{c}}\left(\frac{U}{L}\right)}{\frac{U}{L} \cdot \cosh \frac{\pi}{2\sqrt{c}}} \cdot \cosh \frac{\pi}{\sqrt{c}}\left(\frac{1}{2} - \frac{X}{L}\right) \text{ --- --- } Eq: 2.23b$$
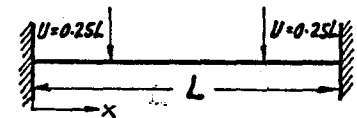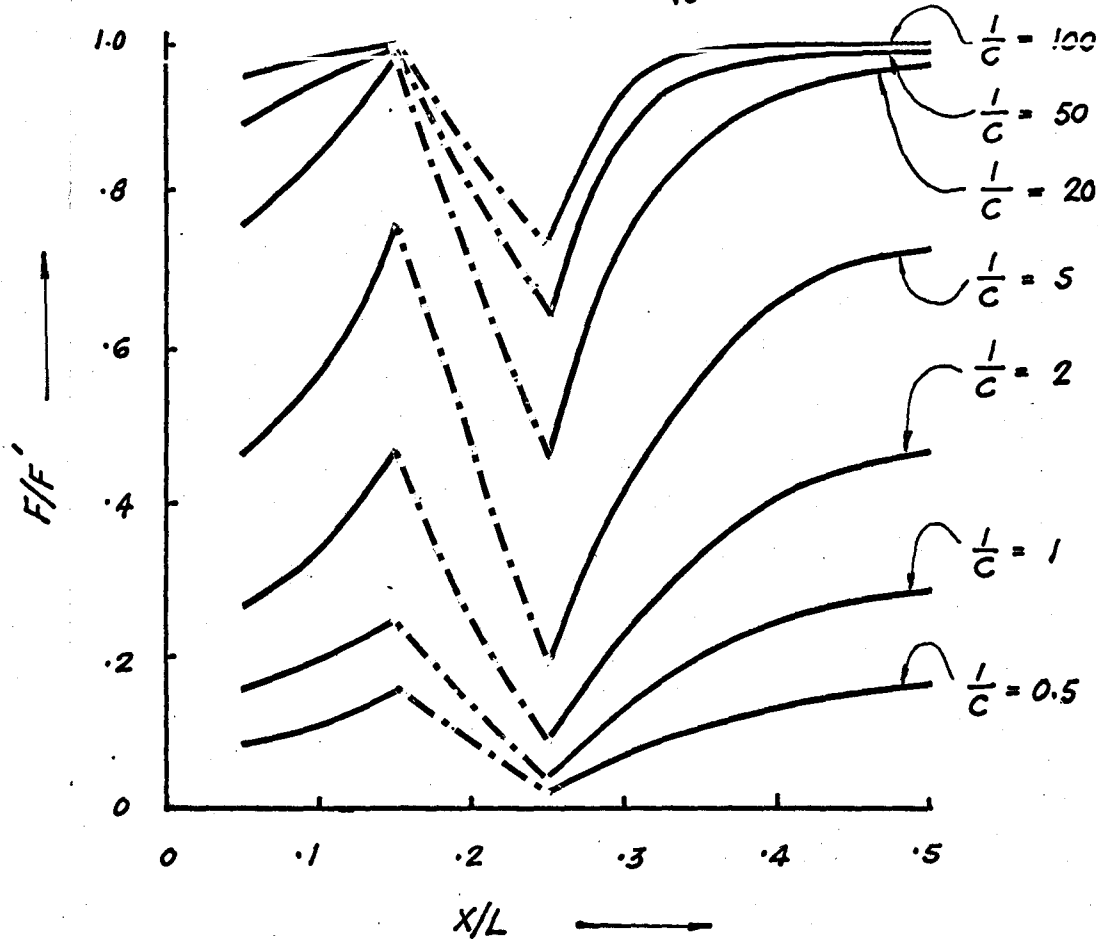
VARIATION IN DEGREE OF INTERACTION — FIXED END BEAM.

FIG . 2.12

$$q_L = \frac{\overline{EA}}{EI} \cdot z \cdot \frac{W}{2} \left\{ \left(\frac{\text{Cosh } \frac{\pi}{2\sqrt{C}} - \text{Cosh } \frac{\pi}{\sqrt{C}} \left(\frac{1}{2} - \frac{u}{L} \right)}{\text{Sinh } \frac{\pi}{2\sqrt{C}}} \right) \text{Sinh } \frac{\pi}{\sqrt{C}} \frac{x}{L} \right.$$

$$\left. - \text{Cosh } \frac{\pi}{\sqrt{C}} \frac{x}{L} + 1 \right\} \qquad 2.24a$$

and

$$q_R = \frac{\overline{EA}}{EI} \cdot z \cdot \frac{W}{2} \left\{ - \left(\frac{1 - \text{Cosh } \frac{\pi}{\sqrt{C}} \frac{u}{L}}{\text{Sinh } \frac{\pi}{2\sqrt{C}}} \right) \text{Sinh } \frac{\pi}{\sqrt{C}} \left(\frac{1}{2} - \frac{x}{L} \right) \right\} \qquad 2.24b$$

Plots showing variations of F, q, and $\frac{F}{F^T}$ along the length of a beam with point loads at quarter span, and for varying values of the interaction coefficient $\frac{1}{C}$, are given in Figs. 2.10, 2.11 and 2.12.

2.2.4 Case IV - Partially Fixed End Beam with Symmetrically
      Placed Two Point Loads - End Slip Restricted

Expressions for this case were obtained by using the following modified values of moment expression in Eq. 2.19 of case III:

$$M_{(x)} = - \mu \frac{Wu}{2L} (L - u) + \frac{W}{2} x \quad \text{for } 0 \leqslant x \leqslant u$$

and
$$\qquad\qquad\qquad\qquad\qquad\qquad\qquad\qquad\qquad\qquad 2.25$$

$$M_{(x)} = - \mu \frac{Wu}{2L} (L - u) + \frac{W}{2} u \quad \text{for } u \leqslant x \leqslant \frac{L}{2}$$

where μ defines degree of end fixity. For $\mu = 0$, case IV reduces to case II and for $\mu = 1$ it is case III.

The corresponding expressions for the degree of interaction $\frac{F}{F^T}$ are given by

$$\frac{F_L}{F_L{}'} = 1 + \frac{\sqrt{C}}{\pi} \cdot \frac{1}{\left[-\mu\frac{u}{L}\left(1-\frac{u}{L}\right)+\frac{x}{L}\right]} \left\{ \left(\frac{\text{Cosh}\frac{\pi}{2\sqrt{C}} - \text{Cosh}\frac{\pi}{\sqrt{C}}\left(\frac{1}{2}-\frac{u}{L}\right)}{\text{Sinh}\frac{\pi}{2\sqrt{C}}}\right)\text{Cosh}\frac{\pi}{\sqrt{C}}\frac{x}{L} \right.$$

$$\left. - \text{Sinh}\frac{\pi}{\sqrt{C}}\frac{x}{L}\right\} \qquad\qquad 2.26a$$

$$\frac{F_R}{F_R{}'} = 1 + \frac{\sqrt{C}}{\pi} \cdot \frac{1}{\left[-\mu\frac{u}{L}\left(1-\frac{u}{L}\right)+\frac{u}{L}\right]} \left\{ \left(\frac{1 - \text{Cosh}\frac{\pi}{\sqrt{C}}\frac{u}{L}}{\text{Sinh}\frac{\pi}{2\sqrt{C}}}\right) \cdot \text{Cosh}\frac{\pi}{\sqrt{C}}\left(\frac{1}{2}-\frac{x}{L}\right)\right\}$$

$$2.26b$$

2.2.5 Discussion of Loading Cases I to IV

The variation of the tensile force F in the steel reinforcement is given in Fig. 2.3, 2.6 and 2.10 for case I, II and III respectively. It can be observed that F = 0 at the free ends and maximum at mid span for case I. This could be expected, since the flexural strain is also maximum at the mid span. Comparing this with case II, it will be found that $F \neq 0$ at free end. This is because of the end anchorages. The effect of the end anchorage is more pronounced as the bond between the concrete and the steel reinforcement $(\frac{1}{C})$ diminishes. Case III exhibits maximum tension at the fixed ends.

Similarly, variation of the load per unit length, q, transmitted between the concrete and the steel reinforcement is given in Fig. 2.4, 2.7 and 2.10 for case I, II, and III respectively.

It can be noticed that in case I, where slip is permitted, the horizontal shear per unit length is maximum at the free ends and diminishes gradually towards the mid span. The value of the horizontal shear between the two point loads is smaller in cases of very high value of $\frac{1}{C}$ (= 100, 50) compared with the smaller values of $\frac{1}{C}$ (= 5.0 etc.)

In cases II and III, where the end slip is restricted, horizontal shear is zero at the ends, and the maximum value occurs at a place between the support and the load point, depending upon the value of $\frac{1}{C}$.

Comparatively in case III, a smaller value of horizontal shear per unit length has been observed between the two load points.

Fig. 2.5, 2.8 and 2.12 are the plots showing variation in the degree of interaction $\frac{F}{F'}$ for the case I, II and III respectively. All these cases show a drop in the degree of interaction under the load point.

Fig. 2.13 shows a comparison of $\frac{F}{F'}$ for case I and case II for $\frac{1}{C}$ = 5. The degree of interaction is generally higher in case II but near the supports it increases rapidly to a value in excess of unity. This reflects the effect of end anchorage (i.e. imposition of condition that $\frac{dF}{dx}_{\text{at } x=0, L}$ =0) and appears also in Fig. 2.6

It can also be noted that for very small values of $\frac{1}{C}$ (= 0.5) the distribution of F, the tension in the reinforcement in Fig. 2.6 is almost constant. This is in
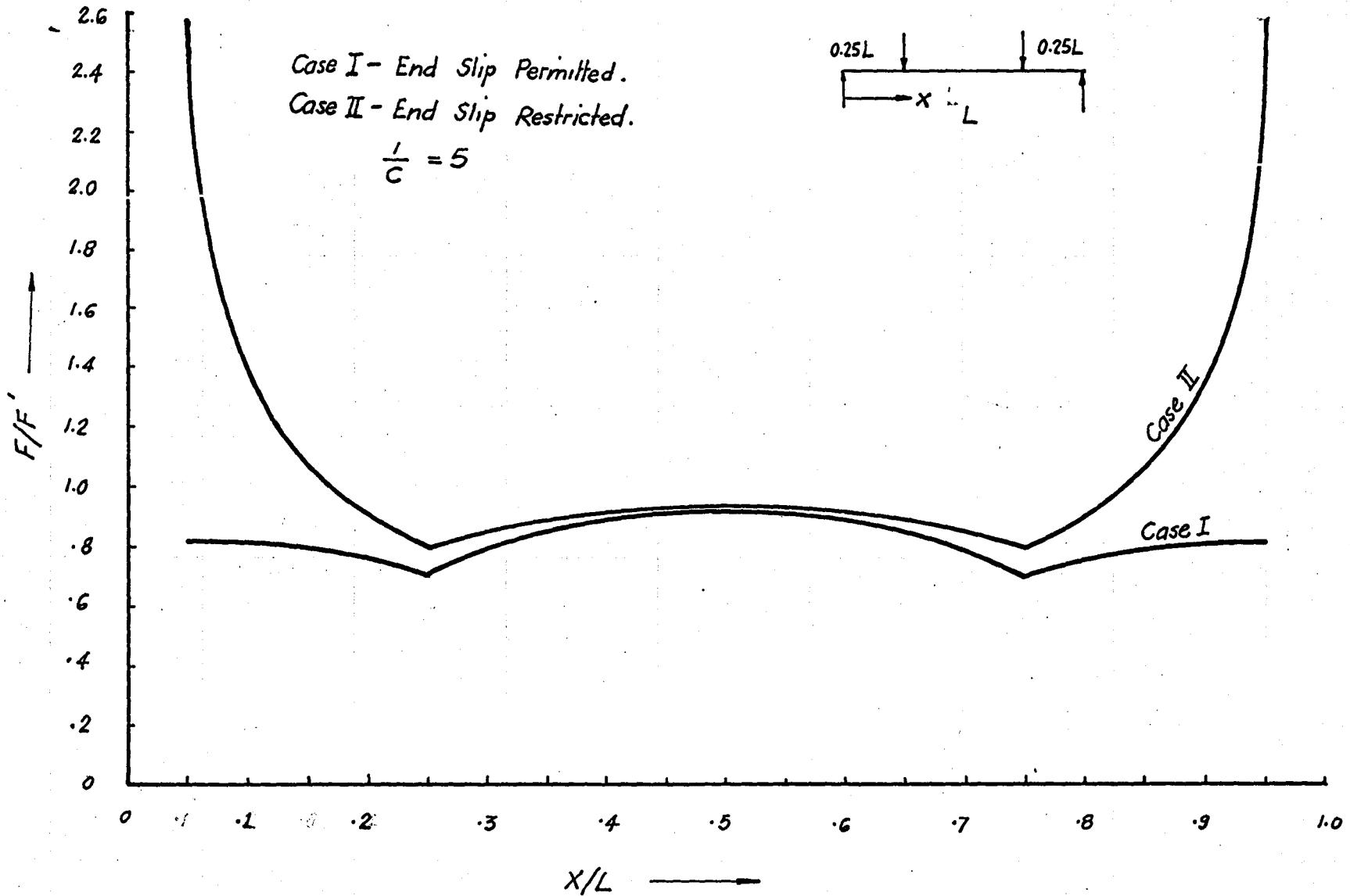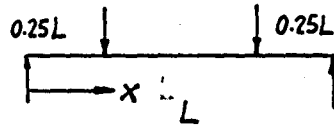
VARIATION IN F/F' - EFFECT OF RESTRICTION OF SLIP AT ENDS OF A BEAM.

FIG. 2.13

Case I - Ends Free

Case III - Ends Fixed

$$\frac{1}{C} = 5$$
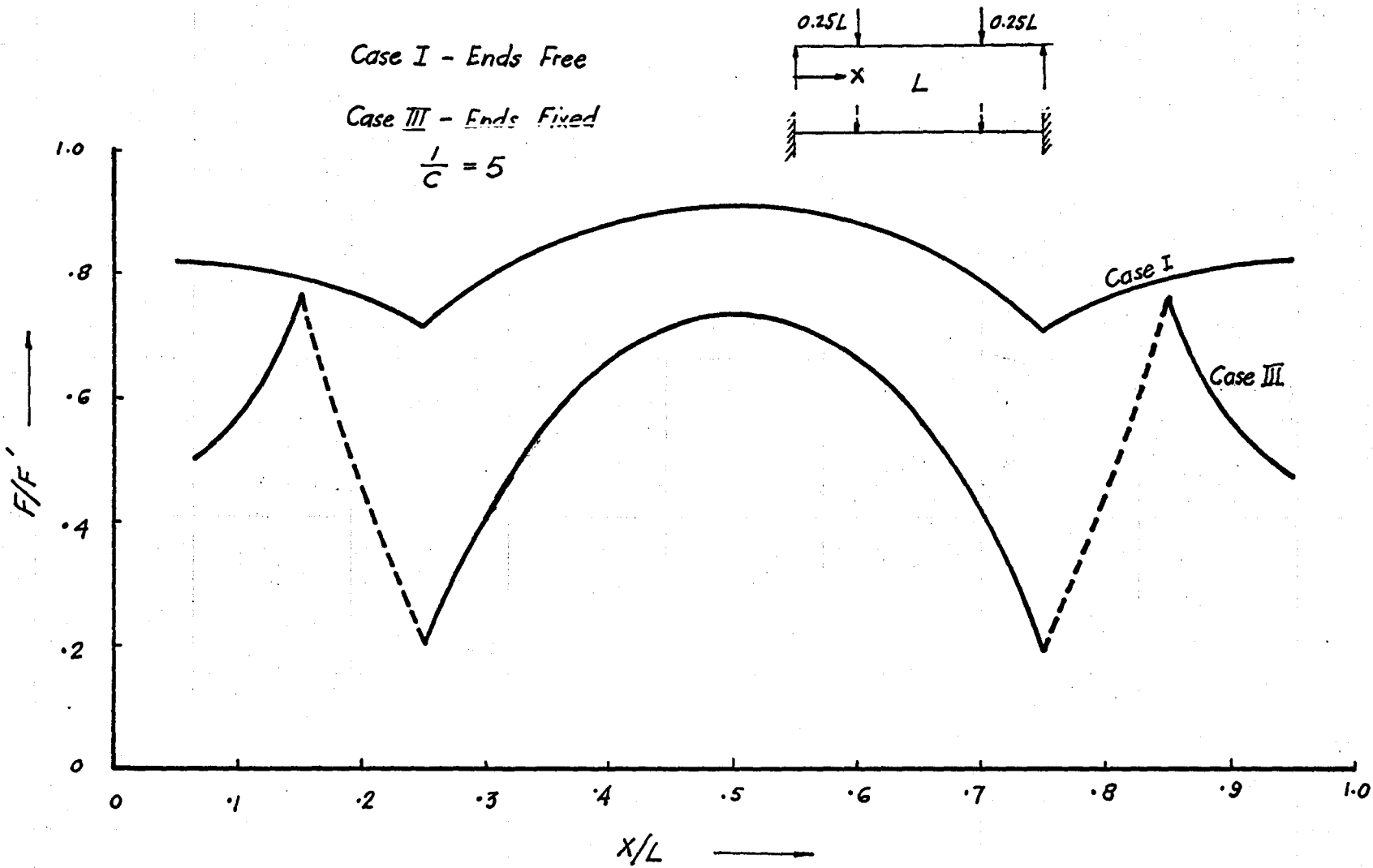
VARIATION IN F/F' - EFFECT OF FIXITY OF ENDS OF A BEAM.

FIG. 2.14

agreement with Kani's[7] findings that "the force in the reinforcement would remain constant with a beam without bond" but with an anchorage.

Fig. 2.14 shows similar plots for case I and case III. For a fixed end beam the $\frac{F}{F^T}$ distributions are generally lower than for the case of simple supports; however, near the point of contra flexure, values conforming to a continuous curve were not obtained, because of computational difficulties in the process of division of two small quantities.

Case III also exhibits a big drop in the value of $\frac{F}{F^T}$ at the fixed ends.

2.3   Interaction Coefficient $\frac{1}{C}$

The dimensionless parameter, the Interaction Coefficient;

$$\frac{1}{C} = \frac{k}{s} \cdot \frac{\overline{EI}}{\overline{EA\Sigma EI}} \cdot \frac{L^2}{\pi^2} = \frac{1}{\frac{1}{m}I_c + I_s} \cdot \frac{1}{E_s A_c} \cdot \frac{z}{y} \cdot \frac{L^2}{\pi^2} \cdot \frac{k}{s} \qquad 2.27$$

was introduced by Newmark et al[3], in the development of the theory for incomplete interaction of composite beams. It is a measure of the degree of interaction between the concrete and the reinforcing steel. Variations in the magnitude of $\frac{1}{C}$ can be considered to represent various accumulative effects of slip between the concrete and steel reinforcement, and deformation of the "concrete teeth".

It can be seen, however, that the magnitude of $\frac{1}{C}$ and hence the loss of interaction in a reinforced concrete beam is significantly influenced also by the geometric properties of the R.C. beam in addition to the bond-slip characteristic k. The effect on $\frac{1}{C}$ of the variation of one parameter at a time and two parameters simultaneously is demonstrated in Fig. 2.15 and 2.16. It should be noted that variation in the geometrical properties can have as significant an effect upon the degree of interaction as a change in the bond-slip modulus k.

2.3.1 Influence of Variation of a Single Parameter

a) Width or depth:

If the length of a beam, percentage of steel and k is kept constant and either width or depth of the section is increased, the value of $\frac{1}{C}$ decreases parabolically, see Fig. 2.15. Decrease in the strength of a beam with increase in depth was also observed experimentally by Kani[22], (see Fig. 2.15a) and Leonhardt and Walther[4]. Decrease in strength due to increase in width, has not been demonstrated experimentally. On the contrary, Kani[22] observes no significant change in the strength by increasing the width. Although it has been shown in Fig. 2.15 that decrease in the interaction coefficient $\frac{1}{C}$ results from increase in depth, the range of $\frac{1}{C}$ which has been shown in this thesis to have significant effect on the performance of a beam is between

For Geometrical Ratio of unity assumed value of $1/c = 100$.

Variation of a single parameter.

Width or depth (p const.)

Geomet. Similar Beam

Percentage steel

Length (p const.)

Geometrical Ratio

Value of $1/c$ ⟶
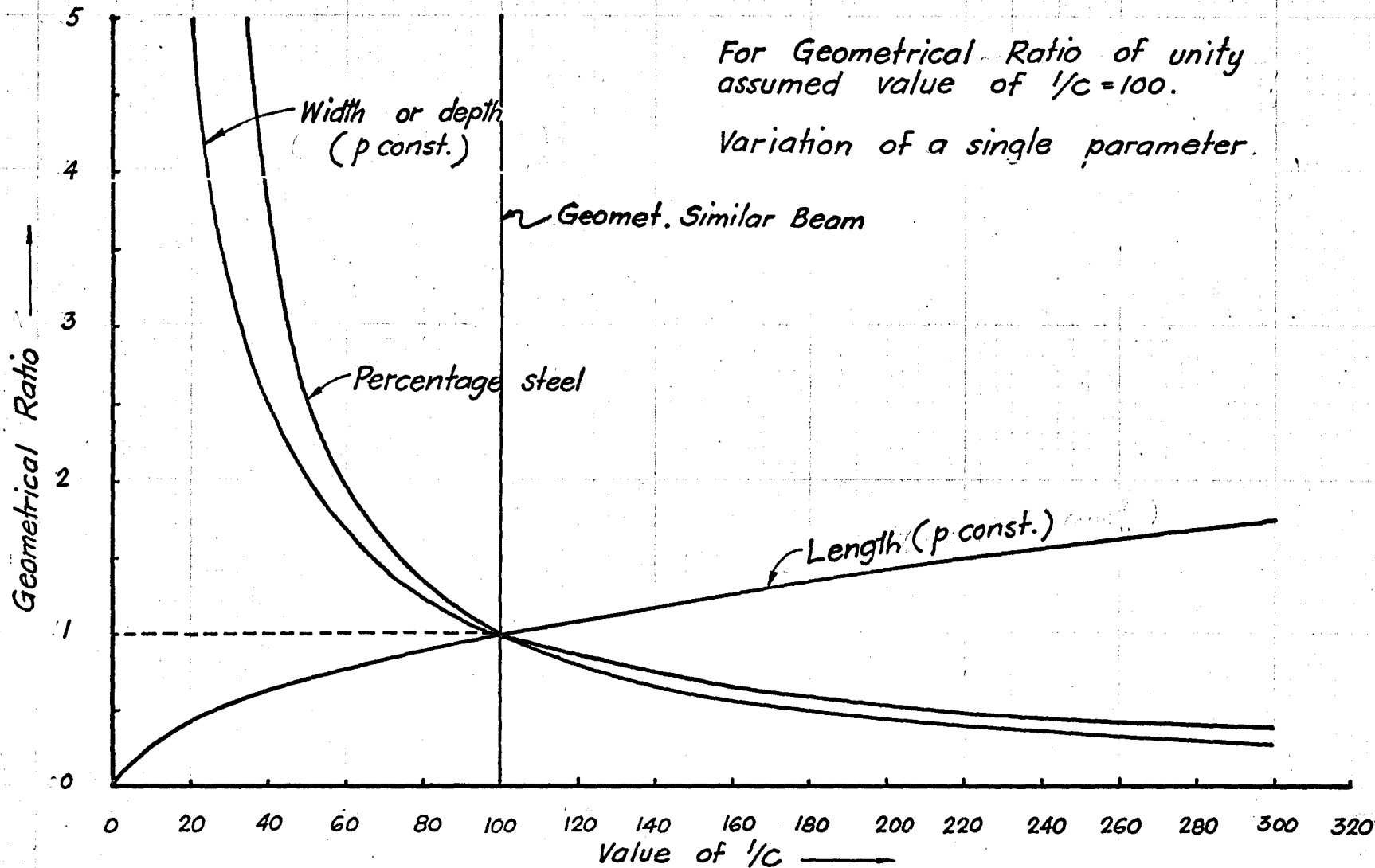
EFFECT OF GEOMETERY OF A BEAM ON VALUE $1/c$.

FIG. 2.15

$$\frac{1}{C} = 0 - 50.$$

b) Length:

If the cross-section of a reinforced concrete beam is kept constant and only the length of the beam is varied it will be found that $\frac{1}{C}$ increases with the square of the length. On close examination of the strength of the beams tested by Kani[19,22] (fig. 2.15b), this fact could also be established, however, the effect of the length was not so pronounced as found theoretically.

c) Percentage of Steel:

Similarly, if all the other parameters are kept constant and only the percentage of steel is varied, the value of $\frac{1}{C}$ decreases with an increase in p. Kani[19] reported a similar reduction in the relative beam strength. The results of his tests, in which $\frac{u}{d}$ ratio ranges between 1 and approximately 6.5, show that for p = 0.5 there was practically no loss in the relative beam strength; however for p = 2.80, a loss of up to 50% was indicated. (See Fig. 5.6, Chapter V.)

d) Geometric Similarity:

It has been found from the computations that varying depth, width, length and the area of the reinforcement simultaneously such that the geometric similarity is maintained, does not vary the value of $\frac{1}{C}$.
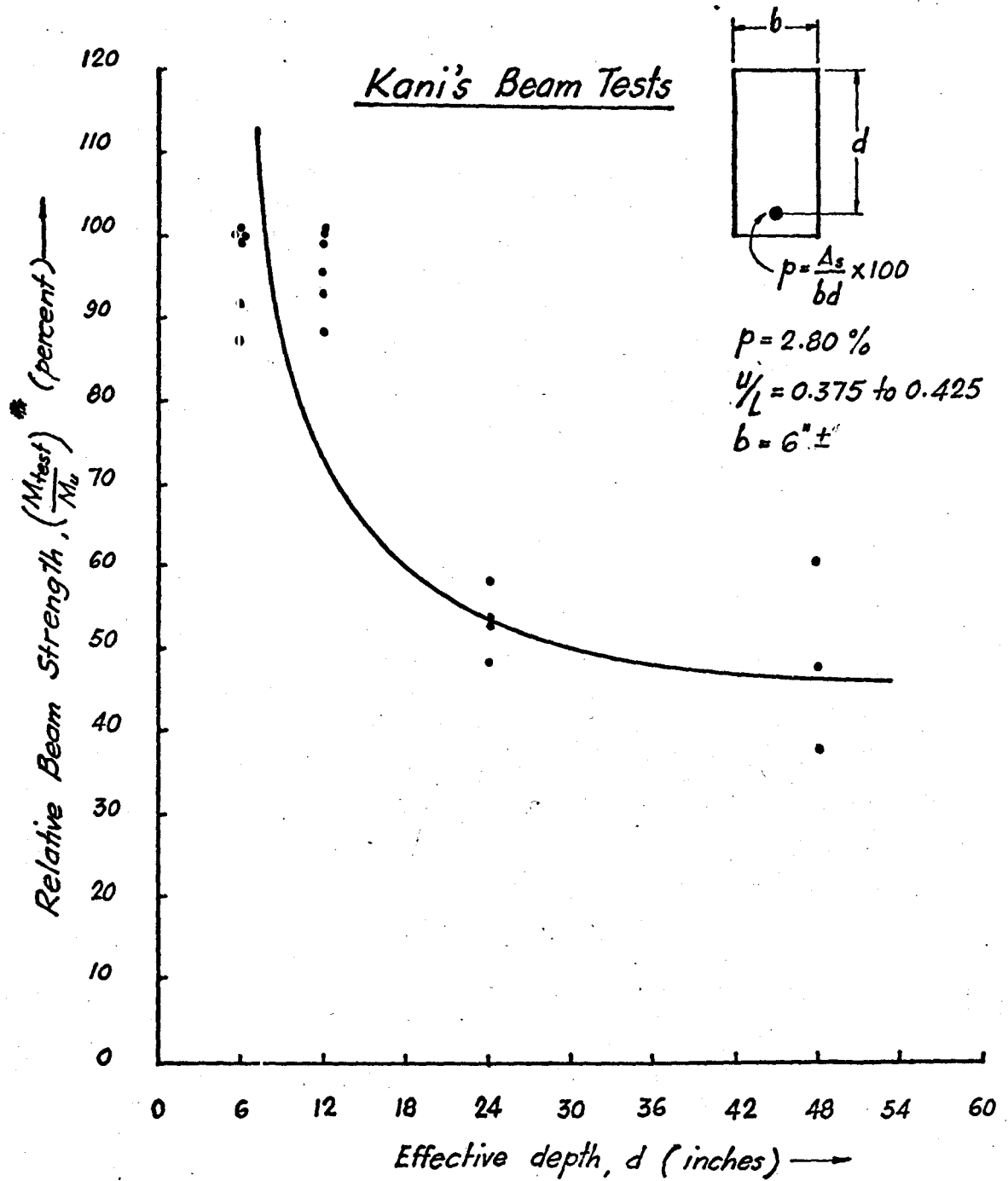
Influence of beam depth on Relative Beam Strength

FIG. 2.15a
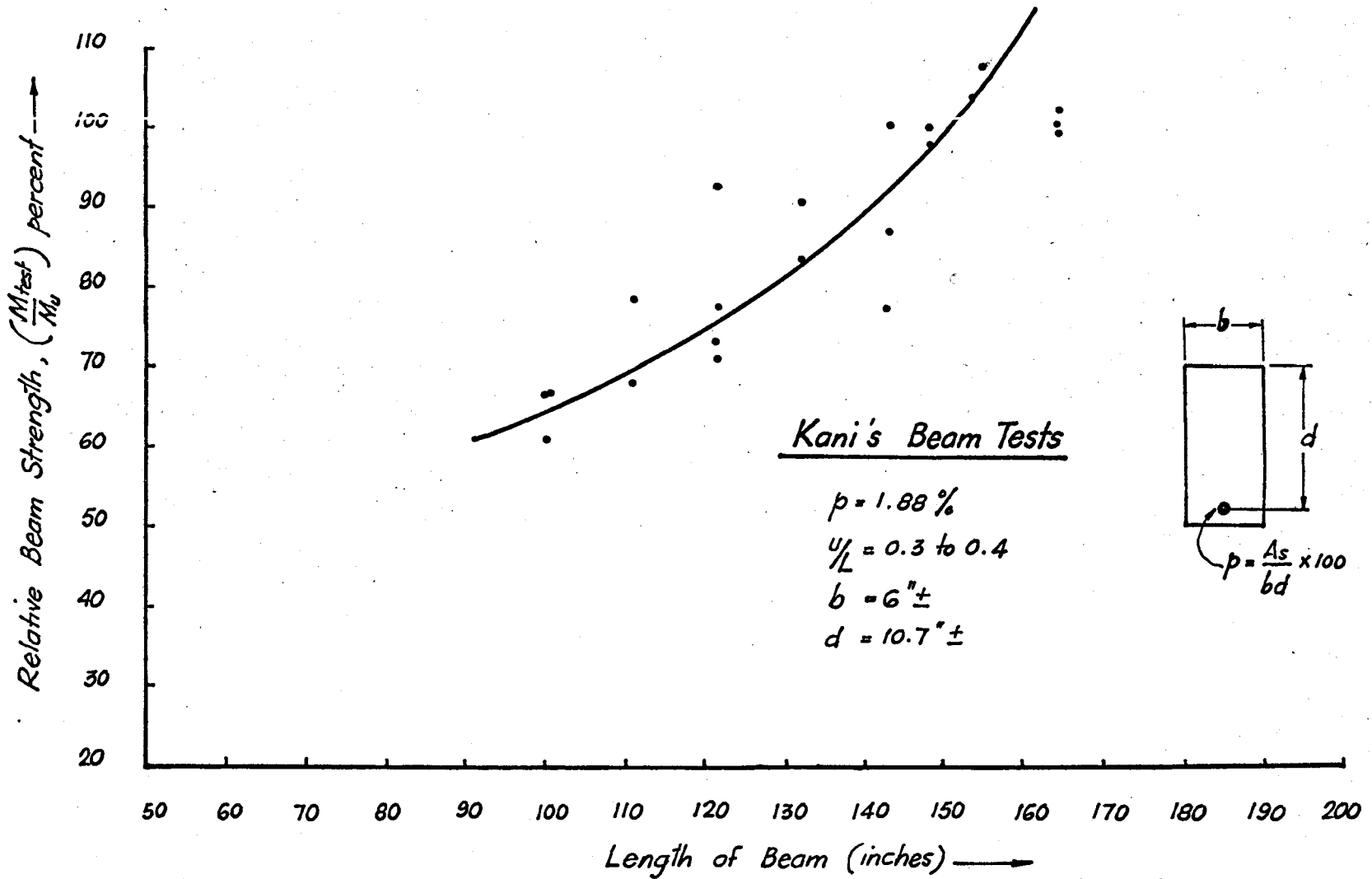
Influence of Length on the Relative Beam Strength.

FIG. 2.15b.

Kani's Beam Tests

$p = 1.88\%$

$u/L = 0.3$ to 0.4

$b = 6'' \pm$

$d = 10.7'' \pm$

$p = \dfrac{A_s}{bd} \times 100$

41

2.3.2 Influence of Variation of Two Parameters

Fig. 2.16 shows that the value of $\frac{1}{C}$ decreases parabolically with increase in either the depth-percentage of steel, width-percentage of steel, or the depth-width ratio in a reinforced concrete beam. The effect of the depth-percentage of steel and width-percentage of steel ratios are exactly similar, where the effect of depth-width ratio is comparatively lower.

The value of $\frac{1}{C}$ increases linearly with increase in either depth-length or width-length ratio. Similarly, the value of $\frac{1}{C}$ also increases with an increase in the length-percentage of steel, but this increase is non-linear.

2.4 Influence Lines for $\frac{F}{F^T}$

From the distribution of the degree of interaction, $\frac{F}{F^T}$ along the length of a beam, the investigation was extended to study the effect of the location of the load point on $\frac{F}{F^T}$. The purpose was to make a comparison of the breakdown in interaction for various ratios of $\frac{u}{L}$ (or $\frac{u}{d}$) with the relative beam strengths determined experimentally by Kani[10], and Leonhardt and Walther[4]. It should be noted that although the influence lines for $\frac{F}{F^T}$ are for the uncracked beam, the general trends of the curves give an indication of the relative efficiency of a beam with variation in the shear span, Fig. 2.17, 2.18a and b, and Fig. 2.19.
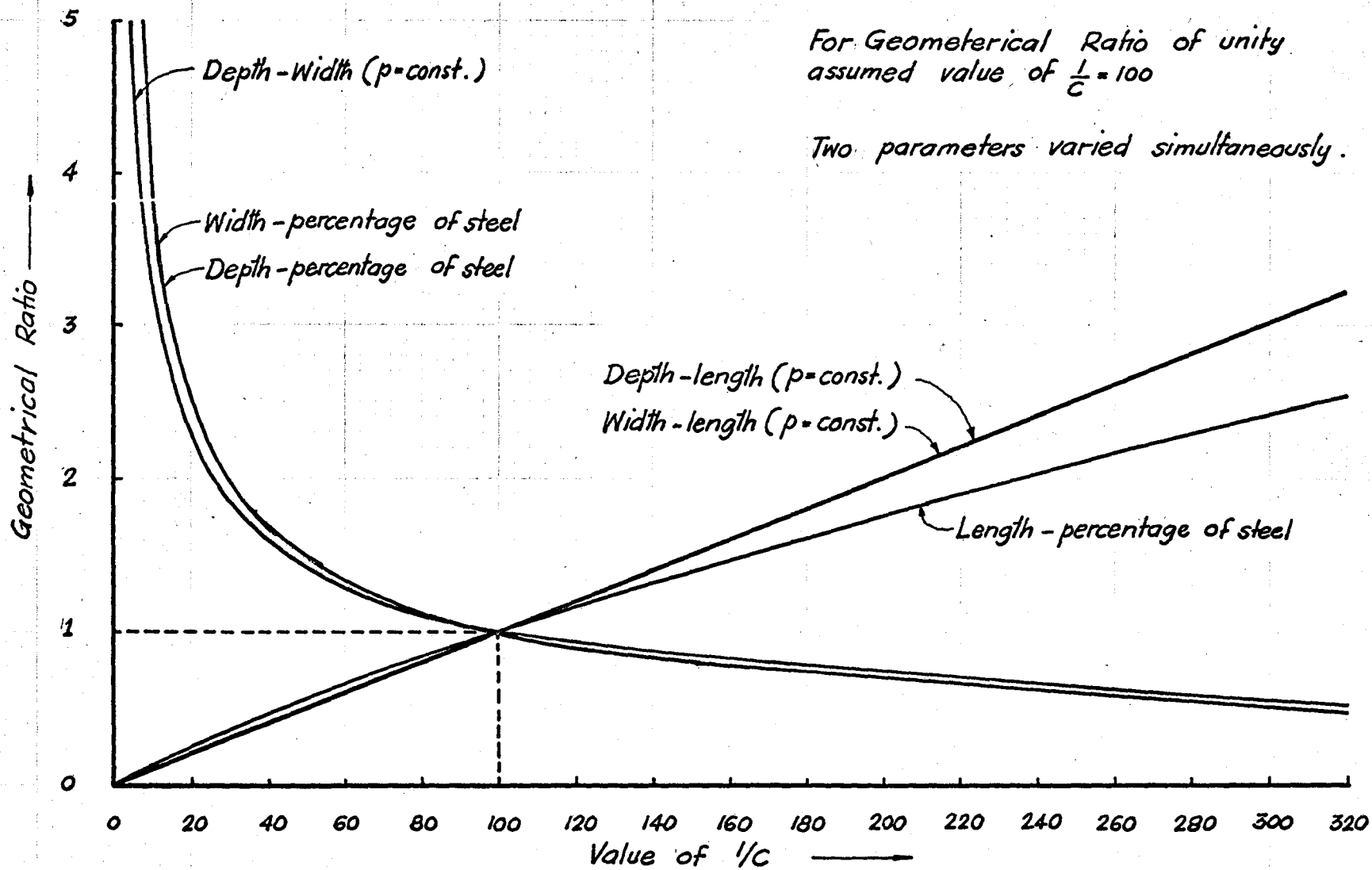
EFFECT OF GEOMETERY OF A BEAM ON VALUE OF $^1/c$.

FIG. 2.16

2.4.1 Simply Supported Beam with Symmetrically Placed Two
       Point Loads

As a first attempt a simply supported beam with
symmetrically placed two point loads was considered, and
computations for $\frac{F}{F_T}$ were carried out under the load point
for intervals of $\frac{u}{L} = 0.05$ and for values of $\frac{1}{C} = 100$, 50,
20, 5, 2, 1 and 0.5.

The results obtained are shown in Fig. 2.17. All
the curves have the same general shape and indicate higher
degree of interaction in the range of $\frac{u}{L}$ between 0.375 to
0.450 decreasing gradually outside this range on each side.
The breakdown in interaction is more pronounced as the load
points approach the supports. The degree of interaction
decreases as the shear span reduces. Similar trends were
demonstrated by Kani[10] in experiments on a large number of
beams. In his tests a decrease in the relative beam
strength was observed by decreasing the shear span ratio $\frac{u}{d}$
to approximately 2.5. However, with further reduction of
the shear span the experimental results gave an increase in
the relative beam strength.

2.4.2 Simply Supported Beam with Symmetrically Placed Two
       Point Loads - End Slips Restricted

In the case of a simply supported beam with two point
loads (case I), the computed variations of horizontal shear
per unit length, q, indicate that maximum slip occurs at the
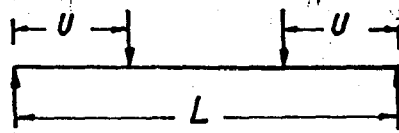
END SLIP PERMITTED
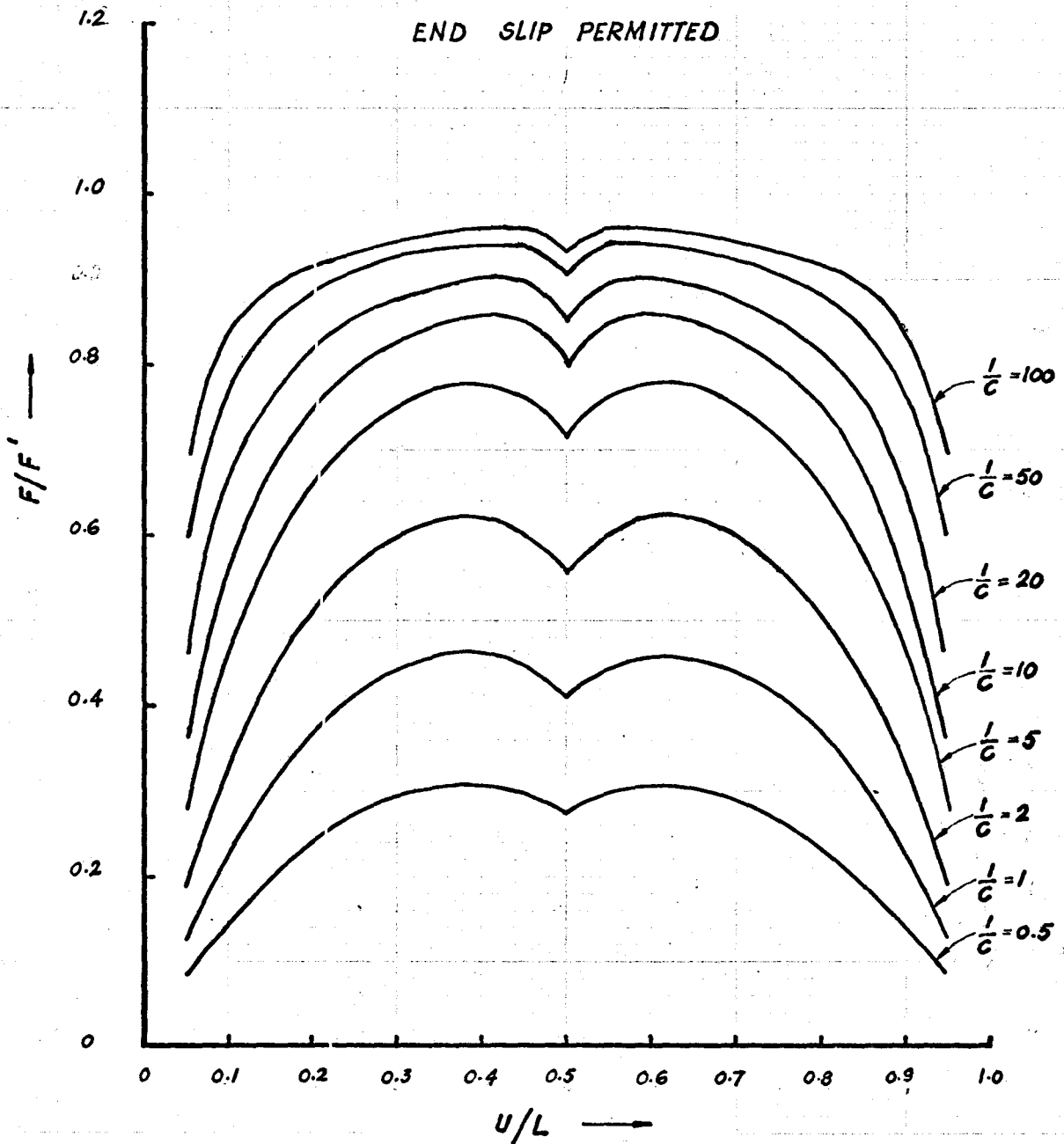
INFLUENCE LINES FOR DEGREE OF INTERACTION, F/F'.

FIG. 2.17

ends of beam, Fig. 2.4; however, in Kani's test beams, the reinforcement was anchored at each end of all the beams by means of bolt and anchor plate. This prevented slip at the ends of the beams. The previous case, (case I), was modified by imposing a boundary condition of $(\frac{dF}{dx}) = 0$, $x = 0$, and $x = L$, i.e. that there is no slip permitted at the ends of the beam. Solutions were obtained for F, q, and $\frac{F}{F'}$ as given in section 2.4.2, Figs. 2.6, 2.7 and 2.8. Computations for the influence lines for $\frac{F}{F'}$ were carried out for $\frac{1}{C} = 100$, 50, 20, 5, 2, 1 and 0.5 and the results are shown in Fig. 2.18a and b.

About the influence of bond on the strength of a beam, Kani[10] wrote, "For two beams, identical in every respect except bond resistance, the one with poor bond, and therefore large Δx (i.e. width between two cracks), will have a higher load carrying capacity than the beam with good bond. The surprising result is: the better the bond the lower the diagonal load-carrying capacity."

He further discussed the test beams, described by Leonhardt and Walther[4] and demonstrating this point he stated: "The beams with poor bond carried at least 31 percent more load than the corresponding beams with deformed bars. The beams with poor bond reached their flexural failure, while the beams with deformed bars stayed far below their full flexural capacity." These comments pertain to
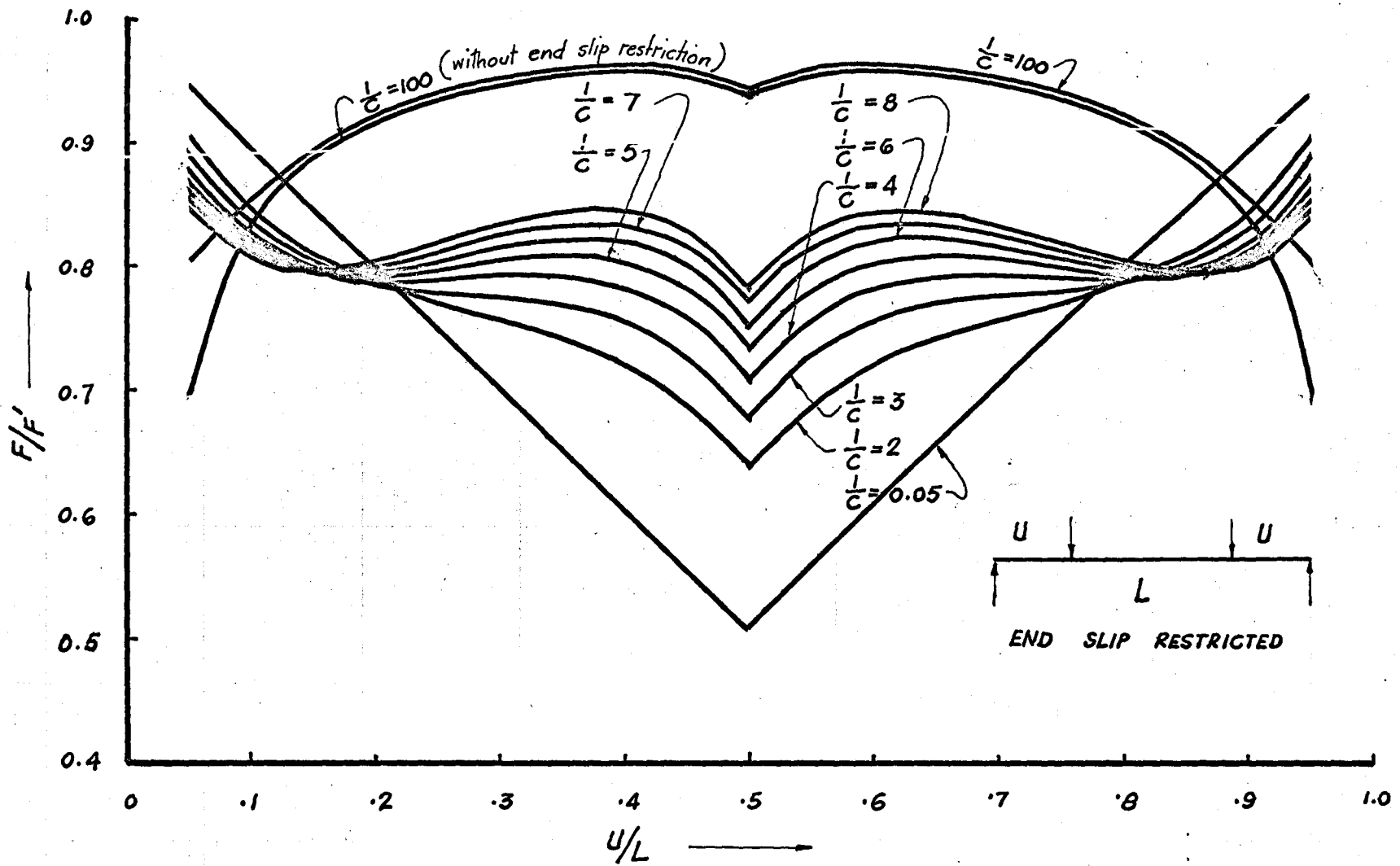
INFLUENCE LINES FOR DEGREE OF INTERACTION, F/F'.

FIG. 2.18 (a)
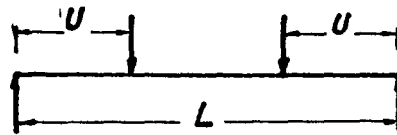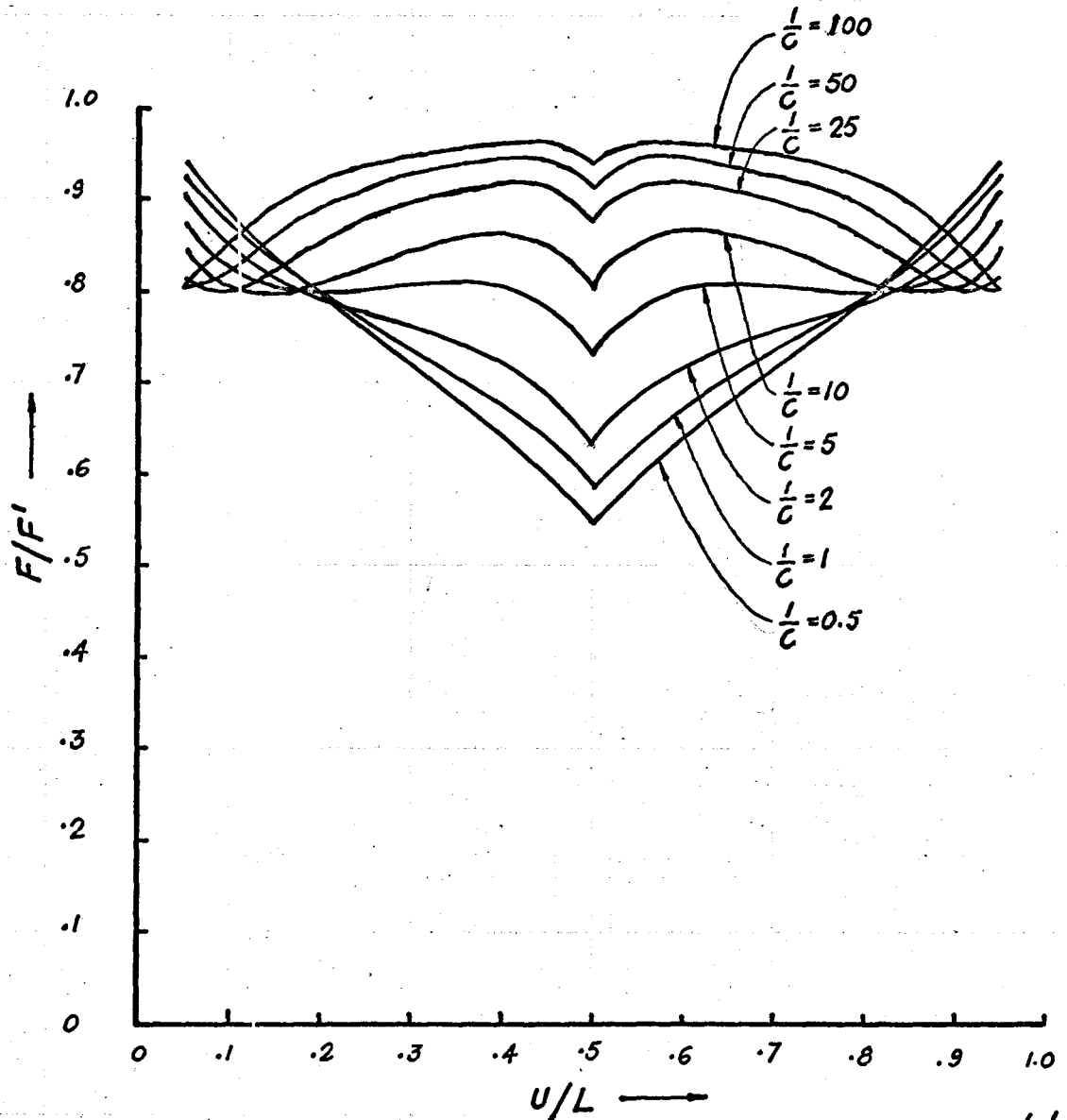
INFLUENCE LINES FOR DEGREE OF INTERACTION, F/F'.

FIG. 2.18(b)
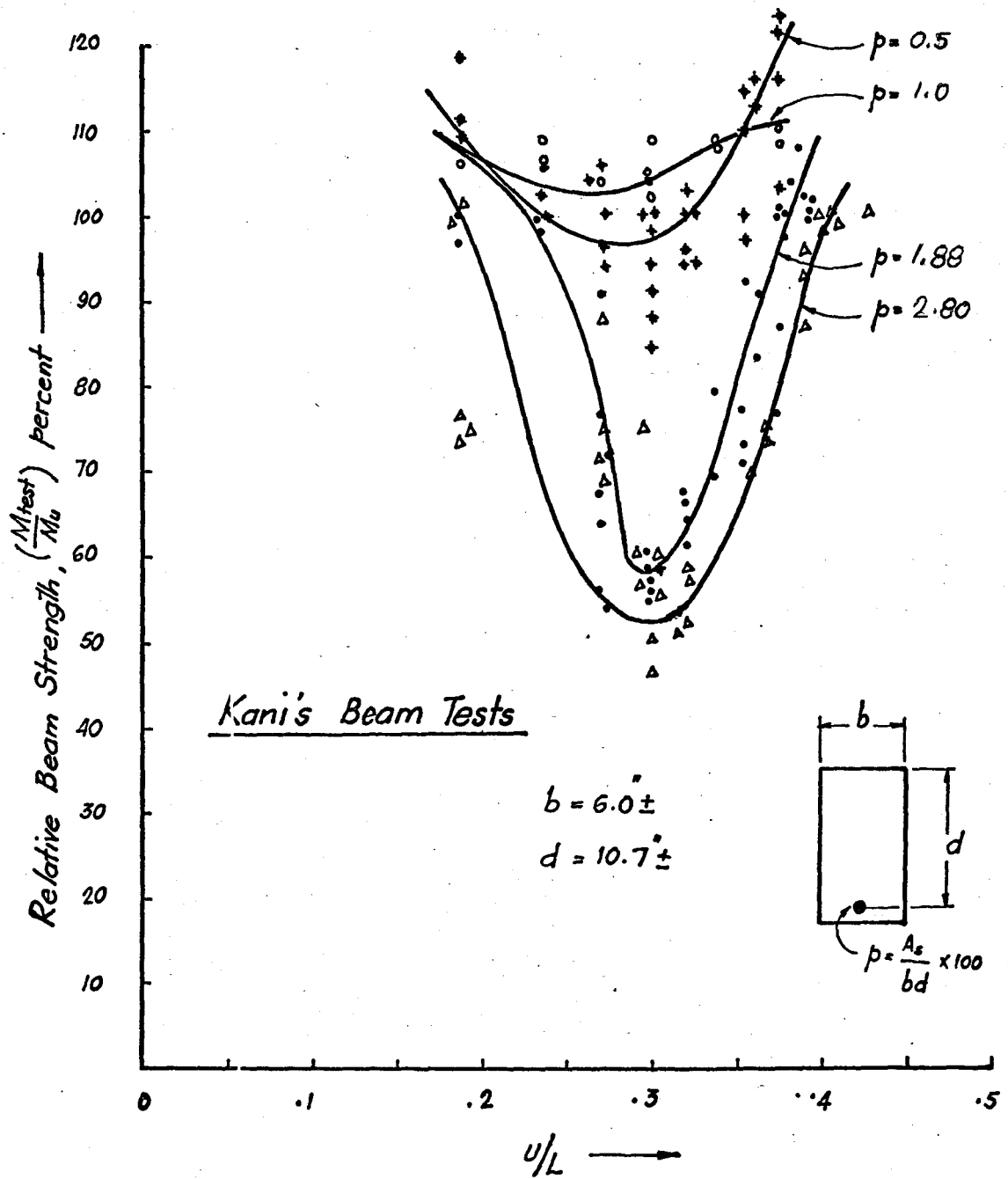
Influence of $^{v}/_{L}$ on Relative Beam Strengths.

FIG. 2.19

2.4.3   Fixed End Beam with Two Symmetrically Placed Point

   Load

   This is an extreme case because in addition to zero

slip at the ends of beam, there are also moments due to end

fixity.   The influence lines for $\frac{F}{F^r}$ are shown in Fig. 2.20.

It can be seen that the $\frac{F}{F^r}$ values are very high near the

supports and depending upon the value of $\frac{1}{C}$, they rapidly

drop off to zero between a range of $\frac{u}{L}$ = 0.10 to 0.25.   After

this range their magnitude increases again gradually towards

the mid span, showing a small drop where both point loads

approach mid span.   It should be noted that values of $\frac{F}{F^r}$ in

this case are generally lower than the previously considered

two cases.   (Figs. 2.17 and 2.18a and b.)
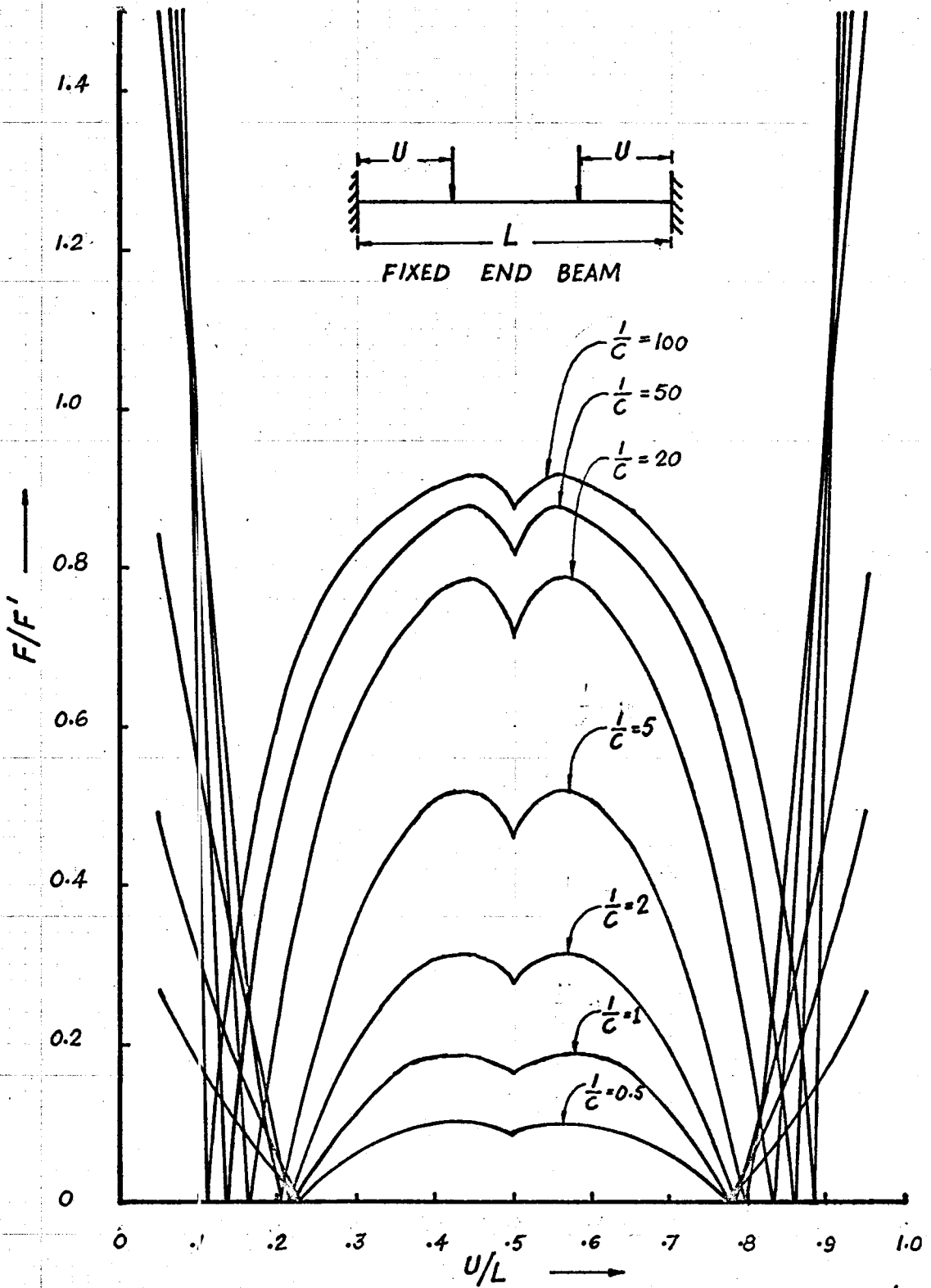
INFLUENCE   LINES   FOR   DEGREE   OF   INTERACTION, F/F'

CHAPTER III

FLEXURAL CRACKING

3.1 Development of a Flexural Crack

In addition to the assumptions made in Chapter II, it is assumed here that the concrete is capable of withstanding flexural tensile strain to some limiting value. If the computed flexural tension strain, ε_{cb} exceeds this critical (or limiting) value, ε_{cr} at any section of the beam, a flexural crack will develop and will extend into the beam until equilibrium between the internal forces and moments, and the applied moment is obtained, and the actual tensile strain ε_{cb} is at the value of the critical strain, ε_{cr}.

From the geometry of the strain distribution across the depth of a reinforced concrete beam, Fig. 3.1, the following can be written:

$$C_h = 2H \ \frac{\varepsilon_{cb} - \varepsilon_{cr}}{\varepsilon_{cb} + \varepsilon_{ct}} \qquad\qquad 3.1$$

where C_h is the first increment in the crack height, and its value can be computed by finding ε_{cb} and ε_{ct} from Eq.2.3 and a knowledge of ε_{cr}. Therefore the remaining uncracked depth of concrete will be

$$2H' = 2H - C_h \qquad\qquad 3.2$$

This value of 2H' can be re-used in Eq.3.1 to work out the successive increments of a developing crack, until

53
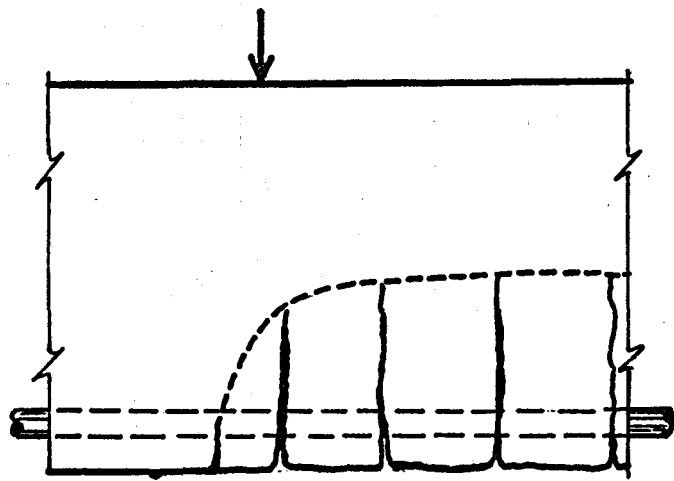
a) Longitudinal Section of a
   Cracked Beam
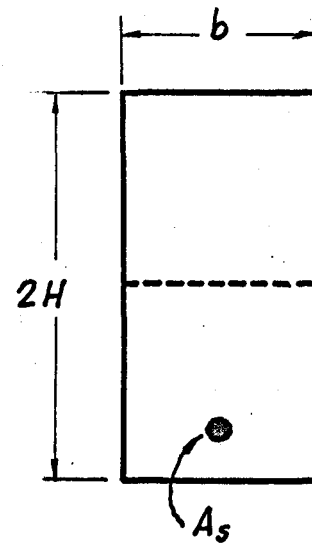
b) Cross-Section
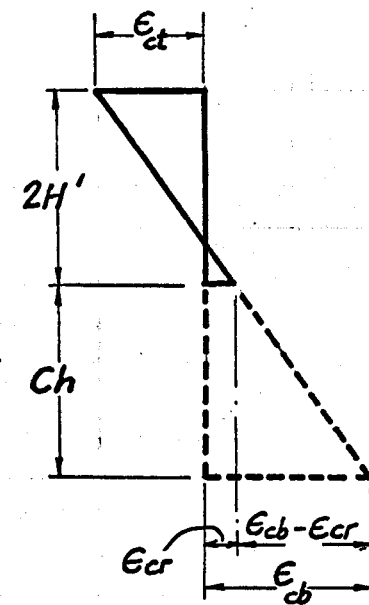
c) Strain Distribution

DEVELOPMENT OF A FLEXURAL CRACK

FIG. 3.1

finally a stage of equilibrium is achieved. The height of a fully developed crack, therefore, can be given by

$$C_{ch} = \sum_{1}^{n_o} C_h \quad \text{where at } n_o \begin{cases} \& C_h = 0 \\ \varepsilon_{cb} = \varepsilon_{cr} \end{cases} \qquad 3.3$$

3.1.1 Flexural Crack under a Load Point

The dimensions of the typical R.C. beam considered in this thesis has the dimension of that tested by Plowman and reported in reference number 8.

It has a concrete cross-section 4" wide x 8.5" deep, with a single $\frac{5"}{8}$ diameter, mild steel reinforcing bar located at an effective depth of 7". No stirrups are used. The span of the beam is 90", simply supported and carrying two symmetric point loads each at a distance of 29.25" from either of the supports. The modulus of elasticity of the concrete and the steel is assumed to be 3.5×10^6 psi and 30×10^6 psi respectively. The beam carries a design moment of 36200.0 lb-in.

Since these dimensions were used in most parts of this report, the beam will be referred to as "Typical Beam".

The concrete is assumed to be capable of withstanding a flexural tensile strain of 100 micro inches per inch. Strains in excess of 100 m "/" will cause cracking.

3.1.2 Equations 3.1, 3.2 and 3.3 were used to derive an iterative technique for computing the crack height under the load point in the "Typical Beam". This was done for

VARIATION OF M_c, F' AND ε_{cb} AS CRACK DEVELOPS.

FIG. 3.2

$4''$

$7.0''$ $8.5''$

$A_s = 0.31 \, \square''$

$U = 29.25''$ $U = 29.25''$

$L = 90.0''$
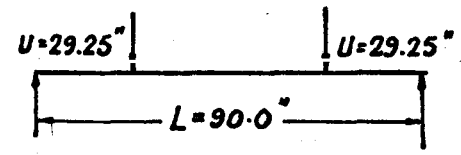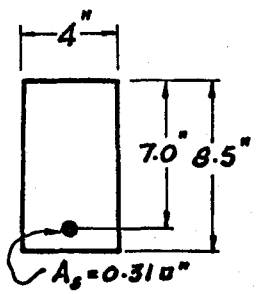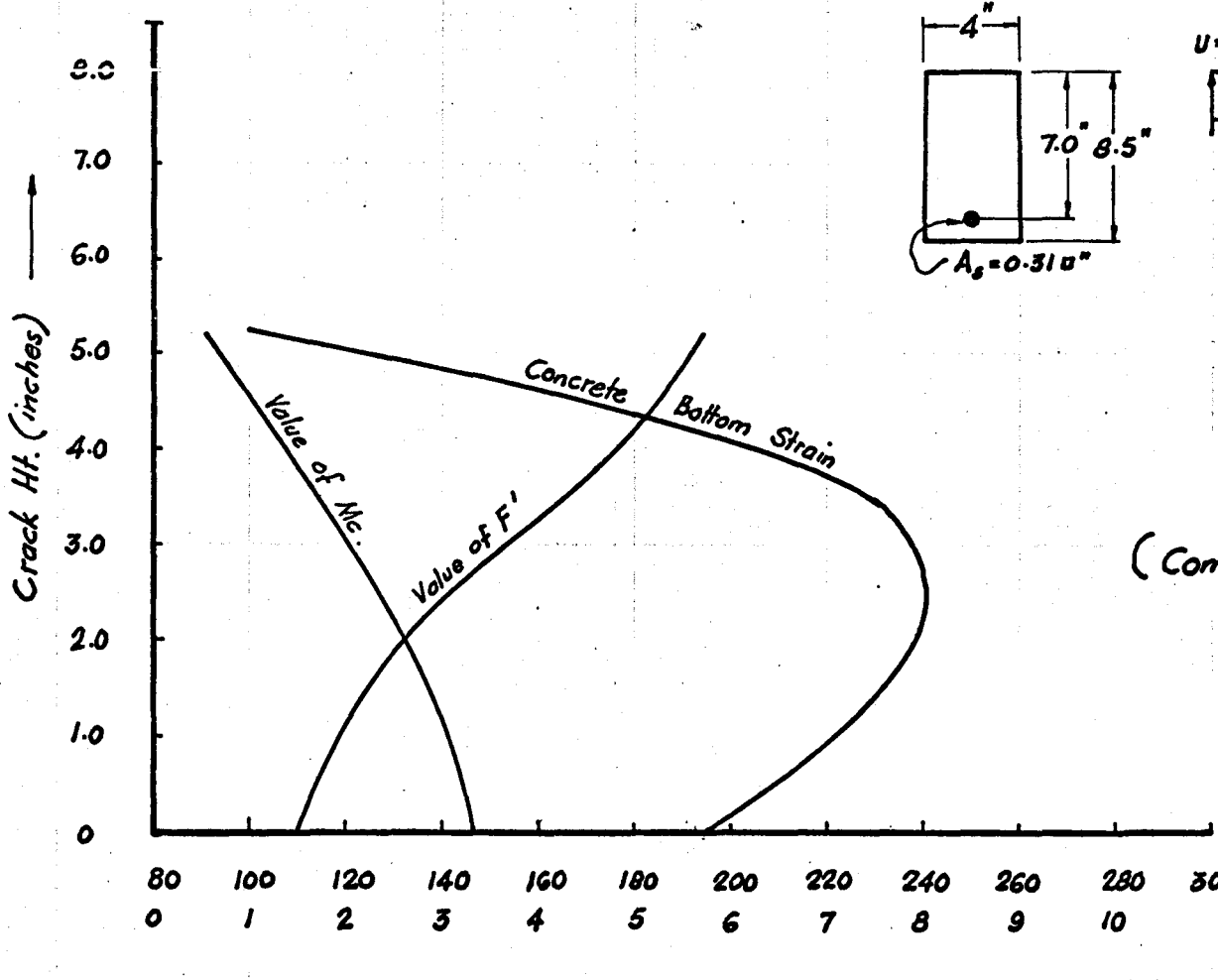
$E_c = 3.5 \times 10^6 \; psi$

$E_s = 30 \times 10^6 \; psi$

$\varepsilon_{cr} = 100 \; mic \; in/in$

$M_t = 36,200 \; lb\text{-}in$

$M_t = M_c + M_s + F' \cdot z$

(Complete Interaction Case)

Crack Ht. (inches)

8.0, 7.0, 6.0, 5.0, 4.0, 3.0, 2.0, 1.0, 0

Value of M_c

Value of F'

Concrete Bottom Strain

80 100 120 140 160 180 200 220 240 260 280 300 $\times 10^{-6} \; in/in \; \varepsilon_{cb}$

0 1 2 3 4 5 6 7 8 9 10 $\times 10^3 \; F' \; lbs$

$\times 10^4 \; M_c \; lb\text{-}in$

56

the cases of complete interaction ($\frac{1}{C} = \infty$) as well as for incomplete interaction ($\frac{1}{C} = 100,50,25,10,5,2,1$ and 0.5). It is assumed that k remains constant. Its value will depend on the choice of $\frac{1}{C}$ at the start of the computation. As the flexural crack develops the cross-section of the concrete diminishes. Assuming that k remains constant, the value of $\frac{1}{C}$ will change due to the change in the concrete cross-section.

During the iteration process, the values of $\frac{1}{C}$ were found to increase due to the change in the geometry of the cross-section. This in turn affected the degree of inter-action $\alpha = \frac{F}{F'},$ causing variations in the quantities such as the concrete top fibre strain ε_{ct}, interaction force F, and the moments in the steel, M_s, and concrete, M_c. The varia-tion of these parameters are shown in Fig. 3.2 and Fig. 3.3.

Curves showing variations in values of ε_{cb}, $\frac{1}{C}$, M_c and F for several initial values of $\frac{1}{C}$ are given in Figs. 3.4 to 3.7.

It is evident from these curves that the choice of $\frac{1}{C}$ value for these analytic computations has a significant influence on the final crack height.

3.1.3 Fig. 3.6 shows that for a certain value of the crack height, M_c does not change much between $\frac{1}{C} = 0.5$ to 200. A comparison of Figs. 3.6 and 3.7 shows a decrease in the moment carried by the concrete, M_c, and an increase in F for increasing height of crack. The moment carrying capacity of
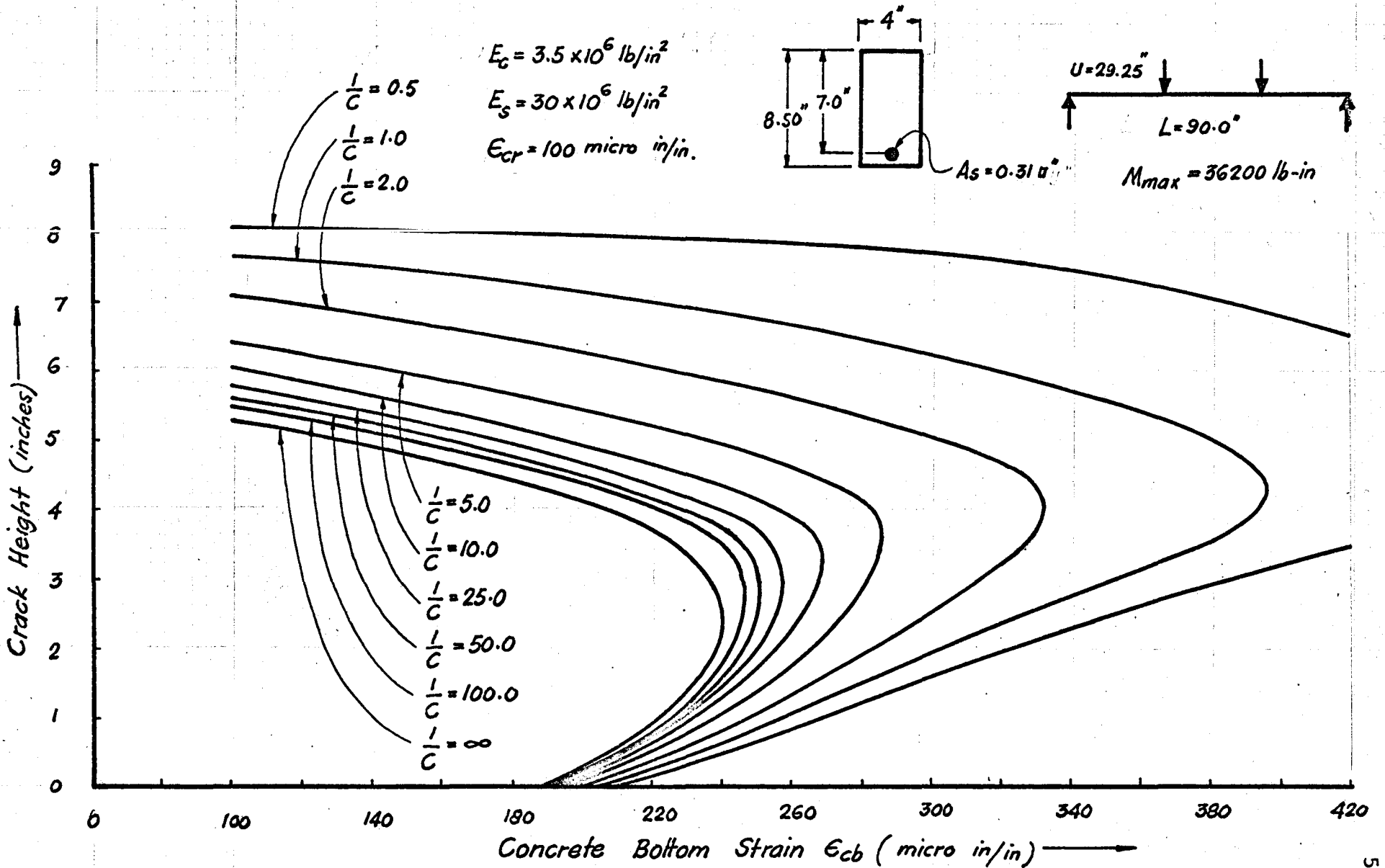
VARIATION IN CONCRETE BOTTOM STRAIN ϵ_{cb} AS CRACK DEVELOPS UNDER THE LOAD POINT

FIG. 3.4

$E_C = 3.5 \times 10^6 \; lb/in^2$

$E_s = 30 \times 10^6 \; lb/in^2$.

$\epsilon_{cr} = 100 \; micro \; in/in$

$M_{max} = 36200 \; lb\text{-}in$

$\frac{1}{c} = 0.5$

$\frac{1}{c} = 1.0$

$\frac{1}{c} = 2.0$

1920

457

179

131

277

461

840

1561

$\frac{1}{c} = 5$

$\frac{1}{c} = 25$

$\frac{1}{c} = 50$

$\frac{1}{c} = 100$

$\frac{1}{c} = 200$

$M_t = M_c^+ + M_s^+ + \alpha F.'z$

Crack Height (in)
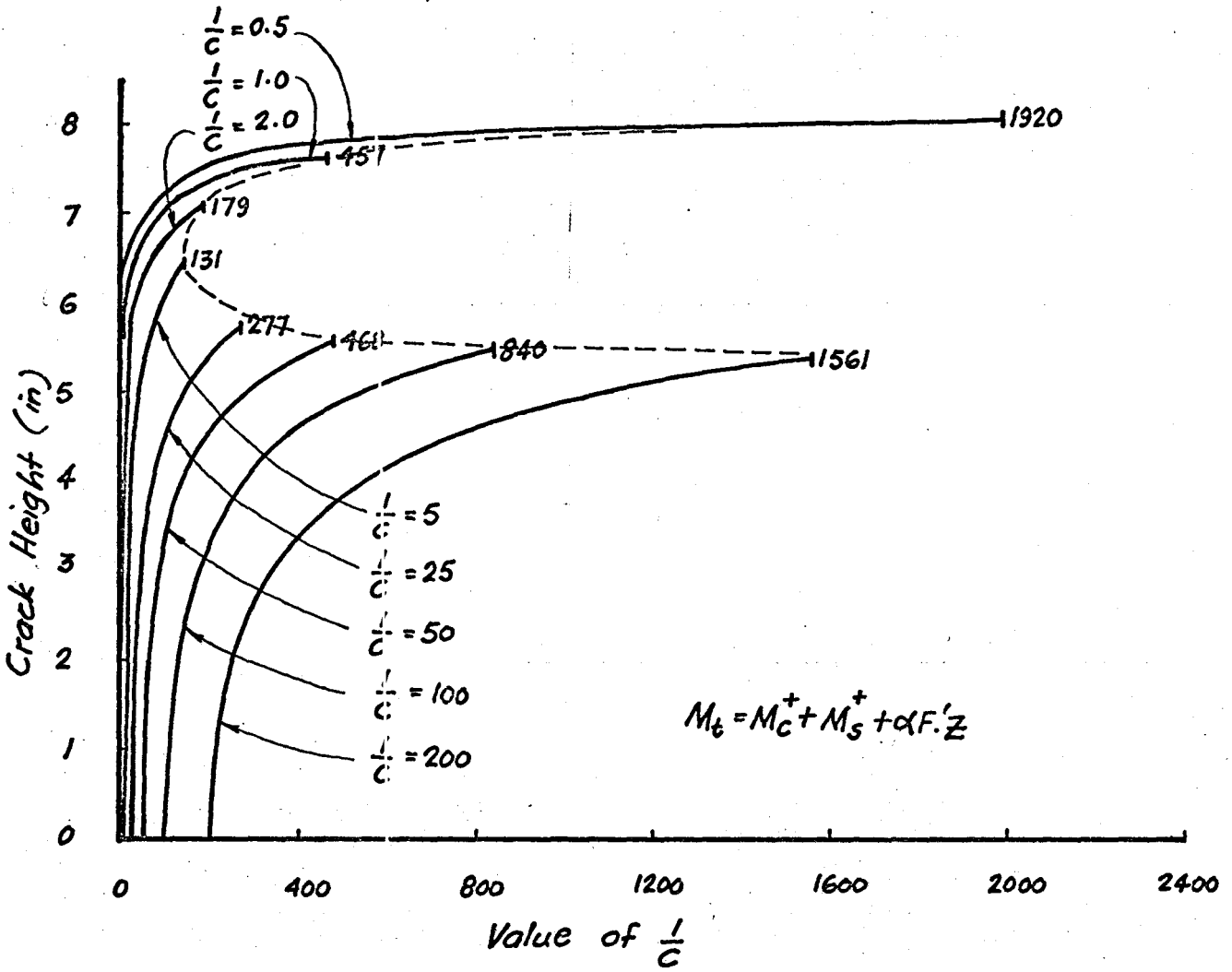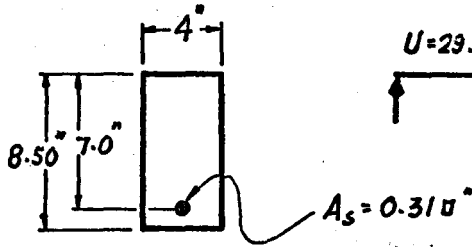
Value of $\frac{1}{c}$

VARIATION IN VALUE OF INTERACTION COEFFICIENT $\frac{1}{c}$ AS CRACK DEVELOPS UNDER THE LOAD POINT

FIG. 3.5

$U = 29.25''$

$L = 90.0''$

$E_C = 3.5 \times 10^6$ psi

$E_S = 30 \times 10^6$ psi

$\epsilon_{cr} = 100$ micro in/in

$M_{max} = 36200$ lb in.

$\frac{1}{C} = 200$

$\frac{1}{C} = 0.5$

$A_s = 0.31\ \square''$
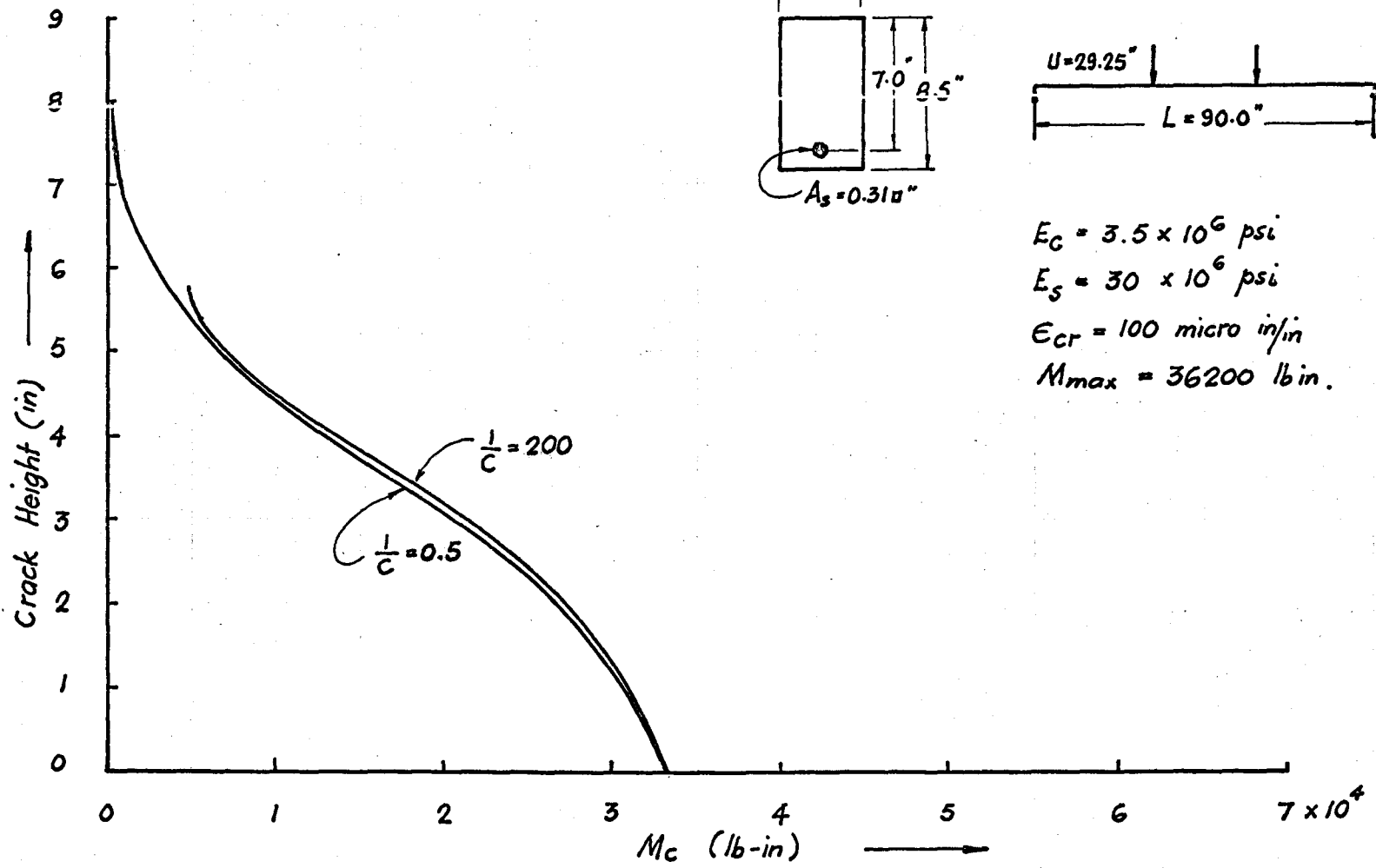
VARIATION IN M_C AS THE CRACK DEVELOPS UNDER THE LOAD POINT.

FIG. 3.6

$E_C = 3.5 \times 10^6 \; lb/in^2$

$E_S = 30.0 \times 10^6 \; lb/in^2$

$G_{cr} = 100 \; micro \; in/in.$

$M_{max} = 36200.0 \; lb\text{-}in$

$\frac{I}{C} = 0.5$

$\frac{I}{C} = 1.0$

$\frac{I}{C} = 2.0$

$\frac{I}{C} = 5.0$

$\frac{I}{C} = 25.0$

$\frac{I}{C} = 50.0$

$\frac{I}{C} = \infty$

Crack Height (inches)

Interaction Force (lbs)
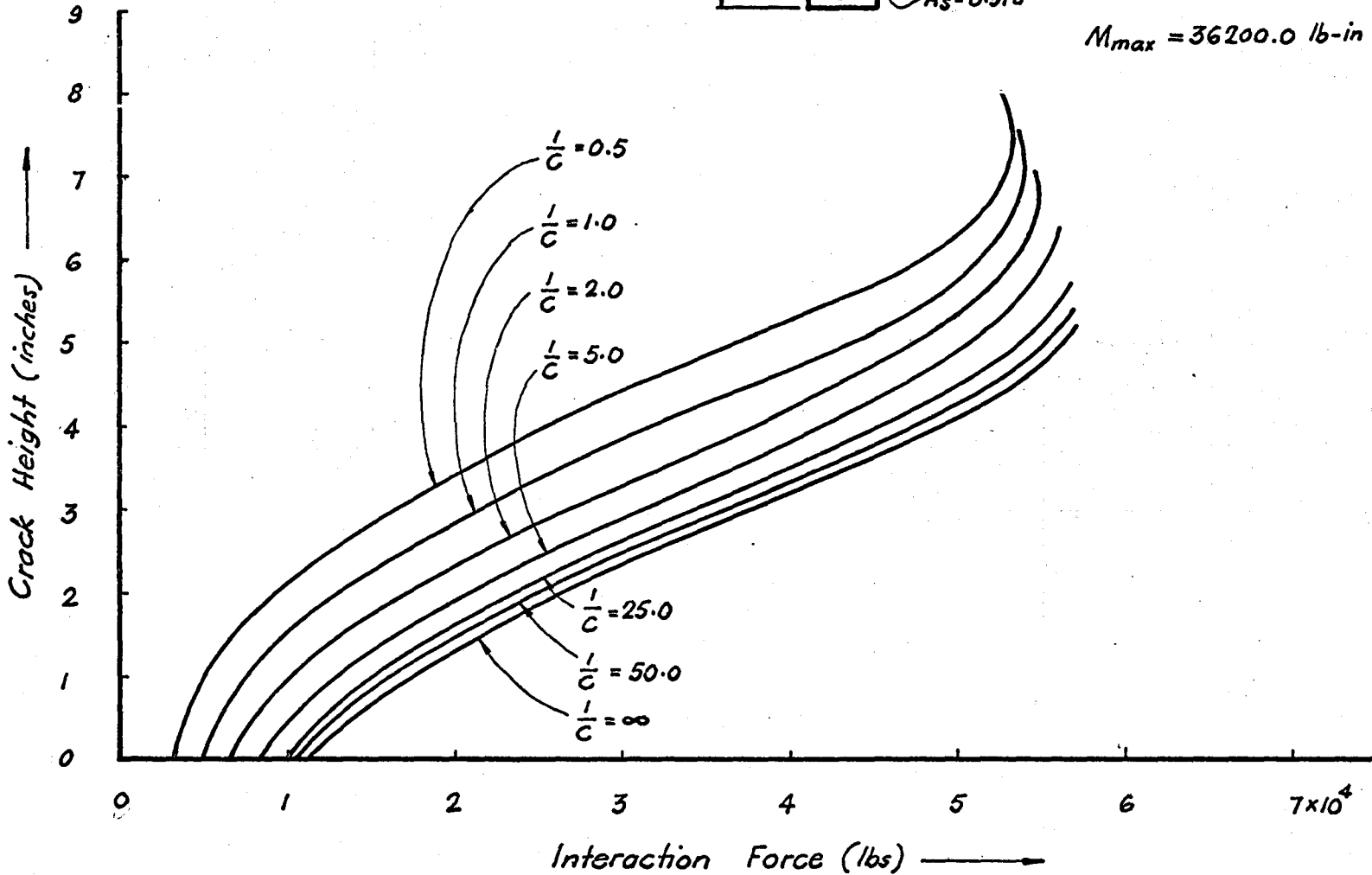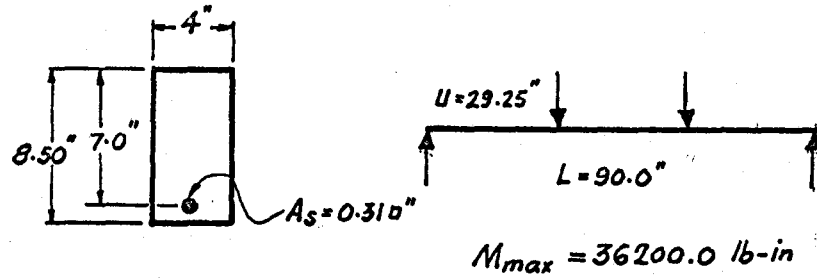
VARIATION IN INTERACTION FORCE AS CRACK DEVELOPS UNDER THE LOAD POINT.

FIG. 3.7

the uncracked concrete section reduces as the uncracked concrete section diminishes. The increase in the horizontal force F, helps to suppress the tensile strains due to bending, preventing continuation of the crack up to the top of the beam. A reduction in the interaction coefficient results in a decrease in the actual compressive force for a specific crack height, Fig. 3.7.

3.1.4 Terminal values of $\frac{1}{C}$, initial as well as terminal values of F, M_c and C_{ch} are plotted against the initial values of $\frac{1}{C}$ in Fig. 3.8, and the resulting plots show that most of these quantities become fairly constant **for** a value of $\frac{1}{C}$ > 50. Therefore the investigations carried out for $\frac{1}{C}$ > 50 would be insignificant for our objectives.

3.1.5 Equations of Equilibrium

From the free-body diagram of Fig. 2.1, the applied moment M_t can, in general form, be expressed in terms of the internal forces and moments as in Eq. 2.5.

If there is complete interaction ($\frac{1}{C} = \infty$) between the concrete and the reinforcement in a reinforced concrete beam, Eq. 2.5 will then be:

$$M_t = M_c + M_s + F'.Z \qquad\qquad 3.4$$

where F' indicates the force of interaction for complete interaction. Assuming that now the moment of the same magnitude as M_t is applied to a beam with incomplete interaction
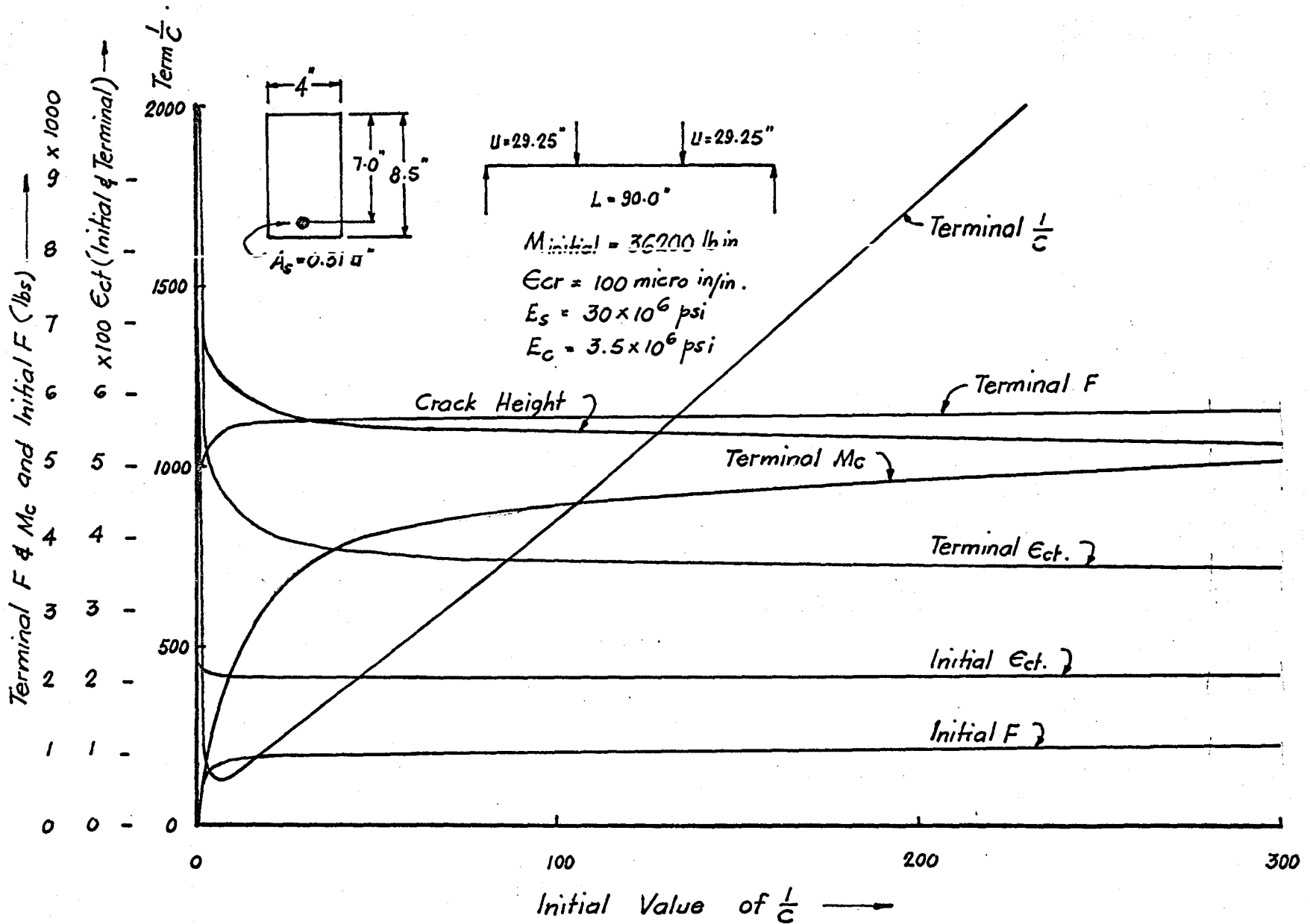
DEVELOPMENT OF CRACK UNDER THE LOAD POINT – VARIATION OF PARAMETER WITH $\frac{1}{C}$.

FIG. 3.8

$(\frac{1}{C} < \infty)$, then Eq. 3.4 would reduce to:

$$M_t = M_c^+ + M_s^+ + \alpha F'Z \qquad 3.5$$

where $M_c^+ > M_c$, $M_s^+ > M_s$ and $\alpha = \frac{F}{F'}$ is the degree of inter-
action between the concrete and the steel reinforcement in
a reinforced concrete beam, at a particular section. The
variation of $\frac{F}{F'}$ along a beam depends upon the external
loading and the support conditions (see Fig. 2.13).

In the case of no interaction $(\frac{1}{C} = 0)$, $\alpha = 0$ and
Eq. 3.5 becomes

$$M_t = M_c^+ + M_s^+ \qquad 3.6$$

This means that the concrete and the steel reinforce-
ment, both carry pure moment and are acting independent of
each other.

Since a reinforced concrete beam is considered to be
a composite beam with incomplete interaction, Eq. 3.5 defines
the state of equilibrium.

This equation must hold for every stable cross-
section in the beam.

3.2 Flexural Crack Profiles

The estimation of crack heights at various sections
along the length of a beam, lead to a profile which divides
the entire beam into two distinct portions, namely a com-
puted potential flexural cracking zone, and the remaining

66

uncracked beam section. The cracking zone defines the extremities of a region within which pure flexural cracks could occur. Formation of the flexural cracks in a beam is shown in Fig. 3.19. As the cracking progresses, the beam takes the form of a 'comblike' structure. The transfer of stresses between the reinforcement and the concrete then is through the bond provided by the concrete 'teeth', when for a certain magnitude of the applied loading, flexural cracking has taken place, the extremities of these cracks will represent a crack profile in the actual beam.

The crack profiles for the "Typical Beam" are considered here. Details of the crack profiles for other cases will be found in subsequent appendices.

The shape and size of a flexural cracking zone was found to be influenced by various parameters, such as interaction coefficient, $\frac{1}{C}$, location of the load points, the percentage of steel p, and the intensity of the point loads λ.

3.2.1 Influence of Interaction Coefficient $\frac{1}{C}$

The significance of the influence of $\frac{1}{C}$ on the crack profile is obvious from Fig. 3.9. With $\frac{1}{C} = \infty$, a minimum extent of the crack profile was obtained for given load conditions. A decrease in the magnitude of the initial value of $\frac{1}{C}$ results in an enlargement of the potentially cracked zones. This is particularly due to increase in the

$E_c = 3.5 \times 10^6 \text{ psi}$
$E_s = 30 \times 10^6 \text{ psi}$
$\epsilon_{cr} = 100 \text{ micro in/in}$
$M_{max} = 36,200 \text{ lb-in.}$

4"

7.0" 8.5"

U=29.25" U=29.25"
L=90.0"

C
Symmetrical

$\frac{1}{C} = 0.5$

$\frac{1}{C} = 1$

$\frac{1}{C} = 2$

$\frac{1}{C} = 5$

$\frac{1}{C} = 50$

$\frac{1}{C} = 10$

$\frac{1}{C} = 20$

$\frac{1}{C} = 100$

$\frac{1}{C} = \infty$
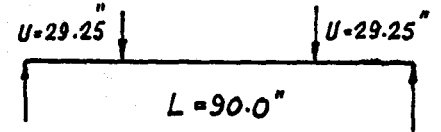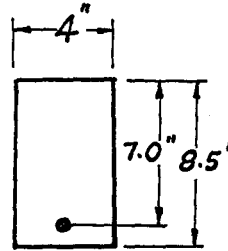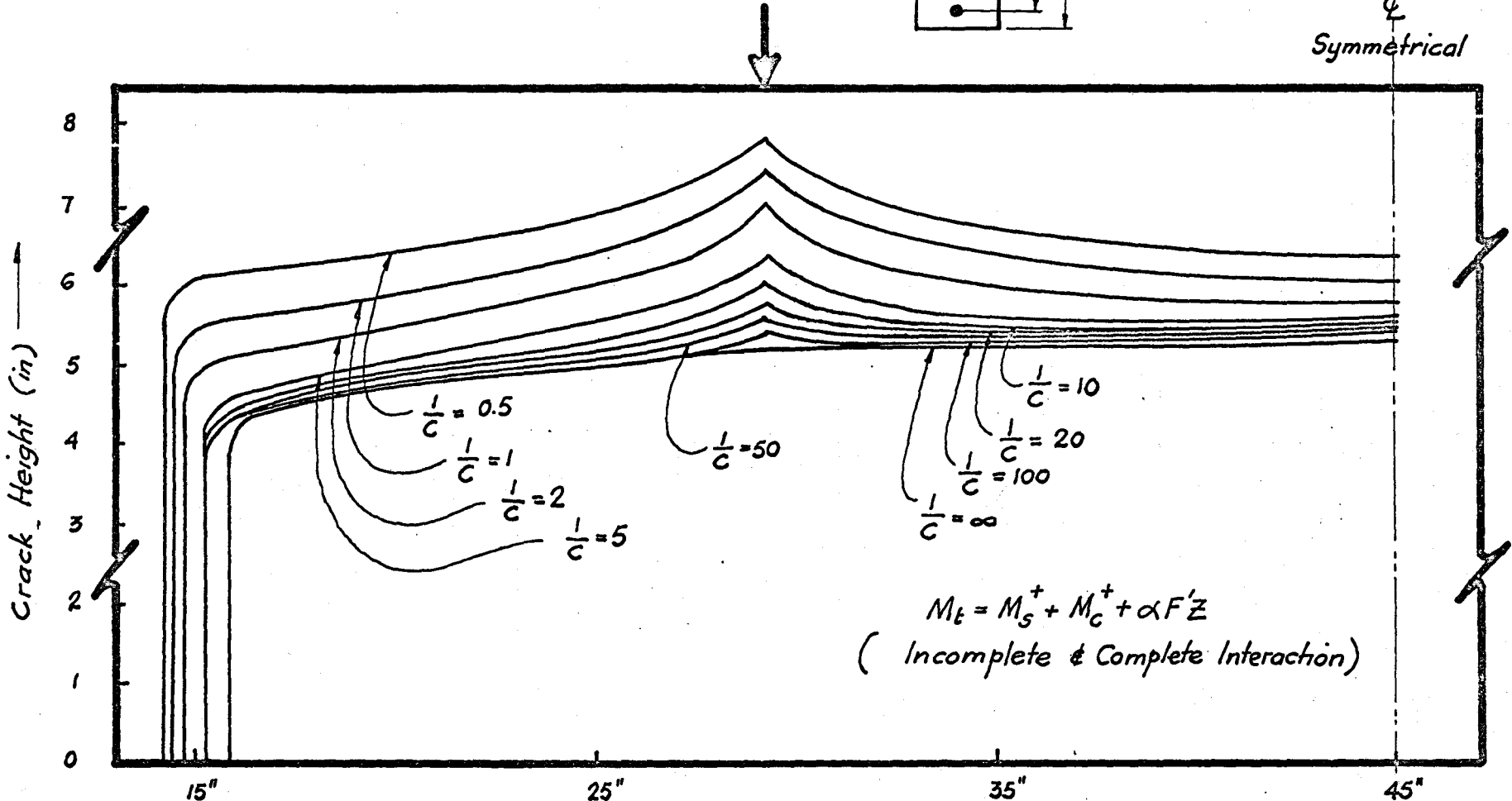
$M_t = M_s^+ + M_c^+ + \alpha F'Z$
(Incomplete & Complete Interaction)

Crack Height (in)

8

7

6

5

4

3

2

1

0

15"   25"   35"   45"

Distance from L.H. Support (in)

EFFECT OF THE VALUE OF $\frac{1}{C}$ ON THE CRACK PROFILES

FIG. 3.9

67

height of cracks. The cracks are higher in a beam with poor bond than in the case of a beam with better bond. Reduction in the interaction coefficient does not significantly affect the longitudinal spread of the flexural crack zone. It should be noted that the magnitude of $\frac{1}{C}$ increases to a magnitude greater than the initial value but this is a reflection of the influence of geometry on $\frac{1}{C}$, namely that as the uncracked section diminishes, the magnitude of successive values of $\frac{1}{C}$ increases (see Eq. 2.27).

3.2.2 Influence of Percentage of Steel, p.

Crack profiles are shown in Fig. 3.9 for the "Typical Beam" in which the reinforcement consisted of $1-\frac{5}{8}$" diameter bar giving p = 1.1 percent. Increase in height and extent of the cracked zone due to reduction in $\frac{1}{C}$ is clearly indicated. In Fig. 3.10 to 3.13 p was varied between 0.5 to 3.0. Fig. 3.10 is a case of complete interaction ($\frac{1}{C} = \infty$), Fig. 3.11 is for $\frac{1}{C} = 100$, i.e. a high bond or interaction case, and Fig. 3.12 is for $\frac{1}{C} = 5$, i.e. a case of moderate bond.

The effect of increase in percentage of steel, p, is to reduce the crack height whereas the reduction in bond modulus, k, reflected in a reduction of the initial value of $\frac{1}{C}$ leads to increase in crack height.

MacGregor and Walters[24], concluding from their investigation, state "In a region of pure flexure the height of flexural cracking is strongly influenced by steel

$E_C = 3.5 \times 10^6 \; lb/in^2$

$E_S = 30 \times 10^6 \; lb/in^2$

$\varepsilon_{cr} = 100 \; micro \; in/in$

$M_{max} = 36200.0 \; lb\text{-}in.$

$A_S = p \dfrac{bd}{100}$

$U = 29.25''$

$L = 90.00''$

$\mathcal{C}$
Symmetrical

$p = 0.5$

$p = 1.0$

$p = 1.5$

$p = 2.0$

$p = 2.5$

$p = 3.0$

$M_t = M_c + M_s + F'z$
(Complete Interaction $\dfrac{I}{C} = \infty$)

Crack Height (in)

Distance from L.H. Support (inches)
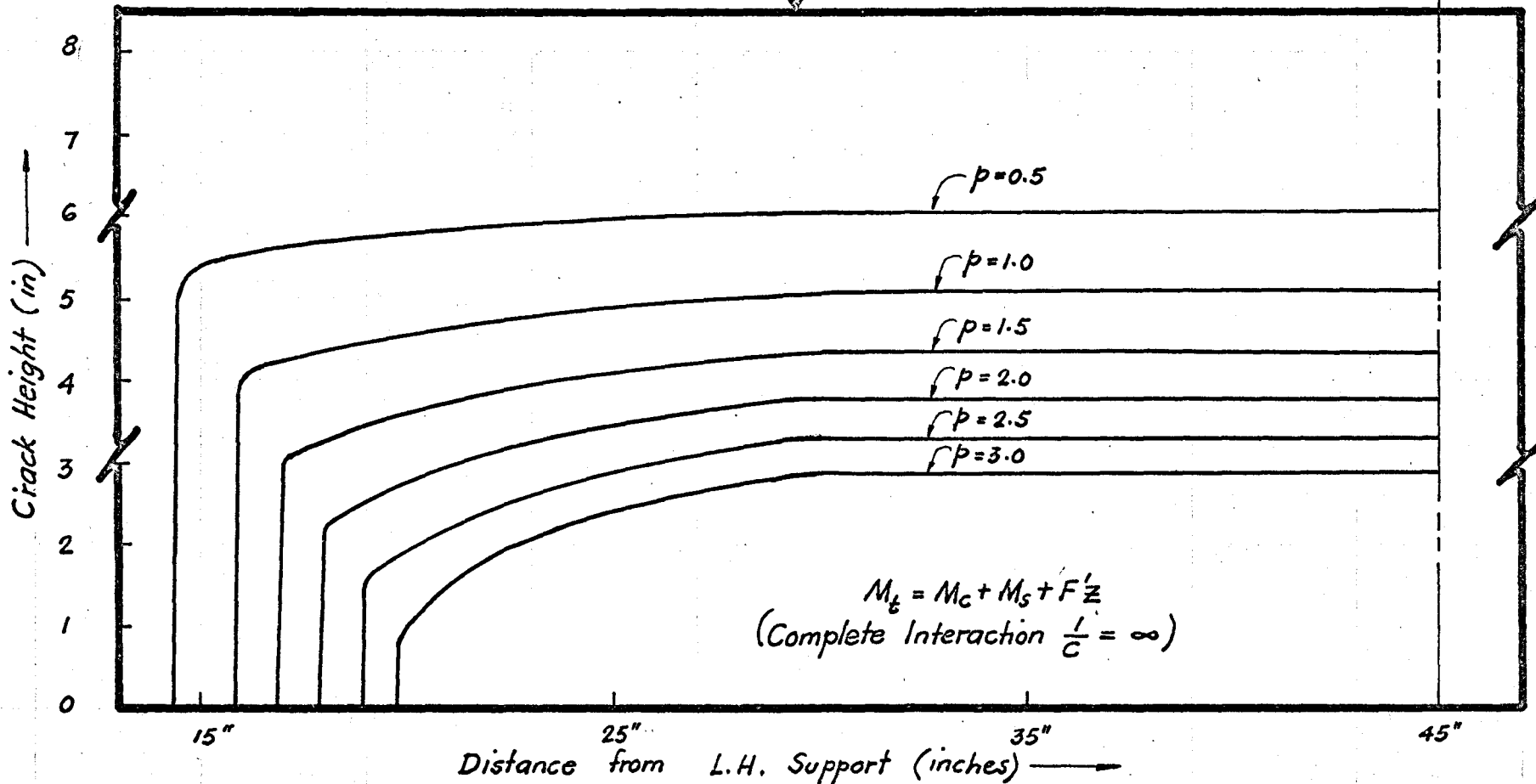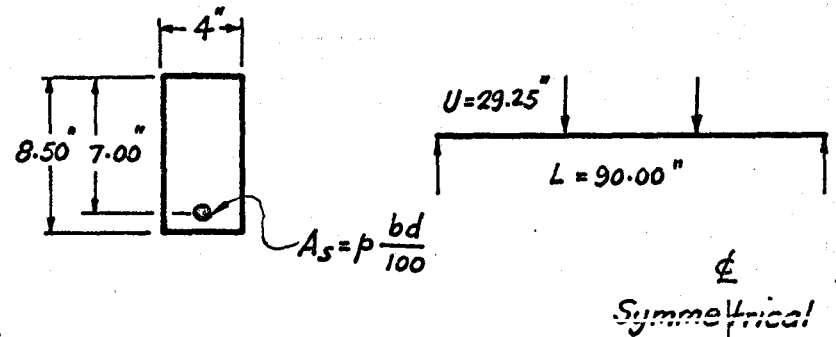
EFFECT OF PERCENTAGE OF STEEL ON CRACK PROFILES

$E_c = 3.5 \times 10^6 \; lb/in^2$.

$E_s = 30 \times 10^6 \; lb/in^2$.

$\varepsilon_{cr} = 100 \; micro \; in/in$

$M_{max} = 36200.0 \; lb\text{-}in$

$A_s = p\dfrac{bd}{100}$

$U = 29.25''$

$L = 90.00$

℄ Symmetrical

$p = 0.5$

$p = 1.0$

$p = 1.5$

$p = 2.0$

$p = 2.5$

$p = 3.0$

$M_t = M_c^+ + M_s^+ + \alpha F \dfrac{'}{z}$

(Incomplete Interaction $\dfrac{1}{c} = 100$)

Crack Height (in) →

Distance from L.H. Support (inches) →

EFFECT OF PERCENTAGE OF STEEL ON CRACK PROFILES

70

$E_c = 3.5 \times 10^6 \ lb/in^2$

$E_s = 30 \times 10^6 \ lb/in^2$

$\epsilon_{cr} = 100 \ micro \ in/in$

$M_{max} = 36200 \ lb\text{-}in.$

4"

8.50" 7.0"

$A_s = P\frac{bd}{100}$

$U = 29.25"$

$L = 90.0"$

$\mathcal{C}$
Symmetrical

$p = 0.5$

$p = 1.0$

$p = 1.5$

$p = 2.0$

$p = 2.5$

$p = 3.0$

$M_t = M_c^+ + M_s^+ + \alpha F'z$

(Incomplete Interaction $\frac{l}{c} = 5$)

Crack Height (in)

Distance from L.H. Support (in.)

EFFECT OF PERCENTAGE OF STEEL ON CRACK PROFILES

$\frac{1}{C} = 5$

$\frac{1}{C} = 10$

$\frac{1}{C} = 25$

$\frac{1}{C} = 50$

$\frac{1}{C} = 100$

$\frac{1}{C} = \infty$

$U = 29.25''$

$L = 90.0''$

4"

7.0"

8.5"

$A_s = p \frac{bd}{100}$

$M_{max.} = 36200 \ lb\text{-}in$

$E_c = 3.5 \times 10^6 \ lb/in^2$

$E_s = 30 \times 10^6 \ lb/in^2$

$\epsilon_{cr} = 100 \ m \ in/in$

EFFECT OF PERCENTAGE OF STEEL ON CRACK HEIGHT UNDER THE LOAD POINT

FIG. 3.13

percentage p. For low values of p the crack will extend a considerable distance into the beam with no increase in load."

Experiments by other research workers also substantiated this fact[10].

Fig. 3.13 shows the variation in the crack height under the load point with different values of p. Each of these curves is for a particular value of $\frac{1}{C}$. A comparison of the influence of $\frac{1}{C}$ as well as of p can easily be made. With a percentage of steel of 0.5, the influence of bond as manifested by $\frac{1}{C}$ causes an increase in crack height from 6.0" to 6.9", or 15% for $\frac{1}{C} = \infty$ and $\frac{1}{C} = 5$ respectively, With a percentage of steel of 3.0, the crack height is increased from 2.8" to 4.3", an increase of 53.6% for the same range of $\frac{1}{C}$.

3.2.3 Influence of Location of the Load Point 'u'

Fig. 3.14, shows the crack profiles for a value of $\frac{1}{C} = 10$, and one times the design load for different locations of point loads (u=15",20",25",30",35" and 40"). The example chosen was for the "Typical Beam" except that the location of the point loads was varied. The load intensity was changed to produce the same magnitude of the applied moment. It is found that crack height under the load point increases as the load moves towards the support. The change in shape of the crack profile resulting from the movement of the load point is also shown.

$E_c = 3.5 \times 10^6 \ lb/in^2$

$E_s = 30.0 \times 10^6 \ lb/in^2$

$\varepsilon_{cr} = 100 \ micro \ in/in$

$M_{max} = 36200.0 \ lb\text{-}in$

$M_t = M_s^+ + M_c^+ + \alpha F'z$

(Incomplete Interaction $\frac{1}{C} = 10$)
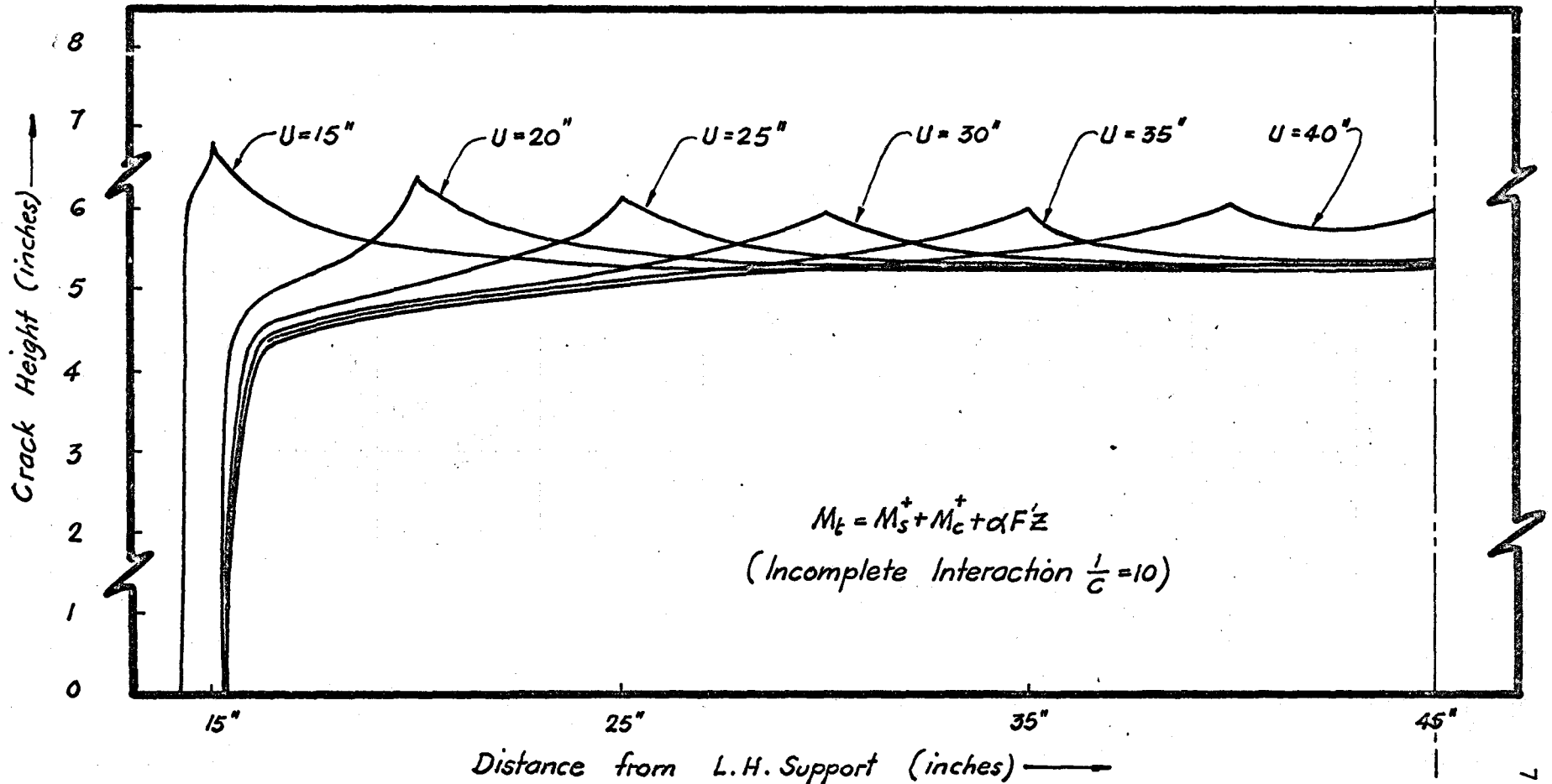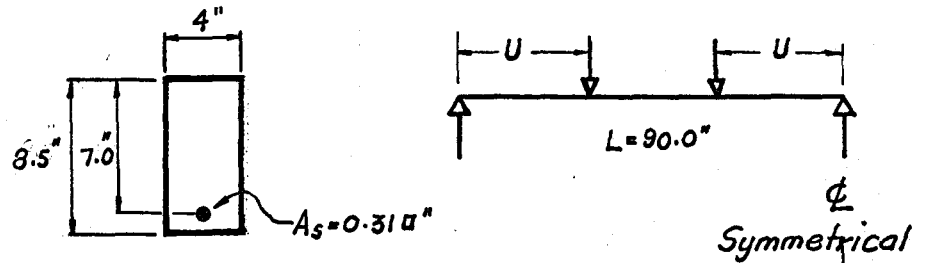
EFFECT OF LOCATION OF LOAD POINT ON THE FLEXURAL CRACK PROFILES

FIG. 3.14

3.2.4   Influence of the Intensity of Load λ

The influence of the intensity of load on the size and shape of the crack profile is shown in Figs. 3.15, 3.16 and 3.17. The load intensities were varied between 1 and 3.5 times the design load.

Fig. 3.15 is again for the case of complete inter-action ($\frac{1}{C} = \infty$) whereas Fig. 3.16 and 3.17 are cases of in-complete interaction, with the interaction coefficient, $\frac{1}{C}$, of 100 and 5 respectively.

The increase in the load intensity λ did not increase the crack heights much, in comparison to the influence of p, or that of $\frac{1}{C}$. However, an increase in λ has the predominant effect of extending the length of the flexural cracking zone. Fig. 3.18 gives the crack height under the load point for varying values of λ as well as $\frac{1}{C}$. Therefore a comparison of the influence of these two para-meters can be made. Loss of interaction has a much more significant effect on the height of the flexural crack than does an increase in load intensity.

3.3   Strain Distribution in a Cracked Beam

3.3.1   Fig. 3.20 and 3.21 show the variation of upper, mid-height and lower fibre strains in the reinforcement and top fibre concrete strain along the length of a cracked beam for $\frac{1}{C} = 100$ and $\frac{1}{C} = 5$ respectively. These correspond to the

$E_c = 3.5 \times 10^6 \ psi$

$E_s = 30 \times 10^6 \ psi$

$\epsilon_{cr} = 100 \ micro \ in/in.$

$M_{max} = 36,200\lambda \ lb\cdot in$

$4''$

$8.5'' \quad 7.0''$

$A_s = 0.31 \, \square''$

$U = 29.25''$ $U = 29.25''$

$L = 90.0''$

$\lambda = 3.5$

$\lambda = 3.0$

$\lambda = 2.5$

$\lambda = 2.0$

$\lambda = 1.5$

$\lambda = 1.0$

$M_t = M_c + M_s + F' \cdot Z$
(Complete Internation)

Crack Height (ins)

Distance from L.H. Support (inches) ⟶
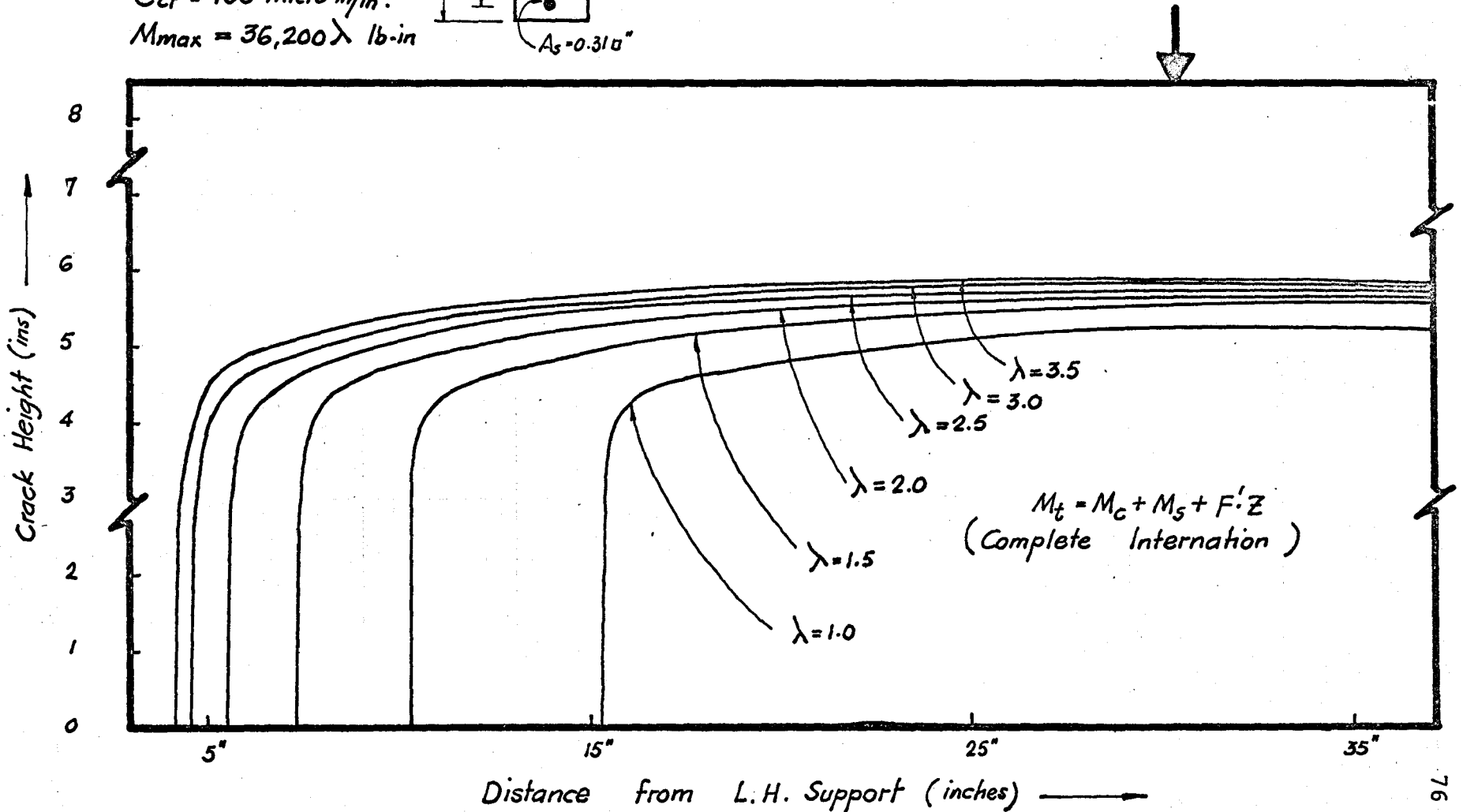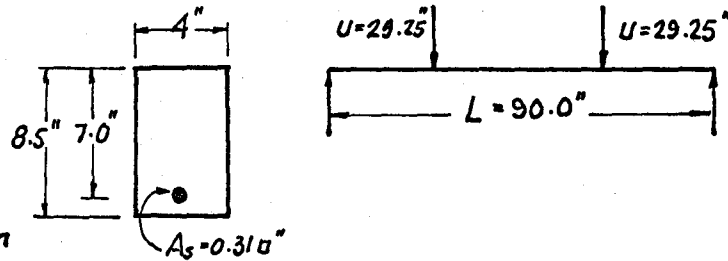
EFFECT OF LOAD INTENSITY ON THE CRACK PROFILES

FIG. 3.15

$E_C = 3.5 \times 10^6 \ psi$
$E_S = 30 \times 10^6 \ psi$
$\epsilon_{cr} = 100 \ micro \ in/in.$
$M_{max} = 36,200 \ \lambda \ lbin$
$\frac{I}{C} = 100$

$4''$

$U = 29.25''$ $U = 29.25''$

$7.0''$ $8.5''$ $L = 90.0''$

$A_S = 0.31 \ in^2$

$\lambda = 3.5$

$\lambda = 3.0$
$\lambda = 2.5$
$\lambda = 2.0$
$\lambda = 1.5$
$\lambda = 1.0$
$\lambda = 0.5$

$M_t = M_c^+ + M_s^+ + \alpha F' Z$

(Incomplete Interaction)

Crack Height (inches)

Distance from L.H. Support (inches) ⟶
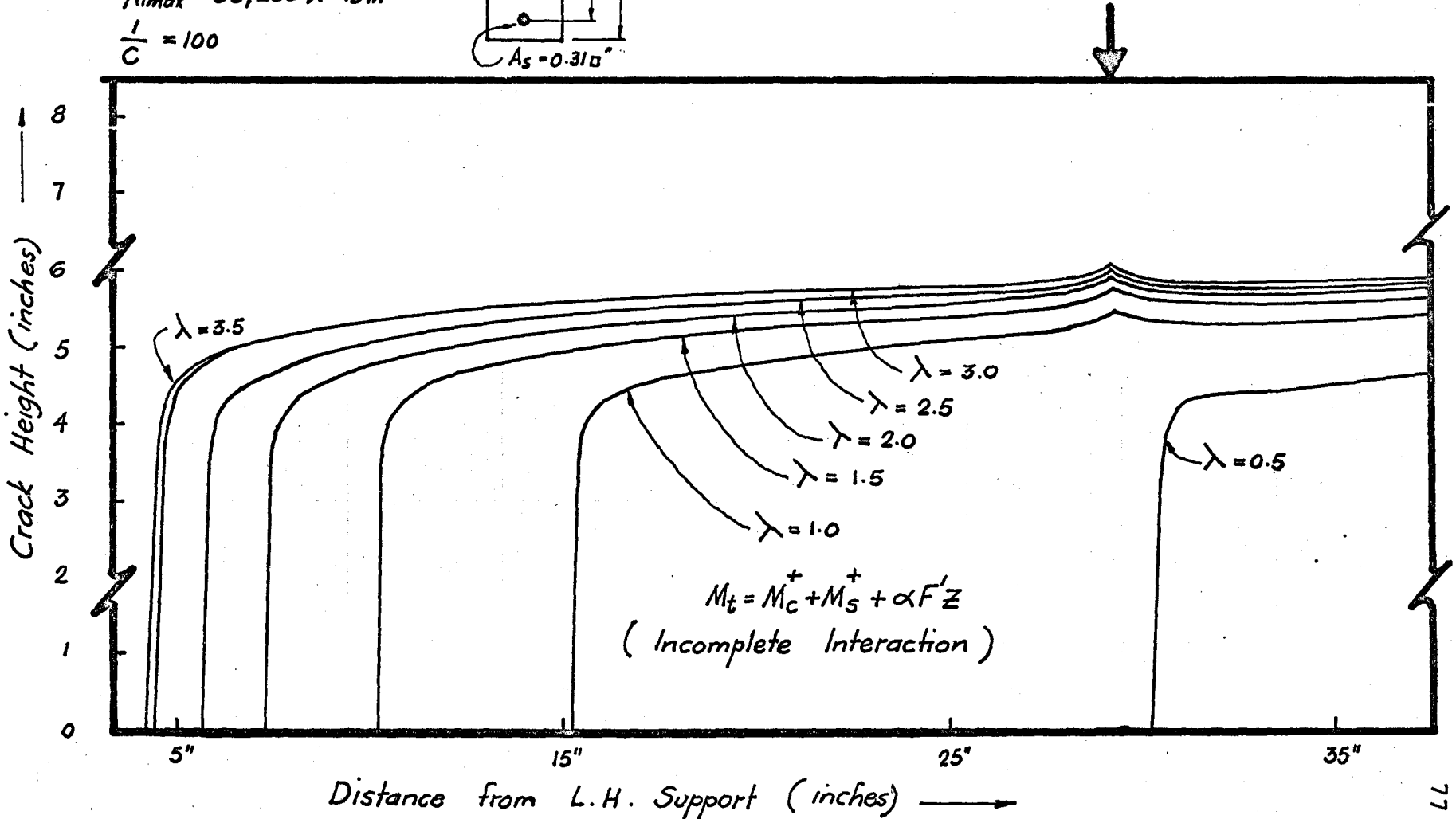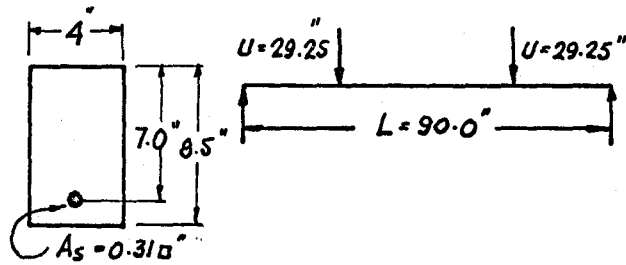
EFFECT OF LOAD INTENSITY ON THE CRACK PROFILES

FIG. 3.16

$E_c = 3.5 \times 10^6$ psi

$E_s = 30 \times 10^6$ psi
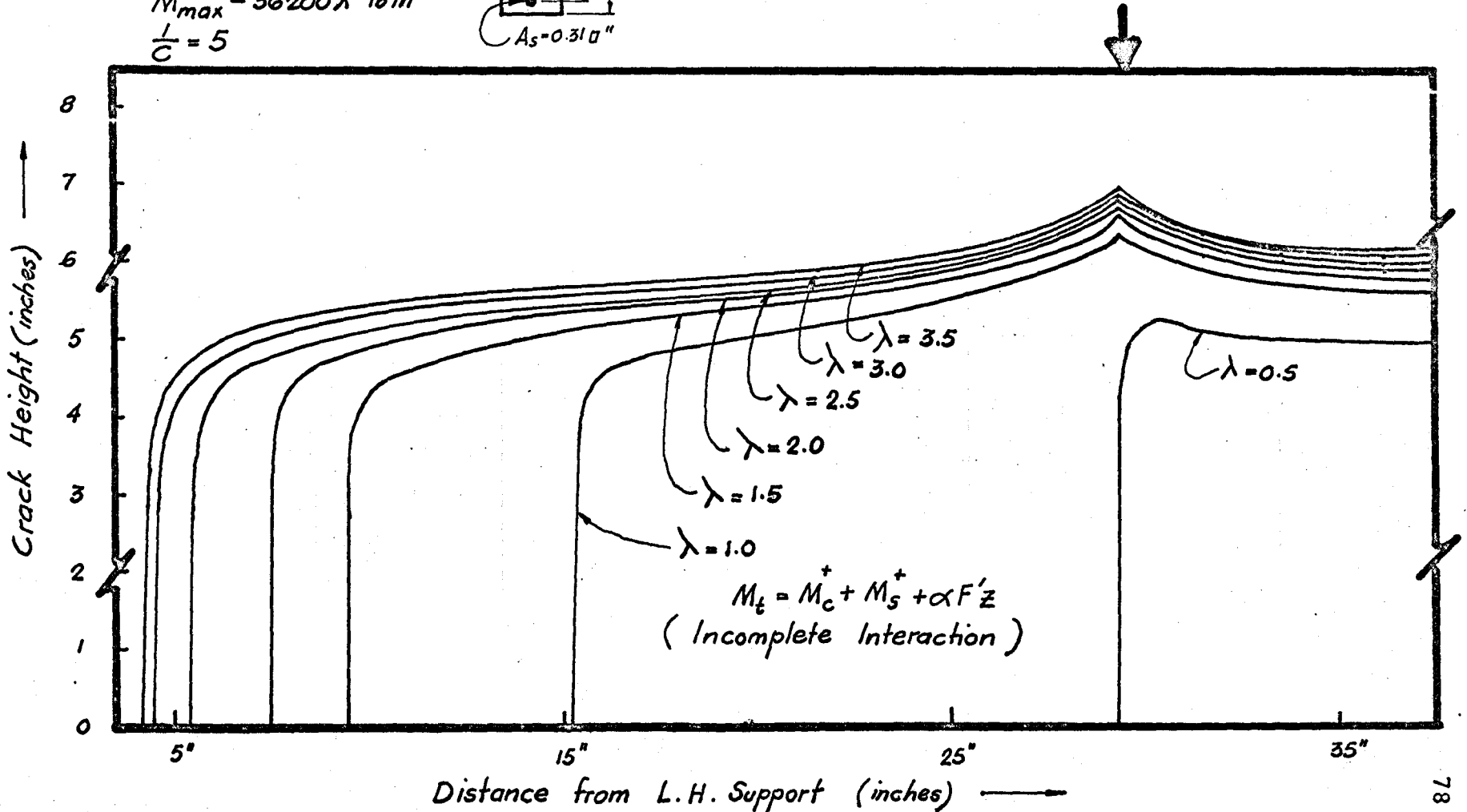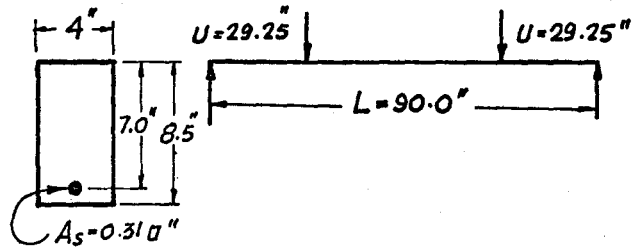
$\epsilon_{cr} = 100$ micro in/in.

$M_{max} = 36200\lambda$ lb in

$\dfrac{1}{C} = 5$

$U = 29.25''$ $U = 29.25''$

$L = 90.0''$

$4''$

$7.0''$ $8.5''$

$A_s = 0.31 \, \Box''$

$\lambda = 3.5$

$\lambda = 3.0$

$\lambda = 2.5$

$\lambda = 2.0$

$\lambda = 1.5$

$\lambda = 1.0$

$\lambda = 0.5$

$M_t = M_c^+ + M_s^+ + \alpha F'z$

(Incomplete Interaction)

Crack Height (inches)

8 7 6 5 4 3 2 1 0

$5''$ $15''$ $25''$ $35''$

Distance from L.H. Support (inches)
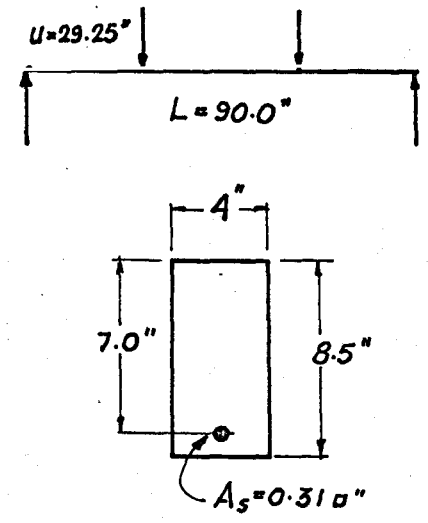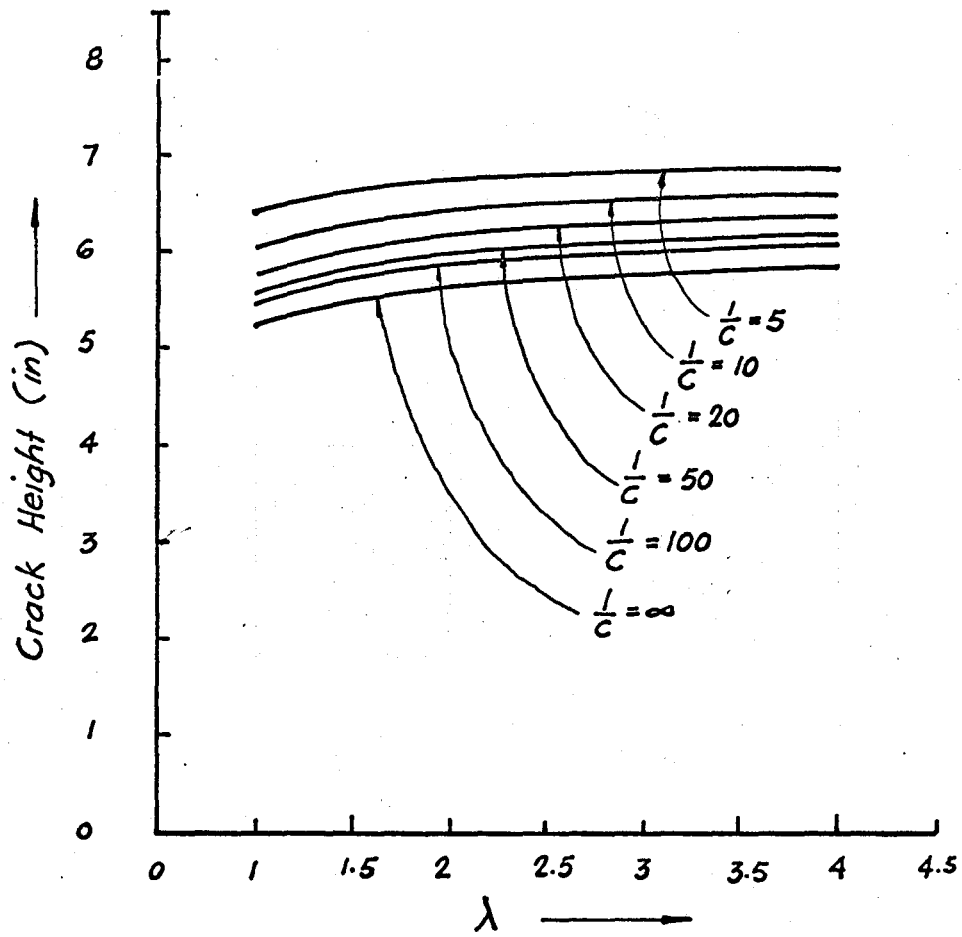
EFFECT OF LOAD INTENSITY ON THE CRACK PROFILES

FIG. 3.17

EFFECT OF INTENSITY OF LOAD ON CRACK HEIGHT UNDER THE LOAD POINT

FIG. 3.18

flexural crack profiles of Fig. 3.9. It may be observed that strains in general, are much higher in a cracked zone than in the uncracked beam. The shape of the concrete top fibre strain distribution resembles that found experimentally by Kar[26], see Fig. 3.23.

The mid-height steel strains measured experimentally by Plowman[8] and Fenwick and Pauley[29] are reproduced in Figs. 3.22 and 3.24 respectively. Observations by Fenwick and Pauley were made only in the cracked portion of the beam. It should be noted, however, that although the computed variations in the mid-height strain show a sudden change in the magnitude at the point where cracking starts, Plowman's results could provide an envelope for this variation. Fenwick and Pauley's results also compare qualitatively with the computed distribution in the zone of potential flexural cracking.

3.3.2 In the vicinity of the load points the steel bottom strain, ε_{cb}, and concrete top strain, ε_{ct}, show an increase in magnitude, whereas the steel top strain, ε_{st}, shows a drop in the magnitude compared to the case for complete interaction. This change in the steel strains, could, in cases of low value of $\frac{1}{C}$, result in a considerable local deformation of the reinforcement.

Also from Fig. 3.27b and 3.28 for the case of a small value of p or of $\frac{1}{C}$, if cracking is quite high, it
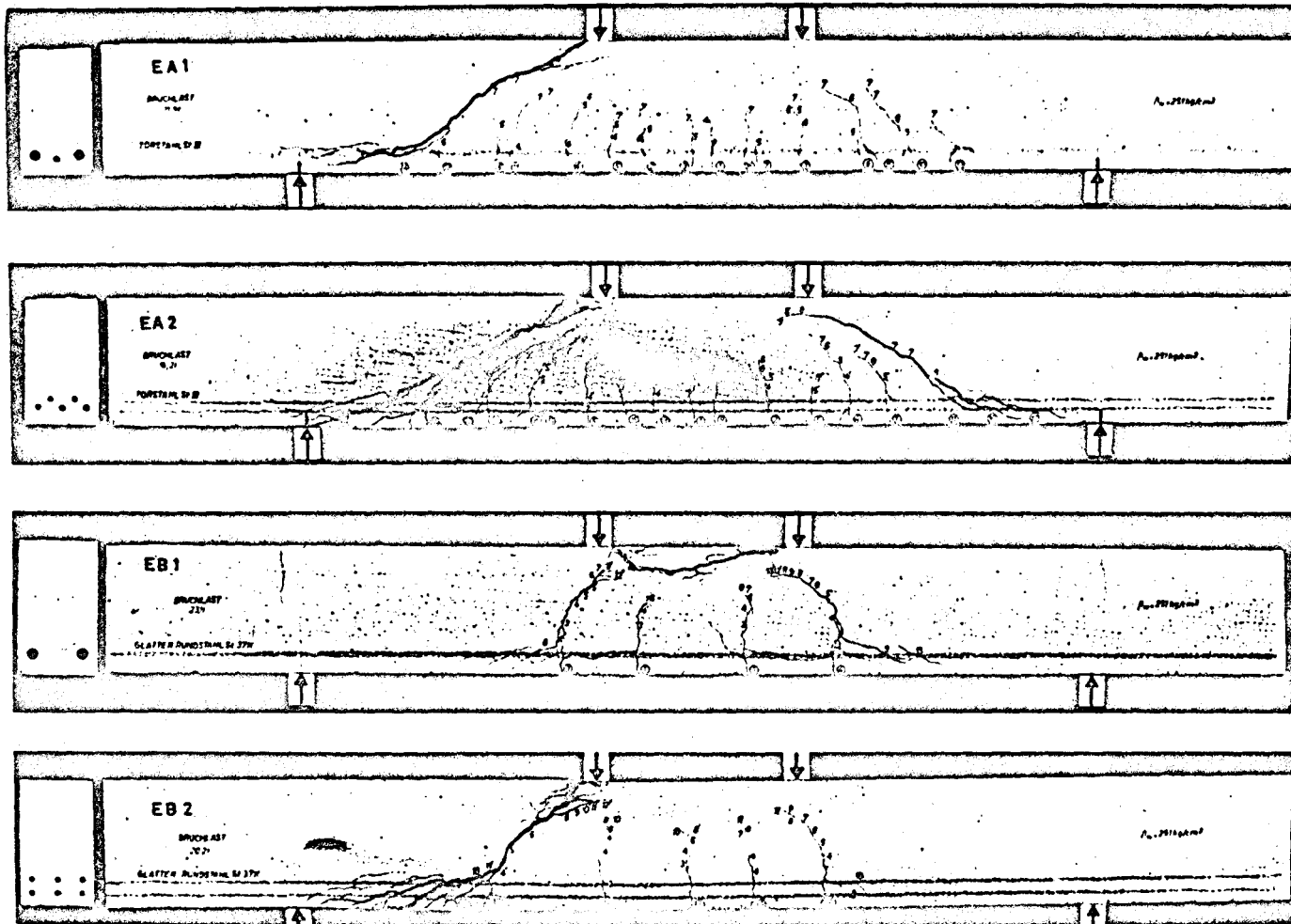
FIG.3.19 Crack pattern and failure pictures for point loads with different bond. (Numbers in circles equal number of occurrence of the cracks. Other numbers equal load increment for which a load has penetrated to the indicated location load increment p = 1.55 tons.)

DUE TO LEONHARDT AND WALTHER
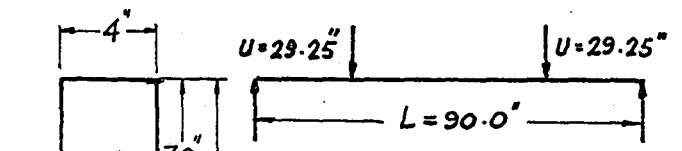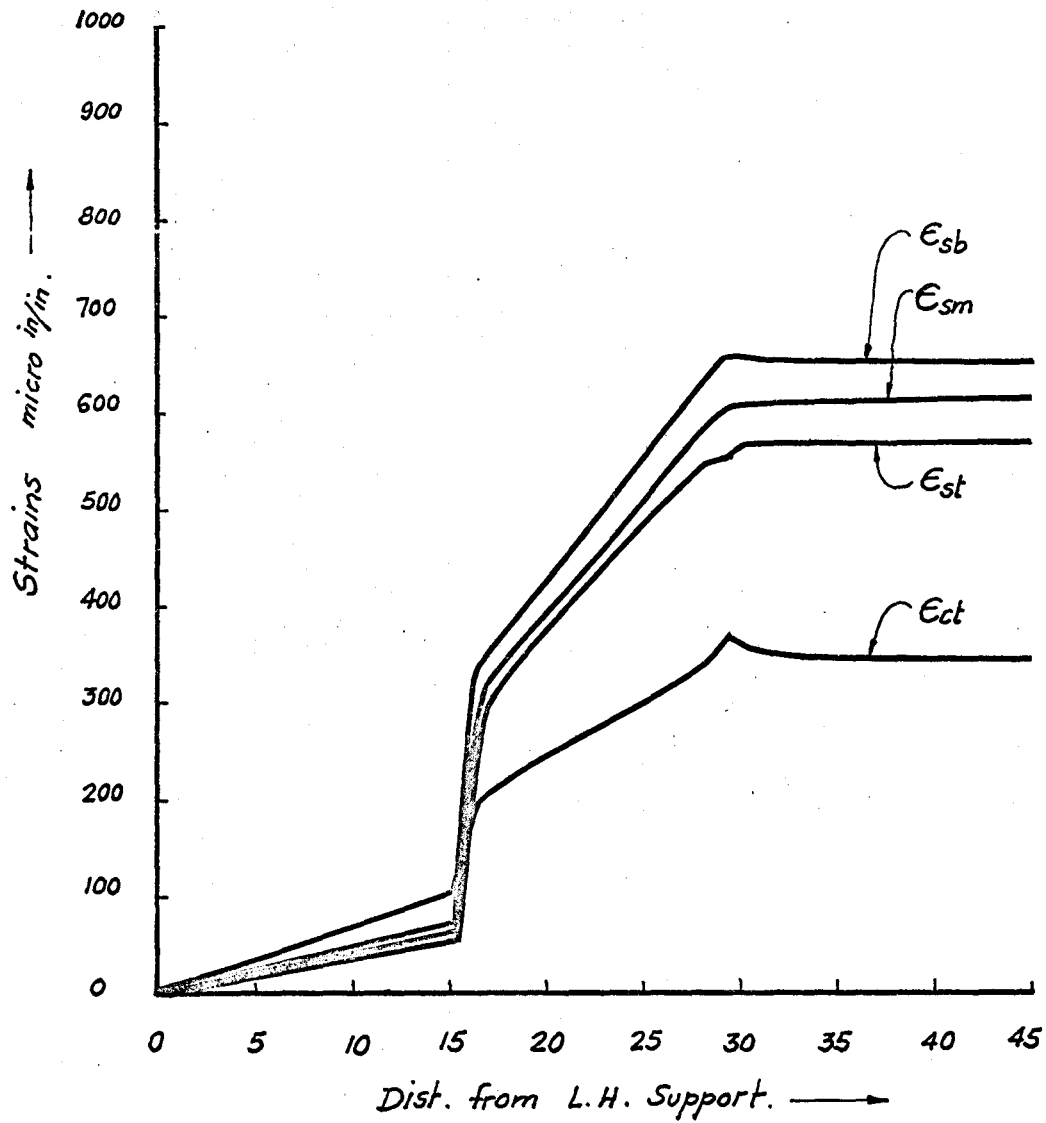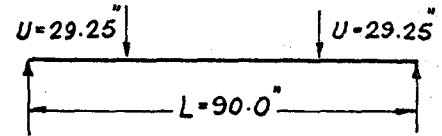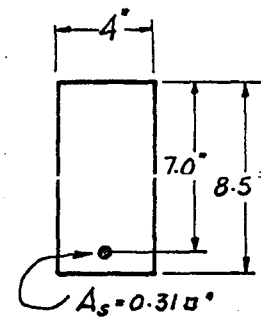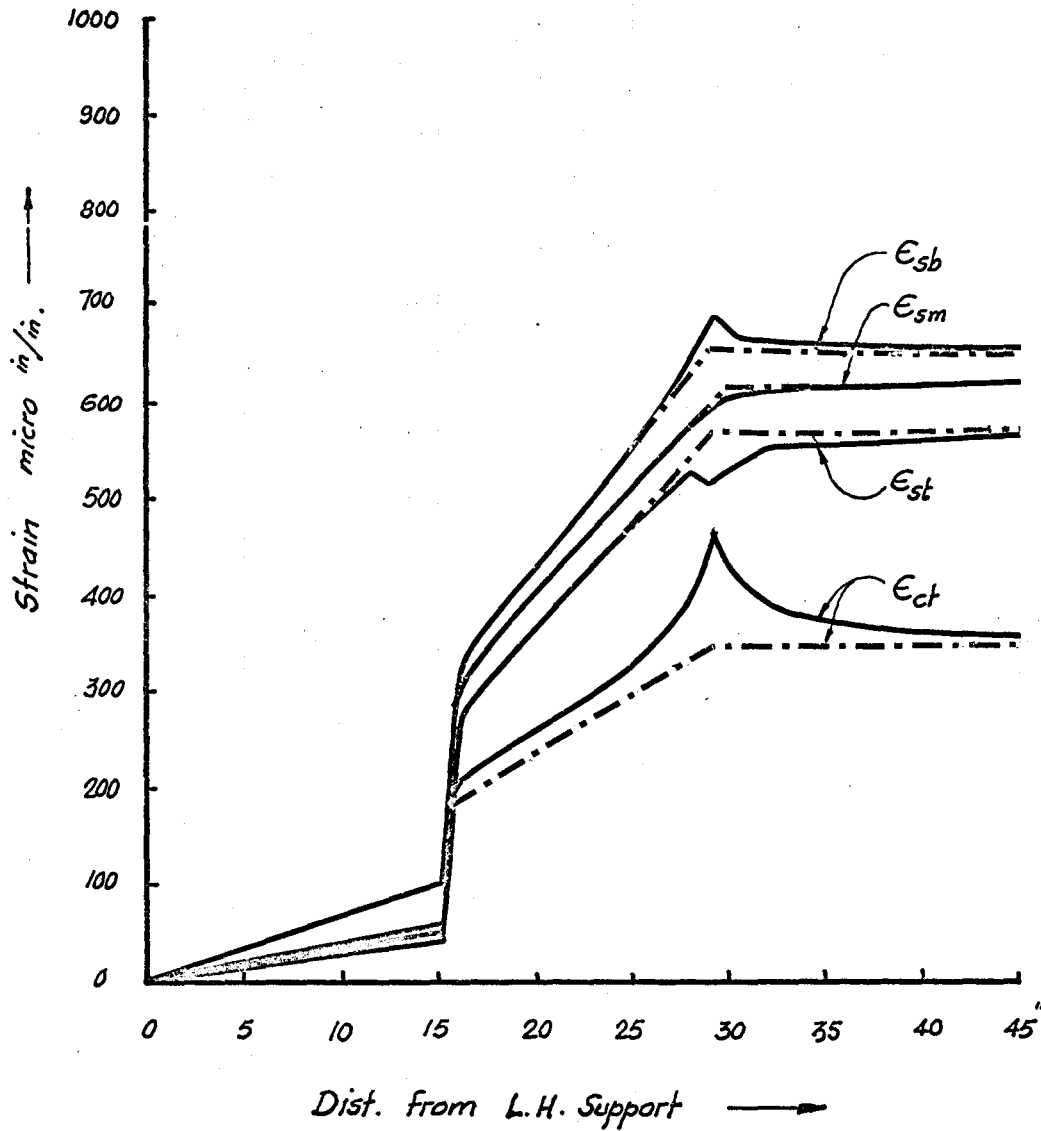
DISTRIBUTION OF THE STRAINS ALONG THE LENGTH OF A CRACKED BEAM.

FIG. 3.20

DISTRIBUTION OF THE STRAINS ALONG THE LENGTH OF A CRACKED BEAM
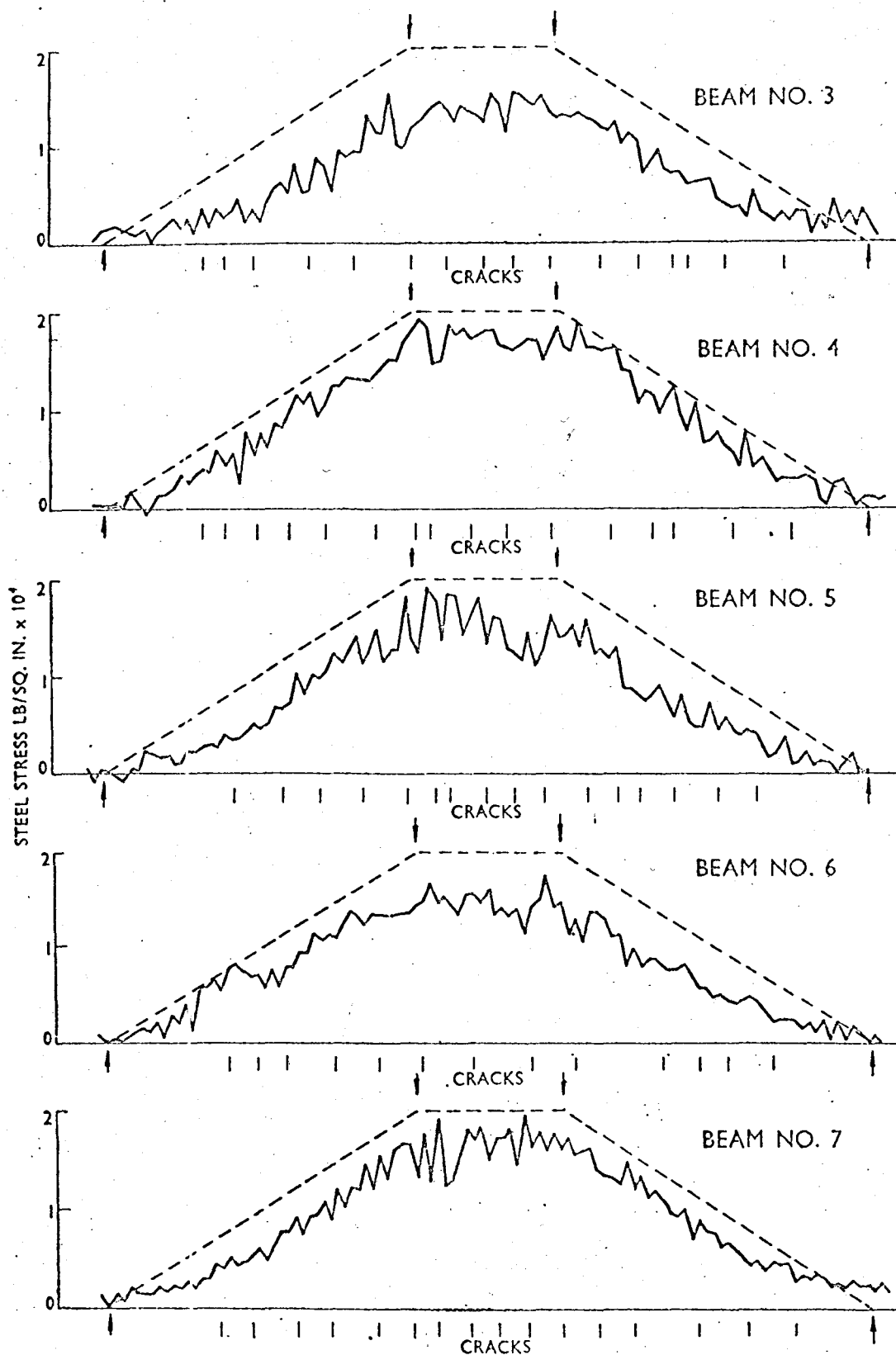
FIG. 3.21

STEEL STRESSES AT DESIGN LOADING IN BEAMS Nos 3, 4, 5, 6, AND 7
Design stress shown by broken line

DUE TO PLOWMAN

FIG. 3.22

BEAM A-12

DISTRIBUTION OF CONCRETE TOP FIBRE STRAIN (DUE TO KAR)
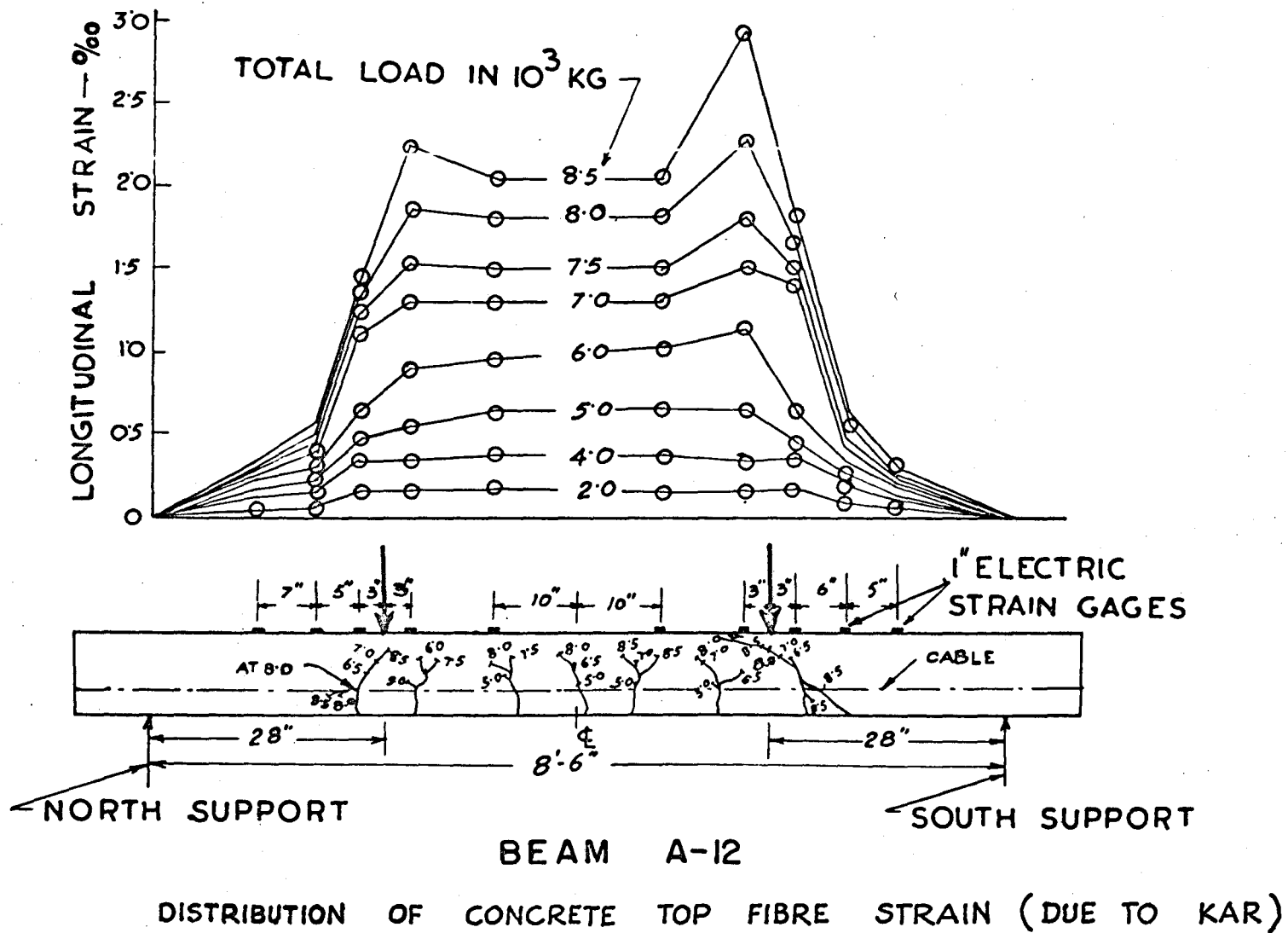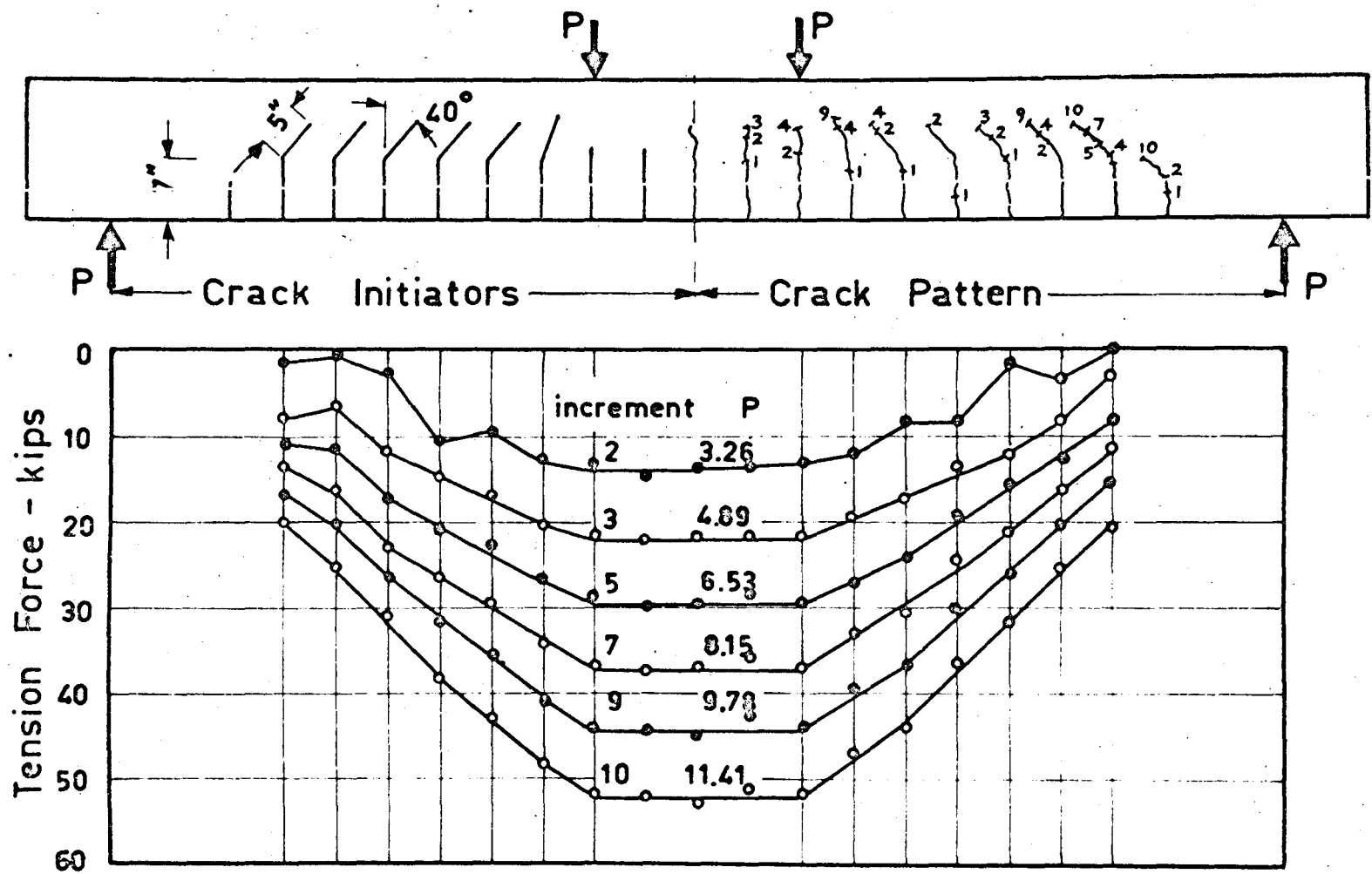
FIG. 3.23

DISTRIBUTION OF TENSION IN STEEL (DUE TO FENWICK AND PAULEY)

FIG. 3.24

would result in a very high magnitude of the top fibre compressive strain, ε_{ct}, in the vicinity of the load point. If this strain exceeds the crushing strain of the concrete, spalling of the concrete will occur, and the beam will finally fail in compression by crushing of the concrete near the load point.

3.3.3 Fig. 3.25 and 3.26 show variation along the length of a beam, of the interaction force F, the moment, M_c, in the remaining section of concrete and the interaction coefficient $\frac{1}{C}$, relating to the strain plots of Figs. 3.20 and 3.21. It may be noticed that the final values of $\frac{1}{C}$ in the cracked beam are quite high due to change in the geometry of the cross-section. This cracking increases the amount of the axial force on the remaining concrete section and reduces the amount of moment, M_c, carried by concrete.

A comparison of the distribution of these quantities, in a beam, between a state before cracking and the one after cracking suggests that the flexural cracking of a reinforced concrete beam causes it to transform into a tied arch.

It should also be noted that an increase in the applied load can increase the axial force F further, and could be responsible for the final failure of the beam. This type of failure could be either due to the buckling of the remaining arch or due to the breakage of bond in the uncracked zone of the beam.

88
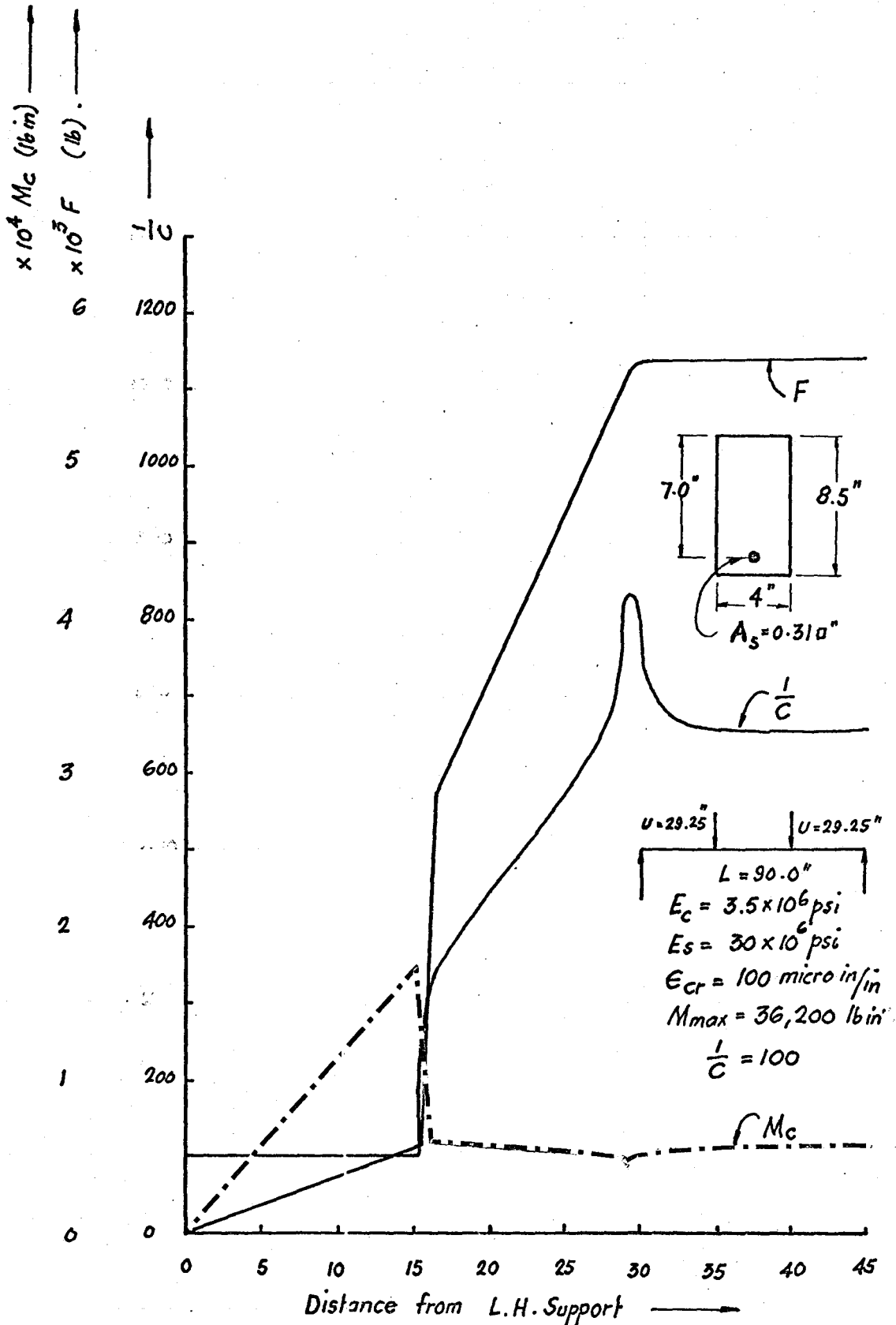
VARIATION IN F, M_c AND $\frac{1}{C}$ ALONG THE LENGTH OF A BEAM.

FIG. 3.25

89
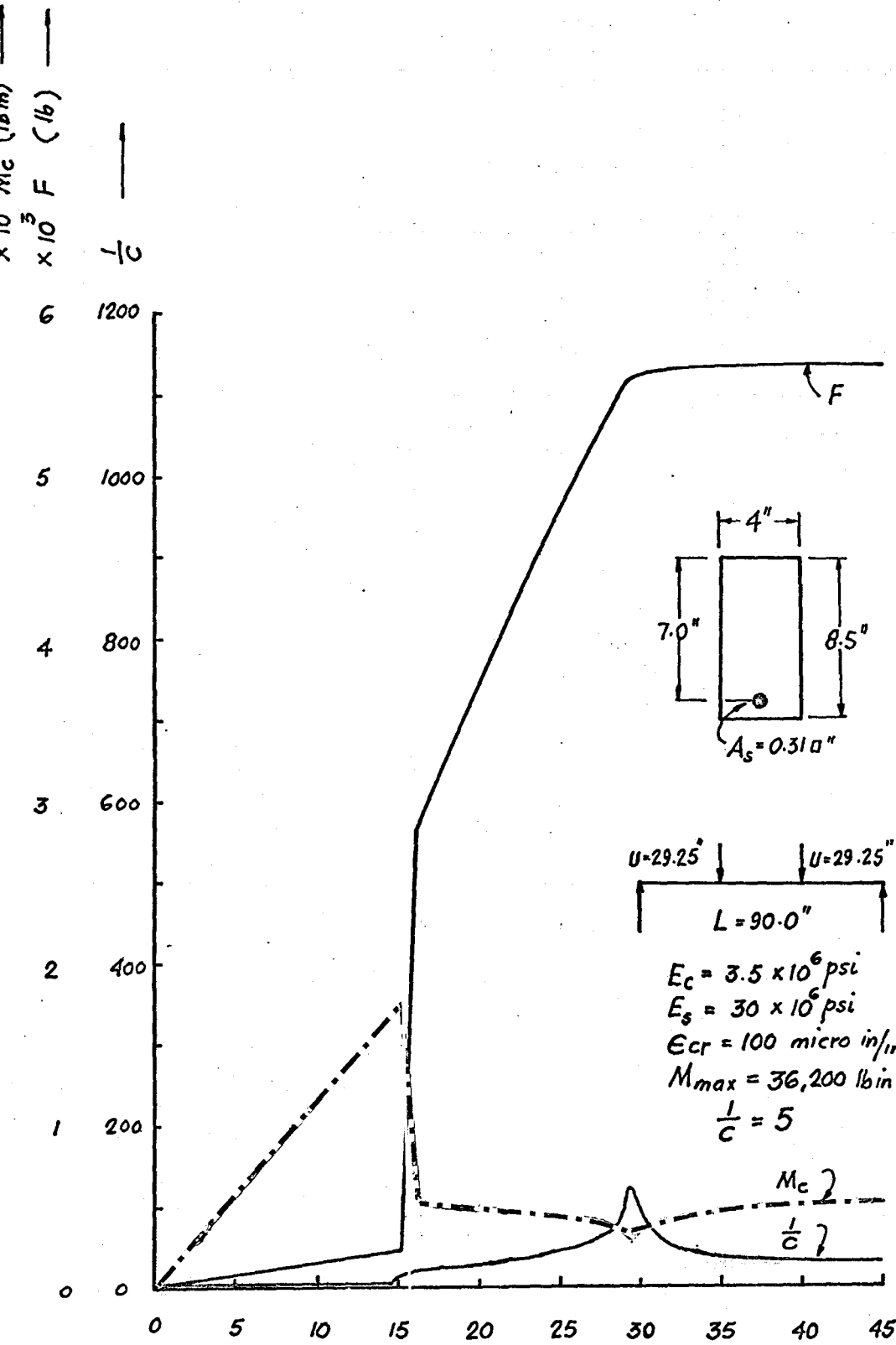
VARIATION IN F, M_c AND $\frac{1}{C}$ ALONG THE LENGTH OF A BEAM.

FIG. 3.26

3.3.4 Fig. 3.27a shows the effect of the ratio of the design load, λ, and the percentage of steel, p, on the values of strain under the point load. The strains exhibit a linear variation with λ. It may also be observed that an increase in the percentage of steel reduces the magnitude of the compressive strain, Fig. 3.27b, for a given load and magnitude of $\frac{1}{C}$.

Fig. 3.28 shows the effect of $\frac{1}{C}$ on the steel strains. For higher values of $\frac{1}{C}$ (i.e. 50 and above), the strains are not markedly affected by a change in $\frac{1}{C}$, as indicated by the straight line portion of these curves. For small values of $\frac{1}{C}$, the effect on strains is significant. The tob fibre strain, ε_{ct}, in the concrete as well as the bottom steel strain, ε_{sb}, show a rapid increase in their magnitude, and strain, ε_{st}, at the top fibre of steel shows a rapid decrease in the magnitude with a decrease in the value of $\frac{1}{C}$.

3.4 Degree of Interaction, $\frac{F}{F'}$, in a Cracked Beam

It was observed in an earlier section of this chapter, that cracking in a reinforced concrete beam leads to an increase in the magnitude of the interaction coefficient, $\frac{1}{C}$, caused by reduction in the cross-section of the uncracked concrete. This in turn causes an increase in the degree of interaction, $\frac{F}{F'}$. (The bond-slip modulus k is assumed to remain constant throughout the entire loading range).

Figure (a): Strains (micro in/in) vs λ, showing curves ϵ_{sb}, ϵ_{ct}, and ϵ_{st}.

Figure (b): Strain (micro in/in) vs p, showing curve ϵ_{ct}.

Beam diagram details:
29.25" and 29.25" load points
$L = 90.0"$
4" width
7.0", 9.5"
$A_s = 100 \, bd \cdot p$

$M_{max} = 36200 \lambda$ lbin.
$\epsilon_{cr} = 100$ micro in/in.
$E_s = 30 \times 10^6$ psi
$E_c = 3.5 \times 10^6$ psi
$\dfrac{1}{c} = 5$.
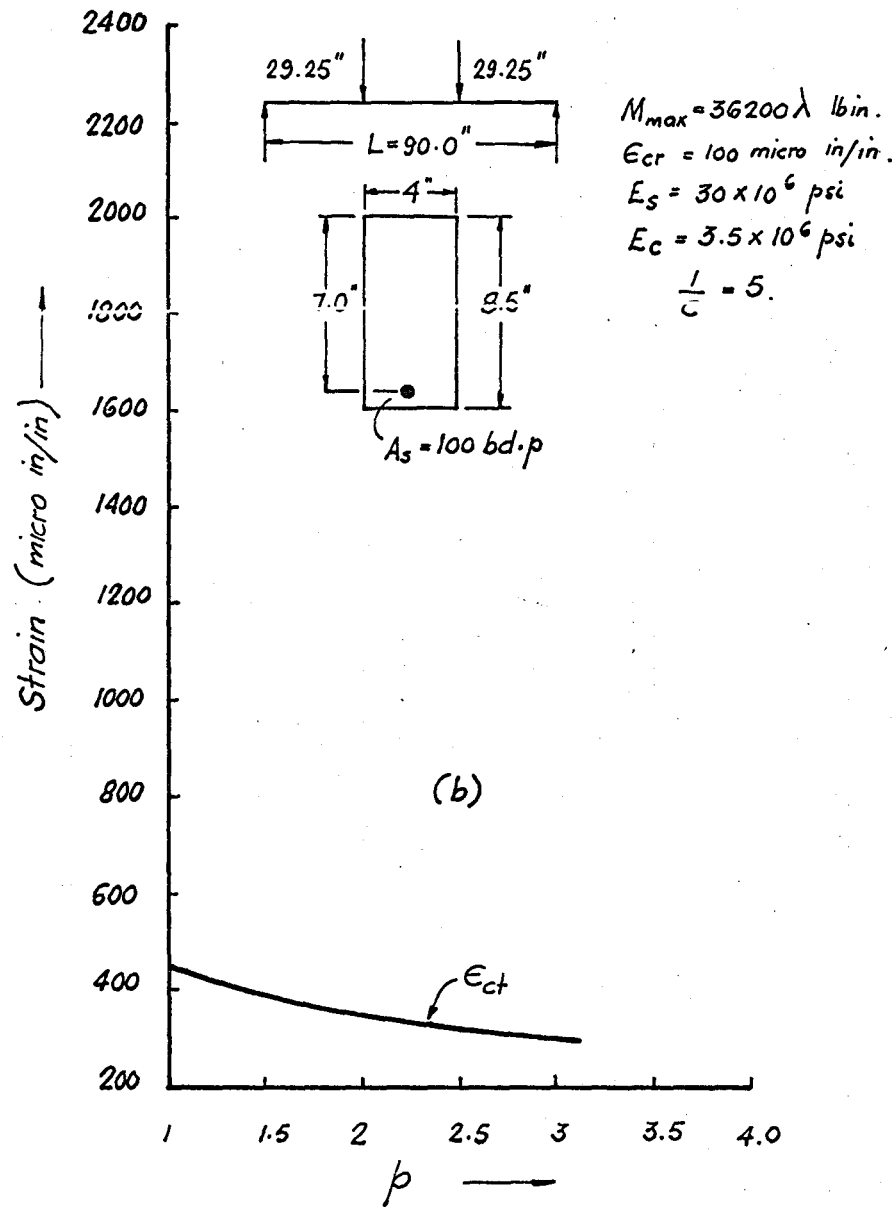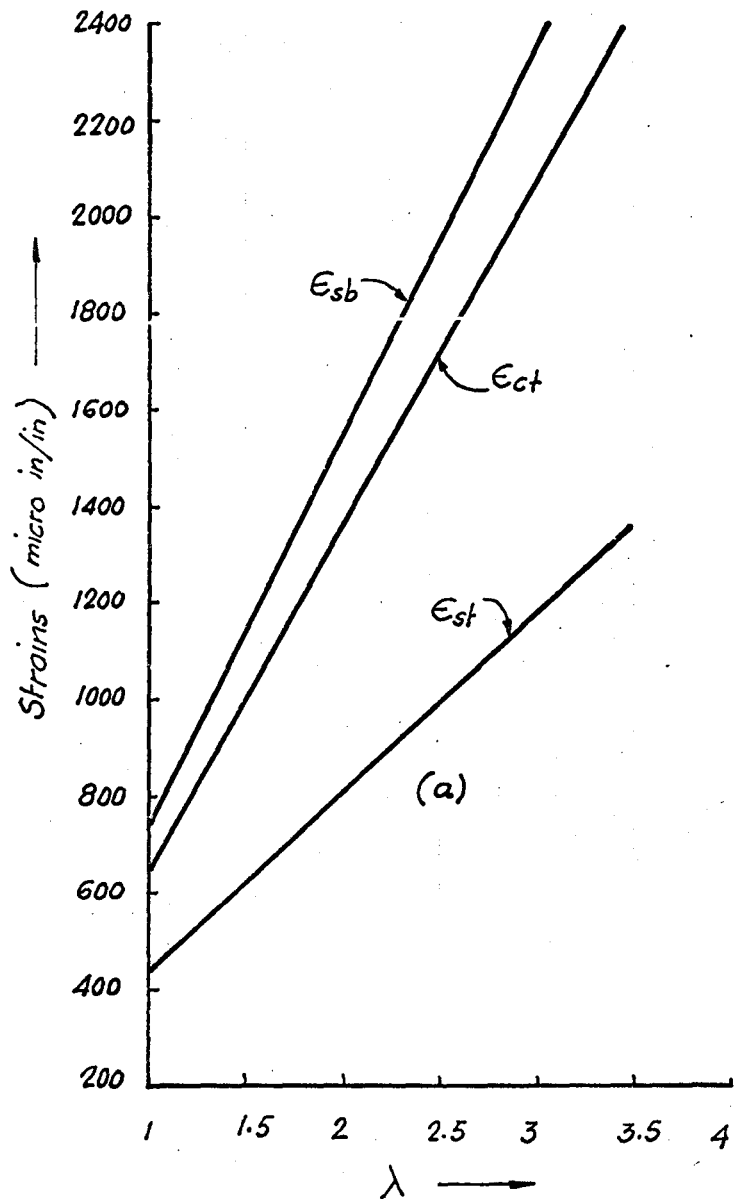
STRAINS UNDER THE LOAD POINT - EFFECT OF λ AND p.

FIG. 3.27 a & b
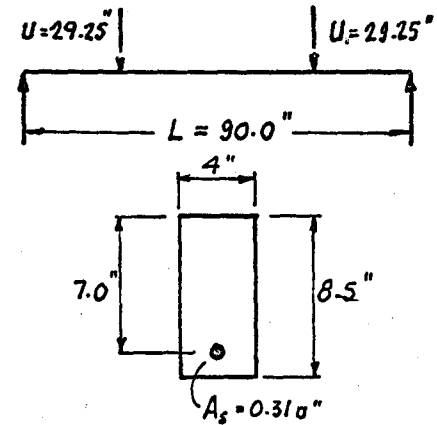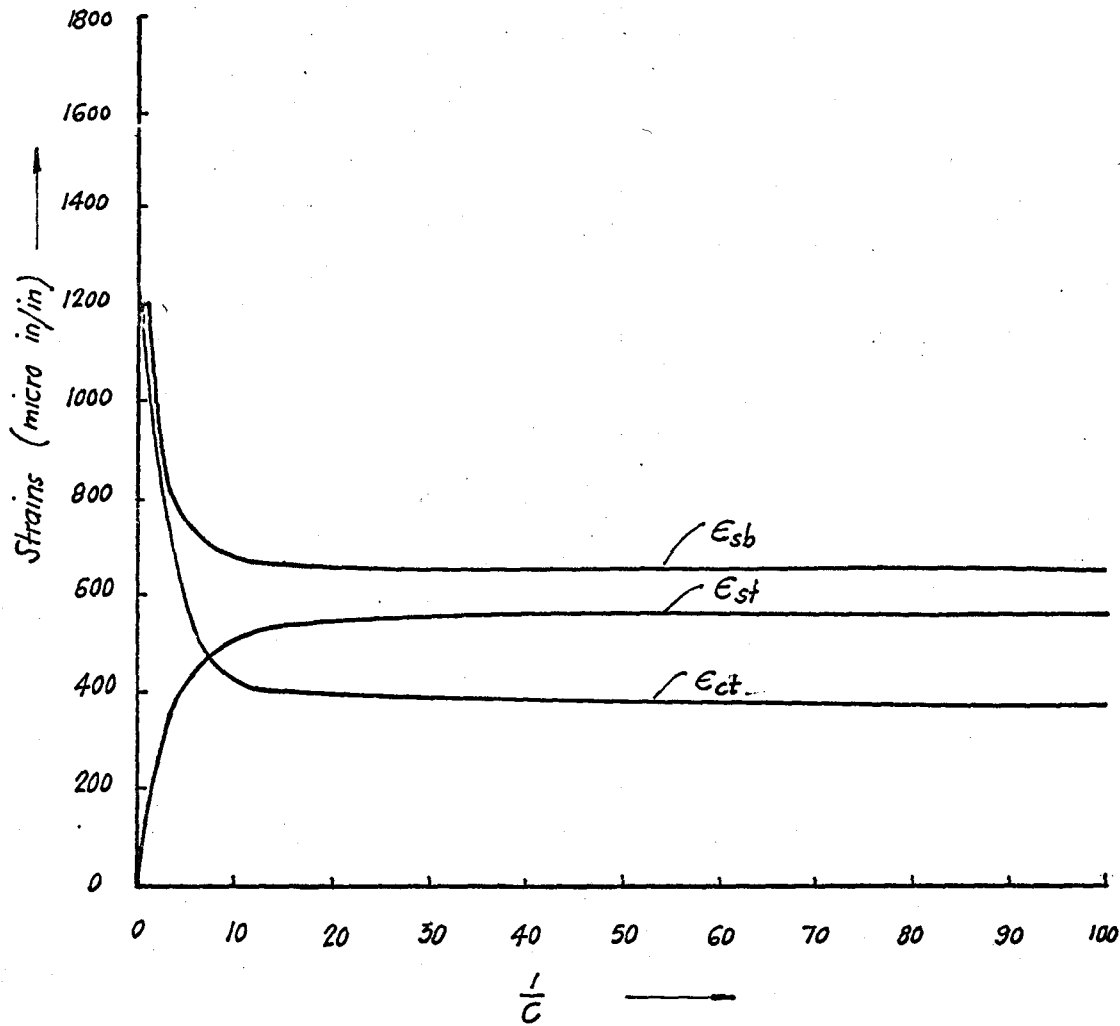
EFFECT OF $\frac{1}{C}$ ON STRAINS UNDER THE LOAD POINT

FIG. 3.28

3.4.1 Figs. 3.29, 3.30 and 3.31 show the distribution of $\frac{F}{F'}$ for a cracked, as well as uncracked beam, for the Cases I, II, and III respectively. These cases have already been described in Chapter II.

It may be seen that while the distribution of the degree of interaction, $\frac{F}{F'}$, remains the same in the uncracked portion, it increases considerably in the cracked portion of the beam. At certain places, $\frac{F}{F'}$ approaches unity as in the case of complete interaction. The terminal distribution of $\frac{F}{F'}$ does not show any significant decrease in magnitude in the region of the load points as has been found for the un-cracked prismatic section, see Fig. 3.29 and 3.30. This is due to an increase in the magnitude of $\frac{1}{C}$ because of reduction of the concrete cross-section and that the bond-slip modulus is assumed to remain constant throughout the entire loading process. In reality the bond-slip modulus is curvilinear. Mathey and Watstein[5] from their tests on reinforced beams with web reinforcement, obtained non-linear bond-slip characteristics.

Bresler and MacGregor[20] in their review state, "The slip is related to interface shear between steel and concrete, usually called "bond stress". As a result, a "bond-slip" law must be formulated to obtain meaningful determination of the stress in steel and concrete."

A curvilinear bond-slip characteristic would have
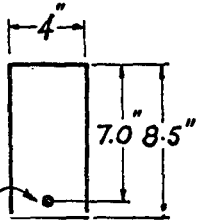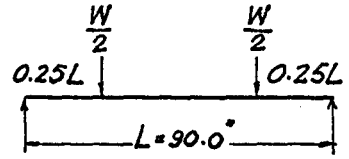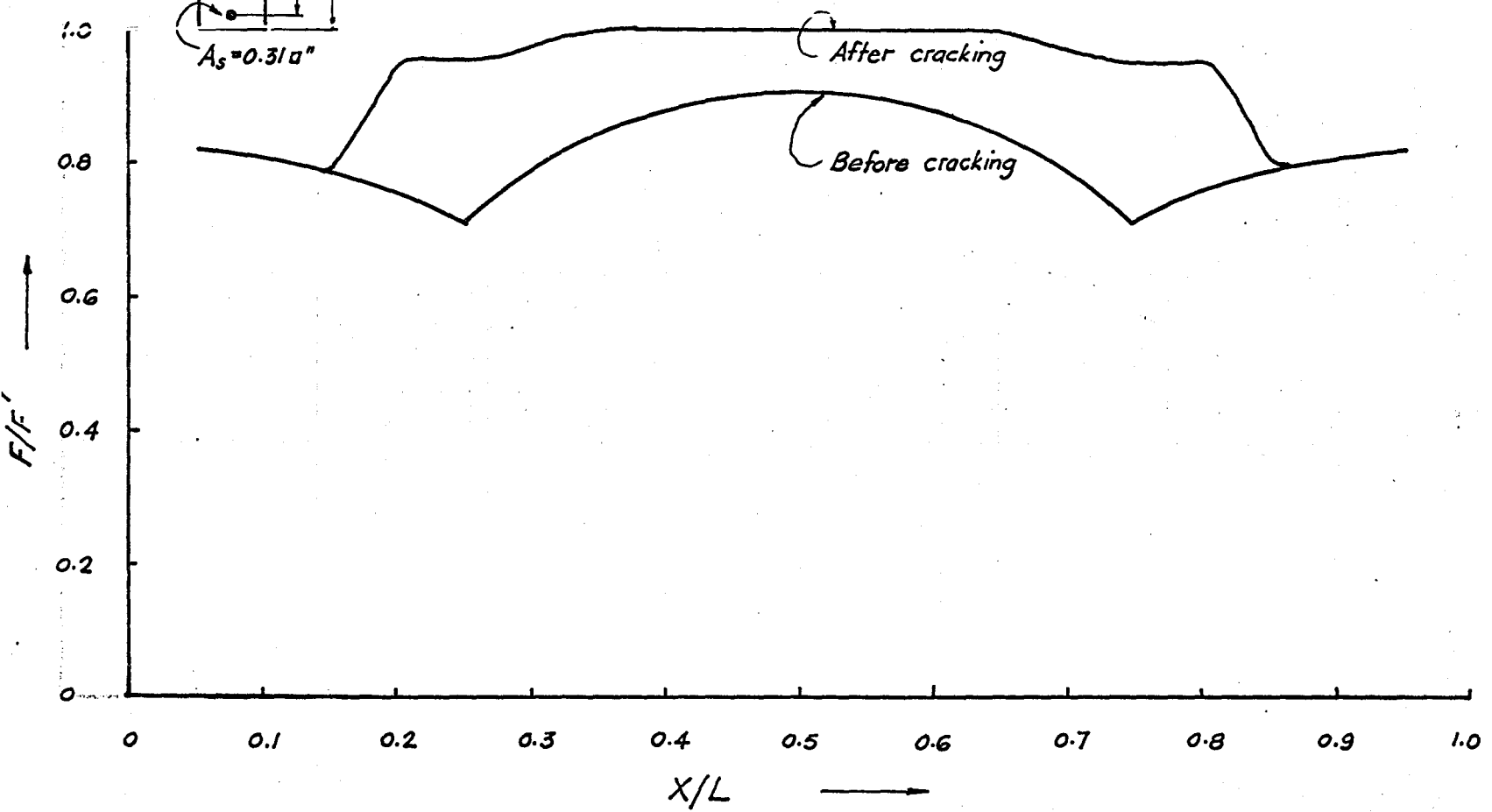
VARIATION IN F/F' VALUE BEFORE AND AFTER CRACKING - CASE I

FIG. 3.29

94
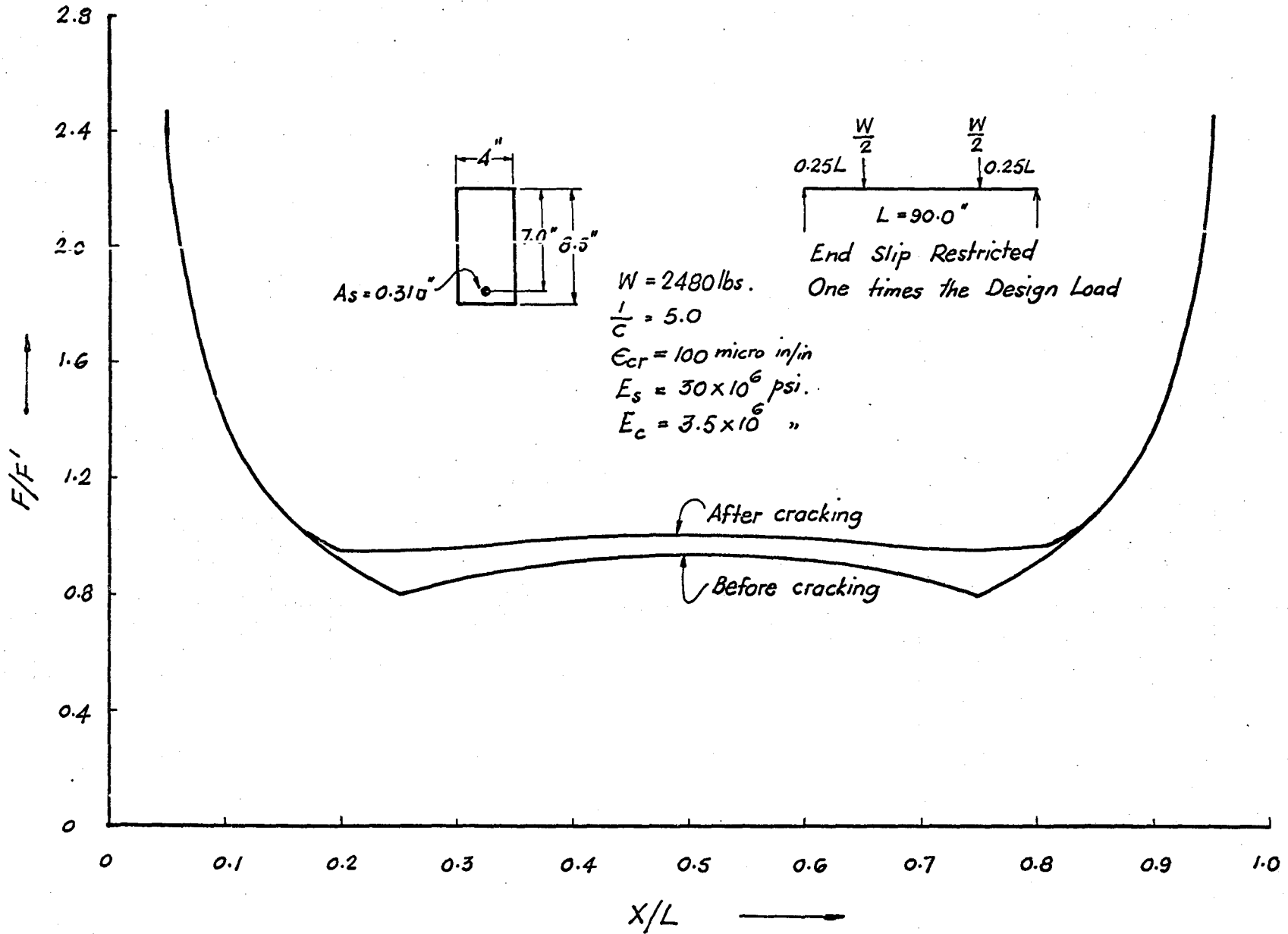
VARIATION IN F/F' VALUE BEFORE AND AFTER CRACKING - CASE II

FIG. 3.30

Figure details (as labelled in the figure):

- 4"
- 7.0"
- 8.5"
- $A_s = 0.31\,□''$
- $\frac{W}{2}$ $\frac{W}{2}$
- 0.25L   0.25L
- L = 90.0"
- One Times the Design Load
- After cracking
- Before cracking
- $W = 4290\ lbs.$
- $\epsilon_{cr} = 100\ micro\ in/in.$
- $E_s = 30 \times 10^6\ psi$
- $E_c = 3.5 \times 10^6\ psi$
- $\frac{I}{C} = 5.$
- F/F'
- X/L
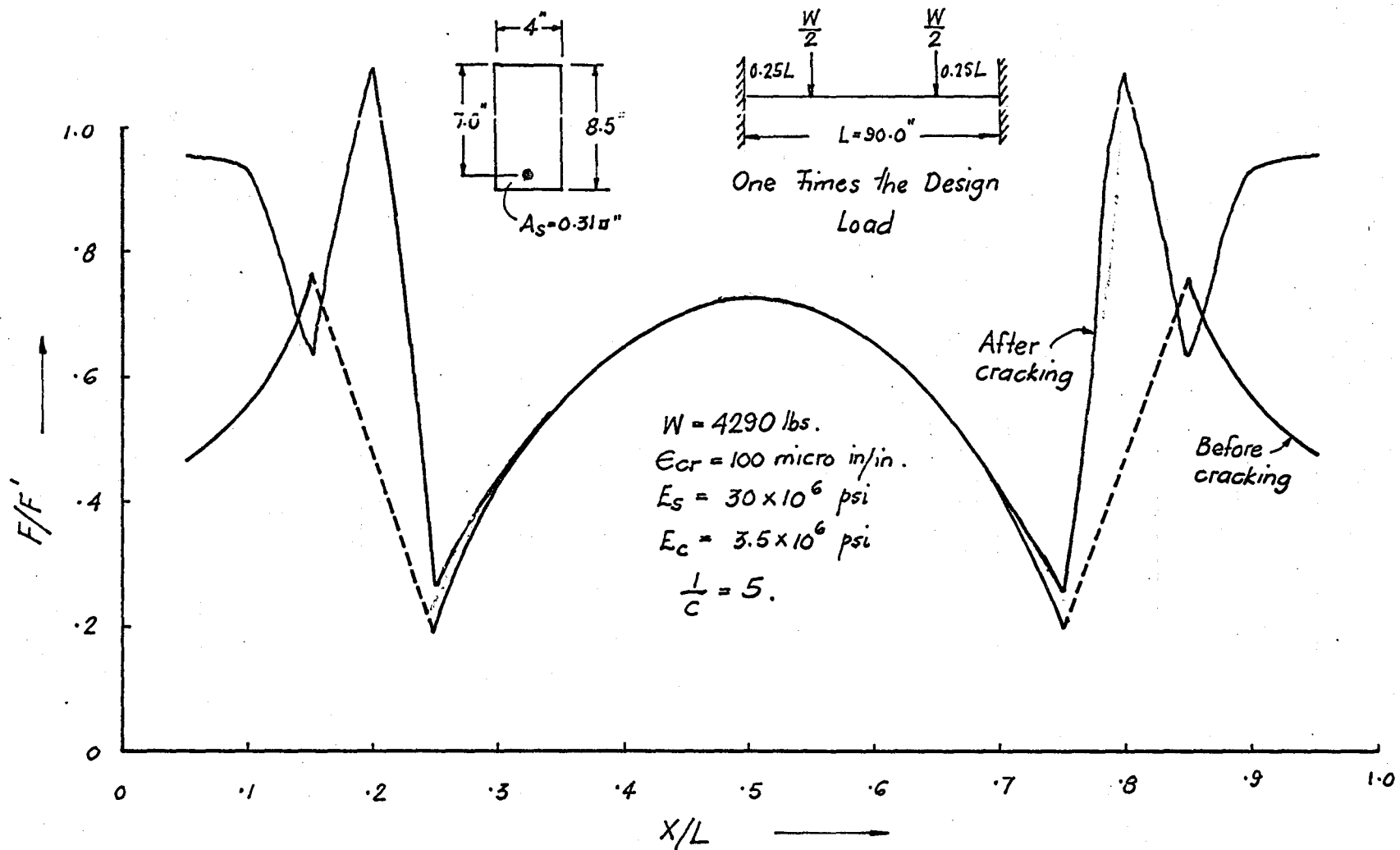
VARIATION IN F/F' VALUE BEFORE AND AFTER CRACKING - CASE III

FIG. 3.31

the effect of offsetting the increase in $\frac{1}{C}$ due to geometric change in the cross-section.

3.4.2   In an actual beam, the degree of interaction, $\frac{F}{F'}$, in an uncracked region of the cracked beam would be affected by the cracking.   This, however, does not show in these computations, because this method of analysis is to compute the magnitude of $\frac{F}{F'}$ only at the section under consideration and does not reflect the geometry of the cross-section in the other parts of the beam.

Therefore an approach which could account for the effect of other sections of the beam, such as the Finite Difference or Finite Element Methods incorporating a non-linear bond-slip characteristic would impart mathematically more correct results.

CHAPTER IV

INFLUENCE LINES

4.1 Influence Lines for Crack Heights

It was observed in the computation of the flexural crack profiles that for a particular load position, maximum crack height occurs under the load point. By moving the point loads along the length of the beam, influence lines for the crack height were computed. These curves show maximum heights to which a flexural crack can possibly go for point loads which produce the same magnitude of moment (36200 lb-in) at the load points, as they are moved outwards from the midspan of the beam. It has been demonstrated in Fig. 3.9 that the height of a crack due to flexure is greatest under the load points or that the degree of inter-action, $\frac{F}{F'}$, is minimum at the load points Fig. 3.29 and 3.30. The flexural capacity of the beam can be seen to be governed by the conditions at the load points.

Fig. 4.1 shows the Influence Lines for crack height under the load points for the "Typical Beam", which is simply supported and carries two symmetrically placed point loads. The case of Fig. 4.2 is the same as for Fig. 4.1, except that in this case, the solution for $\frac{F}{F'}$ was obtained by imposing the condition of zero slip at the ends (see Fig. 3.30). The computed Influence Lines of Fig. 4.2 are very much the same as the Influence Lines of Fig. 4.1. Thus
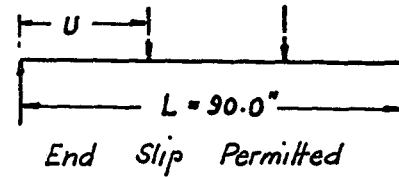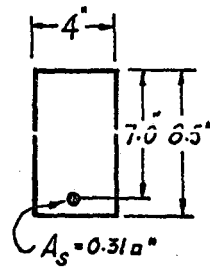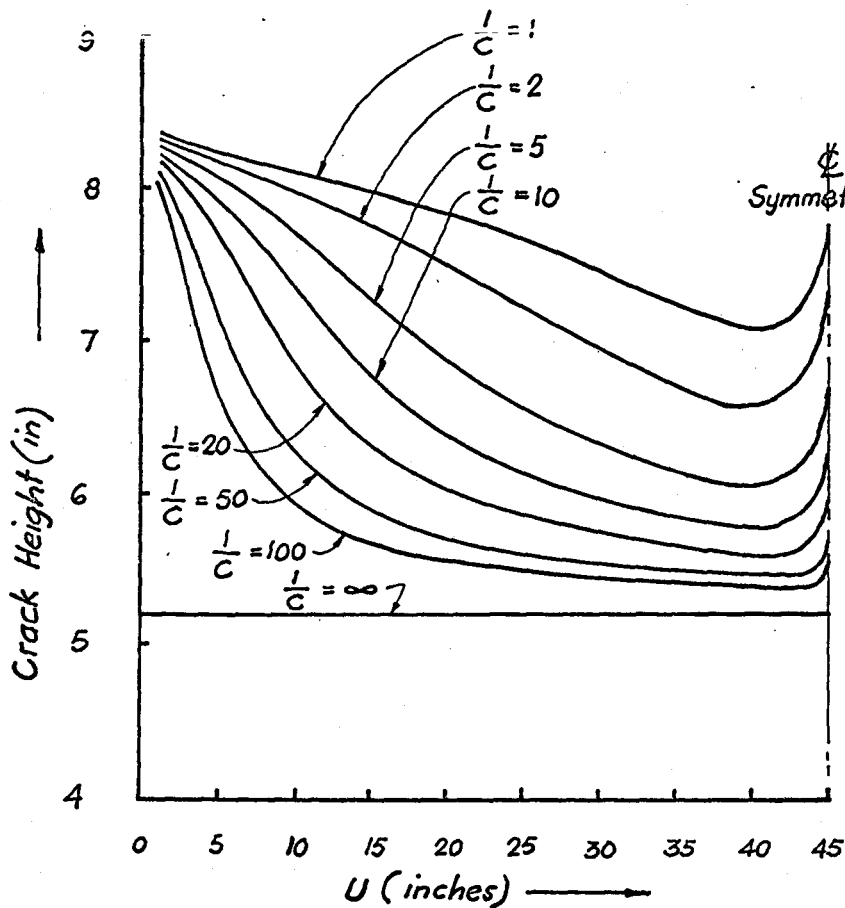
98

EFFECT OF INTERACTION COEFFICIENT ON INFLUENCE LINES FOR CRACK HEIGHTS.

FIG. 4.1
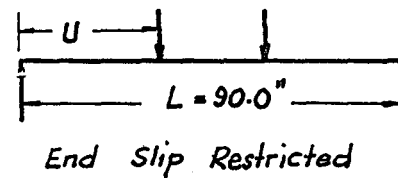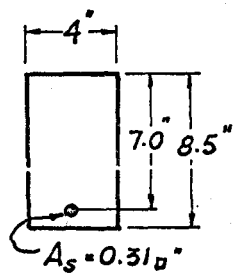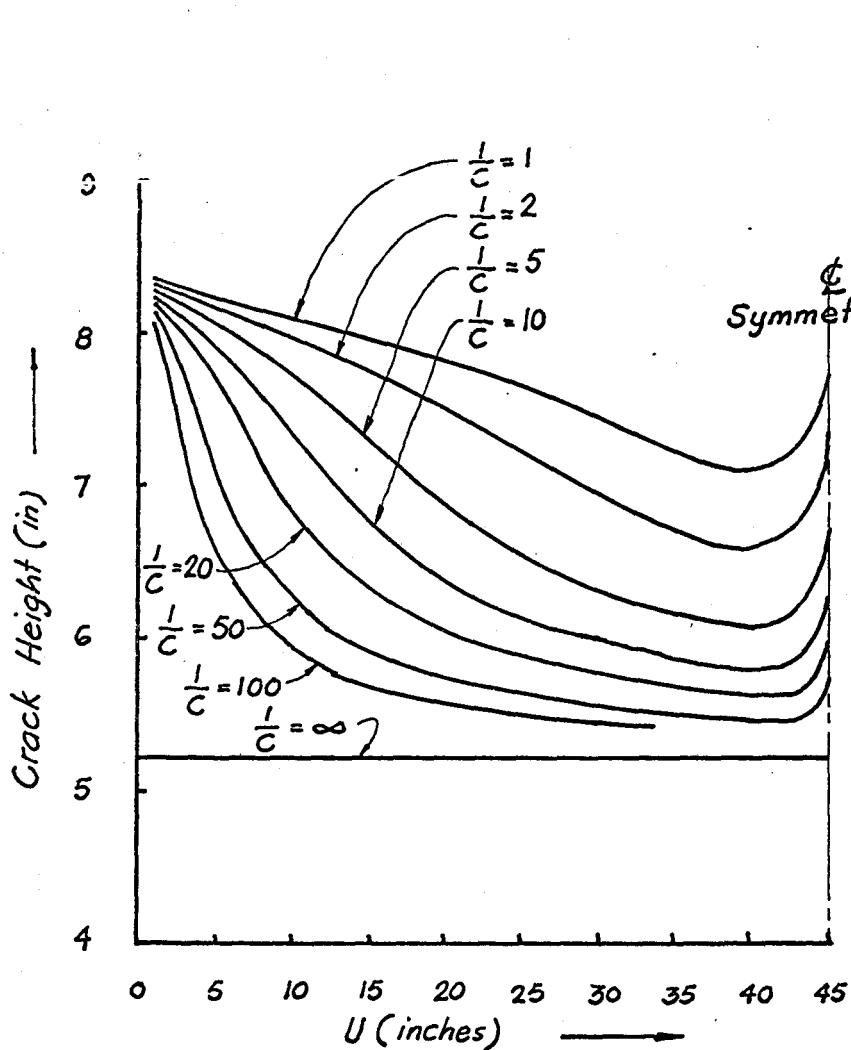
EFFECT OF INTERACTION COEFFICIENT ON INFLUENCE LINES FOR CRACK HEIGHT.

FIG. 4.2

the effect of restriction of end slip on the distribution

of $\frac{F}{F'}$, that was conspicious in an uncracked beam has not

been reflected in computing crack heights. Compare Fig. 2.3

and 2.6 and also Fig. 3.29 and 3.30. This is probably due

to the assumption that the bond-slip characteristic of a

reinforced concrete beam is linear.

It may also be observed that the magnitudes of crack

height are larger for a smaller value of the shear span, u.

The lowest points on these curves occur near the midspan.

As is the case for the crack profiles $\frac{1}{C}$ has a signi-

ficant effect on the Influence Lines for the crack heights.

Influence curves for a large value of $\frac{1}{C}$ are flat in the

middle half of the span, whereas the curves for smaller

values of $\frac{1}{C}$ are flatter in the outer quarter of the span.

This suggests that the flexural capacity of a beam with a

large value of $\frac{1}{C}$ (say 100) would be the same for load

positions within the middle half of the span. On the other

hand, for a medium range value of $\frac{1}{C}$, the flexural capacity

of the uncracked beam varies with the position of the load

point.

Increase in the moment carrying capacity for a

smaller value of the shear arm ratio, $\frac{u}{d}$, have been observed

in the results of experiments by Kani[7] and Leonhardt and

Walther[4].

$E_c = 3.5 \times 10^6 \ lb/in^2$

$E_s = 30 \times 10^6 \ lb/in^2$

$\epsilon_{cr} = 100 \ micro \ in/in$

$M = 36200.0 \ lb\text{-}in$

$\frac{I}{C} = 5$
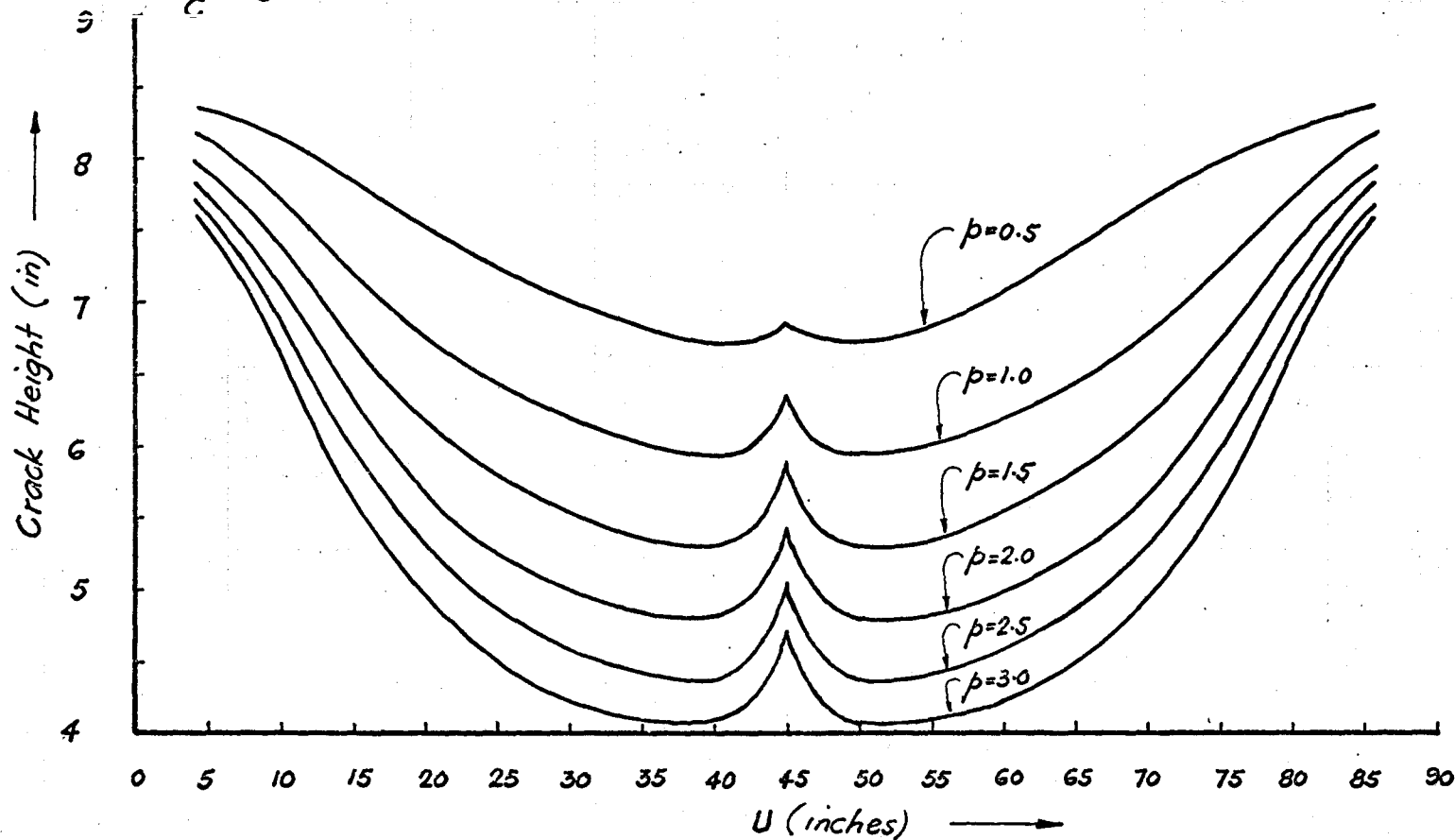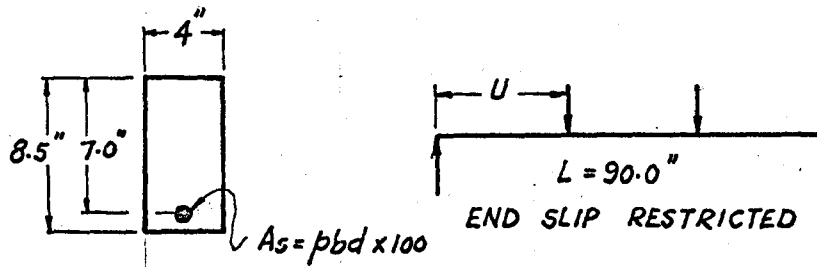
EFFECT OF PERCENTAGE OF STEEL ON INFLUENCE LINES FOR CRACK HTS.

FIG. 4.3

4.1.1 Effect of percentage of steel reinforcement, p.

Fig. 4.3 shows the Influence Lines for the crack heights in the "Typical Beam" with a value of $\frac{1}{C} = 5$, and for varying percentage of steel. Increase in the percentage of steel, p, has been found to result in lesser crack heights and vice versa, and p has a remarkable influence on the flexural capacity of a reinforced concrete beam. It may also be noted that although increase in p lowers crack height considerably in central portion of beam reflecting increase in strength, towards the end of the beam, the effect of loss of interaction markedly reduces the flexural capacity and the reduction of crack height is comparatively smaller.

4.2 Influence Lines for Strains

Fig. 4.4 and 4.5 show the Influence Lines for concrete top strain and mid-height steel strain corresponding to the Influence Lines for the crack height and values of $\frac{1}{C}$ shown in Fig. 4.1 and 4.3 respectively.

Fig. 4.4 indicates the effect of the magnitude of $\frac{1}{C}$ on the values of strains. It may be noticed that the effect of $\frac{1}{C}$ is more pronounced on the concrete top strain, ε_{ct}, than on the mid-height steel strain, ε_{sm}. For larger values of $\frac{1}{C}$, strain values (ε_{ct} as well as ε_{sm}) are constant over most of the span except near the ends where ε_{ct} increases rapidly in magnitude. On the other hand, for small values of $\frac{1}{C}$, ε_{ct} varies significantly from point to point over the
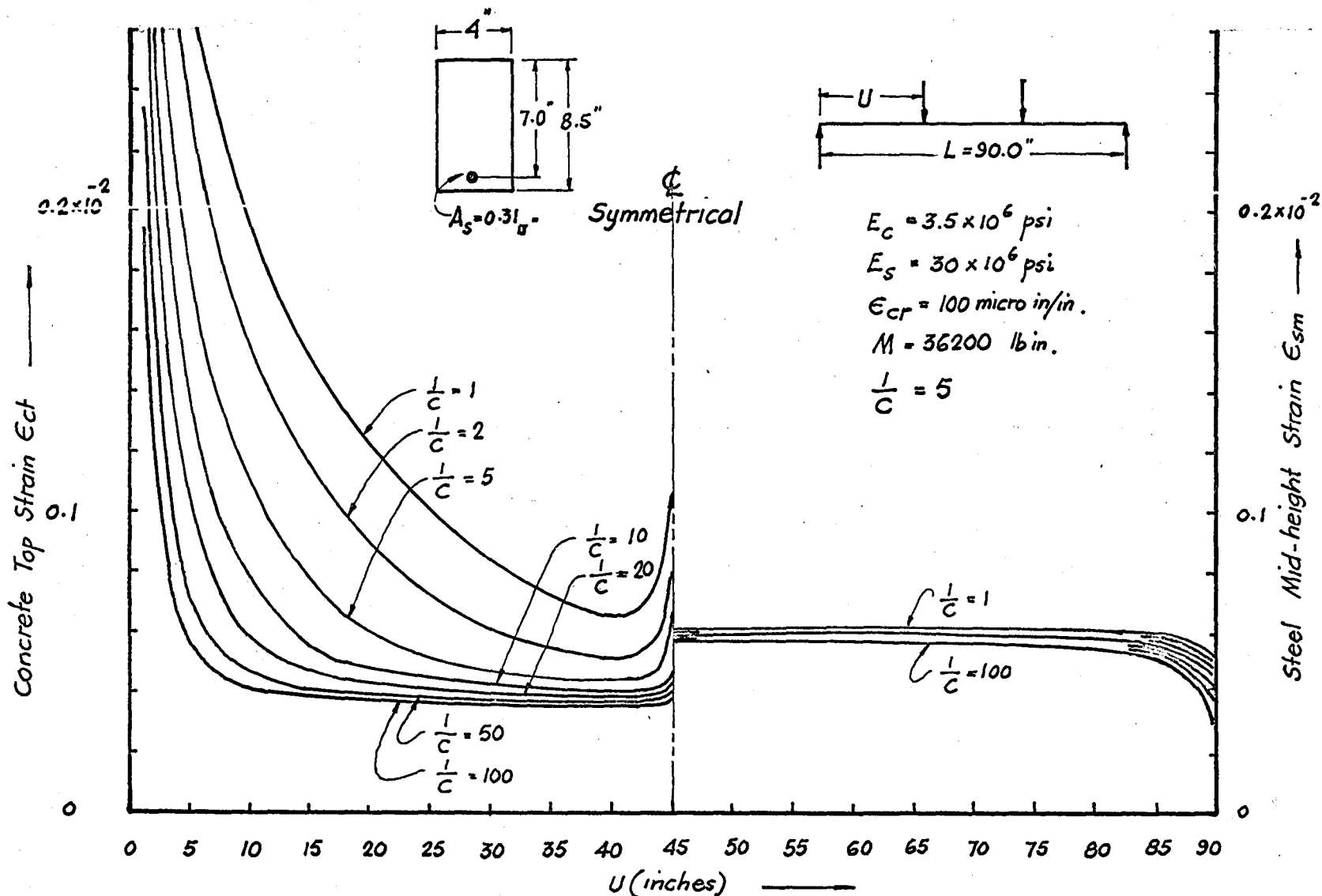
EFFECT OF INTERACTION COEFFICIENT ON THE INFLUENCE LINES FOR STRAINS

FIG. 4.4
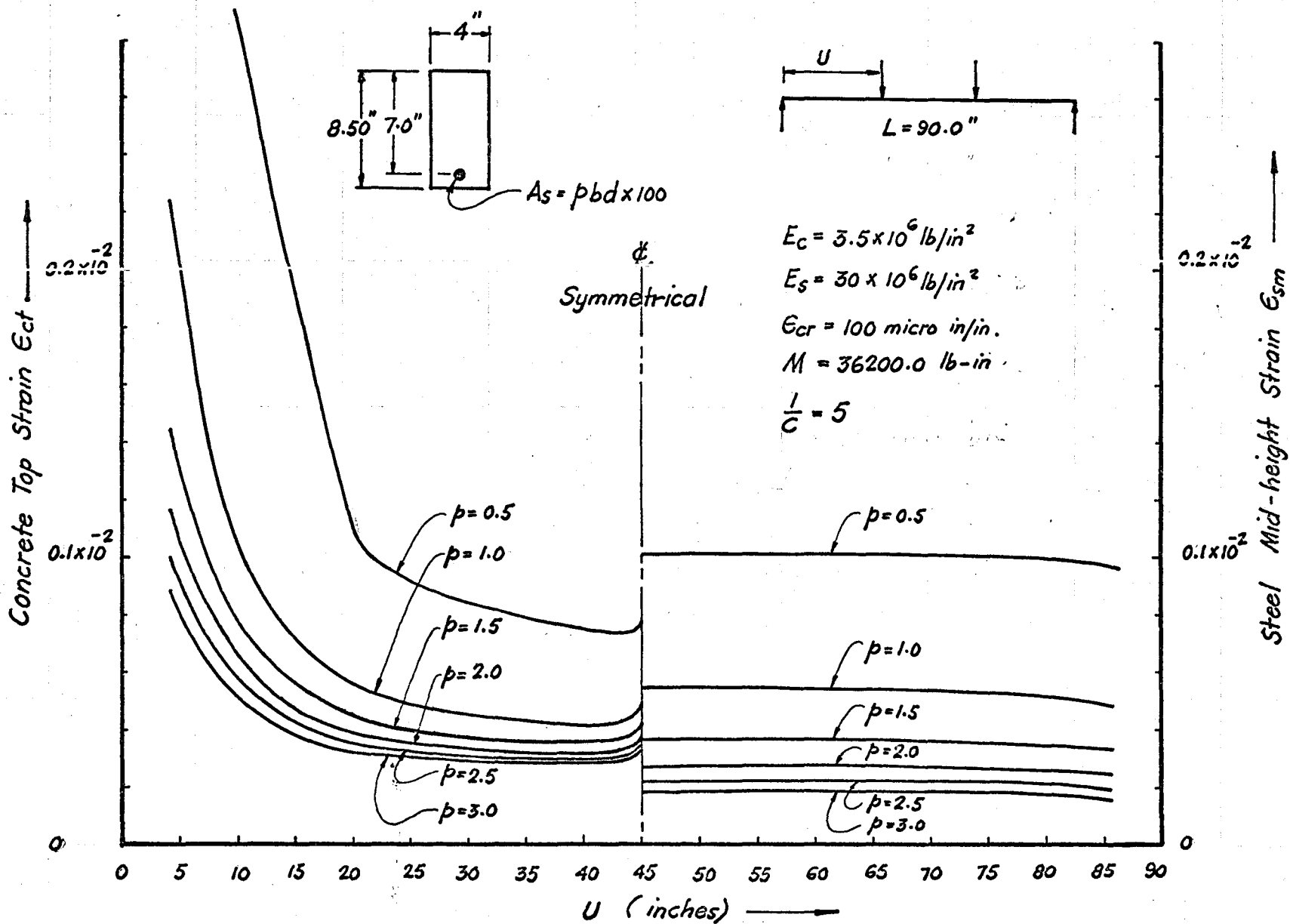
EFFECT OF PERCENTAGE OF STEEL ON THE INFLUENCE LINES FOR STRAINS

FIG. 4.5

entire span.

It may also be observed that when point load is near the mid span, effect of $\frac{1}{C}$ is the least, but as the point load towards the ends of the beam, effect of variation in $\frac{1}{C}$ is more pronounced.

Fig. 4.5 shows the influence of p on the Influence Lines for strains, for a case where $\frac{1}{C} = 5$. It may be seen that increase in p results in decrease in magnitude of the strain in top fibre of concrete ε_{ct} as well as the mid-height strain in steel ε_{sm}. For high percentage of steel, p, the values of ε_{ct} are constant in the middle half of the span, whereas for small values of p, it shows significant variation in magnitude. Fig. 4.5 also shows that ε_{sm} is not affected much by variation in the location of the point load.

A comparison between Fig. 4.4 and 4.5 will show that increase in $\frac{1}{C}$ affects ε_{ct} more than ε_{sm} and an increase in p has more effect on ε_{sm} than on ε_{ct}.

CHAPTER V

MOMENT CARRYING CAPACITY

5.1   The Influence Line plots of Fig. 4.5 give the magnitude of the top fibre concrete strain, ε_{ct}, and the mid-height strain, ε_{sm}, in the steel at the load point for a constant applied moment. Each curve shows the effect of particular value of the steel percentage p. It can be seen that by limiting the magnitude of strains in the steel and the concrete, the strength of a beam can be made to be governed by either the steel or the concrete or both. For example, assume that the crushing strain, $\varepsilon_{ct_{max.}}$, of concrete and yield strain, $\varepsilon_{sm_{max.}}$, in steel are 1000 and 500 micro in/in. respectively. For a beam with p = 0.5 in Fig. 4.5, it may be seen that ε_{ct} is less than $\varepsilon_{ct_{max.}}$ for values of U between 22 in. and 45 in. and ε_{ct} is greater than $\varepsilon_{ct_{max.}}$ for U = 0 to 22 in. On the other hand, ε_{sm} is greater than the assumed $\varepsilon_{sm_{max.}}$ at all locations of the point load along the span. Therefore, for this beam with p = 0.5, the concrete will govern the strength for U = 0 to 22 in. and the steel will govern the strength from U = 22 in. to the midspan.

For the same values of the limiting strains, if a beam with p = 1.0 is examined, it will be found that the concrete governs the strength for U, only between 0 and 12 in. and for all other locations of the load point up to the

midspan, the steel reinforcement governs the strength.

Similarly for the same beam with p = 3.0, it is only the concrete that governs the strength of the beam, since the value of steel strain never approaches the limiting value.

Thus for certain values of $\varepsilon_{ct_{max.}}$ and $\varepsilon_{sm_{max.}}$, the moment capacity of a section at the load point can be determined analytically. This will be the maximum carried by such a section.

5.2   For computing the Influence Line for maximum moment, $M_{max.}$, at the load points, the dimensions of the "Typical Beam" of Chapter II and case I are considered. It is further assumed that the concrete can withstand a maximum compressive strain, $\varepsilon_{ct_{max.}}$ of 2500 micro in/in. and the steel a maximum tensile strain, $\varepsilon_{sm_{max.}}$, of 1200 micro in/in. The interaction coefficient, $\frac{1}{C}$, is taken as 5. The moment carrying capacities have been computed at the load point as the load point moves along the length of the beam. The values of computed moment capacity are plotted against the shear span and are shown in Fig. 5.1.

5.2.1   It may be observed that the plot of Fig. 5.1 consists of two distinct portions, namely one which slopes downwards, and the other which is almost horizontal. In the sloping part, the concrete reaches the limiting strain and so the strength of the beam is governed by concrete; in the
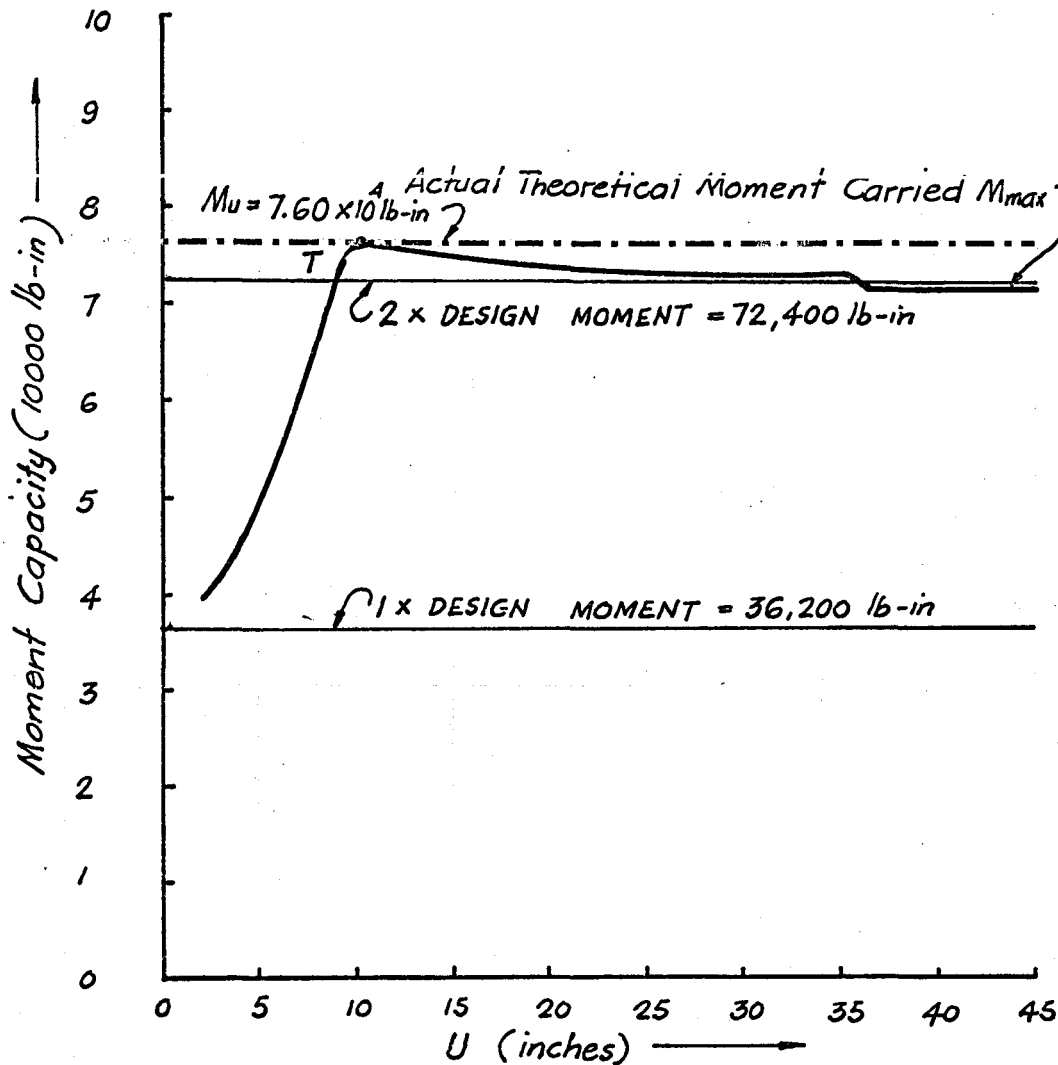
MOMENT CARRYING CAPACITY OF THE "TYPICAL BEAM."

FIG. 5.1
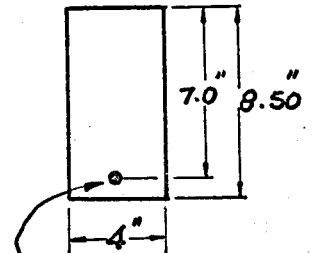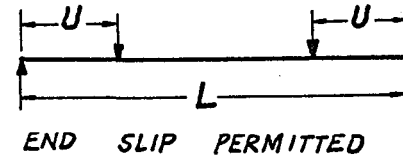
horizontal part the steel governs the strength of the beam. Between the two parts there is a transition point where both concrete as well as steel reach the limiting strains.

5.2.2 The region in which concrete strain governs, the capacity of the beam ranges between 0.6 and 2.1 times the design moment and varies with the location of the load point, whereas in the part where steel strain governs, the moment capacity is fairly uniform and is generally greater than two times the design moment.

5.2.3 The ultimate strength, M_u, of the "Typical Beam" has been computed by the conventional method adopted by Kani[12]

$$M_u = A_s f_y (d - \frac{a}{2}) \qquad\qquad 5.1$$

where
$$a = \frac{A_s f_y}{.85 \; fc.b}$$

and
$$\begin{cases} f_y = E_s \cdot \varepsilon_{sm_{max}} \\[2mm] f_c = E_c \cdot \varepsilon_{ct_{max}} \end{cases}$$

and is indicated by a horizontal line in Fig. 5.1.

A comparison of M_{max} and M_u shows that between $u = 0$ and 10 in., $\frac{M_{max}}{M_u}$ is less than unity. Near the transition point $\frac{M_{max}}{M_u}$ is more than unity and between $u = 12$ in. and the mid span $\frac{M_{max}}{M_u}$ is slightly less than unity.

5.2.4   Experimental data obtained by Kani[10] for a large number of beams tested with two symmetrical load points, are plotted as $\frac{M \text{ test}}{M_u}$ versus the shear arm ratio, $\frac{u}{d}$. A typical plot is shown in Fig. 5.2. It may be observed that the portion VTE (Fig. 5.2) resembles in shape, the computed curve shown in Fig. 5.1. However, in Fig. 5.1, for small values of u, no increase in the computed value, M_{max} is observed. The transition point, T, in Fig. 5.2 is located comparatively nearer to the mid span, than in Fig. 5.1.

5.3   Kani found that the relative beam strength versus $\frac{u}{d}$ plots are influenced by parameters, such as percentage of steel, p, concrete strength, f_c, and depth of the beam. Consequently the effect of certain parameters on the computed values of the flexural capacity have been investigated and are discussed in the following.

5.3.1   Restriction of Slip at Ends of Beam

Fig. 5.3 shows the Influence Line of the moment carrying capacity for Case II, in which the slip at the ends of the beam has been assumed to be zero (due to end anchorage). A comparison of this with Fig. 5.1, shows that both influence lines are very much the same. Therefore, the effect of the end slip restriction does not affect the magnitude of the maximum moments carried by the beam.
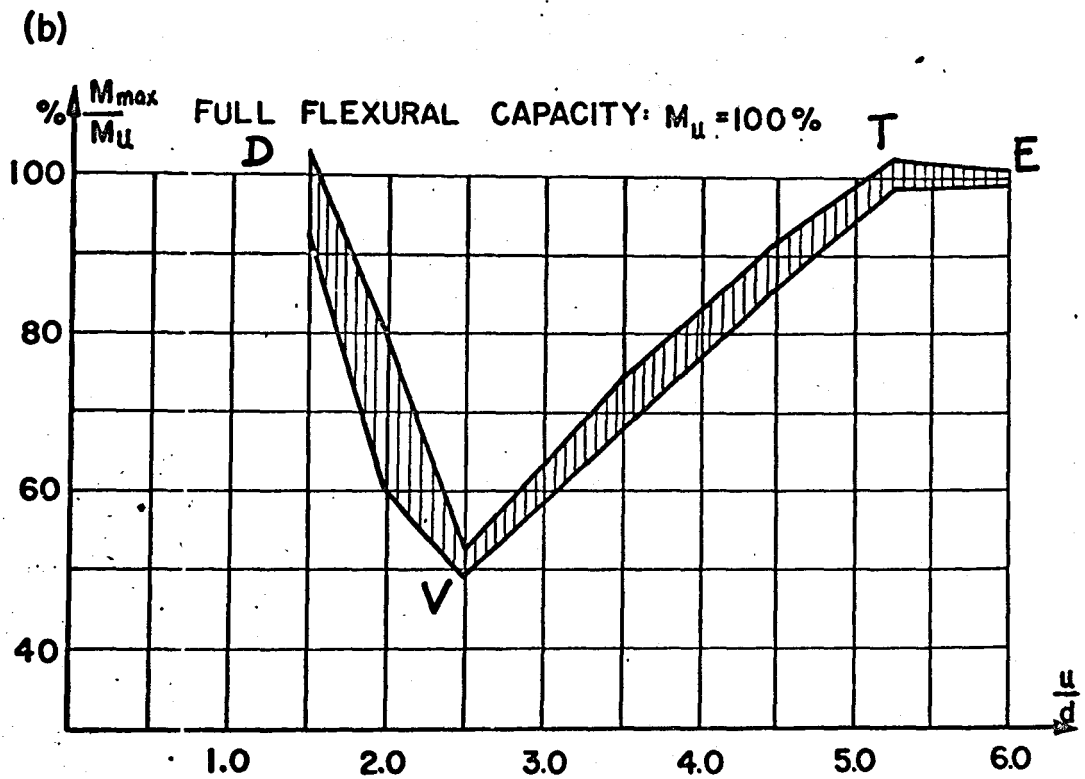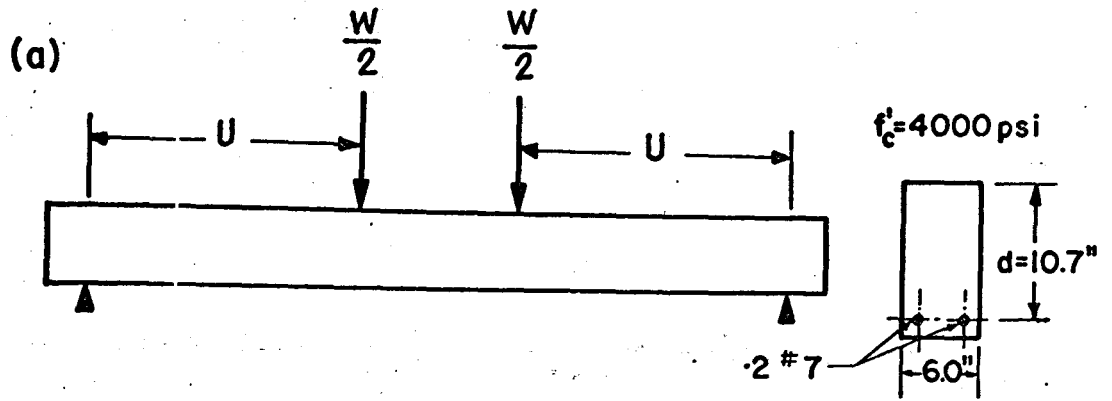
Beam capacities versus u/d ratios of the Toronto Test Series C

DUE TO KANI

FIG. 5.2
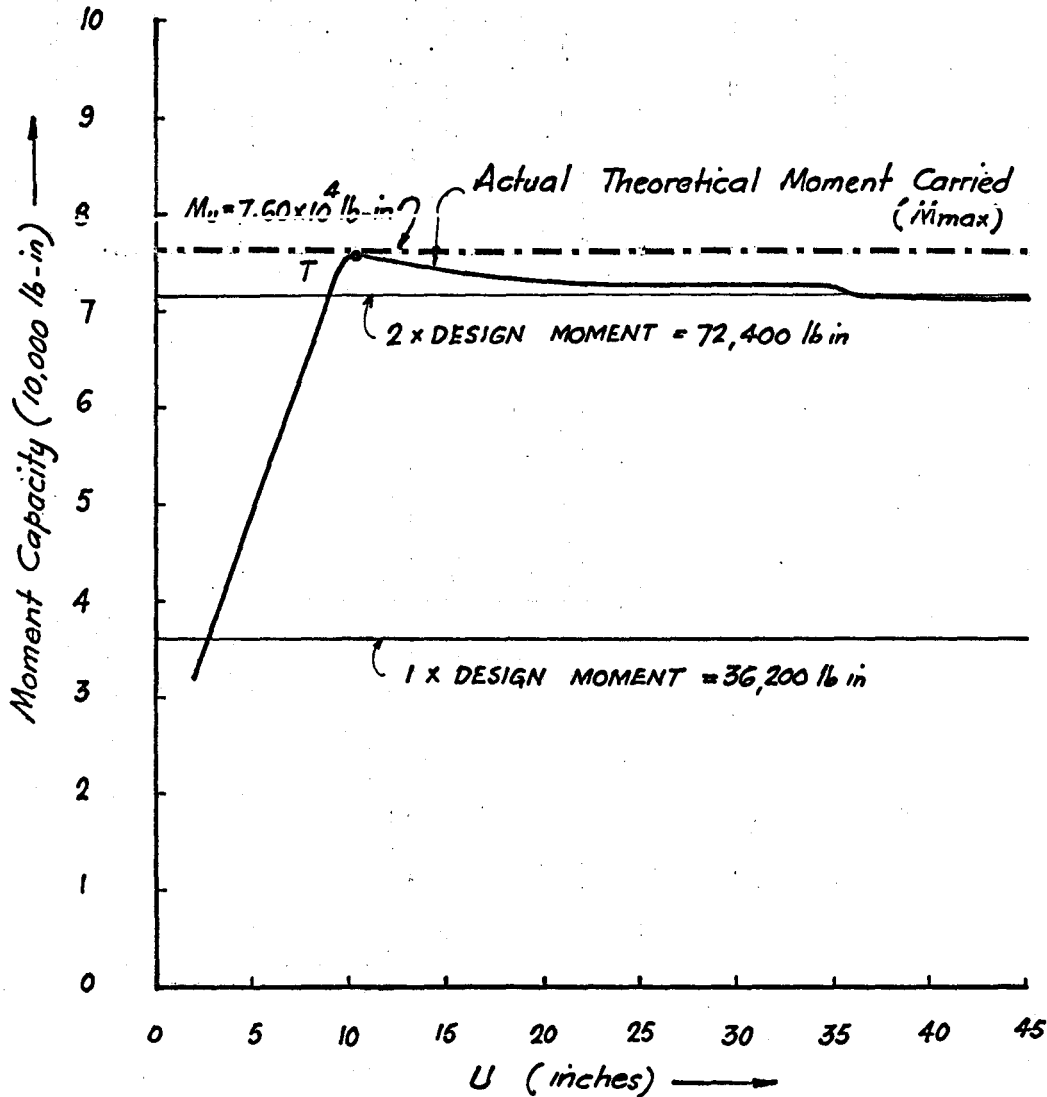
MOMENT CARRYING CAPACITY OF THE "TYPICAL BEAM."

FIG. 5.3
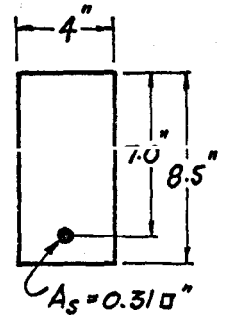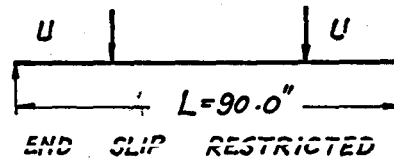
5.3.2 Influence of the Interaction Coefficient, $\frac{1}{C}$

Fig. 5.4 shows plots of moment carrying capacities for case II as in section 5.3.1 but with various values of $\frac{1}{C}$ (= 10, 8, 6, 4, 2 and 1). It may be noticed that decrease in the value of $\frac{1}{C}$ results in moving the transition point towards the centre of the beam. It is also interesting to note that while an increase in $\frac{1}{C}$ increases the moment capacity in the region to the left of the transition point, a decrease in capacity results to the right of the transition point. This means that increase in $\frac{1}{C}$ decreases the strength where the steel strain is the governing factor and increases the strength where the concrete strain is the governing factor.

Kani[10] in evaluating the influence of bond stated "the better the bond, the lower the diagonal load- (moment) carrying capacity". This can be said to apply to the beam in Fig. 5.4 at locations to the right of the transition where a slight reduction in moment capacity results from an increase in the interaction coefficient, $\frac{1}{C}$. An increase in the initial value of the interaction coefficient represents an increase in the bond-slip modulus, k.

5.3.3 Influence of the Percentage of Steel, p.

Figs. 5.5a and 5.5b show the influence line of the computed maximum moment carried by the section at the load point, $M_{max.}$, and the relative moments, $\frac{M_{max.}}{M_u}$ versus shear
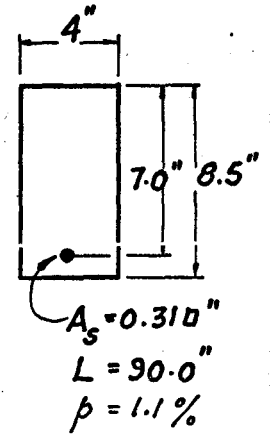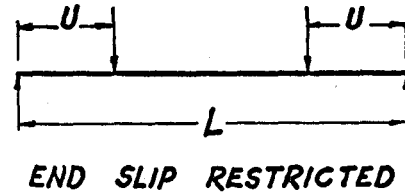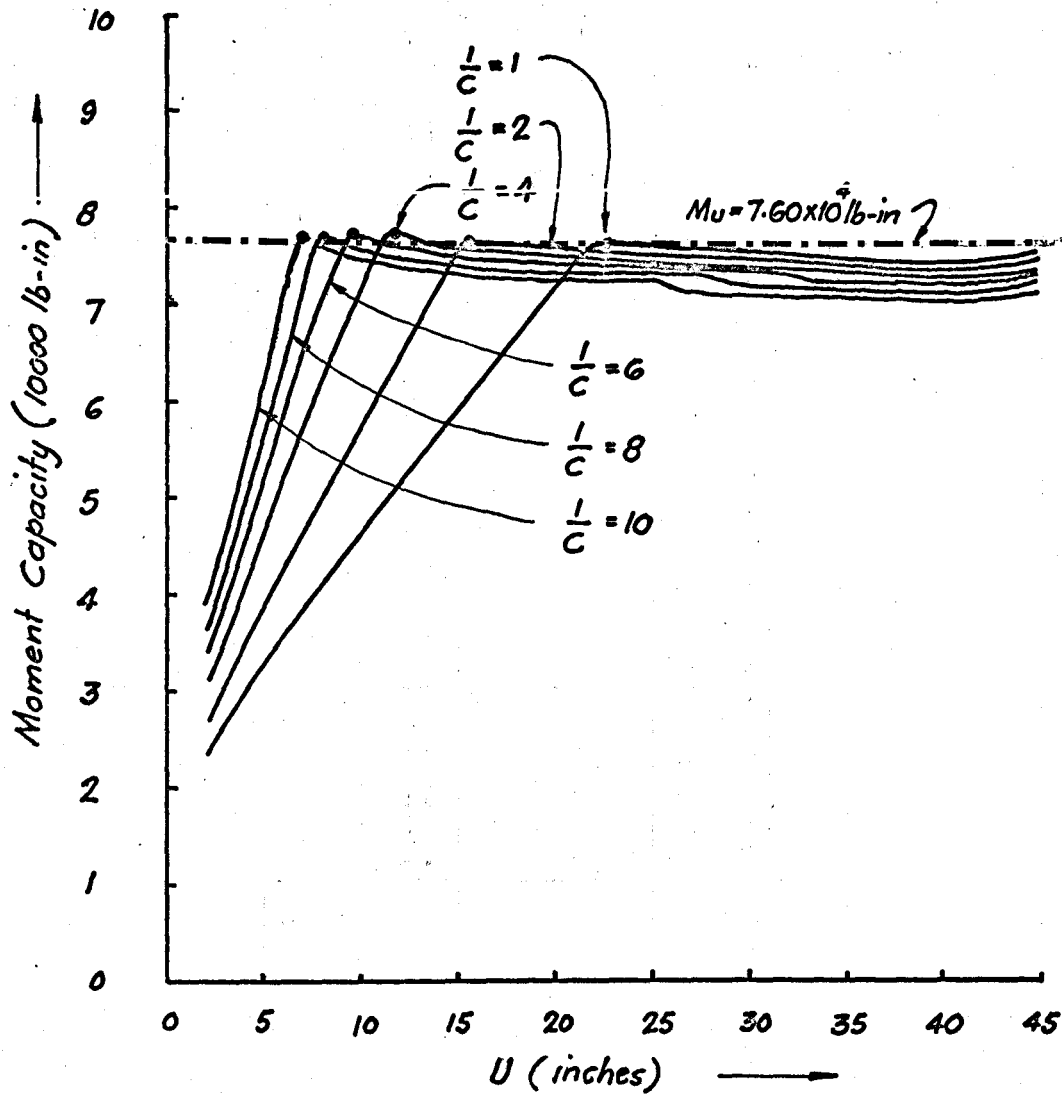
MOMENT CARRYING CAPACITY - EFFECT OF $\frac{1}{C}$ VALUE

FIG. 5.4
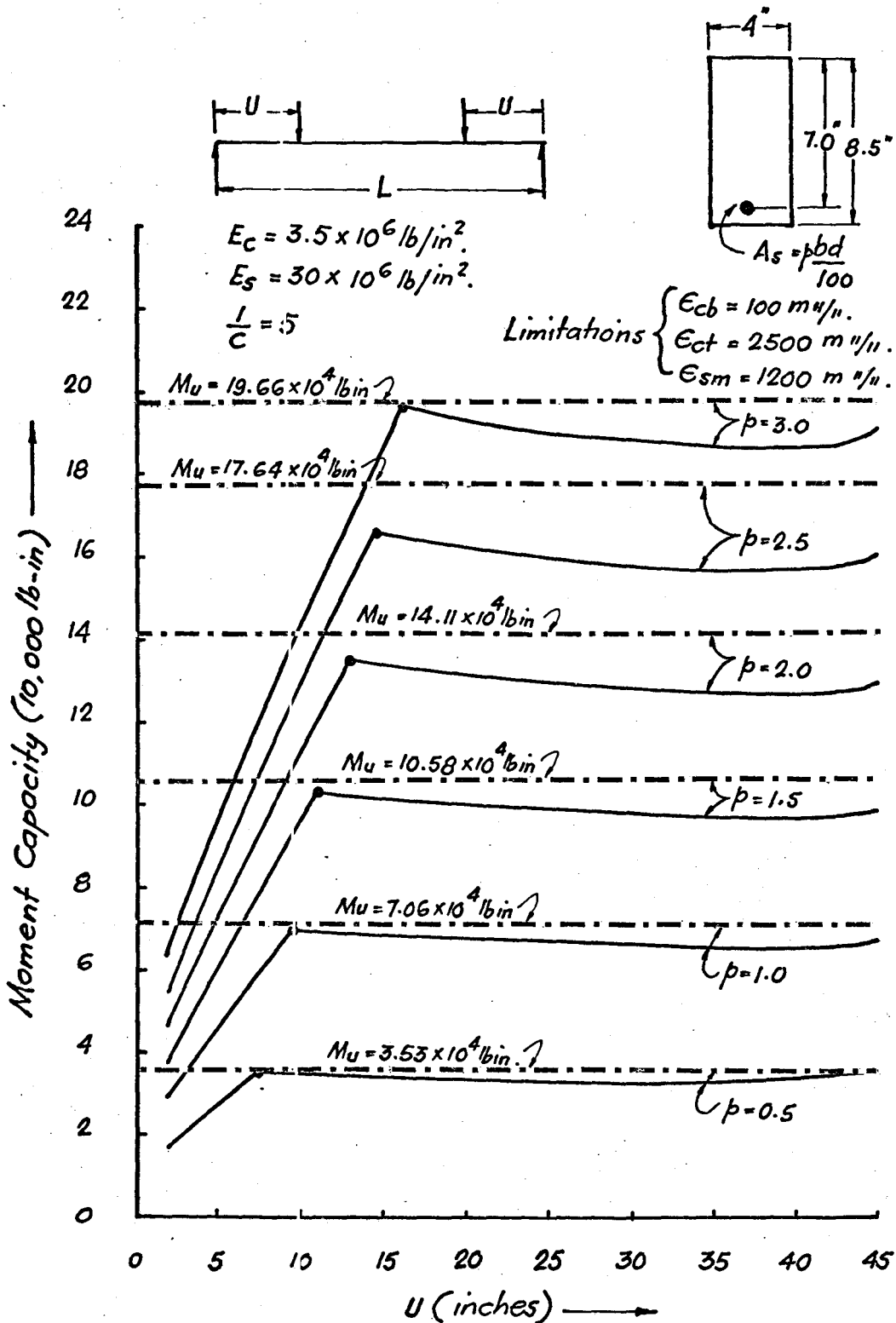
MOMENT CARRYING CAPACITY – EFFECT OF p.

FIG. 5.5(a)
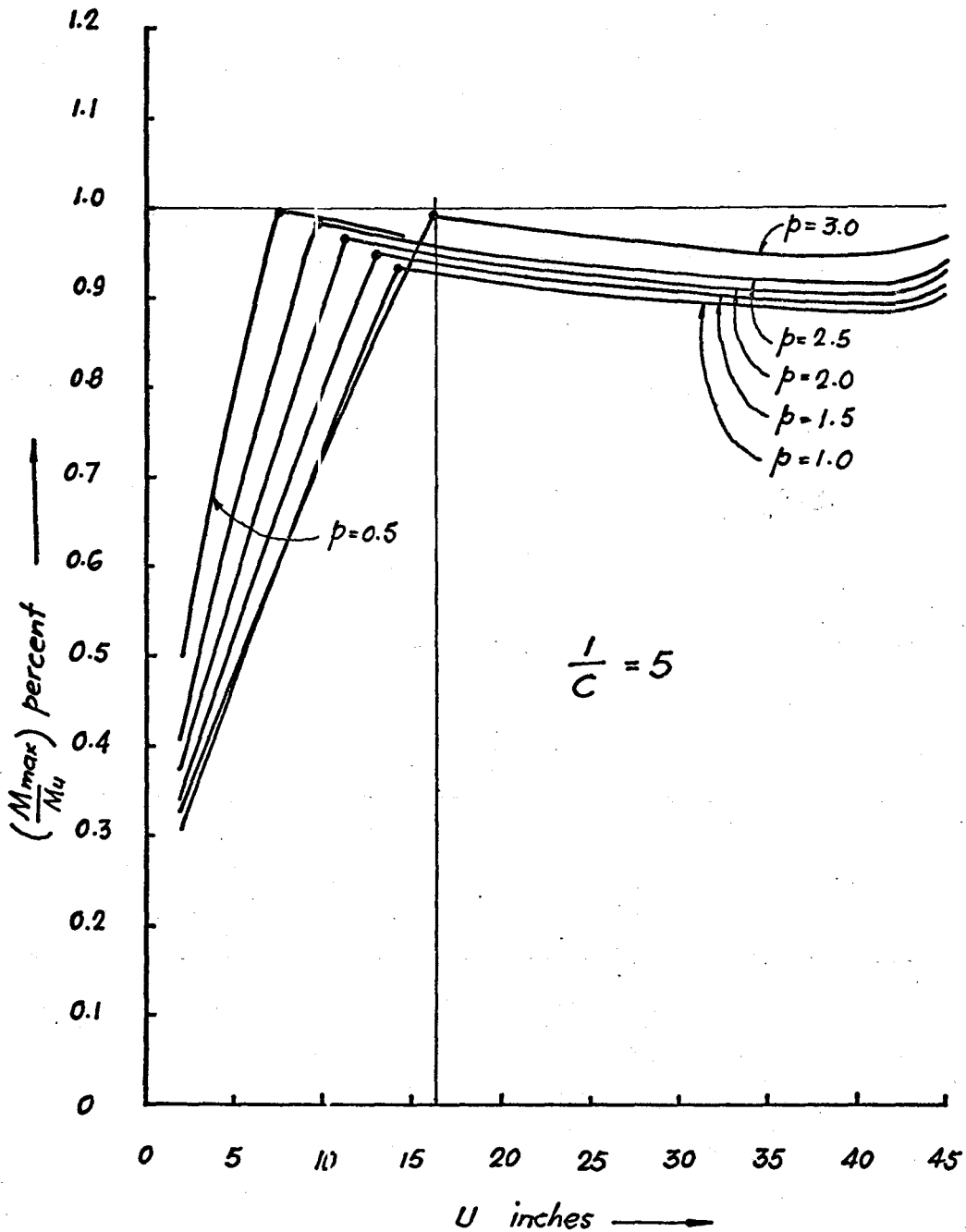
COMPUTED RELATIVE BEAM STRENGTH - EFFECT OF p.

FIG. 5.5 (b)

span, u, respectively for the "Typical Beam" with a value of $\frac{1}{C}$ = 5, and varying percentages of steel, p (= 0.5, 1, 1.5, 2.0 and 2.5). It may be seen that an increase in steel percentage has two effects. It increases the moment carrying capacity and secondly, it causes a shift of the transition point towards the centre of the beam. Increase in the moment capacity with increase in the percentage of steel was also demonstrated by MacGregor and Walters[24]. Kani[12], in describing the influence of p, states "that the amount of main reinforcement influences the location of the transition point, T, ..." (Fig. 5.6). "Varying the main reinforcement from p = 2.80% to 1.88% and 0.80%, the test results produced locations of the transition point, T, at $\frac{u}{d}$ = 6.5, 6.0 and 3.5 respectively". This is also evident in Kani's three dimensional plot of $\frac{M_{test}}{M_u}$ versus $\frac{u}{d}$ and p reproduced in Fig. 5.6.

5.3.4   A comparison of Fig. 5.3 and 5.7 shows the effect of a significant reduction in the magnitude of the interaction coefficient, $\frac{1}{C}$, from 5 to 0.5 for the same beam. The location of the transition point in the latter case has been moved much closer to the centre of the beam. The computed moment capacities to the right of the transition point are essentially the same but at a particular location to the left of the transition point in Fig. 5.7 (say u = 17.5 in., coincident with a $\frac{u}{d}$ ratio of 2.5) the moment capacity is
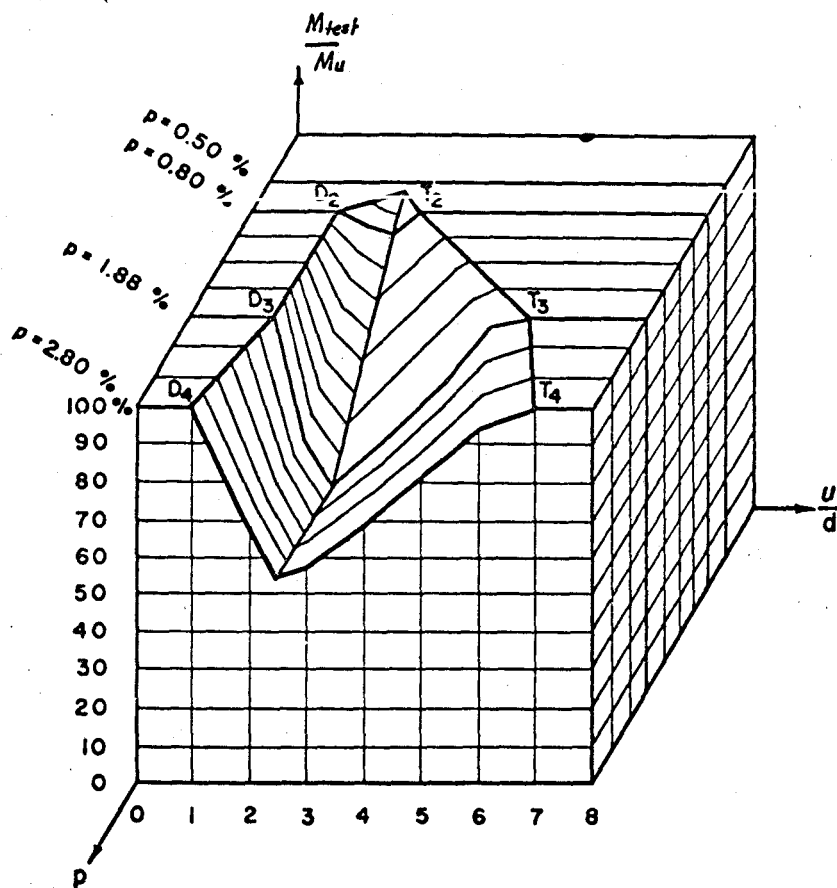
RELATIVE BEAM STRENGTH, $\frac{M_{test}}{M_u}$, versus u/d AND p. (DUE TO KANI)

FIG. 5.6
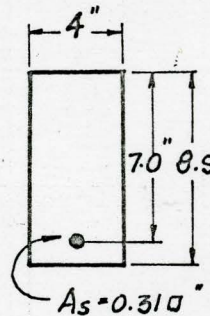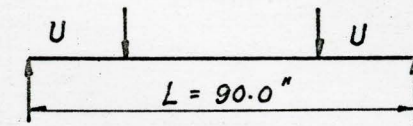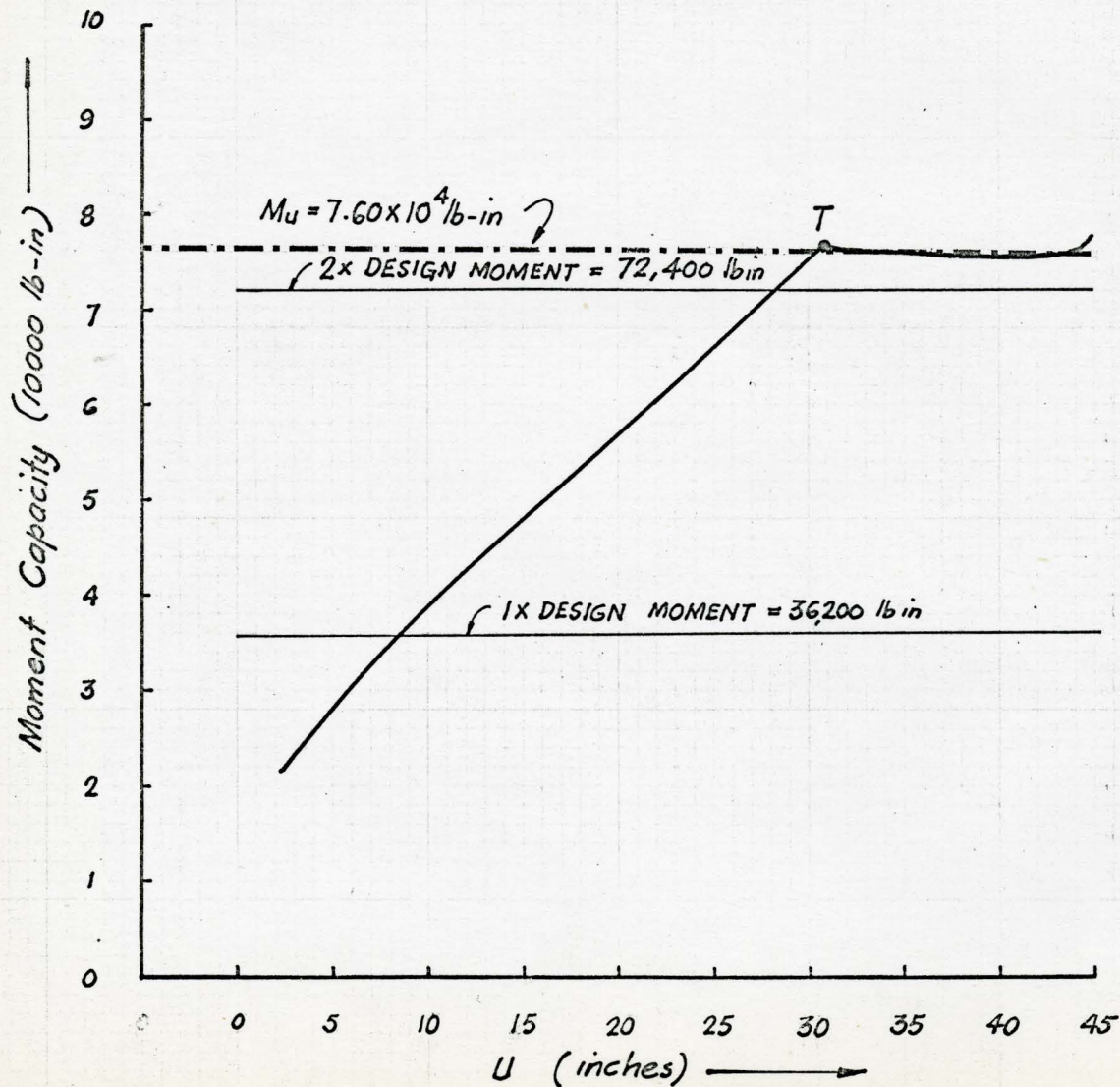
MOMENT CARRYING CAPACITY - EFFECT OF REDUCTION IN VALUE OF $\frac{1}{C}$.

FIG. 5.7

only 72.5% of that at the same location for the beam in Fig. 5.3.

Fig. 5.7 compares qualitatively with the portion VTE of Kani's plot in Fig. 5.1. This comparison suggests that for an actual reinforced concrete beam the value of $\frac{1}{C}$ would be quite small.

5.3.5   Fig. 5.8a demonstrates the effect of the variation of p on the beam with poor bond, i.e. $\frac{1}{C}$ = 0.5. Curves with p = 0.5 and 1.0 are comparable in form with the curves of Fig. 5.5a. The transition points are further moved towards the mid span. The curves with p = 2.0 and above (Fig. 5.8a have no transition points, because of the fact that the concrete strain governs the moment capacity throughout the length of the beam. It may also be observed that the capacity of such beams drops off after reaching a maximum value as the point loads move towards mid span. At this maximum value the strain in the steel is also at a maximum but it never reaches its limiting value.

Fig. 5.8b shows the relative computed moment, $\frac{M_{max.}}{M_u}$ plots corresponding to Fig. 5.8a. A comparison of Fig. 5.5b and 5.8b, indicate that a decrease in the value of $\frac{1}{C}$, causes the transition point to move nearer to mid span.

Kani[12] also stated that from the tests conducted on beams with p = 0.5, there was no transition point obtained.
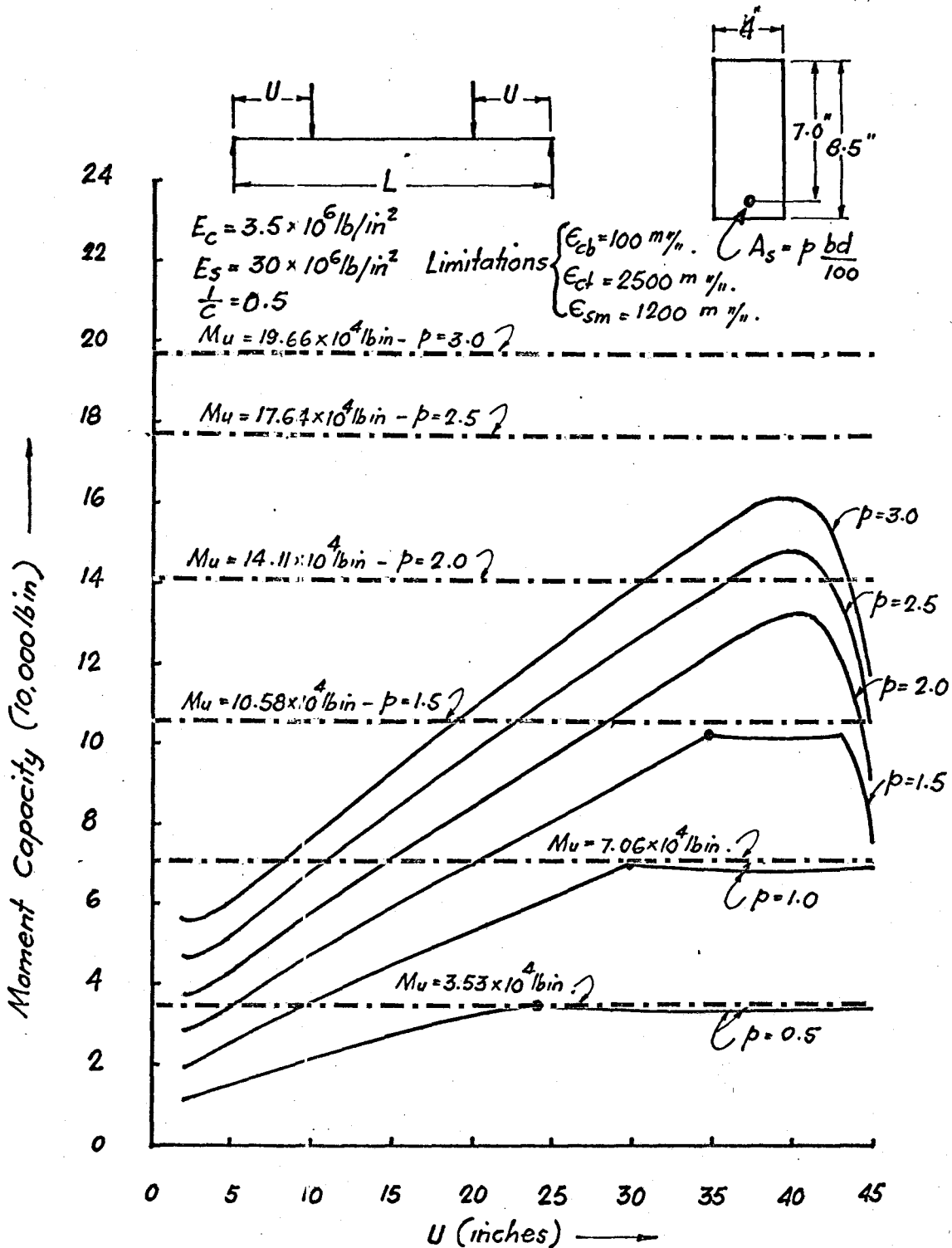
MOMENT CARRYING CAPACITY — EFFECT OF p.

FIG. 5.8 (a)
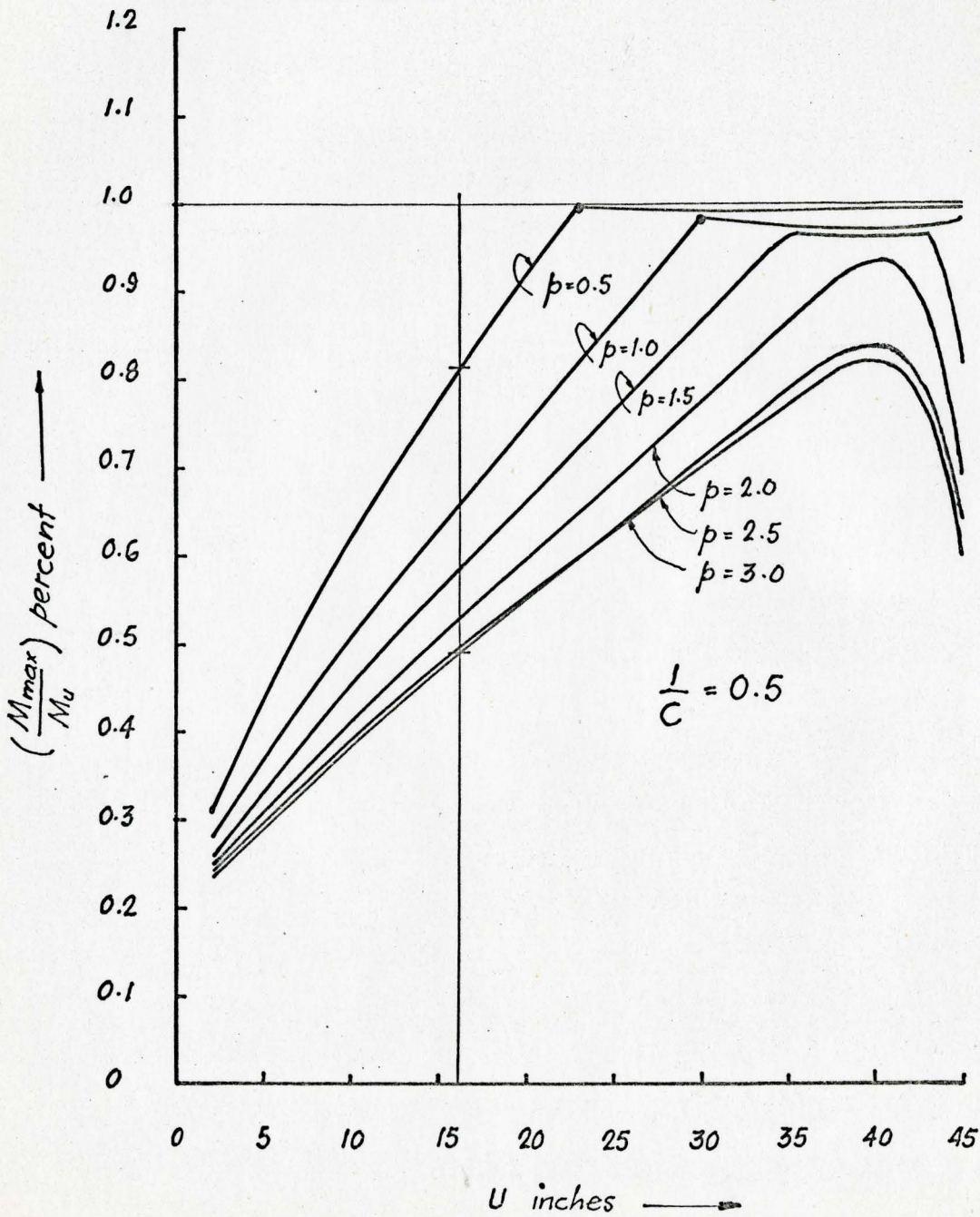
COMUTED RELATIVE BEAM STRENGTHS - EFFECT OF p.

FIG. 5.8 (b)

5.4   Influence of Choice of Limiting Strains

Fig. 5.9 shows the effect of increasing the limiting strain in the steel reinforcement. The strain has been increased from 1200 micro in/in. as in Fig. 5.4 to 1500 micro in/in. (Fig. 5.9). This is analogous to using a higher strength steel. A comparison of Fig. 5.4 and Fig. 5.9 shows a decrease in the capacity to the left of the transition point at any particular value of u and an increase in the capacity to the right of the transition point. For example, at u = 17.5 in. and $\frac{1}{C}$ = 1.0 the moment capacity ratio $\frac{M_{max.}}{M_u}$ for the case in Fig. 5.4 is 87% whereas for the case in Fig. 5.9 at the same location the ratio is 69%. The movement of the transition point towards mid span is a direct result of the increase in the steel yield strain in that the curves in Fig. 5.9 are extensions of those in Fig. 5.4 to the left of the transition points where the concrete strain governs the moment capacity. For the case where $\frac{1}{C}$ = 0.5, Fig. 5.9, no transition point exists and only the concrete governs the strength.

5.5   Kani[10] argued that diagonal failure occurs when the central section of a test beam under pure bending is stronger than the end sections. Under increasing load, a reinforced concrete beam transforms into a comblike structure. In the tensile zone, the flexural cracks create more or less vertical concrete teeth, while the compressive zone represents
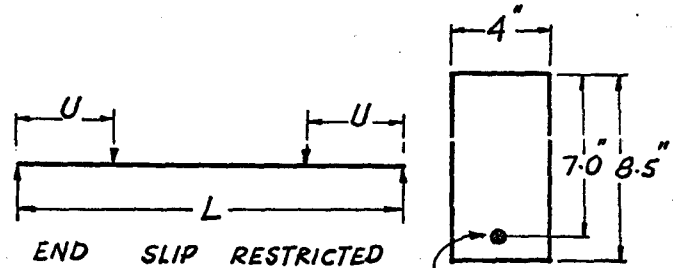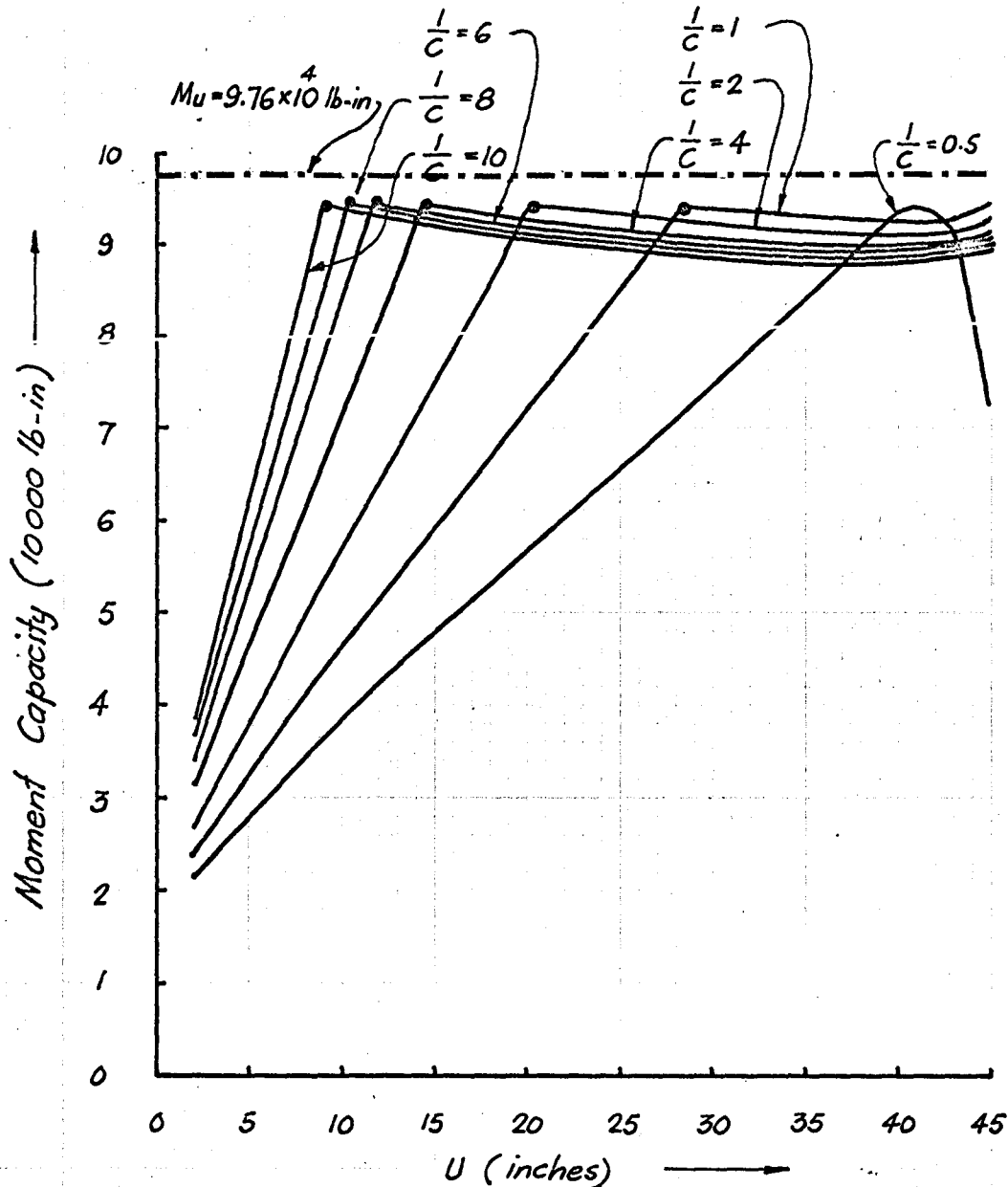
MOMENT CARRYING CAPACITY − EFFECT OF INCREASE IN THE VALUE OF ε_{sm}.

FIG. 5.9

the backbone of the concrete comb. In the comblike structure

the applied load is resisted by transfer of stresses through

the bond existing between the reinforcement and the concrete.

After the resistance of the concrete teeth has disappeared,

the concrete cross-section is reduced and only a tied arch

remains. The transformation of a reinforced beam into a

tied arch may occur suddenly or may develop gradually.

Kani states that for beams with small $\frac{u}{d}$ ratios (i.e.

$\frac{u}{d}$ < 2.5), the capacity of the concrete teeth is lower than

the capacity of the arch. Therefore, under gradually in-

creasing loads, the transformation of the beam into an arch

occurs gradually and the structure fails when the capacity

of the arch is exceeded.

For beams with $\frac{u}{d}$ lying between 2.5 and 5.6, the

capacity of the arch is lower than the capacity of the con-

crete teeth, but of course failure does not occur until the

capacity of the concrete teeth is exceeded at which stage

the transformation begins. Since the arch capacity is lower

than the applied load, a sudden collapse must follow. He

found also from his experiments that in region beyond the

transition point ($\frac{u}{d}$ > 5.6) only normal flexure failure is

possible.

Therefore, in Fig. 5.2, according to Kani[10], the

portion DV represents the relative beam strength values for

$\frac{u}{d}$ ratios between 1 and 2.5 and is due to the strength of the

remaining arch. The portion VTE shows the relative beam

strength values for $\frac{u}{d}$ ratios of more than 2.5, and which are due to the resistance of the concrete teeth. Point V in Fig. 5.2 shows the minimum value of the relative beam strength and point T stands for the transition, beyond which according to Kani[10] only normal flexural failure can take place.

5.5.1 Figs. 5.1 and 5.3 to 5.5 and 5.7 to 5.9 show the computed maximum moment carried by the section at the load point, $M_{max.}$, versus the location of the load point, u. It has been observed that they are influenced by certain parameters in very much the same way as the experimental findings by Kani. However, they have not shown an increase in the relative beam strength for small values of u. This, Kani argued, is due to the strength of the remaining arch.

5.5.2 Kani[10] shows in Fig. 5.2 that diagonal cracking occurs in cases where $\frac{u}{d}$ is between 1 and 5.6 and beyond this range only flexural failures are possible. The diagonal cracking takes place in the shear span, where both shear as well as moment are present. The relative beam strength plots in Fig. 5.6, ($\frac{u}{d}$ ratio between 1 and 5.6) pertain, therefore, to diagonal cracking. Kani suggests that the transition point is a demarcation between modes of failure. The beam with $\frac{u}{d}$ ratio less than at T fails in diagonal tension and the one with $\frac{u}{d}$ ratio greater than at T will fail in normal flexure.

However, the computed values of $M_{max.}$ in this thesis
are only based on flexural consideration and in their com-
putation no account has been made for the applied shear. It
is nevertheless interesting to note that a reduction in
moment capacity does occur as the shear span is reduced and
in spite of the fact that no direct account of diagonal
shear failure is made.

5.5.3   Discussing the influence of the percentage of steel,
p, Kani[12] stated, "For those beams with a high percentage
of reinforcement (p = 2.80 percent), the "valley of dia-
gonal failure" has a low point in the vicinity of $\dfrac{M_{test}}{\overline{M}_u} = 50$
percent, whereas for those beams with a low percentage of
reinforcement (p = 0.50 percent with $\dfrac{M_{test}}{\overline{M}_u} = 100$ percent),
the "valley of diagonal failure" disappears."

He also stated that in most of the cases the lowest
point in the valley occurred in the vicinity of $\dfrac{u}{d} = 2.5$.
This refers to a distance of 7" x 2.5 = 17.5 in. from the
support in case of the "Typical Beam" discussed in this
thesis.   Fig. 5.8b shows a variation in the computed rela-
tive strength between 81 percent for p = 0.5 percent and
49 percent for p = 2.5 at the shear span length of 17.5 in.
(or $\dfrac{u}{d}$ of 2.5).

5.6   As mentioned earlier, the computations of the
influence lines for the moment capacity are based on a beam

model and they did not indicate any rise in the computed

relative beam strength as has been obtained experimentally

by Kani (see portion DV of Fig. 5.2). Kani argues that this

increase is due to the strength of the remaining arch. From

an evaluation of the approach taken in this thesis it seems

unlikely that an increase in relative moment capacity for

very short shear spans ($\frac{u}{d}$ < 2.5) can be achieved even if

more correct curvilinear stress-stress and bond-slip

characteristics are introduced. It is therefore suggested

that perhaps the arch model should be investigated in order

to establish a complete theoretical explanation of the be-

haviour of the reinforced concrete beam.

An outline of the method for investigation of the

strength of the remaining arch is suggested in the following:

1. Select a beam, i.e. dimensions such as width,

depth, length, reinforcement and its location, and the

properties of the material, such as E_s, E_c, ε_{cr}, $\frac{1}{C}$, etc.

2. Choose the limiting strains, $\varepsilon_{ct_{max.}}$ and $\varepsilon_{sm_{max}}$.

3. Assume a moment value M_o, find out the crack

profile corresponding to it, and hence the dimensions of the

remaining arch.

4. Determine moment carrying capacity for such an

arch, M_R, possibly by means of some semi-graphical method

of analysis.

5. Compare M_R with M_o

if $M_R < M_o$ decrease M_o

if $M_R > M_o$ increase M_o and repeat

the steps 1 to 5 until $M_R = M_o = M_{max.}$ within permissible limits of accuracy.

6. Determine $M_{max.}$ in the same way at different sections under the point load along the length of the beam. Plot $M_{max.}$ versus u on the curve for the flexural moment capacity. The point of intersection of the curve for flexural capacity and the curve for the arch capacity will determine the minimum value of the beam strength.

CHAPTER VI

BOND AND SLIP DISTRIBUTION ALONG THE LENGTH OF A CRACKED

REINFORCED CONCRETE BEAM

A reinforced concrete beam, on cracking, usually assumes a 'comblike structure' (10), and between the visible cracks form what are known as the 'concrete teeth'. The concrete teeth provide the remaining interaction through bond between the concrete and steel reinforcement, before either the 'comblike structure' fails or it transforms into an arch. During this transformation, considerable change takes place in the magnitude of bond stress and slip.

The variation in bond stress and slip in the vicinity of a flexural crack was investigated by Evans and Robinson[1] in 1954. They found that the magnitude of bond stress as well as slip were considerably higher at the cracks than between the cracks. Nilson[28] in 1968 carried out similar investigations analytically.

In the analysis carried out by the author, the predominant assumption is that there is an infinite number of cracks in the potential zone of flexural cracking. This is in contradiction with the fact (because then there would be no tooth formation), yet the variations of bond stress and slip obtained being the Influence Lines, are quite informative and yield values of bond stress as well as slip at any point where a crack has already been formed.

131

(a)
NCHES
DISTRIBUTION OF CONCRETE STRAINS

(b)
NCHES
DISTRIBUTION OF STEEL STRAINS

(c)
Tensile fibre
0·08 -dia wire
Centre-line of beam
INCHES
CRACK PATTERN

(d)
DISTRIBUTION OF BOND STRESS

(e)
INCHES
DISTRIBUTION OF SLIP
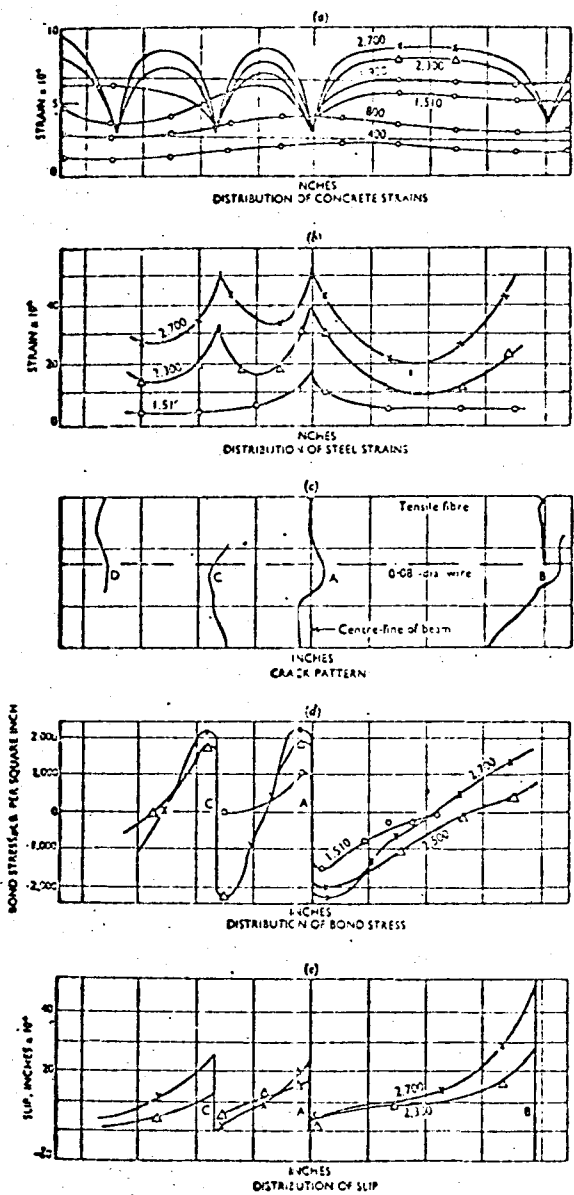
BEAM A4. SLIP, STRAINS, AND STRESSES
(Six 0·08″-dia wires)

(a)
INCHES
DISTRIBUTION OF STEEL STRAINS

(b)
Tensile fibre
0 2″-dia. wire
Centre-line of beam
INCHES
CRACK PATTERN

(c)
INCHES
DISTRIBUTION OF BOND STRESS

(d)
INCHES
DISTRIBUTION OF SLIP
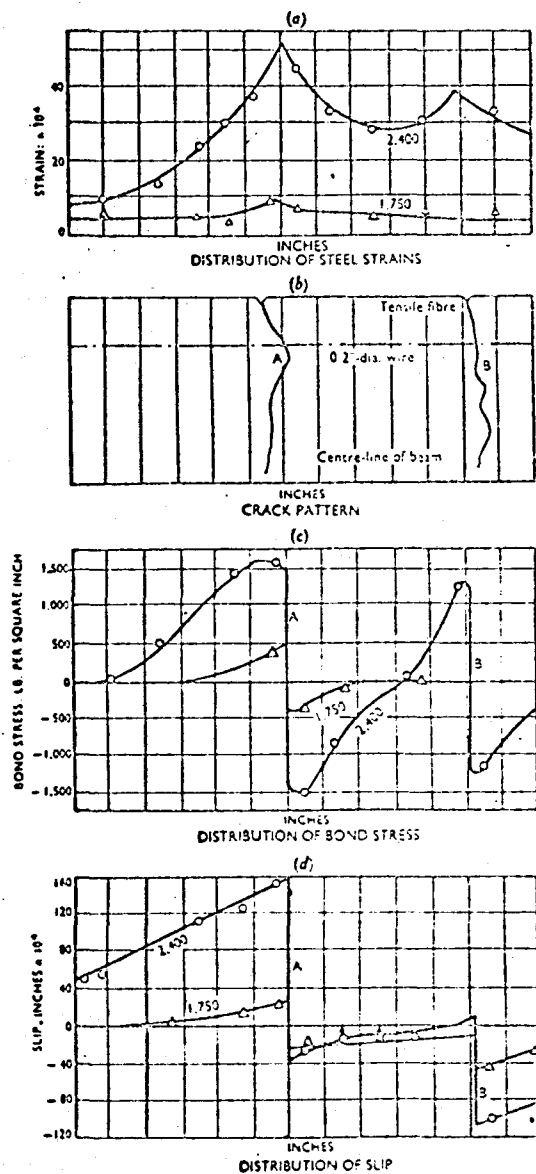
BEAM A10
(One 0·2″-dia wire)

DUE TO EVANS & ROBINSON

FIG. 6.1
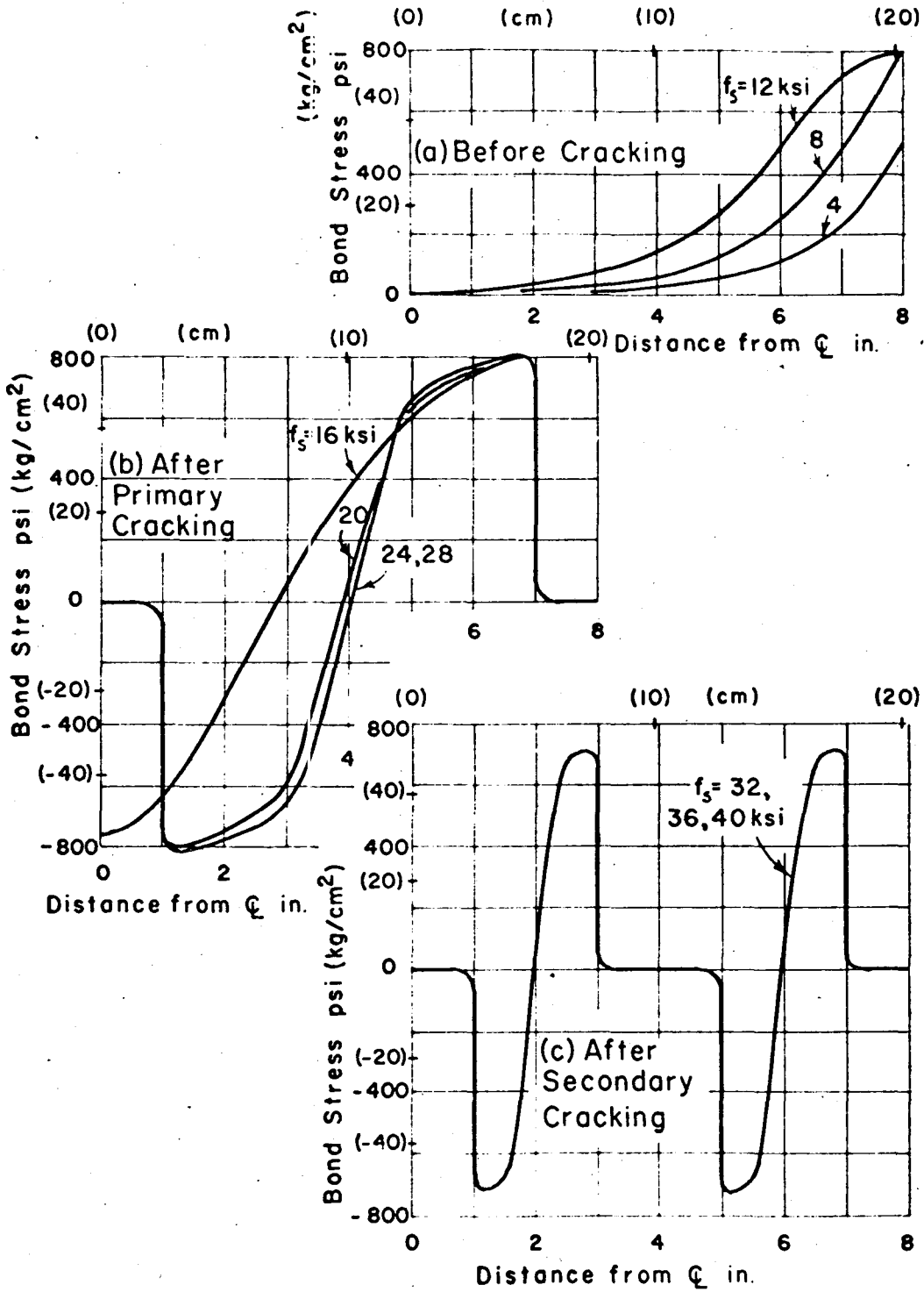
Bond stress distribution

DUE TO NILSON

FIG. 6.2

Flexural Cracks

d

F

$F+\Delta F$
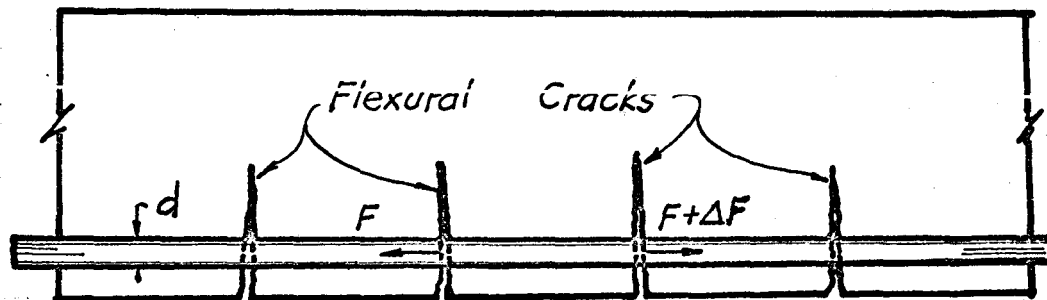
a) Cracked Reinf. Concrete Beam

σ_b

F ⟵ ⟶ $F+\Delta F$

Δx
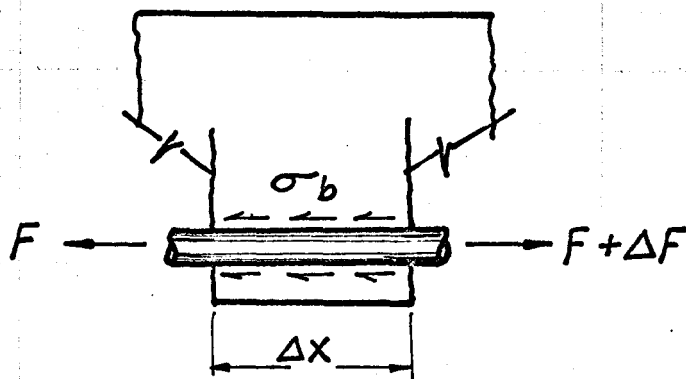
b) Equilibrium of a Concrete Tooth.

DETERMINATION OF BOND STRESS AND SLIP IN A CRACKED R.C. BEAM

FIG. 6.3

6.1 Bond Stress

Considering the horizontal equilibrium of a concrete tooth, Fig. 6.3, the following can be written.

$$\cancel{F} + \sigma_b \cdot \pi d \cdot n \, \Delta x = \cancel{F} + \Delta F$$

or

$$\sigma_b = \frac{1}{\pi dn} \frac{\Delta F}{\Delta x}$$

$$\begin{cases} \text{where } n = \text{no. of the bars} \\ \\ n \cdot \frac{\pi d^2}{4} = A_s \end{cases}$$

or

$$\sigma_b = \frac{4A_s}{d} \frac{\Delta F}{\Delta x}$$

or in the differential form

$$\sigma_b = \frac{4A_s}{d} \frac{dF}{dx} \qquad\qquad 6.1$$

and the equilibrium equation 2.5 pertaining to any composite section can be rewritten as:

$$F = \frac{1}{Z} [M_t - M_c - M_s]$$

differentiating w.γ.t.x and re-substitution gives

$$\frac{dF}{dx} = \frac{1}{Z} \left[\left\{ V - \frac{dM_c}{dx} - \frac{dM_s}{dx} \right\} + F \frac{dZ}{dx} \right] \qquad\qquad 6.2$$

Therefore from Eq. 6.1 and 6.2 σ_b can be written as:

$$\sigma_b = \frac{4A_s}{d} \cdot \frac{1}{Z} \left[\left\{ V - \frac{dM_c}{dx} - \frac{dM_s}{dx} \right\} + F \frac{dZ}{dx} \right] \qquad\qquad 6.3$$

Now for case of conventional working stress theory for reinforced concrete, the beam is uncracked and no slip

is permitted, i.e. $\frac{dZ}{dx} = 0$ (because Z is constant), and for a particular section

$$\frac{dM_c}{dx}, \frac{dM_s}{dx} = 0, \quad \text{Eq. 6.3 reduces to}$$

$$\sigma_b = \frac{4A_s}{d} \cdot \frac{V}{Z} \qquad\qquad 6.4$$

which is the classical expression for bond stress widely used in reinforced concrete design.

6.2 Slip

From Eq. 2.2a and Eq. 2.16 we can write

$$\gamma = \frac{L^2}{\pi^2} \cdot \frac{\overline{EI}}{EA\Sigma EI} \cdot \frac{q}{(\frac{1}{c})} \qquad\qquad 6.5$$

Since according to Eq. 2.6, $q = \frac{dF}{dx}$, therefore Eq. 6.5 can be re-written as

$$\gamma = \frac{L^2}{\pi^2} \cdot \frac{\overline{EI}}{EI\Sigma EI} \cdot \frac{1}{(\frac{1}{c})} \cdot \frac{1}{Z}\left[\left\{V - \frac{dM_c}{dx} - \frac{dM_s}{dx}\right\} + F\frac{dZ}{dx}\right] \qquad 6.6$$

Knowing the forces, and geometry of a cracked section in a beam, Eqs. 6.3 and 6.5 can be used to determine bond stress and slip respectively for any magnitude of $\frac{1}{c}$.

6.3 Numerical Examples

Two cases are considered, one for two symmetrically placed point loads 29.25" from each end, and the other for uniformly distributed loading over the entire span. All the other data pertaining to these examples is the same as for the "Typical Beam" of Chapter II except that the value of
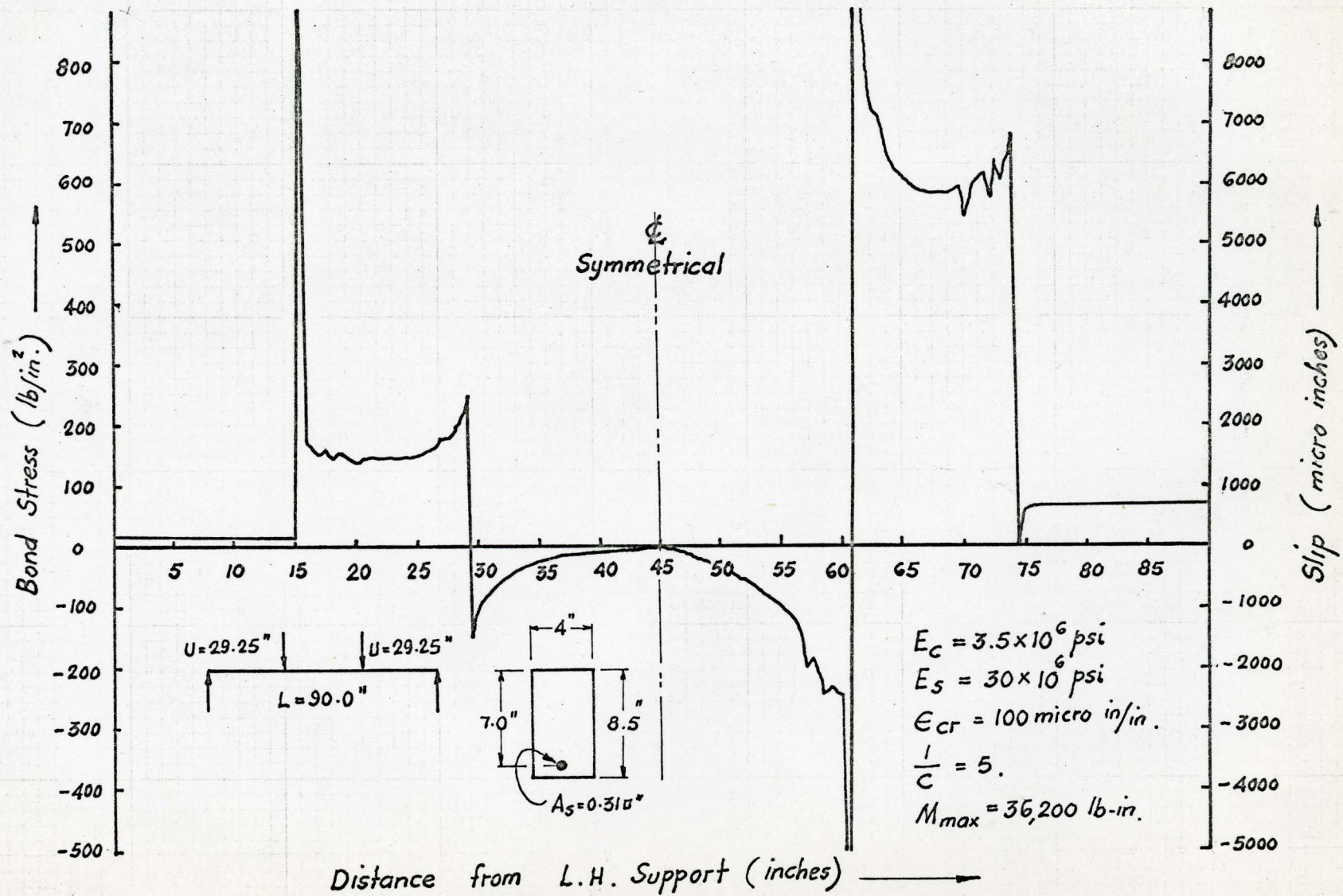
DISTRIBUTION OF BOND STRESS AND SLIP ALONG THE LENGTH OF A CRACKED BEAM.

FIG. 6.4

$\frac{1}{C}$ assumed here is 5. The maximum moment on the beam is equal
to one times the design moment. Eqs. 6.3 and 6.5 were used to
compute the bond stress and slip respectively along the length
of the cracked beam at intervals of $\frac{1}{2}$ inch. These values are
plotted in Fig. 6.4 and 6.5.

The left half of these figures show the plots for
bond stress and on the right half is the variation of slip.
It is interesting to note that the bond stress as well as
the slips are considerably higher in the shear span than in
the portion between two point loads in the cracked region
of the beam. This is because of the applied shear. At the
load point, slip changes its direction, consequently re-
versing the sign of the bond stress, and at the mid span
slip as well as bond is zero. This is what could be
expected for the case of beam loaded symmetrically about its
mid span.

In case 2, i.e. the beam carrying uniformly distri-
buted loading, however, the form of the bond stress and slip
curves are similar to case 1, except that there is no change
in the direction of the bond stress. This is because, for
uniformly distributed loading, slips are directed towards
the ends of the beam.

It can also be observed from Fig. 6.4 and 6.5, that
in the uncracked portion of the beam, slip variation is not
significant. In case 1, Fig. 6.4, maximum slip occurs under
the load point with a magnitude of more than .01". The
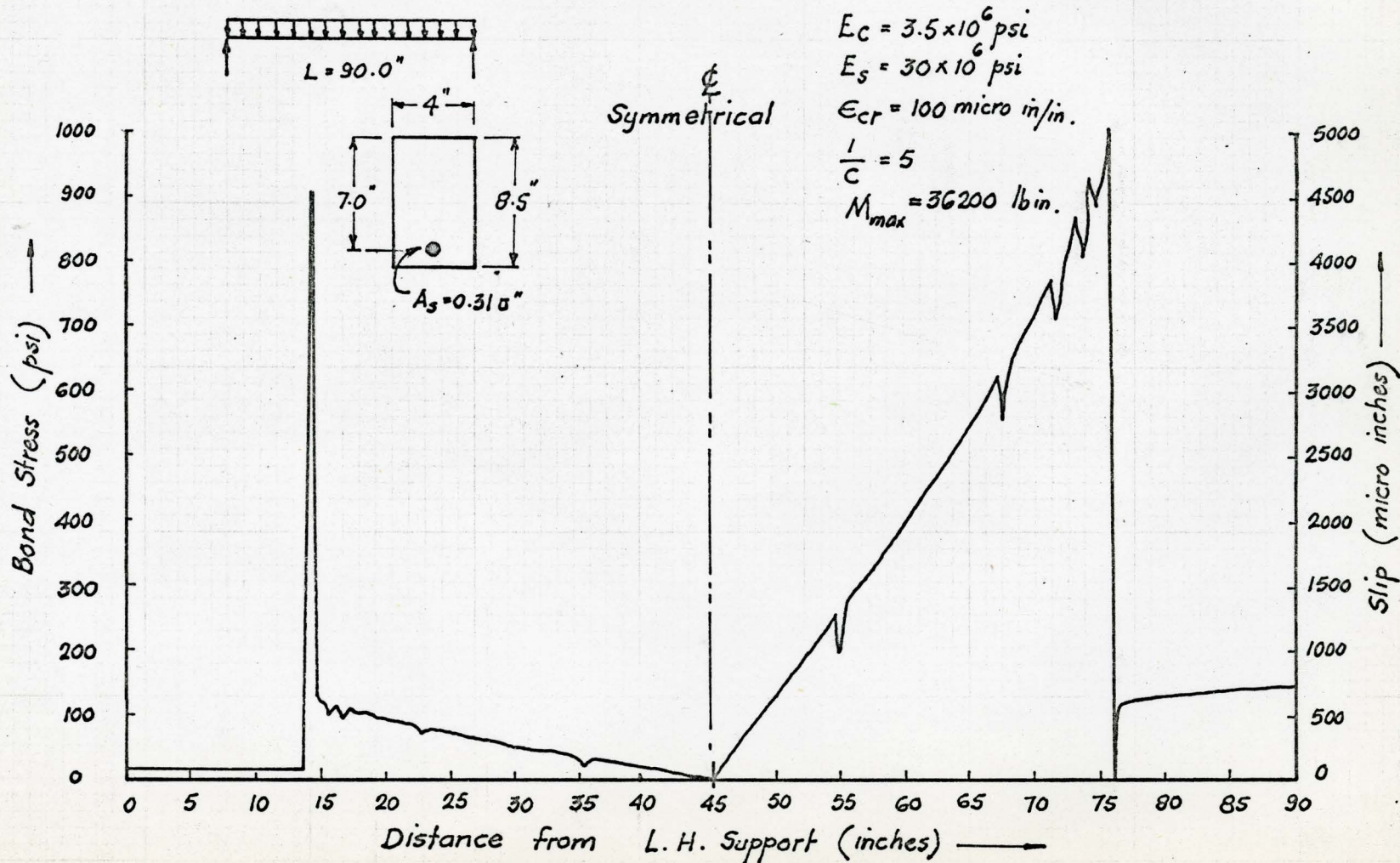
DISTRIBUTION OF BOND STRESS AND SLIP ALONG THE LENGTH OF A CRACKED BEAM.

FIG. 6.5

bond stress corresponding to this slip is approximately
250 psi. The maximum bond stress is, however, at the point
where cracking starts and its value is approximately 900 psi.
In case 2, Fig. 6.5, maximum slip occurs just after the
point where cracking starts. The magnitude of this slip
is 0.005" and the value of the corresponding bond is approxi-
mately 900 psi.

CHAPTER VII

SHEAR AND PRINCIPAL STRAINS

7.1   Since the diagonal cracking is often regarded as being caused by the combined stresses and strains, it was therefore of interest to study the distribution of the shear strain at different sections along the length of a cracked beam, in order to investigate the magnitude and direction of the principal strains.

Two methods were considered, both primarily based upon the equilibrium of the horizontal forces, and these are discussed in the following.

7.2   Method I

7.2.1   In this approach the equilibrium conditions were applied to an uncracked portion between any two sections of a cracked beam. Fig. 7.1a shows such a portion between sections 1-1 and 2-2. The strains at any levels y_1 and y_2 can be given by

$$\left. \begin{array}{c} \varepsilon_{y_1} = \varepsilon_{ct_1} \left(\dfrac{n_1 - y_1}{n_1} \right) \\[2em] \varepsilon_{y_2} = \varepsilon_{ct_2} \left(\dfrac{n_2 - y_2}{n_2} \right) \end{array} \right\} \qquad 7.1$$

where n_1 and n_2 are the positions of the neutral axis in the respective cross-sections.
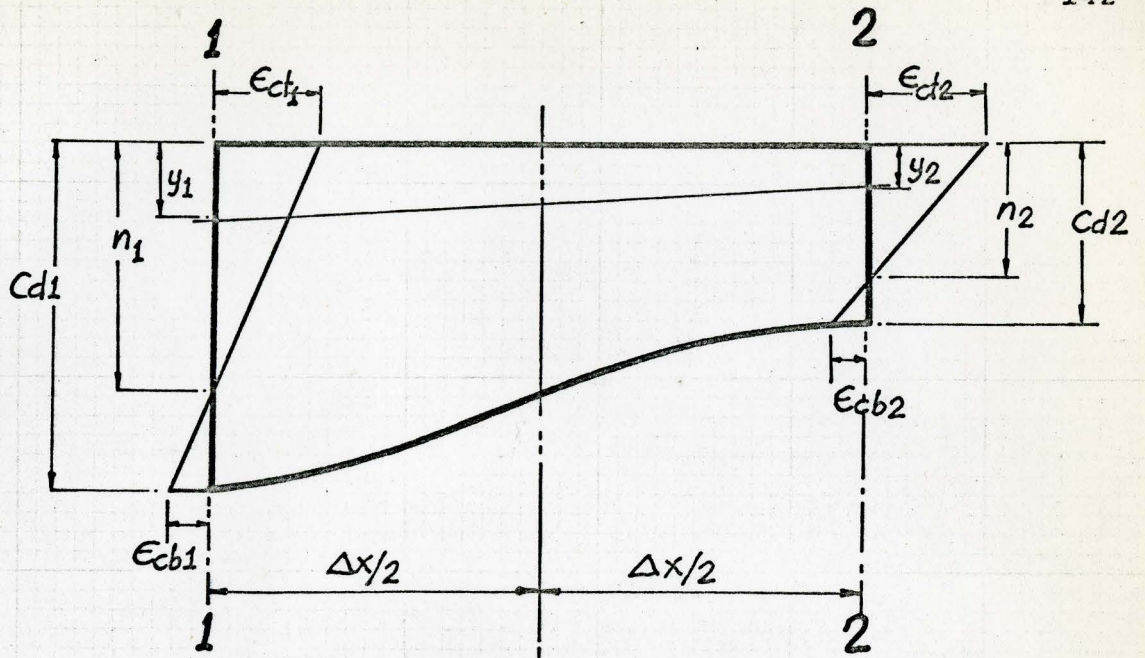
a) Flexural Strains
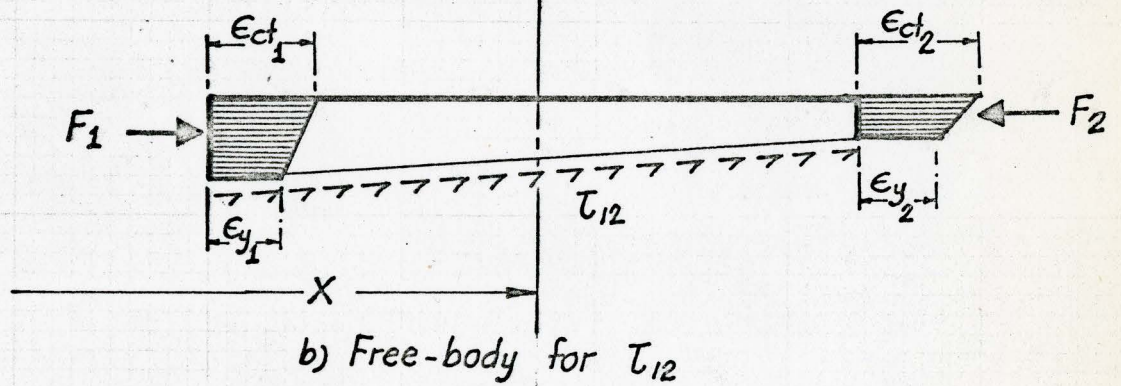
b) Free-body for τ_{12}
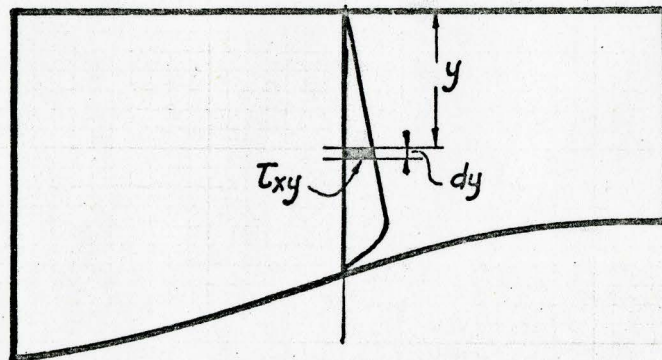
c) Total Shear.

Determination of Vertical Shear Stress Distribution (Method I)

Fig. 7.1

7.2.2 Shear Stress

The uncracked portion between sections 1-1 and 2-2 of Fig. 7.1a can be partitioned into a number of trapizoidal laminas, by dividing each of the two sections into equal number of parts. The average shear stress at the base of any lamina, determined from the equilibrium of the free-body above that base level, would be

$$\tau_{12} = \frac{F_2 - F_1}{b \cdot \Delta x}$$ 7.2

where

$$F_1 = \left(\frac{\varepsilon_{ct_1} + \varepsilon_{y_1}}{2} \right) y_1 b E_c$$

$$F_2 = \left(\frac{\varepsilon_{ct_2} + \varepsilon_{y_2}}{2} \right) y_2 b E_c$$

b is the width of the beam, and τ_{12} is the average shear stress over the base of the free body of Fig. 7.1a. τ_{xy} is the vertical shear at depth y from the top of the beam and is equal in magnitude to τ_{12} Fig. 7.1c.

7.2.3 Shear Force

The total amount of shear, S, carried by the section at x distance from left hand support, as per Fig. 7.1c is given by

$$S = b \int_{o}^{C_d} \tau_{xy} \, d_y$$ 7.3

where $C_d = \dfrac{Cd_1 + Cd_2}{2}$ and $\tau_{xy} = \tau_{12}$ at $y = \dfrac{Y_1 + Y_2}{2}$, see

Fig. 7.1a.

7.2.4 Shear Strain

Similarly the shear strain at any level where τ_{xy} is known, would be

$$\gamma_{xy} = \frac{\tau_{xy}}{G_c} \qquad\qquad 7.4$$

where $\quad G_c = \dfrac{E_c}{2(1 + v)}$

and $\quad v$ is the Poisson's ratio, its value for concrete is taken to be 0.16.

7.2.5 Principal Strains

If $\varepsilon_x = \dfrac{\varepsilon_{y_1} + \varepsilon_{y_2}}{2}$ is considered approximately equal to the flexural strain at any section, distance x from the left hand support, ε_y, the corresponding strain in the transverse direction, would then be equal to $- v\varepsilon_x$. The magnitude and the direction of the principal strains at a point distance, x, from the left hand support and y below the top fibre of concrete in a beam can be written as

$$\left.\begin{array}{c}\varepsilon_{max}\\[4pt]\varepsilon_{min}\end{array}\right\} = \frac{\varepsilon_x + \varepsilon_y}{2} \pm \sqrt{\left(\frac{\varepsilon_x - \varepsilon_y}{2}\right)^2 + \left(\frac{\gamma_{xy}}{2}\right)^2} \qquad\qquad 7.5$$
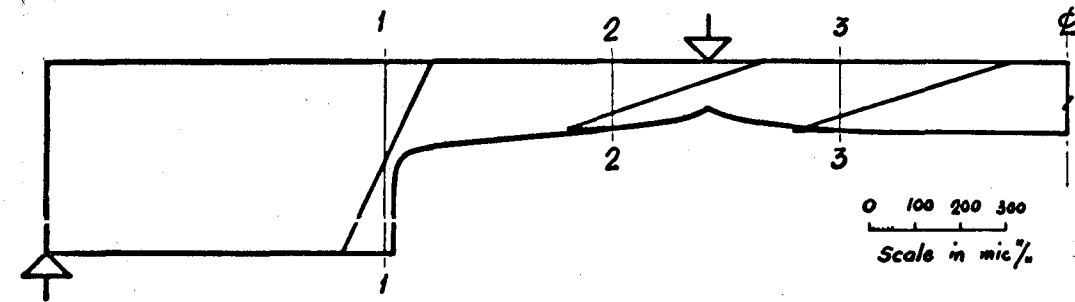
a) Average Flexural Strains

Typical Beam of Chapter II
One Times the Design Load
$\frac{L}{c} = 5$; $\Delta x = 0.1''$; $\nu = 0.16$
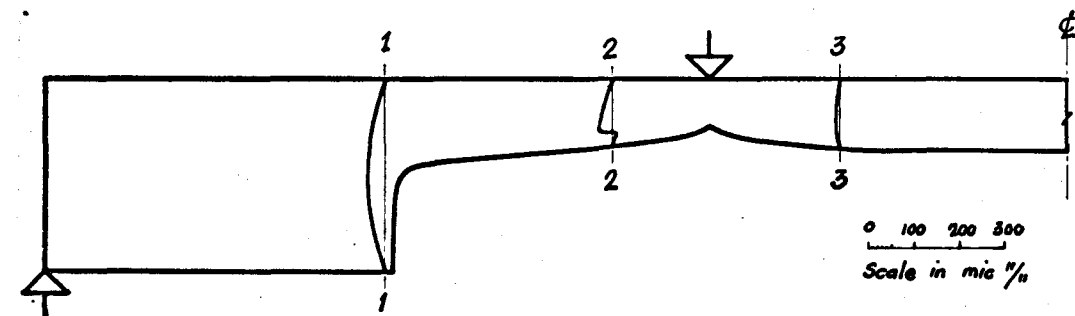
b) Shear Strains

Section	x	Shear Carried 'S'	% of Total Shear 'V'
1-1	15"	1187 lbs.	95
2-2	25"	181 "	14.6
3-3	35"	42 "	3.4
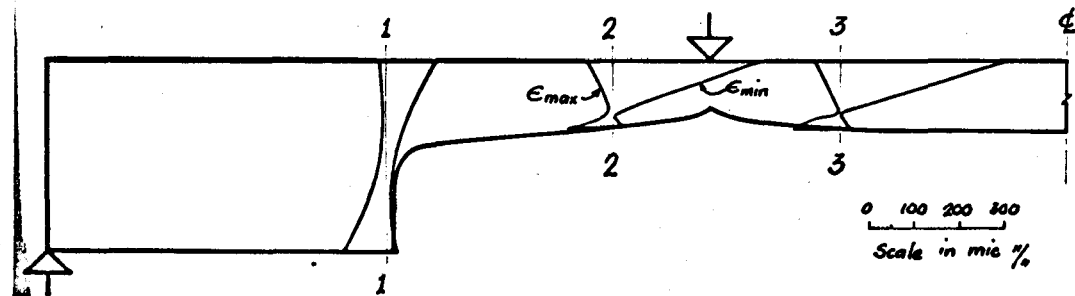
c) Principal Strains

FIG. 7.2   DISTRIBUTION OF FLEXURAL , SHEAR , AND PRINCIPAL STRAINS BY METHOD I

and

$$\theta = \frac{1}{2} \tan^{-1} \left(\frac{\gamma_{xy}}{\varepsilon_x - \varepsilon_y} \right)$$ 7.6

7.2.6   The distribution of shear strain, the magnitude and direction of the principal strain at various levels, and the total shear carried by the concrete section were computed at x = 15", 25", 35" and 45". The values of $\frac{1}{C}$ = 5 and Δx = 0.1" were taken in these computations pertaining to the "Typical Beam" of Chapter II. The results of these computations were plotted and are given in Fig. 7.2.

The amount of shear carried by the uncracked beam varies from section to section. At x = 15", a section where the concrete was about to crack, 95% of the shear was carried by the concrete itself. At x = 25", before the point load in the shear span about 14.6% and at x = 35", between the load points where there is no shear due to the applied loads, only 3.4% of the total shear is carried by the uncracked concrete.

Moreover, the magnitudes of the principal tensile strains, in the uncracked part of the beam, did not exceed the cracking strain, ε_{cr} = 100 micro in/in.

7.3   Method II - Modified Broms' Method[13]

7.3.1   Broms considered that between every two vertical cracks, there was an uncracked section. The computations
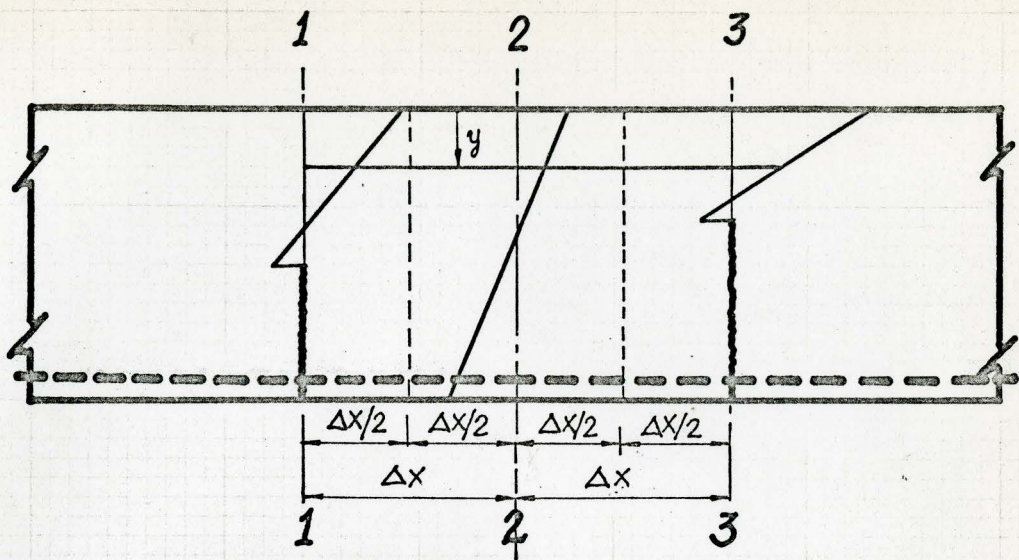
a) Flexural Strains.
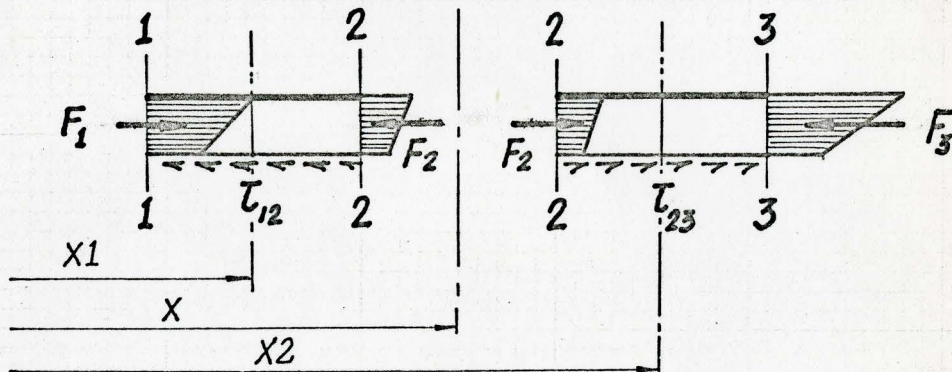
b) Free Bodies.
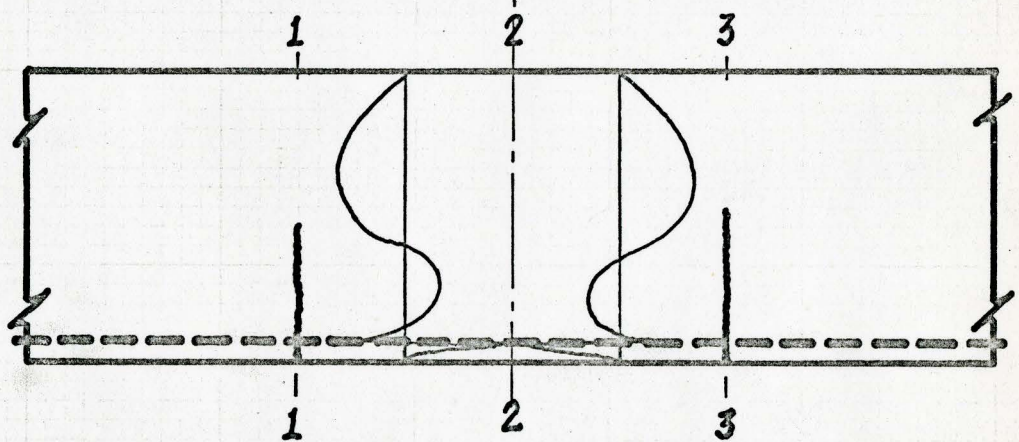
c) Shear Distributions.

Modified Broms' Method (Method II)

Fig. 7.3

Typical Beam of Chapter II
One Times the Design Load

$\frac{l}{c} = 5$; $\Delta x = 0.1''$; $v = 0.16$

a)   Flexural   Strains

The scale at this
section is one tenth
of the indicated

b)   Shear   Strains

ϵ_{min} -----
ϵ_{max} ———

c)   Principal   Strains
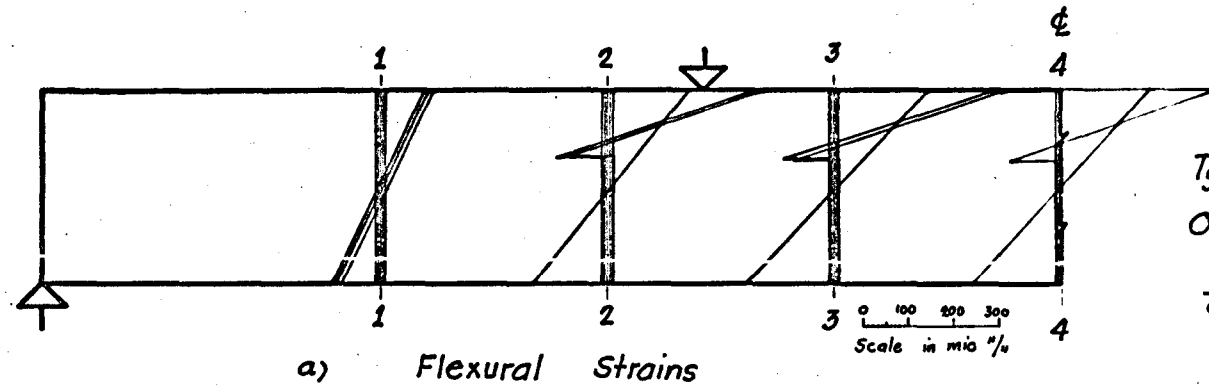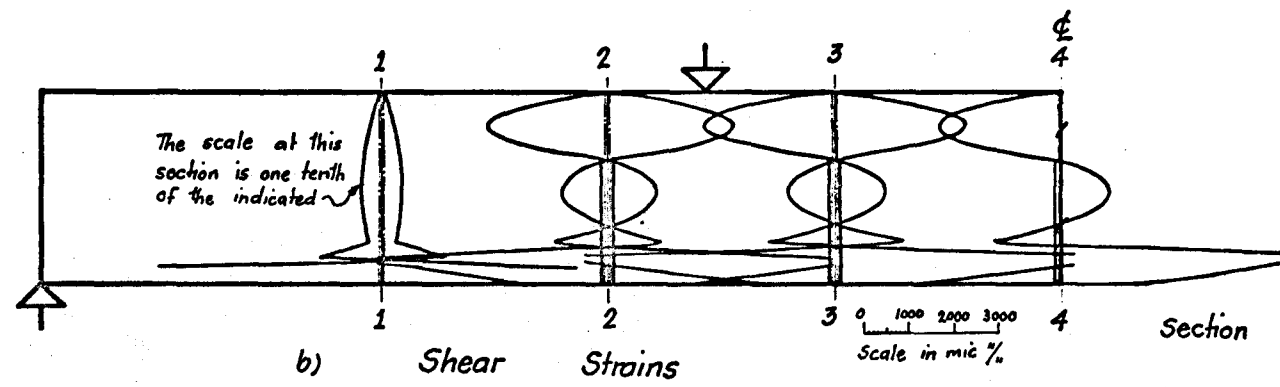
Section	x	Shear Carried	%.age of Total Shear
1-1	15"	4722 lbs.	381
		7425 "	600
2-2	25"	15200 "	1225
		14521 "	1170
3-3	35"	16109 "	1290
		15314 "	1235
4-4	45"	15920 "	1280
		15920 "	1280

148
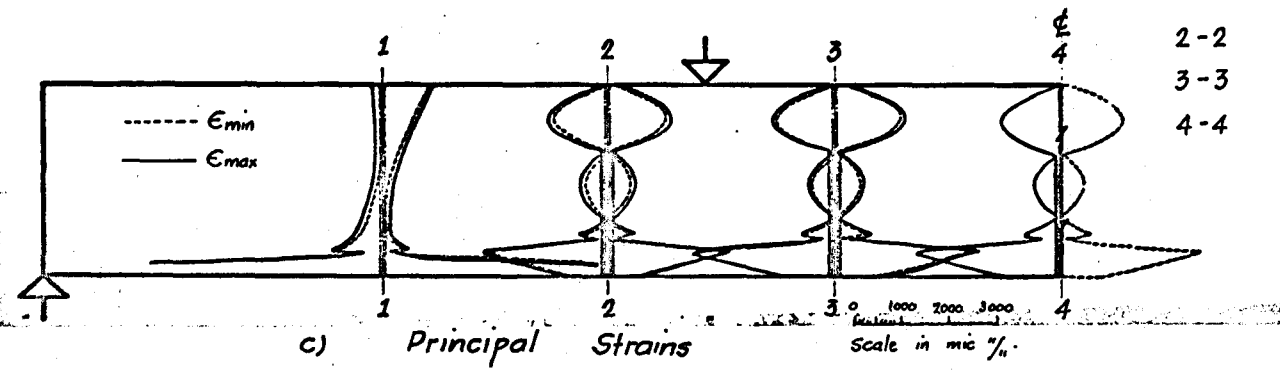
FIG. 7.4   DISTRIBUTION   OF   FLEXURAL ,   SHEAR ,   AND   PRINCIPAL   STRAINS   BY   METHOD II

based on this method will give the shear distribution be-
tween a cracked and an uncracked section, and an uncracked
and a cracked section as shown in Fig. 7.3a.

The portions of the beam between sections 1-1 to
3-3, were partitioned into a number of rectangular lamina
of equal depth. The average shear stresses at the base of
any lamina, between sections 1-1 and 2-2 and sections 2-2
and 3-3 were determined from the equilibrium of the free
bodies above that base level, see Fig. 7.3b.

The other steps involved in these computations are
exactly the same as those of Method I.

7.3.2 The distribution of shear strain, and the magnitude
and direction of the principal strains at various levels of
the depth, were computed for $\frac{1}{C}$ = 5, v = 0.16 and Δx = 0.1.
The results of these computations are shown in Fig. 7.3.

The magnitude of the principal strains were extremely
high and consequently the shear carried by the sections was
also found to be as high as 12 times the shear due to the
applied load.

7.4 Discussion

The basic drawback of Method I is that it only
determines the shear in the sections of the remaining un-
cracked portion of a beam, and its application to the case
of a comblike structure, fails to account for the shear

carried by the dowel action of the reinforcement and through the interlock between the aggregate of the concrete teeth.

Investigations in this regard by Acharya[16] envisage more than 60% of the shear to be carried by the dowel action. Similarly, more recent findings of Fenwick and Pauley[29] put the shear carried by the aggregate interlock and the uncracked section at 60% and 20% of the total, respectively.

In the light of these observations, a value of 14.6% shear carried by the uncracked concrete section at x = 25" could be considered as a reasonable amount, with the remainder to be carried by the aggregate interlock and dowel action.

Broms' approach, on the other hand, gave an unrealistically high value for the shear. The reason for this could be the following drawbacks in his approach.

a) It is assumed that there is an uncracked section between two cracked ones. Also, it was assumed earlier that concrete could only take the tensile strains up to a certain limiting value, ε_{cr}, beyond which it would crack. It can therefore be argued that the strains in the tensile zone of the uncracked section should always be less than ε_{cr}. However the strains computed by the conventional methods were more than ε_{cr} and still the section was considered to be uncracked. Therefore, these conflicting assumptions are

objectionable and probably the unrealistic magnitudes of
the computed quantities are as a result of these assumptions.

b) Another drawback of this approach is that even
in the shear span, cracks were assumed to be vertical, how-
ever observations have shown evidence that generally such
cracks are inclined.

Because of the results (Figs. 7.3 and 7.4), both
approaches could be regarded as two extremes and the actual
situation may be a case of a secondary crack between every
two visible cracks. An analysis based upon this criteria
may reveal results closer to the facts.

Although both of the approaches considered above are
crude, they certainly help to conclude the following:

1. In Broms' approach, which is an upper limit,
principal strains are higher than the cracking strain of
100 micro in/in, above the neutral axes. If this could be
established by a more correct solution then the principal
strains or stresses could be held responsible for the dia-
gonal cracking in the beam.

2. An analysis based on the assumption of a secon-
dary crack between two visible cracks, or an approach based
on the uncracked section of a cracked beam including the
shares of dowel action and aggregate interlock, may reveal
more reliable results.

Therefore, once a more realistic approach is

established, it would then be possible to trace the paths
of diagonal cracks analytically and extend these investi-
gations to study the cause of such a failure.

CHAPTER VIII

DISCUSSION

Analytical studies have shown that cracking is influenced by parameters, such as the interaction coefficient $\frac{1}{C}$, the percentage of steel reinforcement, p, the intensity of loading, λ, and location of the point load. Since the bond-slip modulus, k, was assumed to be constant during computation of the crack height, the variation in $\frac{1}{C}$ reflected the change in the geometry of the cross-section. It was found that a decrease in $\frac{1}{C}$ results in a higher crack height. Crack profiles were studied for a wide range of values of $\frac{1}{C}$, i.e. ∞ to 0.5, Fig. 3.9. This range of $\frac{1}{C}$ produced in general a 40% increase in the height of the crack and 50% at the load points. The height of the crack was always greatest at the load point.

In case of an uncracked prismatic section, for a high value of $\frac{1}{C}$, tension in the reinforcement varied from point to point, whereas for a small value of $\frac{1}{C}$ (= 0.5) in a beam with reinforcement anchored at ends, tension was almost constant, Fig. 2.6. Kani mentioned in his paper [7], "Due to lack of bond, no interchange of forces exists between steel bars and concrete, except at bar ends. The tensile force, F, of the reinforcing bar is constant from one end to the other. At both ends some kind of anchorage is necessary, ..."

It was also seen that the cracking pattern is

affected by the location of the point loads, Fig. 3.14.
Under a constant moment, cracks were higher in the shear
span, for a reduced value of the shear span. On the other
hand, cracks occurring between the two load points were
found to be higher in case of a larger shear span.

It was also established that an increase in the
intensity of the point loads significantly increased the
horizontal spread of the crack zone. It also increased the
crack heights, but at the load points this increase was not
as significant as in the shear span, see Figs. 3.14, 3.15
and 3.16.

It may be observed that the cracking patterns of the
test beams reported by Kani[7,12] and Leonhardt and Walther[4]
generally indicate more increase in the horizontal spread of
cracking under increasing intensity of the point load than it
does to the heights of crack at the load point.

It was also found that the percentage of the steel
reinforcement has the greatest effect on the crack profiles.
Decrease in the reinforcement results in an increase in the
horizontal spread of cracking zone as well as an increase in
the crack heights. For the case of $\frac{1}{C}$ = 5, Fig. 3.12, decrease
in p from 3.0 to 0.5 resulted in an increase in the height of
crack from 4.35" to 7.10", i.e. 63.2% at the load points and
a horizontal spread of the crack zone from 53.4" to 61.2",
i.e. 14.6%. Regarding influence of p on the crack height,

MacGregor and Walters[24] concluding from their analytical studies state, "In a region of pure flexure, the height of flexural cracking is strongly influenced by the steel percentage p. For a low value of p the crack will extend a considerable distance into the beam with no increase in load."

Krahl et al[17] from their analytical studies concluded, "In a region of pure moment, the addition of a small amount of tensile reinforcement to a plain concrete beam changes an unstable crack to a crack that is initially unstable, but then is stabilized. The addition of a large amount of tensile reinforcement can stabilize the entire range of crack development."

However, the approaches followed by MacGregor and Walters and Krahl et al are different from the one considered in this thesis, in the sense that they did not account for the slip between the concrete and the steel reinforcement, the conclusion drawn, as far as p is basically the same.

Treatment of the reinforced concrete beam as a composite beam with incomplete interaction indicated that the degree of interaction reduces as the point loads are moved towards the supports (Fig. 2.17), i.e. shear arm is reduced. This breakdown of the interaction resulted in computed influence lines for the maximum moment capacity essentially similar in form to those obtained experimentally by Leonhardt and Walther, and Kani (see Fig. 5.1, compare with Fig. 5.2,

for $\frac{u}{d} > 2.5$). The computed capacity curves were based solely on flexural consideration and no account was taken of the applied shear. Each curve consists of two parts, namely one sloping down (analogous to portion VT in Fig. 5.2) in which the concrete strain governed the strength and the other which is horizontal (analogous to portion TE in Fig. 5.2) in which steel strain governs the strength of the beam. Between these two parts, there is a transition point, T, at which both concrete and steel strains govern the strength simultaneously.

Kani[10] argued that the transition point, T, (Fig. 5.2) differentiates between two types of failure. Beams with $\frac{u}{d}$ ratio less than T fail by inclined cracking and those with $\frac{u}{d}$ greater than T, only a flexural failure is possible.

It was found that the value of $\frac{1}{C}$ affects the moment carrying capacity of a reinforced concrete beam. For a given value of u, a decrease in $\frac{1}{C}$ causes a decrease in $M_{max.}$ on the left hand side of the transition point and an increase in $M_{max.}$ on the right hand side of the transition point, Fig. 5.4. Decrease in $\frac{1}{C}$ also results in a shift of the transition point towards the mid span. Describing the influence of bond, Leonhardt and Walther[4] stated, "Therefore the quality of the bond influences the failure load considerably more for failure under shear (i.e. left of T) than for bending (i.e. right of T)." Kani[10], in discussing the influence of bond for the beam tests reported by Leonhardt and Walther stated, "the better the bond the lower the diagonal load-carrying

capacity". "The beams with poor bond carried at least 31 percent more load than the corresponding beams with deformed bars. The beams with poor bond reached their flexural failure, while the beams with deformed bars stayed far below their full flexural capacity." This, however, in our analysis holds only for beams with u to the right of T.

The percentage of steel reinforcement has shown a considerable influence on the moment carrying capacity. It was found that increase in p has two effects, namely, an increase in the moment carrying capacity of the beam and, secondly, a shift of the transition point, T, towards the midspan, Figs. 5.5a and 5.8a. It, however, reduces the relative beam strength, Figs. 5.5b and 5.8b.

Kani established similar conclusions experimentally (Fig. 5.6). He stated, "For those beams with a high percentage of reinforcement (p = 2.80 percent), the "valley of diagonal failure" has a low point in the vicinity of $\frac{M_{test}}{M_u^-}$ = 50 percent, whereas for those beams with a low percentage of reinforcement (p = 0.50 percent with $\frac{M_{test}}{M_u^-}$ = 100 percent), the valley of diagonal failure" disappears, and "that the amount of main reinforcement influences the location of the transition point, T, ..." "Varying the main reinforcement from p = 2.80% to 1.88% and 0.80%, the test results produced locations of the transition point, T, at $\frac{u}{d}$ = 6.5, 6.0 and 3.5 respectively."

From the computed results for p = 0.5 to 3.0, the transition point, T, moved from u = 23" (i.e. $\frac{u}{d}$ = 3.28) to u = 40" (i.e. $\frac{u}{d}$ = 5.72) and the computed relative beam strength, $\frac{M_{max}}{M_u}$, reduced from 81% to 49%, Fig. 5.8b. In spite of the fact that certain simplifying assumptions were made for this analytic approach, the computed values are in reasonable agreement with the experimental results.

An attempt was made to study the distribution of bond stress and the amount of slip occurring along the length of a reinforced concrete beam. It was observed that bond stress and slip are considerably higher in the cracked region of a beam than in the uncracked one. The amount of slip varied considerably within the cracked region. Interestingly in case 1, (the beam with two symmetric point loads), reversal of slip was indicated on either side of the load point. The maximum slip at design load was found to be more than .01 inches and took place at the load point. The minimum slip occurred at the point where cracking started. The bond stress was maximum of 900 psi, Fig. 6.4.

In case 2 (the beam with uniformly distributed loading), the maximum slip was 0.005 inches and took place at the extremities of the cracking zone. The minimum slip took place just before the point of maximum slip. Bond stress was highest at the end of cracking zone and had a magnitude of 910 psi, Fig. 6.5.

The variation in the uncracked region of beams was comparatively very small.

Shear studies carried out by the two methods revealed quite different results. Method 2, the modified Broms' method gave unrealistically high magnitudes of the total shear capacity. Method 1, indicated that 14.7% of the total shear is carried by the remaining uncracked section at x = 25". The remainder of the shear is presumably carried by aggregate interlock and dowel action. The opinions of the investigators vary regarding the share of the total shear carried by the remaining uncracked concrete section in a beam. MacGregor and Walters[24] suggested that 11% of shear is carried by the dowel action, 23% of the aggregate interlock and the rest (i.e. 66%) is carried by the uncracked concrete. Fenwick and Pauley[29] put 60% of the shear as carried by the aggregate interlock, 20% by the dowel action and only 20% carried by the uncracked concrete section. Acharya[16] assumes that as much as 60% of the shear is carried by the dowel action.

Therefore more rigorous analysis is required to determine the share of shear carried by different actions in a cracked beam. Such analysis hopefully will lead to further insight into the problem of inclined cracking.

CHAPTER IX

SUMMARY AND SUGGESTIONS FOR FUTURE STUDIES

The reinforced concrete beam has been treated as a composite beam with incomplete interaction. The interaction coefficient, $\frac{1}{c}$, percentage of steel reinforcement, p, intensity of the point load, λ, and the location of the load point, u, were found to affect the extremities of the computed flexural cracking zone. Decrease in the interaction coefficient, $\frac{1}{c}$, increased the height of flexural cracks. It did not, however, significantly affect the horizontal spread of the cracked zone. Increase in the percentage of steel reinforcement, p, on the other hand, decreased the height as well as horizontal spread of the cracked zone for a given load. With a percentage of steel of 0.5, the influence of bond as manifested by interaction coefficient, $\frac{1}{c}$, caused an increase of 15% in the crack height for $\frac{1}{c} = \infty$ to 5. With a percentage of steel of 3, the crack height showed an increase of 53.6% for the same range of $\frac{1}{c}$, Fig. 3.13.

Increase in the intensity of the point load, for a given value of $\frac{1}{c}$, produced proportionately higher crack heights in the shear span, than it did between the load points. It, however, significantly increased the horizontal spread of the flexural cracking zone, Figs. 3.15 to 3.17.

The shape of the flexural crack profile was also influenced by the location of the load points. With a smaller

value of the shear span, u, crack heights in the shear span were greater than the crack heights between the load points whereas for larger shear spans the crack heights between the point loads were greater than those in the shear span, Fig. 3.14.

Influence lines for strains at the load points indicated that a decrease in the interaction coefficient, $\frac{1}{C}$, affects the concrete top fibre strain, ε_{ct}, more than the average steel strain, ε_{sm}, Fig. 4.4, whereas an increase in the steel percentage, p, has more effect on the steel strain, ε_{sm}, than on the concrete fibre strain, ε_{ct}, Fig. 4.5.

The computed influence lines for the moment carrying capacity were similar to the curves for relative beam strengths obtained experimentally by Kani. The transition point, T, divided the computed curves into two parts, one in which the concrete strain governed the strength (to the left of the transition point, T, i.e. for shorter shear spans) and the other in which steel governed (to the right of T, i.e. larger shear spans) the strength of the beam, Fig. 5.1. A decrease in the interaction coefficient, $\frac{1}{C}$, produced a marked reduction in the moment carrying capacity for a value of the shear span, u, to the left of the transition point, T, and increased the moment capacity slightly for a value of the shear span, u, to the right of T. Decrease in $\frac{1}{C}$ shifted the transition point towards the mid span, Fig. 5.4.

With the same percentage of steel (p = 1.1%) and at u = 17.5" (i.e. $\frac{u}{d}$ = 2.5), the moment carrying capacity for $\frac{1}{C}$ = 0.5 was found to be only 72.5% of the case where $\frac{1}{C}$ = 5 and at the same location for the "Typical Beam". The transition point was at u = 10.5" and 35.0" for $\frac{1}{C}$ = 5 and 0.5 respectively, Figs. 5.1 and 5.7.

Increase in the percentage of steel, p, had two effects, it increased the moment carrying capacity of the beam and it shifted the transition point towards the mid-span. It also decreased the ratio of the computed flexural capacity, $M_{max.}$, to the computed ultimate strength, M_u, of the beam with complete interaction, Figs. 5.5a and b and 5.8a and b.

For $\frac{1}{C}$ = 0.5, in the case of the "Typical Beam", an increase of p, from 0.5 to 3.0 resulted in a shift of the transition point from 23" to 35" and a decrease in $\frac{M_{max.}}{M_u}$ from 81% to 49% at u = 17.5" (i.e. coincident with $\frac{u}{d}$ = 2.5).

The shear distribution computed by Method II, indicated that 14.7% of the total shear was carried by the uncracked concrete section at x = 25", i.e. in the shear span. The remaining external shear is probably carried by aggregate interlock and dowel action.

Method II yielded unrealistically high values of both shear stress and total vertical shear capacity.

Suggestions for further work are as follows:

1. The influence of curvilinear bond-slip characteristic on the flexural cracking should be investigated. The method of analysis should be extended to include the study of incremental loading.

2. An arch model should be investigated for determination of the moment capacity of a beam for smaller values of shear span (i.e. $\frac{u}{d} < 2.5$), in order to establish a complete theoretical explanation of the reinforced concrete beam.

3. The distribution of shear stress and strain across the depth of a cracked reinforced concrete beam should be investigated more rigorously, particularly in regard to the magnitude of vertical shear carried by aggregate interlock and dowel action.

This will yield a better assessment of the principal stresses and strains, which may further lead to an insight into the problem of the diagonal cracking.

CHAPTER X

CONCLUSIONS

The conclusions from this study are as follows:

1. The degree of interaction for a composite beam, with symmetrical two point loads is a minimum at the load points. This results in the increase of strains at the top fibre of concrete, ε_{ct}, a decrease in the average steel strain, ε_{sm}, at the load point compared with the usual transformed section.

2. The computed flexural crack profile is similar in form to those observed in tests showing an increase in the height of the flexural crack at the load points due to the fact that there is a lower degree of interaction at the load points.

3. End anchorage of the reinforcement in a reinforced concrete beam, improves the degree of interaction near the supports, compared with one without anchorage. This improvement, however, did not lead to any increase in the moment capacity.

4. In the case of an uncracked, prismatic beam with end anchorages, for a very low value of the interaction coefficient, $\frac{1}{C}$, i.e. poor bond, the tensile force, F, in the reinforcement is constant throughout its length.

5. The interaction coefficient, $\frac{1}{C}$, decreases with an increase in the width, depth or the percentage of steel

in a reinforced concrete beam and it increases with an increase in the length of the beam.

6. When flexural cracking takes place, due to reduction in the depth of the uncracked concrete section, the value of the interaction coefficient, $\frac{1}{C}$, increases. This results in an increase in the degree of interaction as cracking progresses upwards.

7. During flexural cracking, the direct compressive force in the concrete, F, increases, due to a reduction in M_c, the moment carried by the remaining concrete.

8. The influence lines for $\frac{F}{F'}$ at the load point, (in a simple beam with symmetrical two point loads and end slip permitted) indicates a decrease in the degree of interaction as the shear span is reduced.

Restriction of the end slip by means of end anchorages results in an improvement of the degree of interaction near the support which is particularly significant in case of smaller values of the shear span. In spite of this improvement, no significant difference in the flexural capacity is obtained.

9. Loss of interaction, percentage of steel reinforcement, intensity of the point load and location of the load point have an effect on the computed extremities of flexural cracking. Loss of interaction increases the crack height. It does not significantly affect the longitudinal spread of the crack zone. Increase in the percentage of

steel decreases the crack height as well as the horizontal spread of the crack zone.

Increase in the intensity of the point loads has more significant effect on the spreading of the crack zone than of increasing the crack height. The length of the shear span as a whole affects the shape of the crack profile.

10. A decrease in the interaction coefficient, $\frac{1}{C}$, produces a marked reduction in the moment carrying capacity for a value of the shear span, u, to the left of the transition point, T, and increases the moment capacity slightly for a value of the shear span, u, to the right of the transition point. Decrease in $\frac{1}{C}$ also results in a shift of the transition point towards the mid span.

11. Increase in the percentage of steel has two effects, it increases the moment carrying capacity and it shifts the transition point towards the midspan. Increase in p, however, reduces the ratio of $M_{max.}$ to M_u.

12. Method I, for determination of the shear distribution shows that 14.7% of the total shear is carried by the uncracked concrete section. Method II - Modified Broms' Method gives unrealistically high values of the shear carried by a cracked section of beam.

BIBLIOGRAPHY

(1) Evan, R.H., and Robinson, G.W., "Bond Stresses in Pre-
     stressed Concrete from X-Ray Photographs", The
     Institution of Civil Engineers, Proceedings Pt. 1,
     1955, Vol. 4. Paper No. 6025, pp 212-235.

(2) Garson, J.R., Siess, C.P., Newmark, N.M., "An Investi-
     gation of Load-Deformation Characteristics of Rein-
     forced Concrete Beam up to the Point of Failure",
     Structural Research Series No. 40, Reprint June 1959,
     University of Illinois.

(3) Siess, C.P., Viest, I.M., Newmark, N.M., "Studies of
     Slab and Beam Highway Bridges: Part III", University
     of Illinois Engineering Experiment Station, Bulletin
     Series No. 396.

(4) Leonhardt, F. and Walther, R., "Contribution to the
     Treatment of Shear in Reinforced Concrete", National
     Research Council of Canada, Ref. NRC. TT-1172,
     Ottawa, 1965.

(5) Mathey, G., and Watstein, D., "Investigation of Bond
     in Beam and Pull-Out Specimens with High-Yield-
     Strength Deformed Bars", ACI Journal, Proceedings
     V. 57, No. 9, March 1961, pp 1071-1090.

(6) Report of ACI-ASCE Committee 326, "Shear and Diagonal
     Tension", Journal of the ACI, Proceedings V.59,
     January to March 1962.

(7) Kani, G.N.J., "The Mechanism of So-Called Shear Failure",
Trans. of Engng. Inst. of Canada, April 1963.

(8) Plowman, J.M., "Measurement of Stress in Concrete Beam
Reinforcement", The Institution of Civil Engineers,
Proceedings Vol. 25, Paper No. 6659, June 1963,
pp 127-146.

(9) Robinson, H., "Preliminary Investigation of a Composite
Beam with Ribbed Slab Formed by Cellular Steel
Decking", Engineering Dept. Report No. 35, McMaster
University, October 1961.

(10) Kani, G.N.J., "The Riddle of Shear Failure and Its
Solution", Journal of the ACI, Proceedings Vol. 61,
No. 4, April 1964, pp 441-467.

(11) Robinson, H., "Discussion of Paper, Measurement of
Stress in Concrete Beam Reinforcement", The Insti-
tution of Civil Engineers, Proceedings Vol. 28,
July 1964, pp 412-419.

(12) Kani, G.N.J., "Basic Facts Concerning Shear Failure",
Journal of the ACI, Proceedings, Vol. 63, No. 6,
June 1966, pp 675-692.

(13) Broms, B.B., "Stress Distribution, Crack Patterns, and
Failure Mechanisms of Reinforced Concrete Members",
Journal of the ACI, Proceedings, Vol. 61, No. 12,
Dec. 1964, pp 1535-1556.

(14) Barnard, P.R., "Researches into the Complete Stress-
Strain Curve for Concrete", Magazine of Concrete

Research, Vol. 16, No. 49, Dec. 1964, pp 203-210.

(15) Broms, B.B., "Stress Distribution in Reinforced Concrete Members with Tension Cracks", Journal of the ACI, Proceedings Vol. 62, No. 9, Sept. 1965, pp 1095-1108.

(16) Acharya, D.N., and Kemp, K.O., "Significance of Dowel Forces on the Shear Failure of Rectangular Reinforced Concrete Beams Without Web Reinforcement", Journal of the ACI, Proceedings Vol. 62, No. 10, Oct. 1965, pp 1265-1279.

(17) Krahl, N.W., Khachaturian, N. and Siess, C.P., "Stability of Tensile Cracks in Concrete Beams", Journal of the Struct. Division, Proceedings of the ASCE, Vol. 93, No. ST1, Feb. 1967, pp 235-254.

(18) Wong, A.C.C., "The Influence of Loss of Bond on the Mechanics of Failure of Reinforced Concrete Beams", M. of Eng. Thesis, McMaster University, Hamilton, Ontario, Oct. 1964.

(19) Ho, H.H.H., "The Influence of Loss of Bond on the Failure Mechanism of Reinforced Concrete Beams", M. of Eng. Thesis, McMaster University, Hamilton, Ontario, May 1966.

(20) Bresler, B., and MacGregor, J.G., "Review of Concrete Beams Failing in Shear", Journal of the Struct. Division, Proceedings of the ASCE, Vol. 93, No. ST1, Feb. 1967, pp 343-371.

170

(21) Ngo, D., and Scordelis, A.C., "Finite Element Analysis of Reinforced Concrete Beam", Journal of the ACI, Proceedings Vol. 64, No. 3, March 1967, pp 152-163.

(22) Kani, G.N.J., "How Safe are our Large Reinforced Concrete Beams?", Journal of the ACI, Proceedings Vol. 64, March 1967, pp 128-141.

(23) Robinson, H., "Tests on Composite Beams with Cellular Deck", Journal of the Struct. Division, Proceedings of the ASCE, Vol. 93, No. ST4, August 1967, pp 139-164.

(24) MacGregor, J.G. and Walters, J.R.V., "Analysis of Inclined Cracking in Slender Reinforced Concrete Beams", Journal of the ACI, Proceedings Vol. 64, No. 10, Oct. 1967, pp 644-653.

(25) Lutz, L.A. and Gregly, P., "Mechanism of Bond and Slip of Deformed Bars in Concrete", Journal of the ACI, Proceedings Vol. 64, No. 11, Nov. 1967, pp 711-721.

(26) Kar, J.N., "Diagonal Cracking in Prestressed Concrete Beams", Journal of the Struct. Division, Proceedings of the ASCE, Vol. 94, No.ST1, Jan. 1968, pp 83-109.

(27) Bresler, B and Bertero, V., "Behaviour of Reinforced Concrete Under Repeated Load", Journal of the Struct. Division, Proceedings of the ASCE, Vol. 94, No. ST6, June 1968, pp 1567-1590.

(28) Nilson, H.A., "Non-Linear Analysis of Reinforced Concrete by the Finite Element Method", Journal of the ACI, Proceedings Vol. 65, No. 9, Sept. 1968.

(29)   Fenwick, R.C. and Pauley, T., "Mechanism of Shear

Resistance of Concrete Beams", Journal of the Struct.

Division, Proceedings of the ASCE, Vol. 94, No. ST10,

October 1968, pp 2325-2350.

APPENDIX I

Composite Theory

Al.1 General

The type of structure considered in this analysis is shown in Fig. Al.1. It is a T-beam consisting of a beam and a slab tied together by means of a shear connection which transfers horizontal shear from one element to the other. The degree of composite action depends on the effectiveness of the shear connection in preventing the relative movement between the beam and the slab. If no movement or slip is permitted (i.e. the shear connectors are perfectly rigid), the interaction would be complete and the resisting moment of the composite section would be based upon the transformed sectional properties. On the other hand, if the beam and the slab are not interconnected (i.e. no shear connection), slip would take place freely and there would be no inter- action and the resisting moment in this case would be sum of the resisting moments of each element.

Generally the shear connectors in a composite section are not perfectly rigid and so there is a relative movement or slip between the beam and the slab. Such cases are re- ferred to as the composite sections with incomplete inter- action.

Centroidal axis of slab.

C_s

Z C_b

Centroidal axis of beam

F M_s

M_t F M_b

ϵ_s

$-\epsilon_b$

a) Cross - Section

b) Forces

$\left(M_t = M_s + M_c + F \cdot Z \right)$

c) Strains
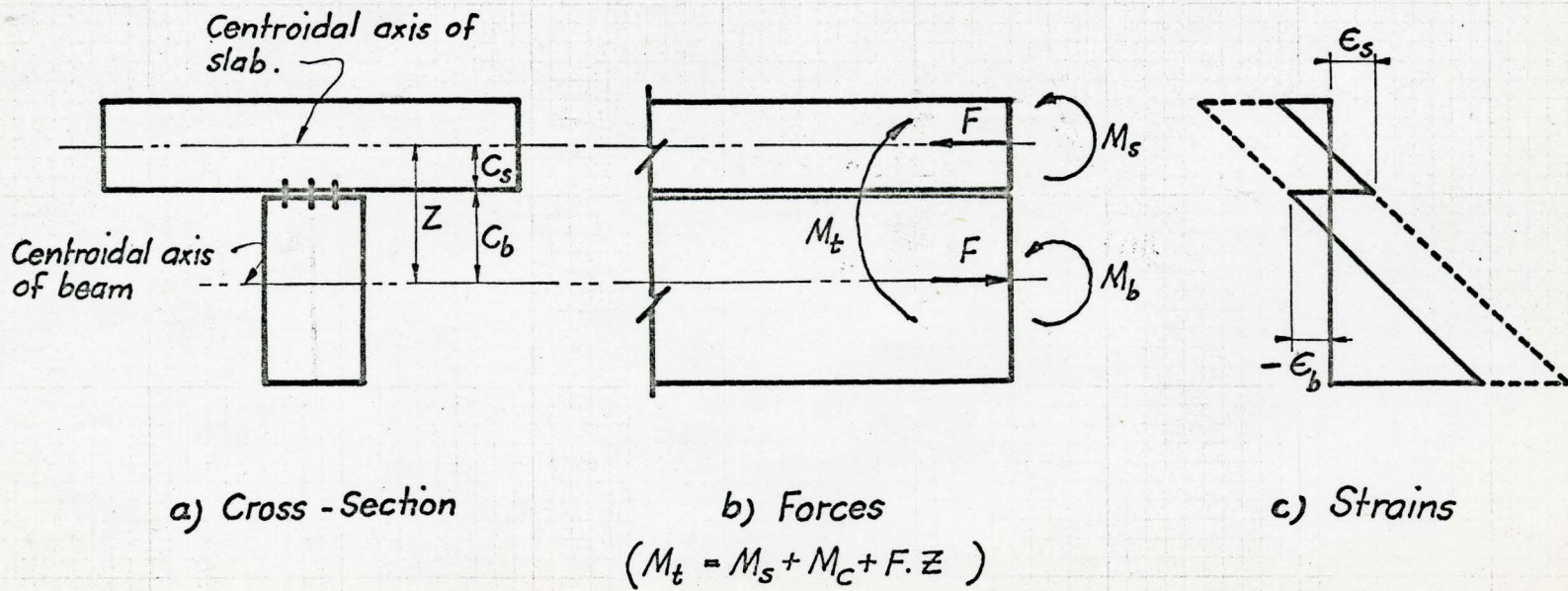
COMPOSITE T-BEAM WITH INCOMPLETE INTERACTION

FIG. A1.1

A1.2   Assumptions

The principal assumptions made in this analysis of a composite section with incomplete interaction are as follows:

1)   The shear connection between the beam and slab is assumed to be continuous along the length of the beam, i.e. connectors are of equal capacities and are equally spaced; then

$$\frac{k}{s} = \text{constant} \qquad \text{A1.1}$$

where   k is so-called modulus of connector and

s is the spacing between connectors.

(If connectors are not equally spaced this assumption will be satisfied only if the capacities of connectors vary directly as their spacings.)

2)   The amount of slip permitted by the shear connection is directly proportional to the load transmitted:

$$\gamma = \frac{Q}{k} \qquad \text{A1.2}$$

where   Q is the load transmitted by a connector, (i.e. the load-slip curve for a connector be a straight line, the slope of which is called the modulus, k, of the connector).

3)   The distribution of strains throughout the depth of the beam and the slab is linear.

4)   The beam and the slab are assumed to deflect equal amounts at all points along their lengths.

The total load on a shear connector, Q, is also expressed as:

$$Q = q.s$$

where q is the load transmitted per unit length of the beam. An alternate form of Eq. A1.2, therefore, is

$$\gamma = q.\frac{s}{k} \qquad\qquad A1.2a$$

A1.3 Basic Relationships

The rate of change of slip along the length of a beam is equal to the difference between the strain in the slab, and the strain in the beam at the level at which slip occurs, i.e. the interface. Using notation of Fig. A1.1c, this may be written as:

$$\frac{d\gamma}{dx} = \varepsilon_b - \varepsilon_s \qquad\qquad A1.3$$

where $d\gamma$ is the change in slip over a length, dx, of the beam.

When a composite beam is subjected to a positive bending moment, the shear connectors exert forces which produce compression in the slab and tension in the beam. These forces act at location of the shear connector, but on each element may be replaced by a couple and a force acting at the centroid of the element. The couples can be added algebraically to the moments that would exist in the beam and slab to obtain the total resistance of the composite section; that is,

$$M_t = M_s + M_b + F.Z \qquad \text{A1.4}$$

Eq. A1.4 is also called an Equilibrium Equation for a section of the composite beam.

Since the distribution of the strains, throughout the depth has been assumed linear, then

$$\varepsilon_b = \frac{F}{E_b A_b} - \frac{M_b C_b}{E_b I_b} \qquad \text{A1.5a}$$

$$\varepsilon_s = -\frac{F}{E_s A_s} + \frac{M_s C_s}{E_s I_s} \qquad \text{A1.5b}$$

where E_b and E_s are moduli of elasticity of the beam,

I_b and I_s are the moments of inertia, and

A_b and A_s are the cross-sectional areas of the beam and the slab respectively.

The load per unit length, q, (or $= \frac{Q}{s}$) which is transmitted between the slab and the beam is equal to the change in the interaction force, F, along the length of the beam. This may be written as

$$q = \frac{dF}{dx} \qquad \text{A1.6}$$

and from Eq. A1.2a

$$\frac{d\gamma}{dx} = \frac{s}{k} \cdot \frac{d^2F}{dx^2} \qquad \text{A1.7}$$

Substitution of Eq. A1.3 and A1.5 in Eq. A1.7 yields:

$$\frac{s}{k} \cdot \frac{d^2F}{dx^2} = F\left(\frac{1}{E_bA_b} + \frac{1}{E_sA_s}\right) - \left(\frac{M_bC_b}{E_bI_b} + \frac{M_sC_s}{E_sI_s}\right) \qquad \text{A1.8}$$

Since the beam and the slab deflect alike at all points, that is, they have equal curvatures, the moments M_s and M_b are related as follows:

$$\frac{M_s}{E_sI_s} = \frac{M_b}{E_bI_b} = \frac{M_s + M_b}{E_sI_s + E_bI_b} \qquad \text{A1.9}$$

or by substitution of Eq. A1.4, Eq. A1.9 becomes

$$\frac{M_s}{E_sI_s} = \frac{M_b}{E_bI_b} = \frac{M_t - F \cdot Z}{\Sigma EI} \qquad \text{A1.10}$$

where $\Sigma EI = E_sI_s + E_bI_b$

Substituting from Eq. A1.10 into A1.8 yields

$$\frac{s}{k} \cdot \frac{d^2F}{dx^2} = F\left[\frac{1}{E_bA_b} + \frac{1}{E_sA_s} + \frac{z^2}{\Sigma EI}\right] - \frac{M_tZ}{\Sigma EI}$$

which may be written as

$$\frac{d^2F}{dx^2} - F \cdot \frac{k}{s} \cdot \frac{\overline{EI}}{\overline{EA}\Sigma EI} = -\frac{k}{s} \cdot \frac{Z}{\Sigma EI} \cdot M_t \qquad \text{A1.11}$$

where the following expressions are introduced for convenience:

$$\overline{EI} = \Sigma EI + \overline{EA} \cdot z^2 \quad \text{and}$$

$$\frac{1}{\overline{EA}} = \frac{1}{E_sA_s} + \frac{1}{E_bA_b}$$

Eq. A1.11 is a second order differential equation in F. The solution of Eq. A1.11, can be obtained by expressing the external moment M_t in terms of the distance x of the

section from the left hand support.

Solutions of a beam with symmetrical two point load, and with different end conditions have been included in Chapter II of this thesis.

The interaction force, F, is related to the effectiveness of the shear connection. Denoting the value of interaction force, for complete interaction by F', the degree of interaction "α" can be written as

$$\alpha = \frac{F}{F'} \qquad\qquad \text{A1.12}$$

A1.5 Strains

Strains in the beam may be determined for any degree of interaction from the equation

$$\varepsilon_b = \frac{F}{E_b A_b} + \frac{M_b y_b}{E_b I_b} \qquad\qquad \text{A1.13a}$$

and in the slab from the equation

$$\varepsilon_s = - \frac{F}{E_s I_s} + \frac{M_s y_s}{E_s I_s} \qquad\qquad \text{A1.13b}$$

where y_b and y_s are the distances from the centroid of the beam or of the slab to the point at which a strain is desired. In both cases, y is positive when measured downwards. The force F in these equations may be computed from the solution of Eq. A1.11 and moment M_b and M_s may be obtained as

$$M_b = \frac{E_b I_b}{\Sigma EI} (M_t - F.Z) \qquad\qquad \text{A1.14a}$$

$$M_s = \frac{E_s I_s}{\Sigma EI} (M_t - F.Z) \qquad\qquad \text{A1.14b}$$

Thus the equations for strains may be written in the form

$$\varepsilon_b = \left[S_b - \alpha . \frac{\overline{EA}}{EI} . z . \left(S_b.Z - \frac{1}{E_b A_b} \right) \right] M_t \qquad \text{A1.15a}$$

$$\varepsilon_s = \left[S_s - \alpha . \frac{\overline{EA}}{EI} . z . \left(S_s.Z + \frac{1}{E_s A_s} \right) \right] M_t \qquad \text{A1.15b}$$

where

$$S_b = \frac{Y_b}{\Sigma EI} \qquad \text{and}$$

$$S_s = \frac{Y_s}{\Sigma EI}$$

The strains for complete interaction ε_b' and ε_s' can be obtained by putting $\alpha = 1$ in above equations for ε_b and ε_s.

APPENDIX II

List of Symbols

A_c Effective cross-sectional area of the concrete (sq. inches)

A_s Cross-sectional area of the steel reinforcement (sq. inches)

b Width of the beam (inches)

$\dfrac{1}{C}$ Interaction coefficient, a dimensionless number

Cd, Cd_1, Cd_2 Effective depths of the concrete in a beam cross-section (inches)

C_{ch} Total crack height (inches)

C_h Increment in the crack height (inches)

C_s, C_s Distances from the centroids of concrete and steel, respectively, to the psuedo interface (inches)

d Effective depth of the section of a reinforced concrete beam (inches)

E_c, E_s Moduli of elasticity of concrete and steel respectively (lb./sq.inch)

ΣEA $E_c A_c + E_s A_s$

$\dfrac{1}{\overline{EA}}$ $\dfrac{\Sigma EA}{(E_c A_c \cdot E_s A_s)}$

ΣEI $E_c I_c + E_s I_s$

$\overline{EI}$ $\Sigma EI + \overline{EA} \cdot z^2$

F, F_1, F_2, F_3, F' Horizontal direct forces acting at the centroids of the concrete and the steel (lbs.)

G_c Shear modulus of concrete

H, H' Half of the uncracked depth of the concrete section (inches)

I_c, I_s Second moments of area of the concrete and steel respectively (inches^4)

jd Depth of lever arm in the conventional reinforced concrete theory (inches)

k Bond-slip modulus in case of a reinforced concrete beam (lb./in.)

L Span length of the beam (inches)

M_c, M_s Internal moments carried by the concrete and steel respectively (lb.-in.)

M_t Moment due to external loads on the beam (lb.-in.)

M_{test} Maximum experimental moment capacity of a beam (lb.-in.)

$M_{max.}$ Maximum computed moment capacity of a beam (lb.-in.) for incomplete interaction.

M_u Computed ultimate moment capacity of a beam (lb.-in.) for complete interaction.

m $\dfrac{E_s}{E_c}$

n Number of reinforcing bars in a reinforced concrete section.

n_1, n_2 Depths of the neutral axes at sections 1 and 2 respectively (inches)

p Percentage of reinforcement in a reinforced concrete section

q, q' Horizontal shear per unit length (lb./in.)

Q   Total shear at a connector in a composite section (lbs.)

s   Spacing between studs in a composite section (inches)

S   Total horizontal shear carried by a concrete section (lbs.)

U or u   Distance from the support to the nearest load point i.e. shear span (inches)

$\frac{u}{d}$ Shear arm ratio

V   Vertical shear due to external loading (lbs.)

W   Magnitude of the external point load (lbs.)

x   Distance from the left hand support to any section within the span (inches)

y   Depth from the top fibre of the concrete to any level within the depth of the section (inches)

$\bar{y}$ Distance between the centroidal axis of the uncracked concrete area and the neutral axis of the transformed area of the cracked reinforced concrete beam (inches)

z   Distance between the centroidal axes of the uncracked concrete section and the steel reinforcement (inches)

α or $\frac{F}{F'}$ Degree of interaction between the concrete and the reinforcement in a reinforced concrete beam

γ Slip between the concrete and the steel (micro inches)

γ_{xy} Shear strain (micro in./in.)

Δx — Distance between two closely spaced cross-sections of a beam (inches)

$\varepsilon_{cb}, \varepsilon_{ct}$ — Strains at the bottom and top concrete fibres respectively (micro in./in.)

ε_{cr} — The critical (cracking) tensile strain of the concrete (micro in./in.)

ε_r — Strain due to the distortion of the concrete 'teeth' in a cracked beam (micro in./in.)

$\varepsilon_{sb}, \varepsilon_{sm}, \varepsilon_{ct}$ — Strains at the bottom, mid height and top fibres respectively of the steel (micro in./in.)

$\varepsilon_{ct_{max}}, \varepsilon_{sm_{max}}$ — Maximum permissible compressive strain at the top fibre of concrete and maximum permissible average tensile strain in the steel reinforcement, respectively (micro in./in.)

$\varepsilon_{min}, \varepsilon_{max}$ — Minimum and maximum principal strains, respectively (micro in./in.)

$\varepsilon_x, \varepsilon_y$ — Flexural longitudinal and transverse strains respectively (micro in./in.)

$\varepsilon_{y_1}, \varepsilon_{y_2}$ — Flexural strains at levels y_1 and y_2 respectively (micro in./in.)

θ — Angle of inclination of the direction of principal strains (degrees)

λ — Ratio of the applied load to one times the design load

μ — Degree of the end fixity

v	Poisson's ratio for the concrete (assumed as 0.16)
σ_b	Bond stress (lb./sq.in.)
τ_{12}	Horizontal shear stress (lb./sq. inch)
τ_{xy}	Vertical shear stress $= \tau_{12}$

```
C
C
C
C
C                           APPENDIX   THREE                              184
C                           -----------------
C
C                      TYPICAL   COMPUTER   PROGRAM
C                      ------------------------------
C
C
C     FUNCTION
C
C         THE PROGRAM COMPUTES THE FLEXURAL CRACK PROFILES IN A REINFO-
C         RCED CONCRETE BEAM - TREATING IT AS A COMPOSITE BEAM WITH
C         INCOMPLETE INTERACTION.
C
C     DESCRIPTION
C
C         ALL DIMENSIONS ARE THOSE OF THE TYPICAL BEAM EXCEPT THE
C         VALUE OF THE INTERACTION COEFFICIENT HAS BEEN VARIED .
C
C     NOTATIONS
C
C         AL           LENGTH OF THE BEAM
C         AC,AS        AREAS OF THE CONCRETE AND STEEL RESPECTIVELY
C         B            WIDTH OF THE BEAM
C         BETA(I)      DEGREE OF INTERACTION
C         CC(I)        INTERACTION COEFFICIENT - TERMINAL VALUE AS OUTPUT
C         CCI          INTERACTION COEFFICIENT - INITIAL VALUE AS OUTPUT
C         CCH          TOTAL CRACK HEIGHT
C         CD           UNCRACKED DEPTH OF CONCRETE
C         CH           INCREMENT IN THE CRACK HEIGHT
C         CM           MOMENT CARRIED BY THE UNCRACKED CONCRETE SECTION
C         ED           EFFECTIVE DEPTH OF THE CONCRETE
C         EC,ES        MODULI OF ELASTICITY OF CONCRETE AND STEEL RESPECTIVELY
C         EPCR         PERMISSIBLE CRACKING STRAIN
C         EPCB,EPCT    STRAINS AT BOTTOM AND TOP FIBRES OF CONCRETE RESPECTIVE
C         EPSB,EPST    STRAINS AT BOTTOM AND TOP FIBRES OF STEEL RESPECTIVELY
C         EPSM         STRAIN AT THE MID-HEIGHT OF STEEL REINFORCEMENT
C         F(I),F1      INTERACTION FORCE FOR INCOMPLETE AND COMPLETE INTER-
C                      ACTIONS RESPECTIVELY
C         H            HALF THE DEPTH OF UNCRACKED SECTION OF CONCRETE
C         TD           TOTAL DEPTH OF CONCRETE
C         TM           EXTERNAL MOMENT
C         PHI          DIAMETER OF THE REINFORCING BAR
C         U            LENGTH OF THE SHEAR SPAN
C         WT           EXTERNAL LOAD
C         X            DISTANCE OF ANY SECTION FROM L.H.S. SUPPORT
C         XIC,XIS      MOMENTS OF INERTIA OF THE CONCRETE AND STEE RESPECT-
C                      IVELY
C         Z            INTERNAL LEVER ARM
C
C     DECK
C
      DIMENSION CC(10),BETA(10),GAMMA(10),F(10)
      U=29.25
      X=4.25
      PI=22./7.
    4 AL=90.0
      WRITE(6,10)X
```

```
   10 FORMAT(10X,42H ********( THE CURRENT SECTION IS AT X = ,F6.2,
     111H )********/)
      B=4.0
      TD=8.50
      TDM=TD*0.5
      ED=7.0
      WT=36200./29.25
      IF(X.GT.U) GO TO 5
      TM=WT*X
      GO TO 6
    5 TM=36200.
    6 AS=0.31
      XIS=(AS*AS)/(PI*4.)
      PHI=SQRT(4.*AS/PI)
      CS=0.5*PHI
      ES=30000000.0
      EC=3500000.0
      EPCR=0.0001
      CC(1)=100.
      CC(2)=50.
      CC(3)=20.
      CC(4)=10.
      CC(5)=5.
      CC(6)=2.
      CC(7)=1.
      DO 200 I=1,7
      CCI=CC(I)
      CCH=0.0
      H=TD/2.
      AC=B*2.*H
      XIC=B*(2.*H)**3/12.
      EABAR=(ES*AS*EC*AC)/(EC*AC+ES*AS)
      EISIG=ES*XIS+EC*XIC
      Z=ED-H
      EIBAR=EISIG+EABAR*Z**2
      THETA=EIBAR/(EABAR*EISIG)
      GAMMA(I)=CC(I)/THETA
      AA=PI*SQRT(CC(I))
      BB=COSH(AA*(0.5-U/AL))
      DD=COSH(AA*0.5)
      EE=SINH(AA*X/AL)
      GG=SINH(AA*U/AL)
      HH=COSH(AA*(0.5-X/AL))
      IF(X.GT.U) GO TO 40
      BETA(I)=1.0-(AL*BB*EE)/(AA*X*DD)
      GO TO 45
   40 BETA(I)=1.-(AL*GG*HH)/(AA*U*DD)
   45 F1=(EABAR/EIBAR)*Z*TM
      F(I)=F1*BETA(I)
      CM=(TM-F(I)*Z)*(EC*XIC)/EISIG
      GO TO 60
   50 AC=B*2.*H
      XIC=B*(2.*H)**3/12.
      EABAR=(ES*AS*EC*AC)/(EC*AC+ES*AS)
      EISIG=ES*XIS+EC*XIC
      Z=ED-H
      EIBAR=EISIG+EABAR*Z**2
      THETA=EIBAR/(EABAR*EISIG)
```

```
      CC(I)=GAMMA(I)*THETA
      AA=PI*SQRT(CC(I))
      BB=COSH(AA*(0.5-U/AL))
      DD=COSH(AA*0.5)
      EE=SINH(AA*X/AL)
      GG=SINH(AA*U/AL)
      HH=COSH(AA*(0.5-X/AL))
      IF(X.GT.U) GO TO 55
      BETA(I)=1.0-(AL*BB*EE)/(AA*X*DD)
      GO TO 56
   55 BETA(I)=1.-(AL*GG*HH)/(AA*U*DD)
   56 F1=(EABAR/EIBAR)*Z*TM
      F(I)=F1*BETA(I)
      CM=(TM-F(I)*Z)*(EC*XIC)/EISIG
   60 SCB=H/EISIG
      SCT=-H/EISIG
      EPCB=((SCB-BETA(I)*(EABAR/EIBAR)*Z*(SCB*Z+1./(AC*EC)))*TM)
      EPCT=((SCT-BETA(I)*(EABAR/EIBAR)*Z*(SCT*Z+1./(AC*EC)))*TM)
      EPSB=F(I)/(AS*ES)+(TM-F(I)*Z)/EISIG*CS
      EPST=F(I)/(AS*ES)-(TM-F(I)*Z)/EISIG*CS
      EPSM=0.5*(EPST+EPSB)
      CH=2.0*H*(EPCB-EPCR)/(EPCB-EPCT)
      CD=2.*H
      CCH=CCH+CH
      H=H-0.5*CH
      IF(EPCB.LE.EPCR) GO TO 90
      IF(ABS(EPCB-EPCR).LT.2.E-6) GO TO 90
      IF (H.LT.0.0) GO TO 200
      IF(H.GT.TDM) GO TO 200
      IF(EPCB.GT.EPCR) GO TO 50
   90 WRITE(6,100)CCH,CD,EPCB,EPCT,EPSB,EPST,EPSM,F(I),CM,CC(I),CCI
  100 FORMAT(2F8.3,8E13.5,F7.2)
  200 CONTINUE
      X=X+1.0
      IF(X.LE.45.0) GO TO 4
  150 STOP
      END

                          CD TOT   0154
```

APPENDIX IV

Computed Flexural Crack Profiles

The flexural crack profiles discussed here, are based on the method of computation, described in the thesis. Therefore, for details on the procedure of calculations, the reader may refer to Chapter III.

A4.1 Partially Fixed End Beam

Figs. A4.1 to A4.3 show the computed crack profiles for the "Typical Beam" with varying degrees of fixity at the ends. The beam in Fig. A4.1 is subjected to one times the design load, and in Fig. A4.2 and A4.3 to 1.5 and 2.0 times the design load respectively. The value of $\frac{1}{C}$ has been taken = 5 , and that the steel reinforcement is only in the tensile zones of the beam. The degree of end fixity, μ, is given by

$$\mu = \frac{M_o}{M_F} \qquad\qquad \text{A4.1}$$

where M_F is the moment due to the complete fixity at the ends. M_o is the moment at the ends for a given value of μ. The degrees of fixity considered are 0, 0.2, 0.4, 0.6, 0.8 and 1.0. One times the design load is approximately 1240 lbs. (i.e. 36200/29.25). The distribution of the bending along the length of a beam for varying degrees of fixity, μ, is shown qualitatively in Fig. A4.0 below.
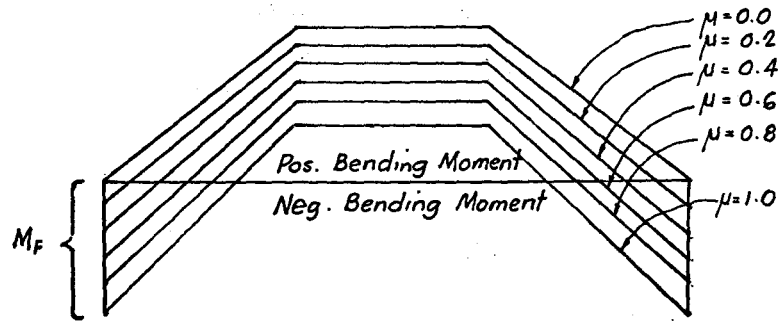
Distribution of Bending Moment

Fig. A4.0

Fig. A4.1 shows the crack profiles for μ = 0.0, 0.2, 0.4 and 0.6 in the region of positive moment and no profile in the region of negative moment. For μ = 1.0, the crack profile is only obtained in the zone of negative moment. It may also be noted, however, that there is no crack profile for μ = 0.8, because the strain in the tensile zones never exceeds the value of ε_{cr}.

Fig. A4.2 shows crack profiles for μ = 0.0, 0.2 and 0.4 in the zone of positive moment, for μ = 0.6 and 0.8 in the zone of positive as well as negative moment.

Similarly, Fig. A4.3 shows the crack profiles for μ = 0.0, 0.2 and 0.4 in the zone of positive bending moment, and for μ = 0.6, 0.8 and 1.0, both in the zone of negative as well as positive bending moments.

A comparison of Fig. A4.2 to A4.3 indicates that increase in the load intensity as well as the degree of end fixity, both have significant influence on the cracking

CRACK PROFILES - EFFECT OF END FIXITY - TWO TIMES THE DESIGN LOAD.

FIG. A4.3

No Crack Profile for $\mu = 0.8$

$\mu = 1.0$

$\mu = 0$

$\mu = 0.2$

$\mu = 0.4$

$\mu = 0.6$

Crack Height (in)

Distance from L.H. Support (in)

M_o 29.25"   29.25" M_o

L = 90.0"

4"

7.0"   8.5"

$A_s = 0.51_{\square}"$
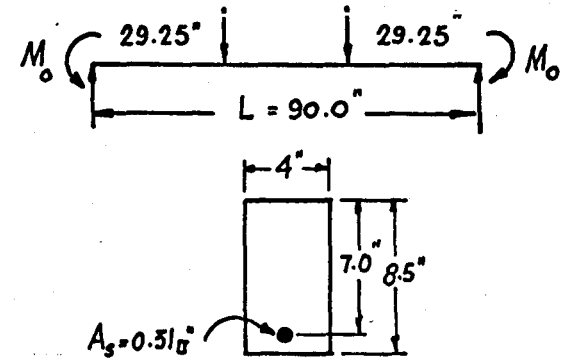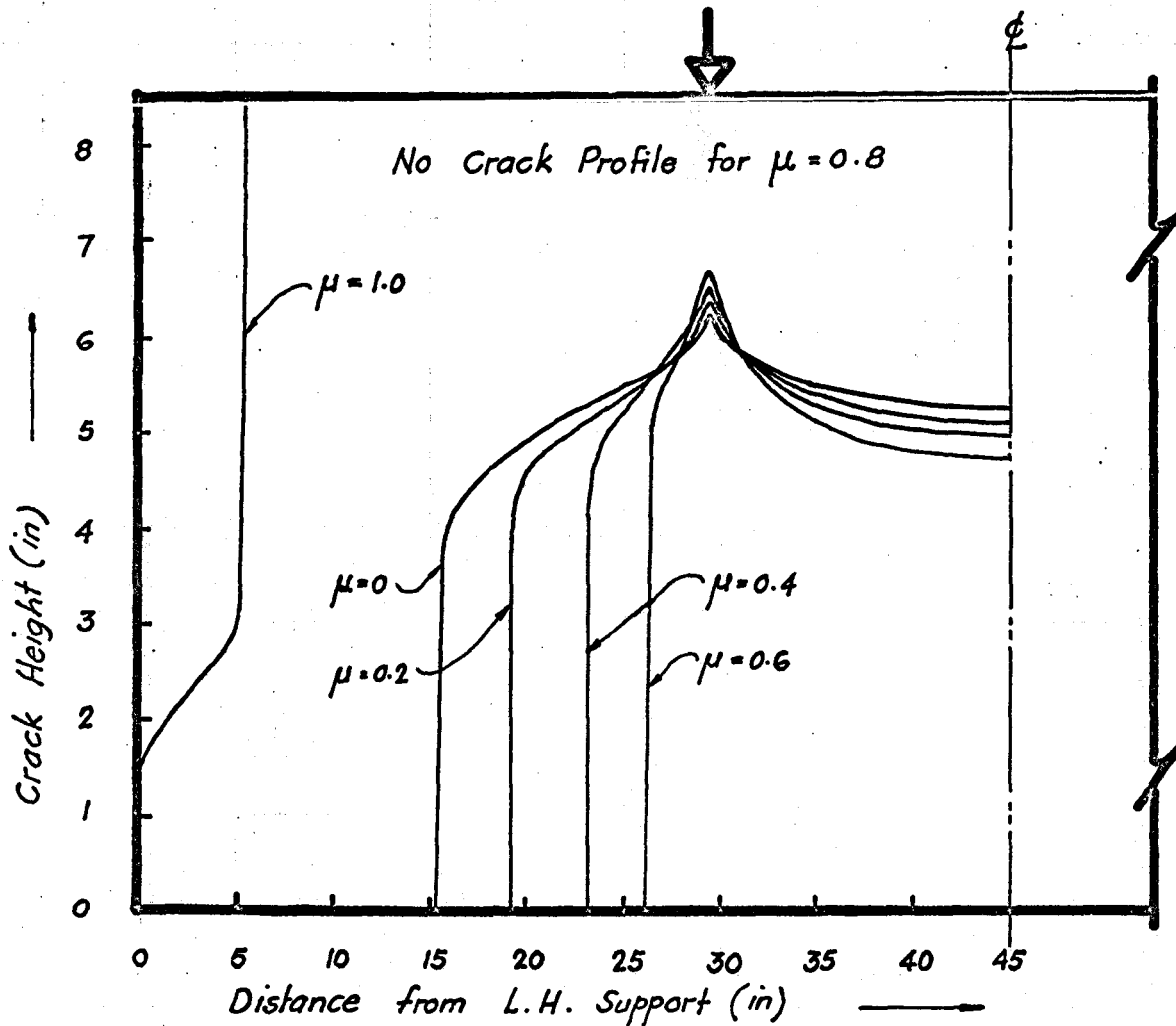
$$\mu = \frac{M_o}{M_F}$$

where :
M_F = Fixed End Moment

$E_s = 30 \times 10^6$ psi

$E_c = 3.5 \times 10^6$ psi

$\epsilon_{cr} = 100$ micro in/in

One Times The Design Load

$\frac{1}{C} = 5$.

CRACK PROFILES - EFFECT OF DEGREE OF FIXITY - ONE TIMES THE DESIGN LOAD.

FIG. A4.1

Graph labels:

- Vertical axis: Crack Height (in), marked 0 to 8
- Horizontal axis: Distance from L.H. Support (in), marked 0, 5, 10, 15, 20, 25, 30, 35, 40, 45
- Curve labels on left: $\mu = 0.6$, $\mu = 0.8$, $\mu = 1.0$
- Curve labels on right: $\mu = 0.0$, $\mu = 0.2$, $\mu = 0.4$, $\mu = 0.6$, $\mu = 0.8$
- ₵ (centre line)

Beam diagram labels:
- M_o ... M_o
- 22.25", 22.25"
- $L = 90.0"$
- 4"
- 7.0", 8.5"
- $A_s = 0.31_o"$
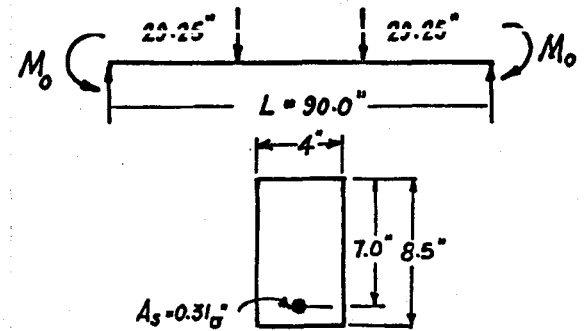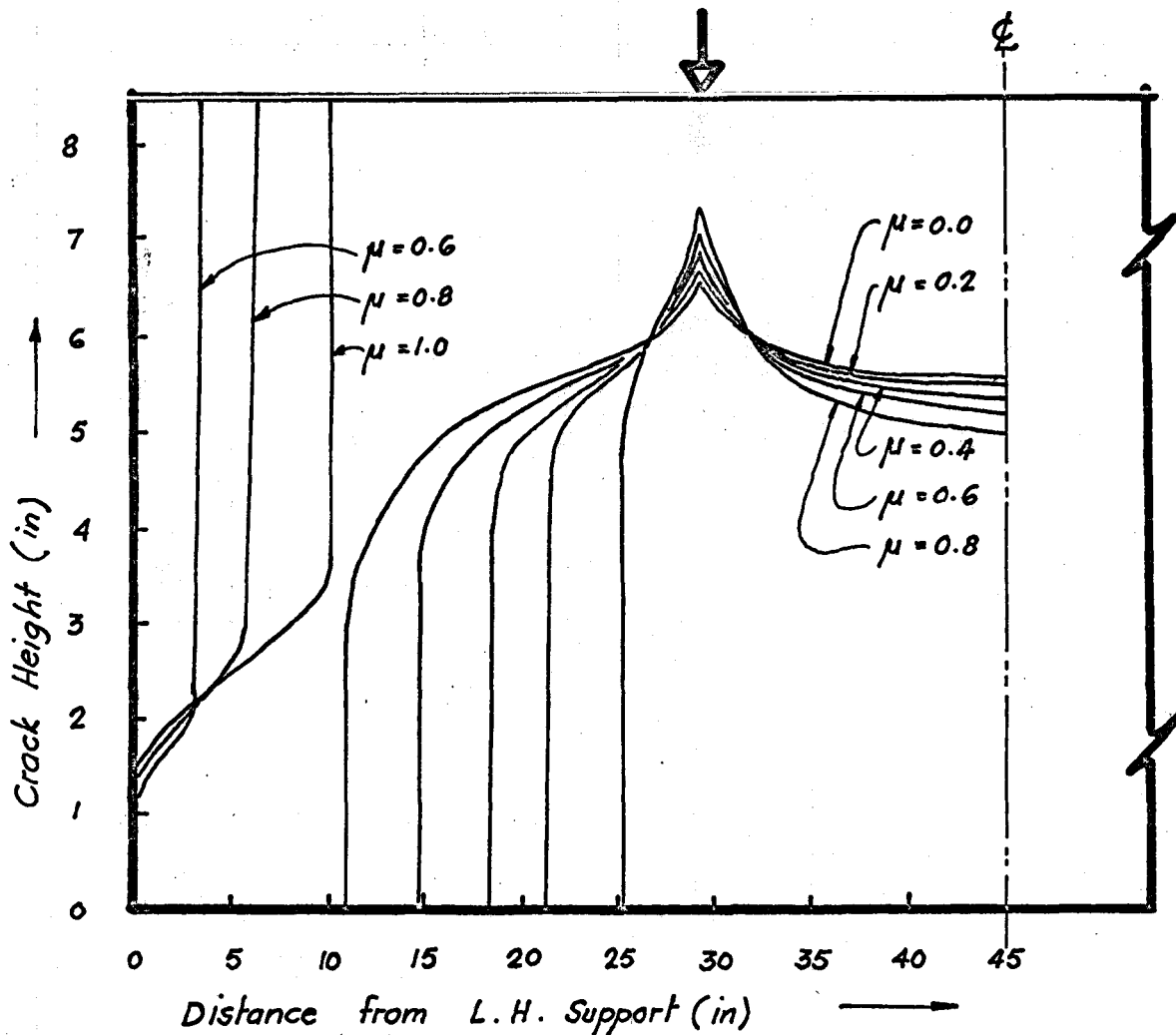
$$\mu = \frac{M_o}{M_F}$$

where: M_F = Fixed End Moment

$E_s = 30 \times 10^6$ psi

$E_c = 3.5 \times 10^6$ psi

$\epsilon_{cr} = 100$ micro in/in.

1.5 Times the Design Load

$\frac{l}{c} = 5$

CRACK PROFILES - EFFECT OF END FIXITY - ONE AND HALF TIMES THE DESIGN LOAD.

FIG. A4.2

pattern. Increase in the load intensity results in higher cracks as well as longitudinal spread. Increase in the degree of end fixity results in increased cracking in the zone of negative bending and suppression of the spread of the crack profile in the zone of positive bending moment.

It may also be noticed that for the same intensity of the point loads, the height of crack in the vicinity of the point load increases with increase in the degree of end fixity. This is due to the fact that $\frac{F}{F'}$ distribution for the fixed end beam is lower than the $\frac{F}{F'}$ distribution for a simply supported beam (see Fig. 2.14). However, the effect of degree of end fixity is opposite in the zone of negative bending. The height of cracks in the vicinity of the supports reduce with an increase in the degree of fixity. This is because the terminal $\frac{F}{F'}$ predominates over the degree of end fixity.

A4.2   Continuous Beams

The continuous beam considered here has two equal spans, each with a length of 90 inches. The cross-sectional dimensions are same as of the "Typical Beam" of Chapter II, except the reinforcement is assumed to exist only in the tensile zones of the beam. Two cases of loading are considered, one with central point load at each span and the other, of uniformly distributed over the entire length of the beam. The intensity of the loading is taken such that
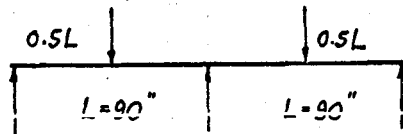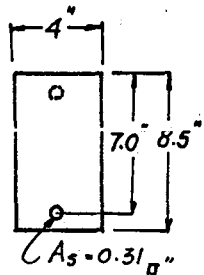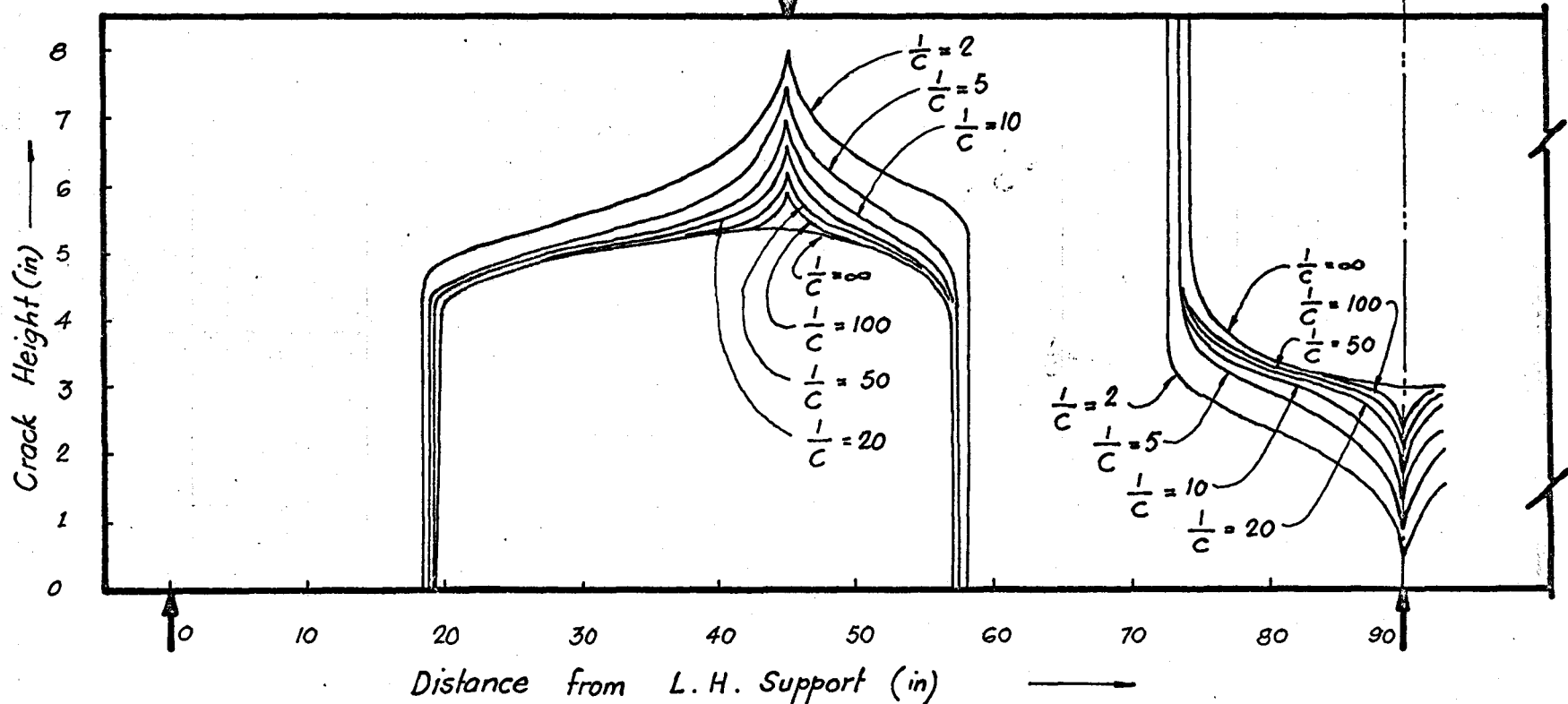
CRACK PROFILES - CONTINUOUS BEAM OF TWO SPANS WITH CENTRAL POINT LOADS.

FIG. A4.4
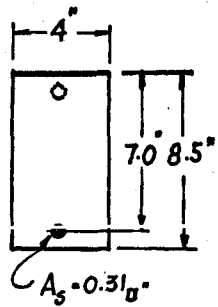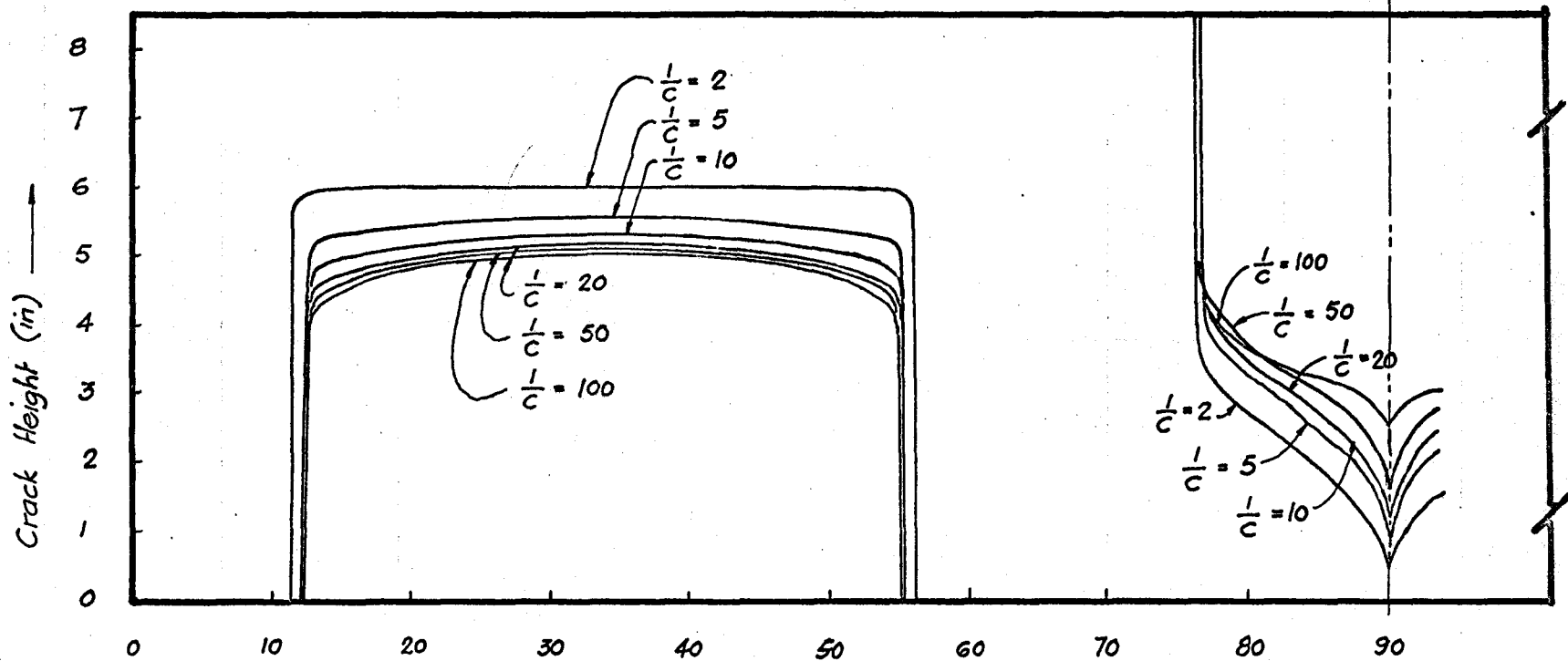
CRACK PROFILES - CONTINUOUS BEAM OF TWO SPANS WITH U.D. LOAD

FIG. A4.5

the magnitude of the maximum applied (i.e. at the central support) is 1.5 times the design load. The computed crack profiles for varying values of the interaction coefficient, $\frac{1}{C}$, are shown in Figs. A4.4 and A4.5.